Aus der Medizinischen Klinik des Universitätsklinikums Heidelberg

Klinik für HÄMATOLOGIE, ONKOLOGIE UND RHEUMATOLOGIE

(Ärztliche Direktor: Prof. Dr. med Carsten Müller-Tidow)

The Effect of Elotuzumab on T cells in Patients with Multiple Myeloma

Inauguraldissertation
zur Erlangung des Doctor scientiarum humanarum
an der
Medizinischen Fakultät Heidelberg
der
Ruprecht-Karls-Universität

vorgelegt von

Mohamed Hemaid Sayed Awwad

aus
Gizeh, Ägypten

2021

Dekan: Herr Prof. Dr. med. Hans-Georg Kräusslich

Doktorvater: Herr Prof.apl. Dr. med. Michael Hundemer

"This work is wholeheartedly dedicated to Hemaid Awwad, my beloved father, whose love for me knows no bounds. In a turbulent life crammed with insecurities, you were always my source of guidance. Without your support, inspiration, and encouragement, this work would not be possible… I owe my success to you… I love you!"

Table of Contents

Abbreviation

ADCC	antibody-mediated cellular cytotoxicity
ADCP	antibody-mediated cellular phagocytosis
APC	antigen presenting cells
BM	bone marrow
BTLA	B- and T-lymphocyte attenuator
C1q	component 1q
CAR	chimeric antigen receptor
CDC	complement-dependent cytotoxicity
CLP	common lymphoid progenitors
CMP	common myeloid progenitors
CPD	cell proliferation dye
CTLA-4	cytotoxic T-lymphocyte-associated Protein-4
CXCL5	C-X-C motif chemokine 5
DAG	diacylglycerol
DC	dendritic cells
EAT-2	Ewing's sarcoma-associated transcript 2
EGR2	early growth response 2
ELISA	enzyme-linked immunosorbent assay
ELK-1	ETS like-1 protein
ERK	extracellular signal-regulated kinase
FACS	flow activated cell sorter
Fc	fragment crystallizable
FDA	food and drug administration

FSC	forward scatter
GEFs	guanine nucleotide-exchange factors
GM-CSF	granulocyte-macrophage colony-stimulating factor
GMMG	German-Speaking Myeloma Multicenter Group
GSEA	gene set enrichment analyses
HPV	human papillomavirus
HSC	hematopoietic stem cells
i.p.	intraperitoneal
i.v.	intravenous
ICI	immune check-point inhibitor
iFISH	interphase fluorescence in situ hybridization
IKZF2	Ikaros family zinc finger 2
IMiD®	immunomodulatory drug
INF-γ	interferon-gamma
IP_3	inositol trisphosphate
IRF4	interferon regulatory factor 4
ISS	international staging system
ITAMs	immunoreceptor tyrosine-based activation motifs
ITK	Interleukin-2-inducible T-cell Kinase
ITSM	immunoreceptor tyrosine-based switch motifs
KLRG-1	killer cell lectin like receptor G1
LAG3	Lymphocyte-activation gene-3
LAT	linker for the activation of T cells
LCK	leukocyte-specific tyrosine kinase
logFC	log-fold changes

MALT	mucosa-associated lymphoid tissue
MAPK	mitogen-activated protein kinase
MGUS	monoclonal gammopathy of undetermined significance
MHC-II	class II major histocompatibility complex
MM	multiple myeloma
NFAT	nuclear factor of activated T cells
NF-κB	nuclear factor kappa-light-chain-enhancer of activated B cells
NK	natural killer
NSCLC	non-small-cell lung cancer
NSG	NOD.Cg-PrkdcscidIL2rgtm1Wjl/SzJ
PAMP	pathogen associated molecular pattern
PC	plasma cell
PD-1	programmed cell death protein 1
PFS	progression-free-survival
PIP2	phosphatidylinositol 4,5-bisphosphate
PKCθ	protein kinase C-θ
PLC	phospholipase C
PRR	pattern recognition receptor
RasGRP	RAS guanyl-releasing protein GRP
RRMM	relapsed/refractory multiple myeloma
s.c.	subcutaneous
SA-β-Gal	senescence-associated-β-galactosidase
SLAMF7	SLAM family member 7
SLP76	SH-2 domain-containing leukocyte protein of 76 KDa

SSC	side scatter
TAA	tumor-associated antigens
TCR	T cell receptor
TIGIT	T cell immunoreceptor with Ig and ITIM domains
TILs	tumor-infiltrating lymphocytes
TIM-3	T cell immunoglobulin, and mucin-domain containing-3
TNF-α	tumour necrosis factor alpha
TOX1	thymocyte selection associated high mobility group
TSA	tumor-specific antigens
VRD	bortezomib, lenalidomide, and dexamethasone
ZAP70	zeta-chain-associated protein kinase 70
ZEB2	zinc finger E-Box binding homeobox 2

1. Introduction

1.1. General Introduction

1.1.1. The Immune System: An Overview

The word “immune” originated from the Latin term “*immunis*”, which means exempt; it is currently used to describe people protected or safe from encountering a disease in the future (Punt et al., C 2019). The concept of immunology can be tracked back to 430 BC, when Thucydides first realized that only people who had recovered from plague disease could nurse new patients without the risk of re-encountering the disease again (Silverstein, 1982). Using evidence-based analyses, Thucydides discovered a new field of knowledge that is known today as immunology.

Advances in biological, chemical, and physical experimental approaches have helped scientists understand the immune system more. With cumulative knowledge gathered through the last centuries, it has become clear that the immune system is one of the most complicated systems in the human body and involves a strictly organized hierarchical system of cells and effector molecules that defend the body against invaders regardless of their spatial and temporal onset (Subramanian et al., 2015). This system comprises a highly adaptable and diverse set of cells that cooperate with each other to assure both efficient and frugal responses to invaders (Punt et al., C 2019). To achieve fast and long-term protection, the immune system has evolved into two different functional branches, innate and adaptive immunity. While innate immunity serves as a non-specific first responder, adaptive immunity implies a more sophisticated, long-lasting, and specific immunity (Netea et al., 2019).

From an organ perspective, in Homo sapiens and most mammals, the immune system consists of primary and secondary lymphoid organs. Primary lymphoid organs include the bone marrow (BM) and thymus, which represent factories for immune cell production, i.e., the proliferation and differentiation of mature immune cells from immature progenitors (Okada and Kondoh, 1986; Boehm and Bleul, 2007). In the BM, haematopoietic stem cells (HSCs) differentiate into common lymphoid progenitors (CLPs) or common myeloid progenitors (CMPs). CLPs differentiate further into B cell progenitor and natural killer (NK) cells in the

BM or travel to the thymus, where they differentiate into T cells (Boehm and Bleul, 2007; Abel et al., 2018). The secondary lymphoid organs include the spleen, lymph nodes, mucosa-associated lymphoid tissue (MALT), and Payer's patches, which are responsible for maintaining an efficient microenvironment for lymphocyte antigen recognition and maturation, thus generating killer and regulatory immune cells (Boehm and Bleul, 2007; Buettner and Lochner, 2016). Notably, while primary and secondary lymphoid organs develop prenatally and exist permanently, transient and less organized lymphoid structures called tertiary lymphoid organs are formed under inflammation or disease conditions. These structures share many structural characteristic elements with lymph nodes, including unique B cell and T cell centres (Luis Munoz-Erazo et al., 2020).

1.1.2. Innate and Adaptive Immunity

While all immune cells have the same goal of protecting the body from foreign antigens derived from either external or internal sources, such as bacteria, viruses, and cancer cells, they achieve this in very different ways. The immune system is classified into innate and adaptive immunity. Innate immune cells carry out the function of being the *first responders* in cases of infection, and they pursue a non-specific immune reaction against foreign antigens. Innate immune cells recognize common structures on pathogens known as pathogen-associated molecular patterns (PAMPs) using pattern recognition receptors (PRRs) (Bonilla and Oettgen, 2010). Such a mechanism allows innate cells to respond to diverse foreign antigens and to serve as antigen-presenting cells (APCs) for adaptive immune cells using class II major histocompatibility complex (MHC-II) molecules (Neefjes et al., 2011). Innate immune cells include macrophages, neutrophils, NK cells, eosinophils, mast cells and monocytes (Bonilla and Oettgen, 2010; Danilova, 2012; Marshall et al., 2018).

Adaptive immunity, on the other hand, represents a slower, and specialized, long-term defence against foreign antigens. In contrast to innate immune cells, adaptive immune cells recognize specific foreign antigens, expand as clonal and specific cells, and eventually develop into long-term specific immunological memory cells that can eliminate similar pathogens in future recurrent infections (Marshall et al., 2018). Adaptive immune cells include T cells and B cells, and they require proper help from innate immune cells to be recruited and activated

through APCs. While both T and B cells behave in a similar antigen-specific way and share many similarities in their activation pathways, they kill target cells in very different ways. T cells provide a cell-mediated immune response, and B cells contribute to the humoral immune response by secreting antibodies (Bonilla and Oettgen, 2010).

1.1.3. T cells

1.1.3.1. T Cell Receptor Activation Signalling

Over the past decades, T cells have captured the focus of scientists as one of the most important players in human immunity. T cell receptor (TCR) activation signalling involves hundreds of cytokines, receptors, and transcription factors that are strictly controlled to avoid both autoimmune and immunodeficient responses (Punt et al., C 2019). The classical consensus understanding is that MHC-I molecules on nucleated cells or MHC-II molecules on APCs present peptides to cytotoxic $CD8^+$ T cells and $CD4^+$ T cells, respectively (Wieczorek et al., 2017).

T cells scan MHC receptors simultaneously until they recognize their specific matching foreign antigen. Once bound, with the help of other co-stimulatory factors, the TCR undergoes a conformational change involving the associated CD3 co-receptor. CD3, which consists of four different chains, the δ-, γ-, ϵ-, and ζ-chains, is phosphorylated by Src kinase leukocyte-specific tyrosine kinase (Lck) after conformational changes that expose immunoreceptor tyrosine-based activation motifs (ITAMs). Phosphorylated tyrosine residues in the CD3 ζ-chain ITAMs recruit zeta-chain-associated protein kinase 70 (ZAP70), which phosphorylates linker for the activation of T cells (LAT). Phosphorylated LAT recruits SH-2 domain-containing leukocyte protein of 76 kDa (SLP76), which is subsequently phosphorylated by ZAP70, forming the LAT-SLP76 complex. Phosphorylated Slp76 also binds to interleukin-2-inducible T cell kinase (ITK). The complex of Zap70, Lck, and ITK has an essential role in the phosphorylation and activation of phospholipase C (PLC)-γ1. Activated PLC-γ1 carries out the crucial activation step of T cell activation by breaking down cell membrane phosphatidylinositol 4,5-bisphosphate (PIP2) into diacylglycerol (DAG), which remains in the membrane, and inositol trisphosphate (IP_3), which binds to the

endoplasmic reticulum and induces calcium ion release. Calcium ions activate calcineurin, which dephosphorylates nuclear factor of activated T cells (NFAT) to enable nuclear delocalization. By remaining in the membrane, DAG recruits protein kinase C-θ (PKCθ), which ultimately activates the nuclear factor kappa-light-chain-enhancer of activated B cells (NF-κB) pathway, and RAS guanyl-releasing protein (RasGRP) through its cysteine-rich sequences. PKC-θ also activates a downstream pathway that involves guanine nucleotide-exchange factors (GEFs) and activates mitogen-activated protein kinase (MAPK) signalling pathways, which activate extracellular signal-regulated kinase (ERK); ERK therefore phosphorylates ETS like-1 protein (Elk-1) and subsequently the transcription factor FOS. Altogether, this leads to the activation of transcription factors and gene reprogramming that transform T cells from a quiescent state to a metabolically active state (Huse, 2009; Paul and Schaefer, 2013; Courtney et al., 2018; Hwang et al., 2020) (Figure 1).

1.1.3.2. Dysfunction of T cells: Exhaustion and Senescence

T cell activation and expansion are highly controlled to avoid both autoimmunity and severe immune reactions; therefore, after repeated proliferation cycles, T cells undergo senescence or exhaustion programmes (Pawelec, 2019). One of the largest challenges in T cell research is to distinguish between exhaustion and senescence; the two states share many common markers, dysfunctional behaviours, lack proliferative activity and feature cell cycle arrest. However, they have different initiation signalling pathways, metabolic profiles, and transcriptional programmes (Akbar and Henson, 2011). Exhaustion programmes are associated with chronic antigen exposure, such as chronic infection and tumours. Transcription factors such as NFAT, nuclear factor Nr4a, and the recently described thymocyte selection-associated high mobility group (TOX1) trigger the first signals for exhaustion in T cells (Mognol et al., 2017; Khan et al., 2019; Sekine et al., 2020). Once the exhaustion state is initiated, surface markers such programmed cell death protein 1 (PD-1), cytotoxic T-lymphocyte-associated protein-4 (CTLA-4), T cell immunoreceptor with Ig and ITIM domains (TIGIT), T cell immunoglobulin and mucin domain-containing-3 (TIM-3), lymphocyte activation gene-3 (LAG3), and B and T lymphocyte attenuator (BTLA)

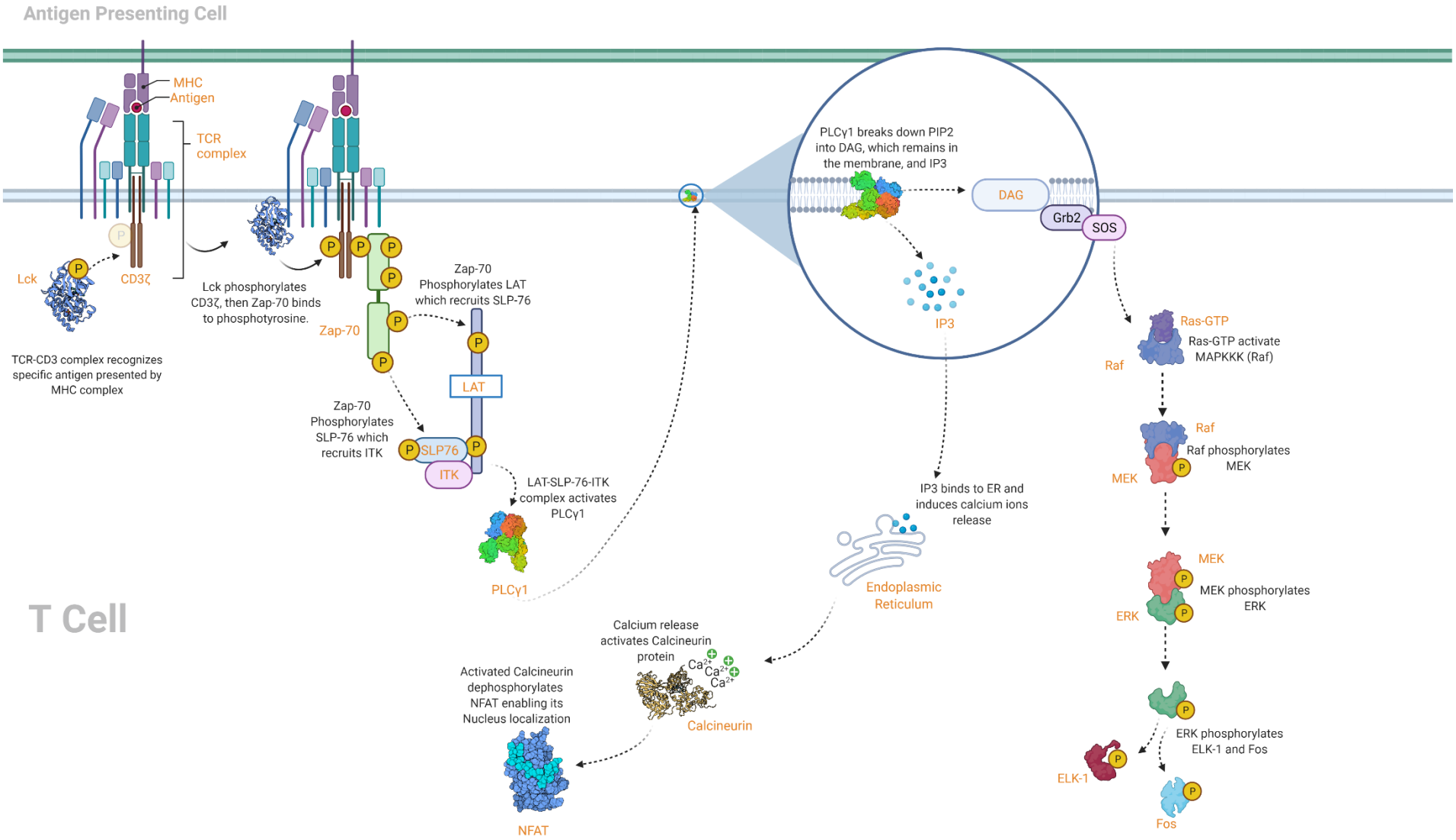

Figure 1. Activation signals in T cells (the figure was created using BioRender.com tools; the TCR-CD3-ZAP-70 complex was adapted from a pre-assembled TCR downstream signalling template at BioRender.com. Protein structures, including 1QPJ(Zhu et al., 2000), 2JOG(Takeuchi et al., 2007), 1MF8(Jin and Harrison, 2002), and 6PBC(Hajicek and Sondek, 2020), were imported from Protein Data Bank (RCSB-PDB)):

Schematic diagram showing T cells molecular pathways. T cells require different activation siganls to transform from a quiescent state to an actively proliferating state. The signals are initiated by the recognition of a specific antigen presented on the surface of an APC by the TCR. TCR intracellular ITAMs initiate activation signals that eventually recruit transcription factors such as NFAT and FOS, which upregulate IL-2 expression.

are upregulated (Matsuzaki et al., 2010; Wherry and Kurachi, 2015; Jiang et al., 2020). The upregulation of these surface markers further induces complex downstream pathways after their binding to the corresponding receptors on APCs or tumour cells, thus eventually leading to a dominant dysfunctional state in T cells (Zhao et al., 2020).

On the other hand, senescent T cells arise more during natural ageing, which could be linked to the weak immune response in elderly individuals (Chou and Effros, 2013; Mittelbrunn and Kroemer, 2021). Nevertheless, senescent T cells are also upregulated in chronic infection and in tumour microenvironments (Huff et al., 2019). The expression of senescence-associated β-galactosidase (SA-β-Gal), CD57, killer cell lectin-like receptor G1 (KLRG-1), and TIM-3 and the downregulation of CD28 and CD27 are hallmarks of T cell senescence (Brenchley et al., 2003; Heffner and Fearon, 2007; Henson and Akbar, 2009; Strioga et al., 2011; Li et al., 2012). Like exhausted T cells, senescent T cells also exhibit a dysfunctional state; moreover, many studies have also reported that senescent T cells can exert immunosuppressive effects on other effector T cells (Filaci et al., 2007; Strioga et al., 2011; Huff et al., 2019).

1.2. Tumour Immunology

1.2.1. Cancer Immunoediting

Over the past decades, immunologists have tried to understand the interaction between immune cells and tumour cells within the microenvironment. The first evidence of tumour immunosurveillance was derived from mice, as researchers demonstrated the ability of the immune system to protect mice from the development of many types of cancer and even showed that mice lacking the interferon-gamma (IFN-γ) gene develop more tumours upon ageing (Vesely et al., 2011).

It is now widely accepted that in the ideal situation, immune cells should be able to eliminate any malignant cells and halt the process of cancer development; however, gene variants in malignant cells can disrupt this idea using three evolutionary steps called the elimination, equilibrium, and escape phases that together generate the process of immunoediting (Schreiber et al., 2011; O'Donnell et al., 2019).

In the *elimination phase*, the immune system identifies novel tumour antigens that could be tumour-specific antigens (TSAs), which are only found in cancer cells, or tumour-associated antigens (TAAs), which are found at high levels in cancer cells but also at lower levels in healthy cells (Haen et al., 2020). After antigen recognition, immune cells cooperate to kill malignant cells, which eventually leads to tumour cell elimination. However, if some tumour cells evolve during the elimination phase in a way that enables them to escape immune surveillance by taking advantage of genetic variants, then the equilibrium phase starts. In the *equilibrium phase*, experienced adaptive immune cells and innate immune cells keep targeting tumour cells and prevent them from overgrowing; however, the tumour cell number remain low in the equilibrium phase, such that the host does not detect their existence. During this phase, because of further mutations and immune stress that selects for the fittest clones, tumour cells acquire the ability to escape immune surveillance by upregulating markers such as programmed death ligand 1 (PD-L1), which binds to PD-1 on exhausted T cells (see 1.1.3.2) and CTLA-4 to induce cell dysfunction. With these new capabilities, tumour cells transform the immunoediting process to the third phase: the *escape phase*. In the escape phase, immune cells lose control and can barely kill tumour cells, even if they do detect the tumour cells, they are dysfunctional and unable to eliminate them. Thus, the selected tumour clones from the previous phases overgrow by taking advantage of the previous immune stress that allowed for natural selection of the least immunogenic clones (Figure 2) (Vesely et al., 2011; O'Donnell et al., 2019; Haen et al., 2020).

1.2.2. Cancer Immunotherapy

The understanding of the cancer immunoediting process inspired the idea to reverse the deterioration of the immune response by targeting the molecular pathways that initiate the exhausted phase. Although the notion of recruiting immune cells to treat cancer can be traced back to the nineteenth century, when William Coley treated cancer patients with extracts of heat-inactivated bacteria that stimulated the immune system (Waldman et al., 2020), the first approved modern immunotherapy targeting exhaustion checkpoints was the antibody ipilimumab, which was approved in 2011 (Hodi et al., 2010; Lipson and Drake, 2011). Currently, almost twenty years after the first approval, cancer

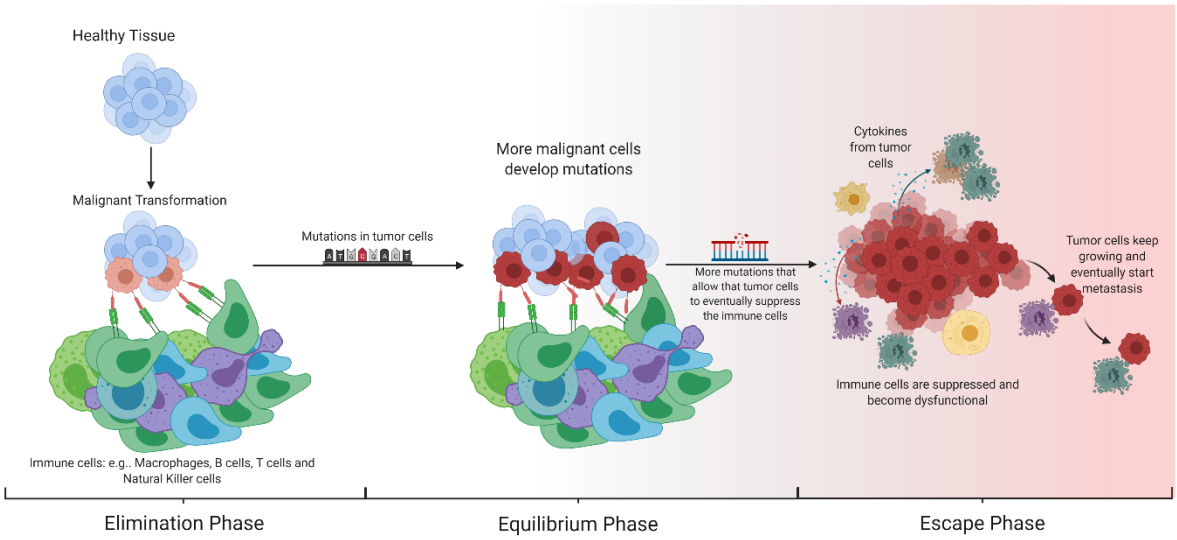

Figure 2. Immunoediting phases (the figure was created using the BioRender.com tool):
The figure describes the transformation of healthy cells into malignant cells, which features three different immunoediting phases: the elimination phase, equilibrium phase and escape phase. Immune stress causes tumour cells with mutations favouring immune escape to be selected and to expand.

immunotherapy has revolutionized the treatment options for patients, and the percentage of eligible patients is rapidly increasing (Haslam and Prasad, 2019).

Most immunotherapy tools can be categorized into immune checkpoint inhibitors (ICIs), chimeric antigen receptor (CAR) T cells, and cancer vaccines. ICIs are antibodies designed to target exhaustion/tolerance pathways in T cells. They block the interaction between ligands expressed on tumour cells and their receptors on T cells that induce exhaustion signals. They can target either ligands or receptors such as PD-1 or PD-L1, and antibody therapy will be discussed in detail in the next section (1.2.3) (Li et al., 2018).

Research advances in the genetic engineering of T cells have enabled the introduction of CAR T cells as a promising therapeutic approach. Genes encoding TSA or TAA receptors are transfected into T cells that are isolated from patients, expanded *in vitro* and reinjected into patients. Given their capability to proliferate *in vivo* and kill tumour cells and even to form long-term memory T cells, they exert robust antitumour activity. First-generation CARs, which contained CD3ζ chains linked to antigen recognition variable regions, did not prove to be successful in the initial clinical trials. However, second-generation

CARs, which include an additional co-stimulatory receptor such as CD28, were more promising in trials (Feins et al., 2019; Larson and Maus, 2021). It is intuitive, therefore, that a combination therapy that includes CAR T cells together with ICIs should have a synergistic outcome; many studies are exploring this approach and are showing promising results (Alard et al., 2020).

Unlike traditional vaccines against bacteria and viruses, cancer vaccines are not used prophylactically; rather, they are mainly used as a therapeutic vaccine to elicit the immune system against existing tumour cells. There are, however, some vaccines against hepatitis B and human papillomavirus (HPV) that can prevent virus-mediated cancers and can be classified as prophylactic vaccines (Waldman et al., 2020). Early studies targeting TAAs have shown modest efficiency and high autoimmune side effects because TAAs can be expressed in normal healthy tissues. On the other hand, frequent genetic variation in tumour cells, which arises due to genetic instability, leads to the generation of novel proteins called neoantigens. Using high-throughput next-generation sequencing, researchers are now able to explore mutations in tumour cells and use in silico algorithms to identify potential immunogenic epitopes that can be used to generate personalized vaccines. Clinical trials with personalized vaccines are still in the early stage; moreover, in one trial, the combination of a personalized neoantigen vaccine with an ICI failed to show a superior response in comparison to ICIs only (Blass and Ott, 2021).

1.2.3. Understanding Antibody Therapy

The development of the hybridoma laboratory approach in 1975 by Köhler and Milstein introduced a new era of antibody therapeutics (Köhler and Milstein, 1975). Since then, therapeutic antibodies have been used unconjugated or conjugated with cytotoxic reagents, and both types have shown strong antitumour efficacy in patients, especially in haematological malignancies (Weiner et al., 2010). Classical antibody therapies can directly kill tumour cells via different mechanisms. One way is complement-dependent cytotoxicity (CDC), which involves an antibody binding to a specific surface protein on tumour cells, recruiting complement component 1q (C1q) through the fragment crystallizable (Fc) domain, and subsequently activating the complement C1r subcomponent (C1r) enzyme, which initiates the signals for downstream

complement proteins. Eventually, this process leads to the formation of membrane pores that kill tumour cells (Weiner et al., 2010; Alfaleh et al., 2020). Other mechanisms include antibody-dependent cellular cytotoxicity (ADCC) or antibody-dependent cellular phagocytosis (ADCP) (Vermi et al., 2018). As of 2021, the United States Food and Drug Administration (FDA) has already approved 100 different antibodies to treat patients, with cancer indications still dominating the approvals (Mullard, 2021).

Meanwhile, the application of ICI antibodies since 2011 has revolutionized antibody therapeutic options for cancer patients. Unlike classical anti-tumour antibodies, ICIs block immune checkpoint pathways to reinstate immunosurveillance and allow immune cells to kill tumour cells. Ipilimumab, the first approved ICI, was designed to block the CTLA-4 receptor on the surface of T cells, which causes cellular inhibition and dysfunction and was approved for the treatment of melanoma (Darvin et al., 2018). Shortly afterwards, antibodies targeting the PD-L1/PD-1 inhibition pathway were developed and approved, e.g., pembrolizumab and nivolumab targeting PD-1 on T cells, which have been used for the treatment of metastatic melanoma and non-small-cell lung cancer (NSCLC). There are currently over 3,000 trials around the world that include at least one T cell modulator, with cancer immunotherapeutics trials representing 2/3 of cancer clinical trials (Darvin et al., 2018; Robert, 2020; Vaddepally et al., 2020).

1.3. Multiple Myeloma

1.3.1. Multiple Myeloma as a Common Haematological Malignancy

Multiple myeloma (MM) is a tumour of plasma cells (PCs) that is characterized by anaemia, bone lesions, and renal impairment that could eventually lead to renal failure in 20-40% of patients (Dimopoulos et al., 2008; Chim et al., 2018). MM is the second most common haematologic cancer, with one in each ten patients diagnosed with haematological malignancies is a myeloma patient (Kazandjian, 2016). MM affects elderly people, with a median age at first diagnosis of 70 years, and only approximately 2% of patients are younger than 40 years (Kyle et al., 2003; Palumbo et al., 2015).

Myeloma cells accumulate in the BM due to uncontrolled proliferation of long-lived monoclonal PCs. Mutations acquired during proliferation endow myeloma cells with the ability to modify and influence other cells to establish a suitable microenvironment. MM is thus believed to evolve from an early non-malignant state called monoclonal gammopathy of undetermined significance (MGUS). One of the widely used staging systems of MM is the international staging system (ISS), which consists of three stages. Although MM has been acknowledged as an incurable disease, with only 30% of patients surviving the first 10 years, recent advances have revolutionized the treatment options (Kuehl and Bergsagel, 2002; Palumbo et al., 2015). The immunomodulatory drug (IMiD) thalidomide and its derivatives lenalidomide and pomalidomide and autologous stem cell transplantation are among the most prominent treatments. In addition to their cytotoxic effect on myeloma cells, IMiDs activate the immune system and exert an anti-angiogenic effect in the bone niche (Raza et al., 2017).

1.3.2. Immunosurveillance in Multiple Myeloma

As previously discussed in sections 1.1.3.2 and 1.2.1, the evolution of tumours requires specific cellular mutations that allow for proper immune escape. While MM progression involves many microenvironmental factors that hamper immunosurveillance, T cell-related mechanisms have gained more focus. Previous studies have shown that myeloma-specific T cells upregulate senescence markers such as CD57 and KLRG-1 but have normal TCR levels (Suen et al., 2016; Lee et al., 2018). Moreover, it has been shown that exhaustion markers such as PD-1 and CTLA-4 are upregulated in the BM of MM patients (Zelle-Rieser et al., 2016). An altered $CD4^+/CD8^+$ T cell ratio and even correlations with the level of $CD8^+$ T cells in tumour-infiltrating lymphocytes (TILs) have also been described in MM patients (Redoglia et al., 1990; Willenbacher et al., 2016).

1.3.3. Antibody Therapy in Multiple Myeloma

The introduction of IMiDs, as discussed in 1.3.1, has remarkably improved MM survival and clinical outcomes, although most of the patients eventually relapse. To overcome this fact, classical antibodies directly targeting tumour cells and ICI antibodies have been extensively tested in MM patients (Ishida, 2018).

Daratumumab was among the first approved antibodies for the treatment of MM, it is an anti-CD38 monoclonal IgG1-kappa antibody that eliminates MM cells via the CDC, ADCC and ADCP mechanisms. Immunomodulatory effects of daratumumab have also been reported: depletion of immunosuppressive cells and expansion of effector T cells. Trials have proven that patients treated with a combination therapy that includes daratumumab have a lower risk of disease progression or death and better prognosis (Krejcik et al., 2016; Ishida, 2018; Mateos et al., 2018). Of note, isatuximab is another antibody targeting CD38 for the treatment of MM with similar mechanisms (Richardson et al., 2020). Elotuzumab is an anti-SLAMF7 antibody that also directly targets myeloma cells and will be reviewed in the next section (see 1.3.4).

PD-L1 is also expressed on the surface of myeloma cells; hence, investigators were encouraged to test PD-1 blockers such as nivolumab and pembrolizumab in the treatment of MM. However, trials involving PD-1 blockers were not very encouraging. Monotherapies with only PD-1 blockers were not effective, and no response was observed (Ishida, 2018; Ribrag et al., 2019). Thus, combinational therapies were tested, and pembrolizumab combined with IMiDs and dexamethasone showed promising outcomes in relapsed/refractory MM (RRMM); however, the FDA decided to halt all clinical trials involving pembrolizumab plus IMiDs after there were reports of immune-related cytotoxicity (Jelinek et al., 2018).

1.3.4. Anti-SLAMF7 Antibody: Elotuzumab

Elotuzumab is a humanized monoclonal antibody developed for the treatment of MM that targets the SLAMF7 receptor, also known as CD319 or CS1. Located on chromosome 1, the CS1 gene encodes the transmembrane SLAMF7 protein in NK cells, T cells, B cells, and dendritic cells (DCs). Studies analysing primary myeloma cells and myeloma cell lines have shown that the majority of myeloma cells express SLAMF7. Moreover, this high expression of SLAMF7 was found to be consistent among different disease stages and clones (Tai et al., 2009; Campbell et al., 2018).

In NK cells, the SLAMF7 protein is known to have an activation function. Two SLAMF7 isoforms are expressed, a long isoform that contains immunoreceptor

tyrosine-based switch motifs (ITSMs) and a short isoform that lacks these motifs and therefore cannot activate NK cells. Upon activation, by crosslinking SLAMF7 with antibodies or self-ligands, the long SLAMF7 isoform is capable of recruiting an adaptor protein called Ewing's sarcoma-associated transcript 2 (EAT-2) through a phosphorylated tyrosine in the ITSM. Recruited EAT-2 then initiates a downstream cascade that phosphorylates and activates PLC-γ and ERK (Malaer and Mathew, 2017; Campbell et al., 2018; Nishida and Yamada, 2019; O'Connell et al., 2019).

Elotuzumab therapy for MM is thought to have different mechanisms of action against myeloma cells:

- *Activation of NK-dependent ADCC:* In a mechanism that involves ADCC, elotuzumab binds to myeloma cells through SLAMF7 and to the NK cell receptor FcγRIIIA (CD16) through its Fc domain. Upon binding to FcγRIIIA, elotuzumab induces strong downstream activation signals in NK cells. Intuitively, the simultaneous binding to myeloma and NK cells by elotuzumab should also help to bring effector and target cells into closer proximity. As expected, studies have also showed that blocking CD16 deteriorates elotuzumab-induced ADCC of myeloma cells (Hsi et al., 2008; Campbell et al., 2018).
- *Direct activation of NK cells:* The binding of elotuzumab to SLAMF7 on NK cells was also shown to directly activate downstream activation signals in a CD16-independent manner. This mechanism, as described above, involves the recruitment of the EAT-2 protein and the phosphorylation of PLC-γ (Pazina et al., 2017).
- *Activation of macrophage-dependent ADCP:* Kurdi and his colleagues showed for the first time that elotuzumab can also induce ADCP in myeloma cells in a mouse xenograft model. In their model, which involved an immunodeficient mouse that lacked all immune cells but contained macrophages, elotuzumab was able to eliminate myeloma cells. Moreover, the researchers were able to show *in vitro* that the activation of ADCP is mediated through an FcγR-dependent pathway (Kurdi et al., 2018).

The different mechanisms described above (summarized in Figure 3) made elotuzumab an excellent candidate as a potential effective therapy for the treatment of MM. In a phase 1b-2 study performed by Lonial and colleagues in which elotuzumab was tested in RRMM patients, 68% of patients who received elotuzumab plus lenalidomide and dexamethasone achieved 1-year progression-free survival (PFS), whereas only 57% of patients who received only lenalidomide and dexamethasone achieved PFS. In a follow-up study after 5 years, patients in the elotuzumab group had a 27% decrease in the rate of progression or death related to the disease (Dimopoulos et al., 2017; Lonial et al., 2018). In another study that recruited 117 patients with RRMM, patients who received elotuzumab plus pomalidomide and dexamethasone showed a median PFS of 10.3 months, while that in patients who received pomalidomide and dexamethasone only was 4.7 months (Dimopoulos et al., 2018).

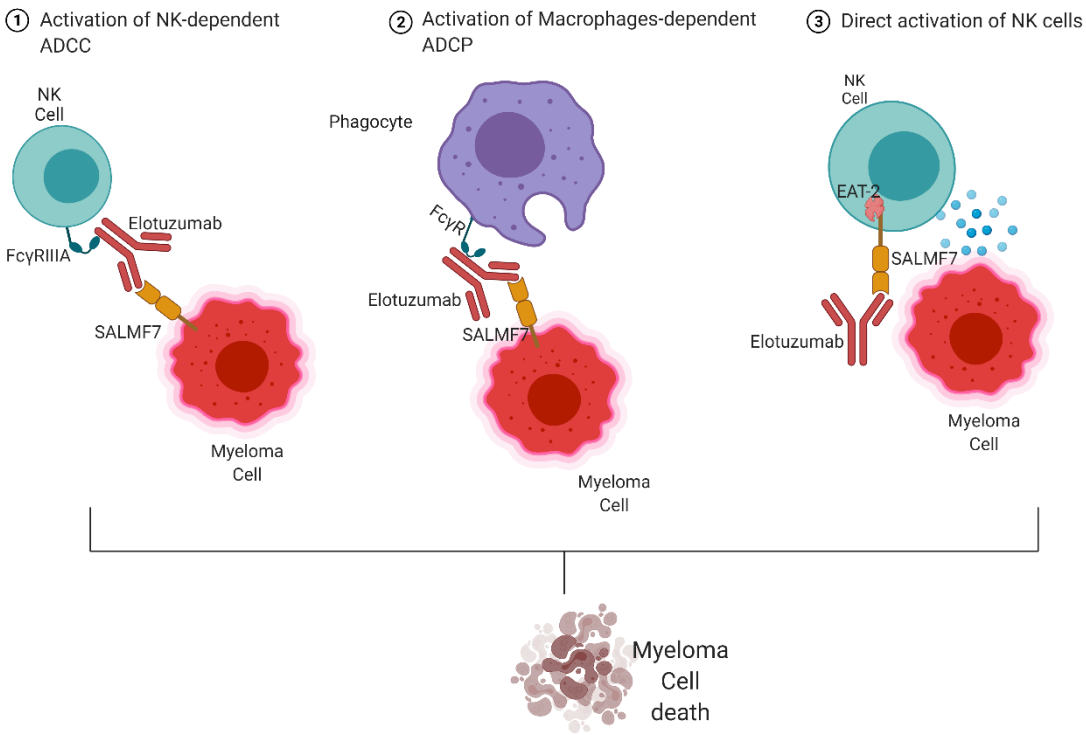

Figure 3. Elotuzumab machanism of action (the figure was created using the BioRender.com tool)
Thus far, three different mechanisms of action have been described for elotuzumab. It can induce ADCC by simultaneously binding to myeloma cells and to FcγRIIIA on NK cells, it can induce ADCP via a similar mechanism, and it can directly activate NK cells by binding to the SLAMF7 receptor on the surface of NK cells.

1.4. Hypothesis and Aims

The aim of the dissertation is to explore the expression of SLAMF7 on T cells, understand the functional relevance of its expression, investigate the effect of anti-SLAMF7 antibody (elotuzumab) therapy on T cells in patients with Multiple Myeloma, and eventually translate all the findings clinically by correlating them with the disease prognosis in patients to provide a rationale for future trials.

To explore SLAMF7 expression on T cells, I sought to answer the following questions:

- Is SLAMF7 expressed in remarkable levels on T cells in Multiple Myeloma Microenvironment? If yes, what kind of T cells do express SLAMF7?
- What is the functional relevance of SLAMF7 expression on T cells? Is it an activation or exhaustion marker?
- How does SLAMF7 expression affect T cells antigen-specific T cell cytotoxicity i.e. enhances or suppresses?
- What would it mean to knock SLAMF7 out in T cells?

In order to study the effect of Elotuzumab therapy on T cells in Multiple Myeloma patients, I investigated the following questions:

- What is the abundance of $SLAMF7^{+}$ T cells in patients with Multiple Myeloma?
- What happens to $SLAMF7^{+}$ T cells after receiving Elotuzumab? And how is it compared to patients who did not receive Elotuzumab?
- Can SLAMF7 expression on T cells contribute to the clinical outcomes in patients with MM, from a prognostic point of view?
- Is there a clinical correlation of SLAMF7 expression on T cells and the clinical outcomes in patients treated with Elotuzumab, from a predictive point of view?

Overall, the study aimed to provide a better understanding of the role of SLAMF7 expression on T cells and how this can be translated into a clinical meaning.

2. Material and Methods

2.1. Material List

Table 1. List of materials used in the experimental approaches.

Reagent	Source	Identifier
RPMI 1640	Sigma-Aldrich Chemie GmbH, Germany	R8758
Penicillin/streptomycin	Sigma-Aldrich Chemie GmbH, Germany	P4333
Pancell human	Pan biotech, Germany	P04-601000
IL-2	Novartis	
Human Serum	Sigma-Aldrich Chemie GmbH, Germany	P2918
CD3/CD28 microbeads	Gibco, Germany	11131D
Elotuzumab	Provided by Bristol-Myers Squibb, USA	
Granzyme B Elisa	Mabtech, Germany	3485-1H-20
Human IFN-γ ELISA Set	BD Biosciences, United States	555142
Human IL-2 ELISA BASIC kit (ALP)	Mabtech, Germany	3445-1A-6
Human Perforin ELISA BASIC kit (HRP)	Mabtech, Germany	3465-1H-20
ELISA microplates	Greiner Bio-one, Germany	655061
PBS1x	Sigma-Aldrich Chemie GmbH, Germany	D8537-500ml
Tween 20	Carl Roth, Germany	9172
Bovin Serum Albumin (BSA)	Sigma-Aldrich Chemie GmbH, Germany	A9418
Streptavidin	Agilent-DAKO, Germany	F0422
IL-4	R&D, Wiesbaden, Germany	204-IL/CF
IL-6	ImmunoTools GmbH	11340064
rhTNF-a	R&D, Wiesbaden, Germany	210-TA
Prostaglandin E_2	Biomol/ Enzo, Germany	P6-007-0001
CD8 MicroBeads, human	Miltenyi Biotec, Germany	130-045-201

Elispot plates	Merck Millipore, Germany	MAHAS4510
EDTA	Sigma-Aldrich Chemie GmbH, Germany	03690-100ml
Cell Proliferation Dye eFluor® 670	Thermo Fisher-Invitrogen, Germany	65-0840-90
FACS tubes	Corning Science, Germany	352052
Cas9-GFP	Sigma-Aldrich Chemie GmbH, Germany	CAS9GFPPRO
CD3/CD28/CD2 T Cell Activ	Stemcell, Germany	10990
ImmunoCult™-XF T Cell Expansion Medium	Stemcell, Germany	10981
TRIzol	Thermo Fisher-Invitrogen, Germany	15596018
High-capacity cDNA Reverse Transcription Kit	Thermo Fisher, Germany	4368813
AmpliTaq Gold DNA polymerase	Thermo Fisher, Germany	4398813
$CD8^+$ T Cell Isolation Kit	Miltenyi Biotec, Germany	130-096-495
RNeasy Mini Kit	Qiagen, Hilden, Germany	74104

2.2. Blood Samples and Ethics Statement

To analyze the expression of SLAMF7 protein expression on the surface of T cells, buffy coats from blood donators (Institute for Immunology/IKTZ, Heidelberg University, Germany) and samples from the PB/BM from patients diagnosed with MM from Heidelberg or from the German-Speaking Myeloma Multicenter Group (GMMG) study centers were obtained. Samples were only received from patients who have signed written informed consent in accordance with the Declaration of Helsinki, the study secretary was responsible for gathering and organizing all the legal documents. The clinical trials in which patients has been enrolled were based on institutional guidelines, and human studies have been approved by the Ethics Committee of the Medical Faculty at Heidelberg University. The clinical trial is a randomized phase III trial on the

effect of adding elotuzumab in bortezomib, lenalidomide, and dexamethasone (VRD) induction /consolidation and lenalidomide maintenance in patients with newly diagnosed myeloma, with European clinical trial register number: 2014-003079-40, and a national institute of health number: NCT02495922.

2.3. Cell Culture Medium and Reagents

Adapted from Awwad et al. (Awwad et al., 2021): T cells were cultured in T cell medium which is RPMI 1640 medium, supplemented with penicillin/streptomycin, 2 mM L-glutamine (all from PAA Laboratories, Pasching, Austria), 5% heat-inactivated human serum (PAA Laboratories) and 50 IU/ml IL-2 (Proleukin, Chiron GmbH, Munich, Germany). To isolate mononuclear cells (MNCs) from PB or BM samples, I used Ficoll-Hypaque density gradient centrifugation (Biochrom, Berlin, Germany) for 20 min at 1200xg without brake and then isolated the buffy coat layer between plasma and erythrocytes.

2.4. Molecular Cytogenetic Testing

The laboratory of Professor Anna Jauch from the institute of human genetic, Heidelberg University Hospital, has performed the molecular cytogenetic testing of Myeloma cells for patients enrolled in the GMMG-HD6 clinical trial.

Adapted from Awwad et al. (Awwad et al., 2021) and from the laboratory protocols provided by the laboratory of Professor Jauch: $CD138^+$ BM PCs were sorted from the BM of newly diagnosed MM patients using automated magnetic-activated cell sorting (MACS) with anti-CD138 beads as previously described (Granzow et al., 2017). Interphase Fluorescence In Situ Hybridization (iFISH) analyses has been performed to detect numerical changes at the chromosomal loci 1q21/13q14, 5p15/5q35, 8p21/19q13, 9q34/15q22, and 11q22.3/17p13; the IgH translocations t(11;14)(q13;q32), t(4;14)(p16;q32), and t(14;16)(q32;q23); and any other IgH rearrangement as previously described (Awwad et al., 2021). Hybridization was performed according to the manufacturer's instructions (MetaSystems, Altlussheim, Germany) with a minimum of 100 evaluated interphase nuclei per probe using an automated spot counting system (Applied Spectral Imaging, Edingen-Neckarhausen, Germany). A 10% threshold was set to detect gains, deletions, and translocations. A patients was considered as a

high-risk cytogenetic profile if the presence of deletion 17p and/or t(4;14) or t(14;16) was detected, as previously described (Krönke et al., 2017).

2.5. Flow Cytometry

Adapted from Awwad et al. (Awwad et al., 2021): The expression of T cell surface markers was analyzed by flow cytometry. Cells were counted and resuspended in PBS and incubated according to the manufacturer's instructions with the following fluorochrome-labeled antibodies:

Table 2. List of antibodies used in the experimental approaches.

Antibody	Source	Identifier
anti-human IFN-γ mAb 1-D1K, purified	Mabtech, Germany	3420-3-1000
anti-human IFN-γ mAb 7-B6-1, biotinylated	Mabtech, Germany	3420-6-250
APC-Vio 770 Anti-CD11b antibody	Miltenyi Biotec, Germany	130-113-794
APC-H7 mouse anti-human CD45 clone 2D1	BD Biosciences, Heidelberg, Germany	560178
PE-Cy7 mouse anti-human CD3 clone SK7	BD Biosciences, Heidelberg, Germany	557851
PerCP mouse anti-human CD8 clone SK1	BioLegend GmbH, Fell, Germany	347314
PE mouse anti-human CD28 clone CD28.2	BD Biosciences, Heidelberg, Germany	555729
Alexa Fluor 647 mouse anti-human CRACC (CD319 or SLAMF7) clone 235614	BD Biosciences, Heidelberg, Germany	564338
PE mouse anti-human CD197 (CCR7) clone 150503	BD Biosciences, Heidelberg, Germany	560765
V450 mouse anti-human CD45RA clone HI100	BD Biosciences, Heidelberg, Germany	560362
PE mouse anti-human CD152 (CTLA-4) clone BNI3	BD Biosciences, Heidelberg, Germany	557301
PE-Cy7 mouse anti-human CD62L clone DREG-56	BD Biosciences, Heidelberg, Germany	565535
BV421 mouse anti-human CD279 (PD-1) clone EH12.1	BD Biosciences, Heidelberg, Germany	562516

PE mouse anti-human CD16 clone 3G8	BD Biosciences, Heidelberg, Germany	555407
BV421 mouse anti-human CD57 clone NK-1	BD Biosciences, Heidelberg, Germany	563896
V450 mouse anti-human CD56 clone B159	BD Biosciences, Heidelberg, Germany	560360
PE mouse anti-human LAG-(CD223) clone T47-530	BD Biosciences, Heidelberg, Germany	565616
BV421 mouse anti-human TIM-3 (CD366) clone 7D3	BD Biosciences, Heidelberg, Germany	565562
PE/Cy7 mouse anti-human TIGIT clone A15153G	BioLegend GmbH, Fell, Germany	372714
FITC anti-human CD47 clone CC2C6	BioLegend GmbH, Fell, Germany	323106

Control cells were stained with the corresponding isotype antibodies at the same concentration. Flow cytometry analyses were performed on a BD FACSLYRIC™ or BD FACSCanto™ flow cytometer with BD FACSDiva software, data were analyzed using FlowJo software.

2.6. Nonspecific Activation of T cells and Enzyme-Linked Immunosorbent Assay (ELISA)

Adapted from Awwad et al. (Awwad et al., 2021): To analyze the effect of elotuzumab on the nonspecific activation of T cells by measuring cytokines secretion, $CD3^+$ T cells were isolated from MNCs using the MACS system (Miltenyi, Germany) according to manufacture instructions and were activated with anti-CD3/CD28 microbeads (Dynabeads, Invitrogen Dynal, Oslo, Norway) for 24 h at a cell:bead ratio of 1:4. Afterwards, the concentrations of granzyme B, IFNγ, IL-2 and perforin in the culture supernatants were determined with ELISA kits (Mabtech, Germany). ELISA microplates (Greiner Bio-One, Frickenhausen, Germany) were first coated with a capture antibody overnight to allow antibody binding to the wells. Next day, plates were washed twice with PBS and blocked for 1 h with blocking buffer (PBS with 0.05% Tween 20 and 0.1% BSA); the plates were then washed 5 times with wash buffer (PBS containing 0.05% Tween 20). Cell supernatants or standards were then added

to the wells, and the plates were incubated for 2 h at room temperature. Then, the plates were washed, and a detection antibody was added for 1 h. A streptavidin solution was added to the wells for 1 h. After a final wash, an appropriate substrate solution was added, and the optical density was measured using an ELISA reader.

2.7. Expansion of MART-1$_{aa26-35*A27L}$-specific T cells

Adapted from Awwad et al. (Awwad et al., 2021): peripheral blood mononuclear cells (PBMCs) from "HLA-A*02^{+}" HD were used to generate MART-1aa26-35*A27L-specific T-cells. T-cells specific for this antigen show cross-reactivity for HM1.24, a highly-expressed antigen on MM cells, and are able to lyse autologous MM cells (Christensen et al., 2009). Immature dendritic cells (DC) were obtained by culturing plastic-adherent PBMCs for 5 days in RPMI 1640 medium containing Granulocyte-macrophage colony-stimulating factor (GM-CSF) (800 U/ml, Sargramostim, Bayer, Seattle, WA, USA), Interleukin 4 (IL-4) (500 U/ml, R&D Systems, Minneapolis, MN, USA) and 5% heat-inactivated human serum. The maturation of immature DCs was then induced by supplementing Tumor Necrosis Factor Alpha (TNF-α) (10 ng/ml, R&D Systems), Interleukin 6 (IL-6) (1000 U/ml, PromoCell) and prostaglandin E_2 (1 µg/ml, Biomol/Enzo Lifesciences, Lörrach, Germany) for 2 days in the presence of the MART-1$_{aa26-35*A27L}$ peptide (10 µg/ml) to load the DCs. Afterwards, autologous PBMCs were incubated for 7 days together with mature DCs loaded with MART-1$_{aa26-35*A27L}$ peptide in T-cell medium to expand the MART-1$_{aa26-35*A27L}$-specific T-cells.

2.8. IFN-γ ELISPOT Assay

Adapted from Awwad et al. (Awwad et al., 2021): CD8^{+} cells were purified from the MART-1$_{aa26-35*A27L}$-activated T-cell population by positive immunomagnetic cell sorting (MACS-system, Miltenyi Biotec). Purified CD8^{+} cells were then incubated with the MART-1$_{aa26-35*A27L}$ peptide- or irrelevant peptide-pulsed T2 cells (loaded by a 2 h incubation in serum-free RPMI 1640 media containing 10 µg/ml peptide) for 24 h in anti-IFN-γ antibody- (Mabtech, Nacka Strand, Sweden) coated nitrocellulose-plates (Millipore, Schwalbach, Germany) in an effector-cell:target-cell (E:T) ratio of 1:5. Afterwards, plate-bound IFN-γ was detected as

previously described (Hundemer et al., 2006). ELISPOT experiment was considered functional if at least 10 dots were detected and if the mean of the MART-$1_{aa26\text{-}35*A27L}$ wells showed more dots than the control peptide wells.

2.9. Preparation of Human Macrophages and Phagocytosis Assay

The laboratory of Dr. Heiko Bruns in the University Hospital Erlangen has performed the macrophages and phagocytosis assays.

Adapted from Awwad et al. (Awwad et al., 2021) and the written protocols from the laboratory of Dr. Bruns: After isolating the MNCs by density gradient centrifugation, monocytes were isolated from the PB of HDs by adherence on plastic plates and cultured in the presence of M-CSF (50 ng/ml, R&D, Wiesbaden, Germany) to generate macrophages, which were detached with EDTA (1 mM, Sigma) after 6 days of culture. For immunofluorescence, macrophages were stained with a green fluorescent dye (CellTracker Green, Thermo Fisher) according to the manufacturer's recommended protocol and plated in 8-chamber slides (Nalgene Nunc International). For flow cytometry, macrophages were stained with an anti-CD11b antibody (M1/70.15.11.5, Miltenyi Biotec), washed with PBS and incubated in capped, sterile FACS tubes (BD Biosciences). Isolated T cells were labeled with CPD (Cell Proliferation Dye eFluor® 670, Thermo Fisher) according to the manufacturer's recommended protocol. Next, macrophages were coincubated for 2 h with CPD-labeled T cells (E:T=1:1, 37°C) in the absence or presence of elotuzumab (10 µg/ml) or an irrelevant IgG1 antibody (isotype control). The cells were then washed, fixed with paraformaldehyde (4%), mounted with VECTASHIELD Mounting Medium with 4',6-diamidino-2-phenylindole (DAPI) and analyzed by z-stack sections creating up to 10 optical slices (0.5 µm thick each) using a confocal microscope (LSM700, Zeiss) at 630X magnification.

2.10. NSG Mouse Model

The laboratory of Dr. Hakim Echchannaoui, University Medical Center (Umc) of the Johannes Gutenberg University, has performed the mouse model experiments.

Adapted from Awwad et al. (Awwad et al., 2021) and the written protocols from the laboratory of Dr. Echchannaoui: NOD.Cg-Prkdc^{scid}IL2rg^{tm1Wjl}/SzJ (NSG) 8 weeks-old mice were injected subcutaneously (s.c.) with 2x10^6 NCI-H929 myeloma cells in the right flank. T cells were isolated from PB of HD and were retrovirally transduced with a TCR for a novel HLA-A2.1-restricted myeloma associated antigen. 5x10^6 TCR positive T cells highly expressing SLAMF7 were adoptively transferred intravenously (i.v.) 7 days later. All mice received an additional intraperitoneal (i.p.) injection of 7.2x10^5 international unit (IU) human recombinant IL-2 on the day of T cell transfer to trigger T cell expansion. Mice were further divided into two groups that received either elotuzumab (200 µg per mouse, i.p.) or PBS on days 3, 10, and 14 after T cell transfer. Mice were sacrificed when the tumors reached 1 cm^3 and TILs were isolated as described (Echchannaoui et al., 2018). Briefly, freshly isolated tumor cells (from sacrificed animals) were dissociated by mincing the tissue with scalpels into 0.5-mm small pieces. Dissociated tissue was further triturated and filtered through a 100-mm cell strainer to obtain single-cell suspension. Cell suspension was then analyzed by flow cytometry to determine the frequency of the specific T cell populations. Animal experiments were performed according to approved protocol from the local animal welfare authorities of Rheinland-Pfalz (protocol AZ 23 177-07/G16-1-016).

2.11. CRISPR-Cas9 SLAMF7 Knockout

Adapted from Awwad et al. (Awwad et al., 2021): To analyze the functional role of SLAMF7 expression in CD8$^+$ T cells, permanent genome editing of healthy human CD8$^+$ T cells, pre-enriched using MACS sorting, was achieved by the CRISPR-Cas9 RNP and synthetic guide RNA (sgRNA) electroporation approach using Cas9-GFP from Sigma-Aldrich (Steinheim, Germany). Cells were first activated using Human CD3/CD28/CD2 T Cell Activator and cultured in ImmunoCult™-XF T Cell Expansion Medium (both from STEMCELL Technologies, Köln, Germany). After 2 days, the cells were electroporated with Cas9-GFP preincubated with either sgRNA targeting SLAMF7 (crRNA sequence: 5’ AAA GAG CUG GUC GGU UCC GU 3’) or Scrambled sgRNA (crRNA sequence: 5’ GUA UUA CUG AUA UUG GUG GG 3’) using the Invitrogen Neon Transfection System (Thermo Fisher, Germany). The

electroporation parameters were adjusted, by testing different conditions, to 1400 V, pulse length of 30 ms and 1 pulse. Cells were then directly cultured in pre-warmed ImmunoCult™-XF T Cell Expansion Medium for 2 h. Afterwards, the medium was changed, and the cells were cultured for 2 more days. Knockdown efficiency was then assessed using flow cytometry analysis.

2.12. SLAMF7 Isoform PCR

Adapted from Awwad et al. (Awwad et al., 2021): RNA was isolated from dry cell pellets using TRIzol method as previously described (Rio et al., 2010). cDNA was then synthesized from RNA using a High-capacity cDNA Reverse Transcription Kit (Thermo Fisher) according to the manufacturer´s instructions. In order to amplify SLAMF7, the following primers have been used: forward 5`GTG ACC AAT CTG ACA TGC TGC 3´ and reverse 5´CTG CTC ACG ATG CCA GAC AC 3´. PCR was performed using AmpliTaq Gold DNA polymerase (Thermo Fisher) with 0.2 µM of each primer and 0.2 mM of each dNTP. The PCR program was as follows: initial denaturation at 95°C for 5 min, followed by 40 cycles of denaturation (95°C, 30 s), annealing (64°C, 1 min), and elongation (72°C, 1 min), with a final elongation step at 72°C for 5 min.

2.13. RNA Sequencing

Adapted from Awwad et al. (Awwad et al., 2021): $CD8^+$ T cells were isolated from MNCs of patients or HDs using a $CD8^+$ T Cell Isolation Kit (Miltenyi Biotec, Bergisch Gladbach, Germany) according to the manufacturer's protocol. The cells were sorted using Flow Activated Cell Sorter (FACS) according to a standard protocol into the $SLAMF7^+$ and $SLAMF7^-CD8^+$ T cell populations. RNA was isolated using an RNeasy Mini Kit (Qiagen, Hilden, Germany) according to the manufacturer's protocol. RNA-Seq libraries were prepared and sequenced in the Genomics and Proteomics Core Facility, German Cancer Research Center, Heidelberg, Germany. Libraries were prepared using an Illumina RNA-Seq preparation Kit and sequenced on a HiSeq 4000 with paired-end 100-bp sequencing, yielding 200 million reads per lane after passing quality control (QC) analyses.

2.14. Statistical and RNA Sequencing Analyses

Statistical analysis has been performed by me and then revised and controlled by Axel Benner from the Division of Biostatistics, German Cancer Research Center (DKFZ). The RNA sequencing analysis has been performed by Abdelrahman Mahmoud from the Division of Applied Bioinformatics, German Cancer Research Center.

Adapted from Awwad et al. (Awwad et al., 2021): The impact of elotuzumab treatment on T cells expressing SLAMF7 in patients enrolled in GMMG-HD6 clinical trial was evaluated by analyzing paired patient samples before and after induction therapy by Wilcoxon's signed rank test using the R computing environment (version 3.6.1). Other comparisons between different patient groups were performed by t-tests using GraphPad (version 8.0) software. A result was considered significant at $p < 0.05$ with $*$, $**$, and $***$ representing $p < 0.05$, $p < 0.01$, and $p < 0.001$ in graphical displays, respectively.

Adapted from Awwad et al. (Awwad et al., 2021): For RNA sequencing, RNA-paired FastQ files were aligned using STAR aligner (Version 2.5.3a)(Dobin et al., 2013) to the reference genome (1KGRef_PhiX), which was generated from the 1000 Genomes assembly and gencode 19 gene models. Sambamba (version 0.6.5)(Tarasov et al., 2015) was used to perform merging and duplicate marking of BAM files. Additionally, SAMtools software (version 1.6)(Li et al., 2009) was used to perform a quality control (QC) analysis using the SAMtools flagstat command and RNA-SeQC software (version 1.1.8)(DeLuca et al., 2012). The featurecounts(Liao et al., 2014) implementation in the R/Bioconductor package subread (version 1.5.1) was used to perform gene-specific read counting over exon features based on the gencode 19 gene models. Both reads of a paired fragment were used for counting, and the quality threshold was set to 255. The gene expression data were then derived after preprocessing unnormalized read counts of all six samples (SLAMF7 positive and SLAMF7 negative) through several statistical learning methods in the R computing environment. Prefiltering was performed to include only nonzero reads per gene for the downstream analysis. The R/Bioconductor package DESeq2 (version 1.22.1)(Love et al., 2014) was used to perform a differential expression analysis between SLAMF7-positive and SLAMF7-negative replicates by Wald tests within

negative binomial generalized linear models. The procedure of Benjamini–Hochberg (BH) was then applied to calculate adjusted p-values to control the false discovery rate at 0.05. To determine relevant effects, we used LFCs with a threshold of 2, and performed a shrinkage of effect size analysis (LFC estimates) using the R/Bioconductor package apeglm (version 1.4.2)(Zhu et al., 2018) to approximate the posterior estimation for GLM to reduce variance for the genes with low information for statistical inference. DE Genes software was then used to perform a functional analysis (FA), and GSEA was performed using the R/Bioconductor package clusterProfiler (version 3.10.1)(Yu et al., 2012) and the MSigDB Collections database (C2: curated gene sets of canonical pathways)(Liberzon et al., 2015).

2.15. Cytokine Profile Screening for Supernatants

The cytokine profile screening assay has been performed by Sciomics GmbH, Heidelberg, after I provided them with cell culture supernatants.

Adapted from Awwad et al. (Awwad et al., 2021) and from the written protocols provided by Sciomics GmbH: The samples were concentrated by filtration and purified by size exclusion chromatography. The bulk protein concentration was determined by BCA assay. The samples were then labelled at an adjusted protein concentration for two hours with scioDye 1 and scioDye 2. After two hours the reaction was stopped, and the buffer was exchanged to PBS. All labelled protein samples were stored at -20° C until use. The samples were analysed in a dual-colour approach using a reference-based design on 10 scioCD antibody microarrays (Sciomics, Germany) targeting different CD surface markers and cytokines/chemokines. Each antibody is represented on the array in four replicates. The arrays were blocked with scioBlock (Sciomics, Germany) on a Hybstation 4800 (Tecan, Austria) and afterwards the samples were incubated competitively using a dual-colour approach. After incubation for three hours, the slides were thoroughly washed with 1x PBSTT, rinsed with 0.1x PBS as well as with water and subsequently dried with nitrogen. Slide scanning was conducted using a Powerscanner (Tecan, Austria) with identical instrument laser power and constant PMT settings. Spot segmentation was performed with GenePix Pro 6.0 (Molecular Devices, Union City, CA, USA). Acquired raw data

were analysed using the linear models for microarray data (LIMMA) package of R-Bioconductor after uploading the median signal intensities. For normalisation, a specialised invariant Lowess method was applied. For analysis of the samples a one-factorial linear model was fitted with LIMMA resulting in a two-sided t-test or F-test based on moderated statistics. All presented p values were adjusted for multiple testing by controlling the false discovery rate according to Benjamini and Hochberg. Proteins were defined as differential for [LogFC] > 0.5 and an adjusted *p* value < 0.05.

Differences in protein abundance between different samples or sample groups are presented as log-fold changes (logFC) calculated for the basis 2.

3. Results

3.1. Global Characterization of SLAMF7 expression on T cells

3.1.1. SLAMF7 Expression on T cells in Myeloma Patients

As SLAMF7 has been described to be expressed on myeloma cells, NK cells, macrophages and T cells (Boles et al., 2001; Boles and Mathew, 2001; Hsi et al., 2008), I sought to investigate the phenotype and frequency of T cells expressing SLAMF7. Therefore, I analysed BM samples from patients newly diagnosed with MM from our GMMG-HD6 clinical trial for the expression of SLAMF7 using flow cytometry. First, I gated on singlet cells to avoid including doublets using a dot plot of forward scatter (FSC)-A vs FSC-H. Then, I gated lymphocytes using a dot plot of side scatter (SSC) vs CD45 expression, with lymphocytes being considered CD45 positive and SSC low. After plotting only lymphocytes on a dot plot of CD3 vs CD8 expression, I gated on either $CD8^+$ T cells or $CD4^+$ T cells (Figure 4A). I then analysed whether the $CD8^+$ T cells and $CD4^+$ T cells expressed SLAMF7 using a histogram. The results showed that SLAMF7 was expressed at high levels on the surface of $CD8^+$ T cells; however, $CD4^+$ T cells expressed less SLAMF7 than $CD8^+$ cells ($p<0.0001$, Figure 4B).

Thus, I concluded that SLAMF7 is expressed at substantial levels on the surface of $CD8^+$ T cells in the BM of patients newly diagnosed with MM. I then sought to determine whether the expression of SLAMF7 is correlated with or affected by tumour micromovement features, so I measured SLAMF7 expression on T cells in 5 BM and 5 peripheral blood (PB) samples from identical patients, i.e., the BM and PB samples were derived from the same patient. Interestingly, I observed no significant difference, and SLAMF7 expression was similar between the PB and BM samples (Figure 5C).

I then sought to determine the consistency of SLAMF7 expression on $CD8^+$ T cells among different patients. As such, I together with the help of my colleagues Michael Benn, Larissa Schönhoff, Lena Richards, and Mandy Medenhoff analysed 263 PB samples from patients newly diagnosed with MM using flow cytometry as previously described. The average abundance of SLAMF7-expressing $CD8^+$ T cells was 48.29%, with the lowest percentage being 0.4% and the highest being 94.2%, and half of the patients showed an abundance

between 31.4% and 66.4% (Figure 5D). Taken together, these results led me to conclude that SLAMF7 is an important molecule that has high expression on a specific population of T cells.

3.1.2. Immunological Profiling of SLAMF7-expressing $CD8^+$ T cells in Myeloma Patients

Adapted from my written and experimental contribution to (Awwad et al., 2021):

Having confirmed that SLAMF7 is highly expressed on the surface of $CD8^+$ T cells and not $CD4^+$ T cells, I further focused my experiments on analysing SLAMF7 expression in the $CD8^+$ T cell compartment. I then sought to determine whether SLAMF7 expression could influence or was at least associated with a specific phenotype of $CD8^+$ T cells. Thus, I performed in-depth flow cytometry analyses of 9 BM samples obtained from patients newly diagnosed with MM. In the flow cytometry analyses, I included antibodies to detect CD45, CD4, CD8, CD3, CD45RA and CD62L. I then acquired the measurements and calculated the percentages of $SLAMF7^+$ and $SLAMF7^-$ T cells in each state, i.e., $CD8^+$ effector cells were considered $CD62L^-$ $CD45RA^+$; $CD8^+$ naïve cells were considered $CD62L^+$ $CD45RA^+$; $CD8^+$ central memory cells were considered $CD62L^+$ $CD45RA^-$; and $CD8^+$ effector memory cells were considered $CD62L^-$ $CD45RA^-$ (Figure 5A). I found no significant difference between $SLAMF7^+$ and $SLAMF7^-$ $CD8^+$ T cells; however, $SLAMF7^+$ $CD8^+$ T cells exhibited fewer cells in the central memory state and more cells in the effector memory state than $SLAMF7^-$ $CD8^+$ T cells, although the difference was not significant (Figure 5B, C, & D).

Previous studies have shown that a subset of $CD8^+$ T cells can exert an immunosuppressive effect on other effector $CD8^+$ T cells in the MM microenvironment. These cells are characterized by the expression of CD8 and CD57, and they lack CD28 expression (hereafter called $CD8^+$ regulatory T (Treg) cells). It was also shown that the cells achieve such immunosuppression without the need for cell-cell contact and rather do so via soluble factors (Filaci et al., 2004). Only cells with this phenotype isolated from tumour microenvironment showed such immune inhibitory capability, while no effect was seen if such cells were isolated from healthy donors (HDs) (Filaci et al., 2007). Our group was able to show previously that the immunosuppressive activity of $CD8^+$ Treg cells isolated

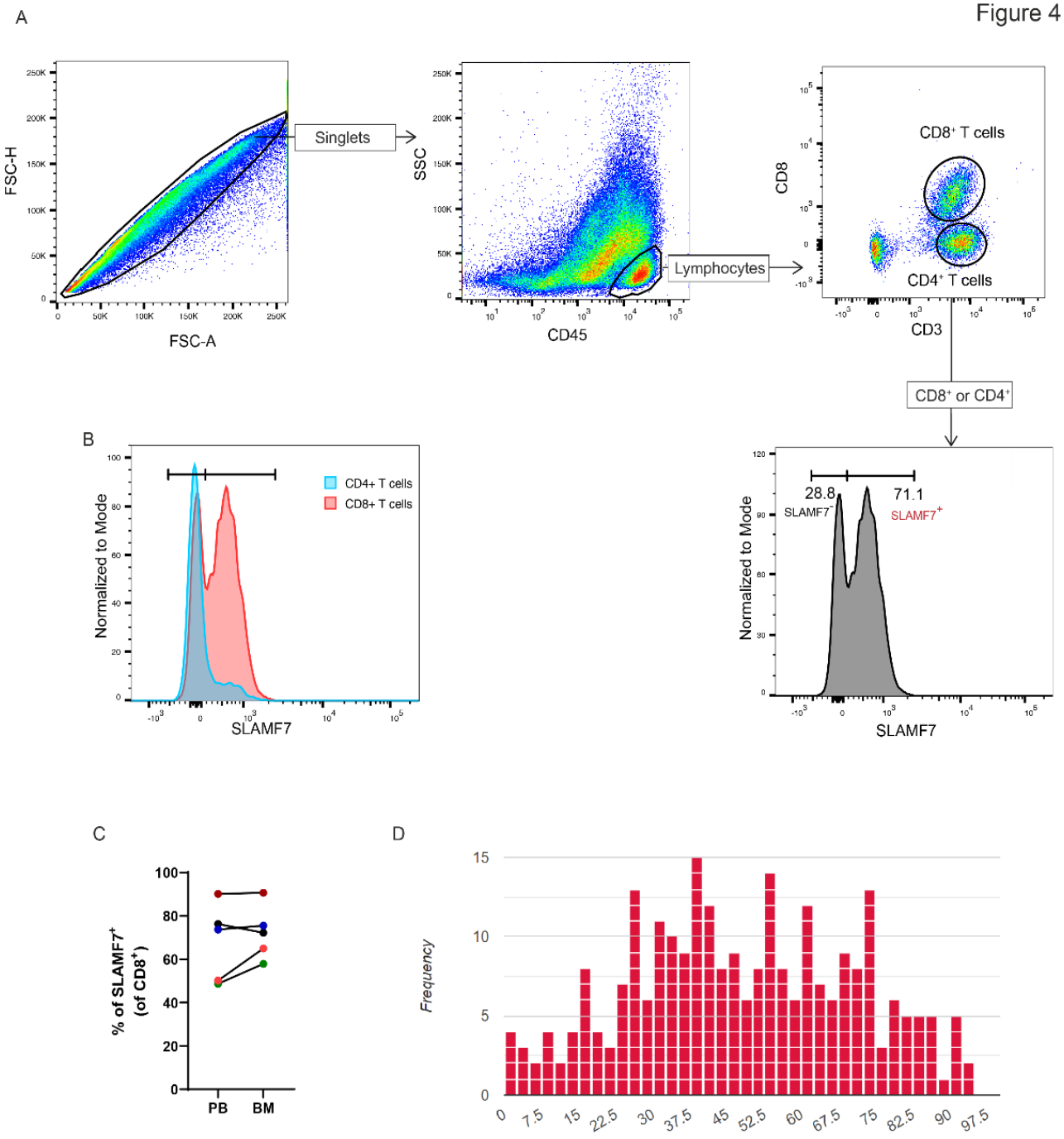

Figure 4. SLAMF7 expression on T cells in myeloma patients:

(A) Representative flow cytometry plots showing the gating strategy for SLAMF7-positive/negative cells. **(B)** Histogram showing the difference in SLAMF7 expression between $CD8^+$ and $CD4^+$ T cells. **(C)** Scatter plot showing SLAMF7 expression on $CD8^+$ T cells from PB and BM; each colour represents one patient (n=5). **(D)** Histogram showing the distribution of SLAMF7-expressing $CD8^+$ T cells in the PB of patients with newly diagnosed MM (n=263).

from HDs could be induced by culturing the cells in the presence of interleukin (IL)-10 (Filaci et al., 2004; Plaumann et al., 2018). Therefore, I decided to assess the expression of SLAMF7 on those $CD8^+$ Treg cells from the BM of MM patients. To explore this, I assessed 6 BM samples from patients newly diagnosed with MM using flow cytometry. Strikingly, I found that SLAMF7 was highly expressed on the surface of $CD8^+$ Treg cells in comparison to other $CD8^+$ T cells ($p<0.0001$, Figure 5E), a finding that highlighted SLAMF7 as a potential further marker for suppressive T cells.

As I previously highlighted in sections 1.1.3.2 & 1.2.1, T cell exhaustion is a critical process in the immunological response, and throughout the last decades, many exhaustion markers have been identified. Therefore, I assessed the expression of PD-1, CTLA-4, TIGIT, TIM-3, and LAG-3 in BM samples from patients newly diagnosed with MM. By comparing exhaustion marker expression between $SLAMF7^+$ $CD8^+$ T cells and $SLAMF7^-$ $CD8^+$ T cells, I found that PD-1, TIGIT, and LAG-3 were significantly highly expressed on the surface of $SLAMF7^+$ $CD8^+$ T cells ($p=0.0003$, $p=0.0002$, & $p=0.02$, respectively). CTLA-4 also showed a trend of higher expression on $SLAMF7^+$ $CD8^+$ T cells that was not significant ($p=0.24$), but TIM-3 did not ($p=0.79$) (Figure 5F, G, & H).

3.1.3. Transcriptomic Analyses of $SLAMF7^+$ and $SLAMF7^-$ $CD8^+$ T cells from MM Patients

Adapted from my written and experimental contribution to (Awwad et al., 2021):

When confirming the consistent expression of SLAMF7 on the surface of $CD8^+$ T cells and its high expression on the surface of exhausted T cells and Treg cells using flow cytometry, I could not detect more than 6 different proteins simultaneously with SLAMF7 on $CD8^+$ T cells due to fluorochrome limitations. However, I realized that with an RNA sequencing approach, I would be able to detect and quantify the expression of most genes and would be able to delineate the phenotype in deeper analyses. Therefore, I decided to collaborate with Abdelrahman Mahmoud from the Division of Applied Bioinformatics in the German Cancer Research Center to perform an RNA sequencing experiment. I sorted $CD8^+$ T cells from the PB of 3 different patients newly diagnosed with MM into $SLAMF7^+$ $CD8^+$ T cells and $SLAMF7^-$ $CD8^+$ T cells using FACS. I then isolated the total RNA from the cells and submitted the samples to the Genomics

Figure 5

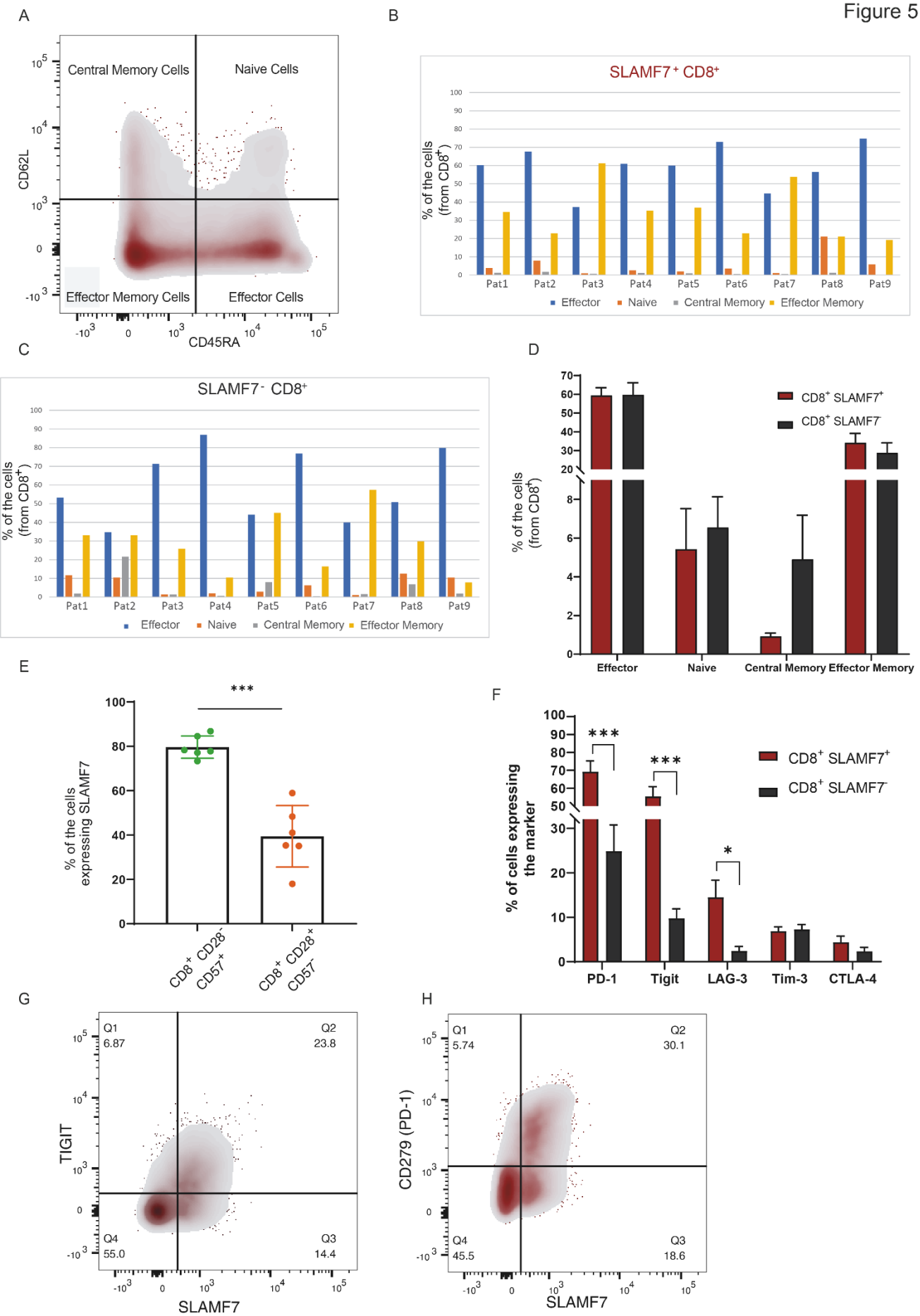
A
Central Memory Cells
Naive Cells
Effector Memory Cells
Effector Cells
CD62L
CD45RA
B
SLAMF7+ CD8+
% of the cells (from CD8+)
Pat1 Pat2 Pat3 Pat4 Pat5 Pat6 Pat7 Pat8 Pat9
Effector Naive Central Memory Effector Memory
C
SLAMF7- CD8+
% of the cells (from CD8+)
Pat1 Pat2 Pat3 Pat4 Pat5 Pat6 Pat7 Pat8 Pat9
Effector Naive Central Memory Effector Memory
D
% of the cells (from CD8+)
CD8+ SLAMF7+
CD8+ SLAMF7-
Effector Naive Central Memory Effector Memory
E
***
% of the cells expressing SLAMF7
CD8+ CD28- CD57+
CD8+ CD28+ CD57-
F
% of cells expressing the marker
CD8+ SLAMF7+
CD8+ SLAMF7-
***
***
*
PD-1 Tigit LAG-3 Tim-3 CTLA-4
G
Q1 6.87
Q2 23.8
Q4 55.0
Q3 14.4
TIGIT
SLAMF7
H
Q1 5.74
Q2 30.1
Q4 45.5
Q3 18.6
CD279 (PD-1)
SLAMF7

Figure 5. Immunological profiling of SLAMF7-expressing CD8+ T cells in myeloma patients (adapted from my written and experimental contribution to (Awwad et al., 2021)):

(A) Representative flow cytometry plot showing how different $CD8^+$ T cells phenotypes were identified using CD45RA and CD62L markers: $CD8^+$ effector: $CD62L^-$ $CD45RA^+$; $CD8^+$ naïve: $CD62L^+$ $CD45RA^+$; $CD8^+$ central memory: $CD62L^+$ $CD45RA^-$; and $CD8^+$ effector memory: $CD62L^-$ $CD45RA^-$). **(B&C)** Bar graph showing how each $CD8^+$ T cell phenotype contributed to the total $CD8^+$ $SLAMF7^+$ (B) and $CD8^+$ $SLAMF7^-$ **(C)** populations in 9 different BM samples from newly diagnosed MM patients. **(D)** Bar graph summarizing the mean percentages of $SLAMF7^+$ and $SLAMF7^-$ T cells in each phenotype from 9 BM samples from patients newly diagnosed with MM. **(E)** The percentages of SLAMF7-expressing cells in $CD8^+$ $CD28^+$ $CD57^-$ (right) and $CD8^+$ $CD28^-$ $CD57^+$ (left) cells from BM samples from patients newly diagnosed with MM (n=6). **(F)** Bar graph showing a comparison of the abundances of $SLAMF7^+$ and $SLAMF7^-$ $CD8^+$ T cells expressing exhaustion markers; samples were taken from the BM of patients newly diagnosed with MM (for PD-1: n=6; for other markers: n=4). **(G&H)** Density flow cytometry plots showing a direct correlation between SLAMF7 expression in $CD8^+$ T cells and TIGIT (left) and PD-1 (right) expression.

Differences between groups were evaluated using Student's t-test; $*p < 0.05$, $**p < 0.01$, and $***p < 0.001$. Bar plots show the mean value with the standard deviation.

and Proteomics Core Facility at the German Cancer Research Center, where they prepared sequencing libraries and performed quality control and sequencing. Afterwards, Abdelrahman Mahmoud performed downstream analyses of the RNA FastQ data and performed differential gene expression analyses as described in section 2.14.

I, in collaboration with Abdelrahman Mahmoud, identified 1,662 genes that we considered significantly upregulated or downregulated in $SLAMF7^+$ $CD8^+$ T cells based on the following threshold: the $\log_2$ fold-change (LFC) must have been more than 2 ([LFC] >2), and the Benjamini and Hochberg (BH)-adjusted p value must have been less than 0.05 (p-value <0.05) (Figure 6A; a full list of differentially expressed genes between $SLAMF7^+$ and $SLAMF7^-$ T cells can be found in the appendices). Consistent with the flow cytometry findings, I found that upregulation of many differentially expressed genes related to exhaustion markers, including LAG3, TNFRSF1B, CD244 (2B4) and TIM-3, in $SLAMF7^+$ $CD8^+$ T cells. I then assessed the PD-1 and TIGIT RNA levels, as they were found to be highly upregulated in $SLAMF7^+$ $CD8^+$ T cells in my flow cytometry analyses, and I could not confirm consistent upregulation in all samples; some samples showed high expression of these markers in $SLAMF7^+$ $CD8^+$ T cells, while others did not show a similar pattern (Figure 6B).

I then determined whether genes identifying $CD8^+$ Treg cells were also upregulated, as I observed in the flow cytometry analysis. All genes encoding $CD8^+$ Treg cell markers, i.e., LFA-1, GZMB, CD57, and PRF1, were significantly upregulated in $SLAMF7^+$ $CD8^+$ T cells, while CD28 was downregulated, showing an identical phenotypic signature to $CD8^+$ Treg cells (Figure 6C).

In collaboration with Abdelrahman Mahmoud, I decided to perform a global transcriptomic overview. As such, we generated and analysed the expression of transcription factors that have been described to play a role in the exhaustion of $CD8^+$ T cells (Martinez et al., 2015). The analysis showed that IKAROS family zinc-finger 2 (IKZF2), early growth response 2 (EGR2), and zinc-finger E-box binding homeobox 2 (ZEB2) were significantly upregulated in $SLAMF7^+$ $CD8^+$ T cells in comparison to $SLAMF7^-$ $CD8^+$ T cells. Moreover, TOX and interferon regulatory factor 4 (IRF4) showed a trend of higher expression in $SLAMF7^+$ $CD8^+$ T cells (Figure 7A).

In collaboration with Abdelrahman Mahmoud, I performed gene set enrichment analysis (GSEA) to explore the global transcriptomic differences between $SLAMF7^+$ and $SLAMF7^-$ cells using pre-described datasets (Subramanian et al., 2005). The analysis showed that the gene set "*positive regulation of interleukin-6 production*" was upregulated in $SLAMF7^+$ $CD8^+$ T cells (p=0.001, Figure 7B). This result indicates that the upstream IL-6 pathway is upregulated in $SLAMF7^+$ $CD8^+$ T cells. IL-6 is an important cytokine that is upregulated in the BM of MM patients, and it functions as both a growth factor and survival factor for myeloma cells (Gadó et al., 2000; Matthes et al., 2016). Furthermore, the "*reactome immunoregulatory interactions between a lymphoid and a nonlymphoid cell*" gene set was upregulated in SLAMF7+ CD8+ T cells (p=0.001, Figure 7C); this set includes genes that suppress the immune response of T cells to self-antigens and tumour antigens.

Taken together, the results of these transcriptomic analyses confirmed the high expression of exhaustion markers and $CD8^+$ Treg cell markers in $SLAMF7^+$ $CD8^+$ T cells. The analyses also showed that exhaustion-related transcription factors and pathways for IL-6 production were upregulated in $SLAMF7^+$ $CD8^+$ T cells. I concluded, therefore, that $SLAMF7^+$ $CD8^+$ T cells should also function as suppressors of $CD8^+$ effector T cells in the MM microenvironment, as has been previously described for the $CD8^+$ Treg cell population that shares an identical phenotype. The upregulation of the IL-6 gene set also supports the immunosuppression notion, as a colleague has shown before that lenalidomide inhibits IL-6 production and that the lenalidomide-induced immunomodulatory effect can be counteracted by the addition of IL-6 (Neuber et al., 2017).

Figure 6

A

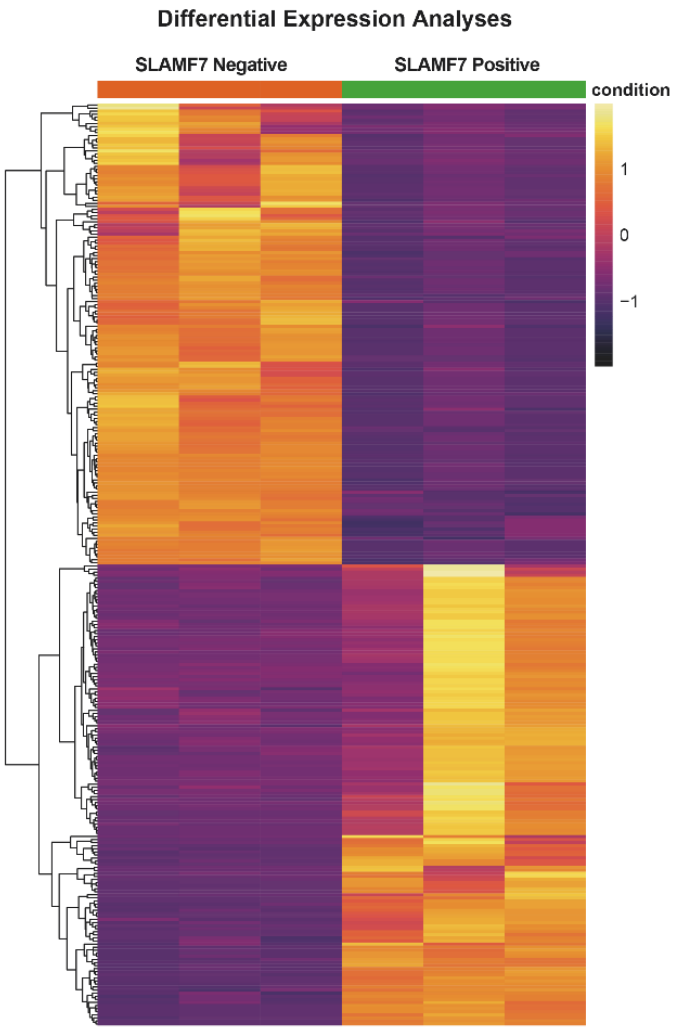
Differential Expression Analyses
SLAMF7 Negative
SLAMF7 Positive
condition
1
0
−1

B

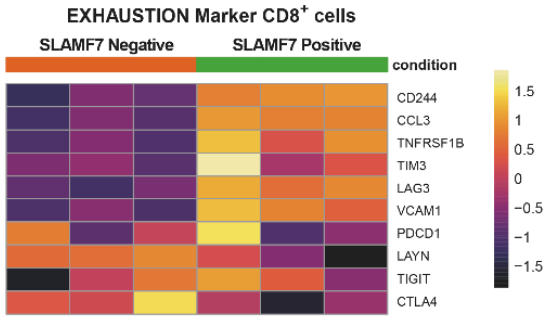
EXHAUSTION Marker CD8+ cells
SLAMF7 Negative
SLAMF7 Positive
condition
CD244
CCL3
TNFRSF1B
TIM3
LAG3
VCAM1
PDCD1
LAYN
TIGIT
CTLA4
1.5
1
0.5
0
−0.5
−1
−1.5

C

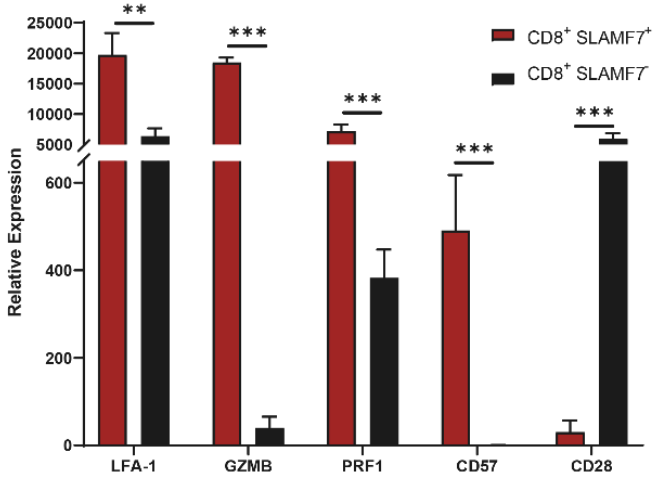
CD8+ SLAMF7+
CD8+ SLAMF7−
Relative Expression
25000
20000
15000
10000
5000
600
400
200
0
**
***
***
***
***
LFA-1
GZMB
PRF1
CD57
CD28

Figure 6. Transcriptomic analyses of SLAMF7^{+}CD8^{+} and SLAMF7^{-}CD8^{+} T cells (adapted from my written and experimental contribution to (Awwad et al., 2021)):

(A) Heatmap showing the top 300 upregulated and downregulated genes in SLAMF7^{+}CD8^{+} T cells in comparison to SLAMF7^{-}CD8^{+} T cells from PB of 3 patients newly diagnosed with MM. **(B)** Heatmap for the relative RNA expression of exhaustion-related surface markers in SLAMF7^{+}CD8^{+} T cells and SLAMF7^{-}CD8^{+} T cells (n=3). **(C)** Barplot showing the relative expression of Treg cell markers on the surface of SLAMF7^{+}CD8^{+} T cells and SLAMF7^{-}CD8^{+} T cells (n=3).

Differences in gene expression levels were tested by Wald tests within negative binomial generalized linear models. BH analysis was then applied to calculate the adjusted p-values to control the false discovery rate at 0.05. To determine relevant effects, we used LFCs with a threshold of 2. The bar plots show the mean value with the standard deviation.

Figure 7

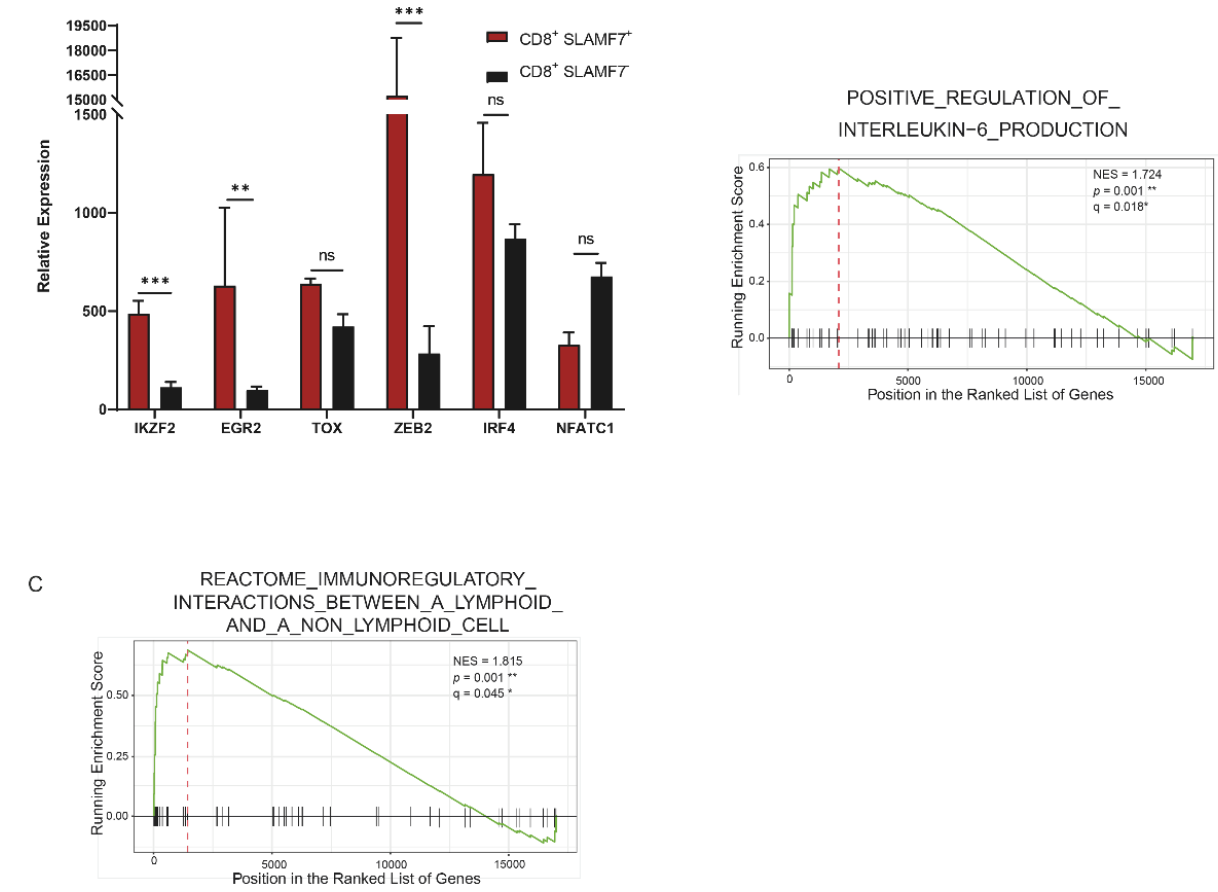

Figure 7. Transcriptomic analyses of exhaustion markers and GSEA of SLAMF7^{+}CD8^{+} and SLAMF7^{-}CD8^{+} T cells (the figures were adapted from my written and experimental contribution to (Awwad et al., 2021)):

(A) Barplot showing the relative expression of exhaustion-related transcription factors in SLAMF7^{+}CD8^{+} and SLAMF7^{-}CD8^{+} T cells (n=3). **(B)** GSEA plots showing the upregulation of "positive regulation of interleukin-6 production" in SLAMF7^{+}CD8^{+} T cells. **(C)** GSEA plots showing the upregulation of "reactome immunoregulatory interactions between a lymphoid and a nonlymphoid cell" in SLAMF7^{+}CD8^{+} T cells.

Differences in gene expression levels were tested by Wald tests within negative binomial generalized linear models. BH analysis was then applied to calculate the adjusted p-values to control the false discovery rate at 0.05. To determine relevant effects, we used LFCs with a threshold of 2. The bar plots show the mean value with the standard deviation.

3.2. Functional Analyses of CD8$^+$ SLAMF7$^+$ T cells

3.2.1. Antigen-specific T Cell Response Assessment and Cytokine Screening

Adapted from my written and experimental contribution to (Awwad et al., 2021):

To determine the effect of the abundance of SLAMF7$^+$ CD8$^+$ T cells on the antigen-specific T cell response, I used the myeloma antigen MART-1$_{aa26–35*A27L}$ ELISPOT model developed by our laboratory (Hundemer et al., 2006). In this experiment, I isolated MNCs from the PB of 7 different HDs, captured immature DCs via adhesion on plastic plates, enhanced their proliferation and transition into mature DCs and loaded them with MART-1$_{aa26–35*A27L}$ peptide as described in section 2.7. Afterward, I co-cultured pre-loaded DCs with autologous PB mononuclear cells that contained T cells to expand MART-1$_{aa26–35*A27L}$-specific T cells. During the expansion phase, I sorted SLAMF7$^+$ CD8$^+$ T cells from the BM of patients newly diagnosed with MM and added them to the co-culture with a transwell insert that allows the exchange of cytokines and proteins only without cell-cell contact, thus avoiding allograft rejection. Control co-cultures with cells from identical donors were also setup without SLAMF7$^+$ CD8$^+$ T cells from patients. After 5 days of incubation, I enriched CD8$^+$ T cells with magnetic beads and quantified their ability to kill T2 target cells with the MART-1$_{aa26–35*A27L}$ peptide in their HLA-A2 surface receptor on a pre-coated ELISPOT plate (Figure 8A).

The results showed that the addition of SLAMF7$^+$ CD8$^+$ T cells from MM patients was able to significantly suppress the expansion of antigen-specific CD8$^+$ T cells and eventually even suppress their cytotoxic activity against target cells (p=0.038, Figure 8B). The suppression capacity of SLAMF7$^+$ CD8$^+$ T cells from MM patients without cell-cell contact inspired me to explore the supernatants of the co-cultures that contained SLAMF7$^+$ CD8$^+$ T cells and compare them to the control co-culture supernatants. Therefore, I collaborated with Sciomics GmbH in Heidelberg, which is a company specialized in performing quantitative cytokine screening assays using antibody microarray chips to capture different surface markers and cytokines. I submitted the supernatants from the previous experiment, and Sciomics GmbH performed the assay as described in section 2.15. Of note, the assay captures 351 different proteins.

The results were analysed by me and visualized in figures by my colleague George Steinbuss. I found that IL-6 and IL-8 were upregulated in the supernatant of SLAMF7$^+$ CD8$^+$ T cells. IL-6, as indicated in section 3.1.3, is a vital factor for the survival of myeloma cells, and my RNA sequencing data showed that the IL-6 upregulation gene set was upregulated in SLAMF7$^+$ CD8$^+$ T cells. IL-8 was also previously described as a vital cytokine for the proliferation of myeloma cells (Herrero et al., 2016). Interestingly, I found that IL-2 and IL-5 were upregulated in the control samples, indicating a more activated state of T cells in those wells. C-X-C motif chemokine 5 (CXCL5), a chemokine that has been described to enhance the frequency of CD4$^+$ Treg cells (Shi et al., 2014), was also upregulated in the SLAMF7$^+$ CD8$^+$ T cell supernatants (Figure 8C and D; a full list of the measured proteins is available in the appendices).

Taken together, my data show that IL-6, IL-8 and CXCL5 are potential effector molecules supporting the SLAMF7$^+$ CD8$^+$ T cell suppression capacity. Therefore, I sought to determine whether the number of these cells in patients is directly correlated with T cell cytotoxicity.

3.2.2. Effect of CD8$^+$ SLAMF7$^+$ T Cell Abundance in Myeloma Patients on the T Cell Response

Adapted from my written and experimental contribution to (Awwad et al., 2021):

I then performed a new set of experiments to evaluate whether the abundance of SLAMF7$^+$ CD8$^+$ T cells in the PB of newly diagnosed MM can be reflected in their antigen-specific T cell response. I used the same MART-1$_{aa26–35*A27L}$ ELISPOT model but without any further variables. Thus, PB samples from 45 newly diagnosed MM patients were used to generate mature peptide-loaded DCs that were then used to expand MART-1$_{aa26–35*A27L}$-specific T cells. I measured the ability of those cells to lyse target T2 cells with the ELISPOT approach. As the abundances of SLAMF7$^+$ CD8$^+$ T cells were already measured in the previous experiments (see section 3.1.1), I divided the patients into SLAMF7$_{high}$ patients, i.e., patients with SLAMF7$^+$ CD8$^+$ T cell abundances higher than or equal to the median SLAMF7$^+$ CD8$^+$ T cell frequency of all patients, and

Figure 8

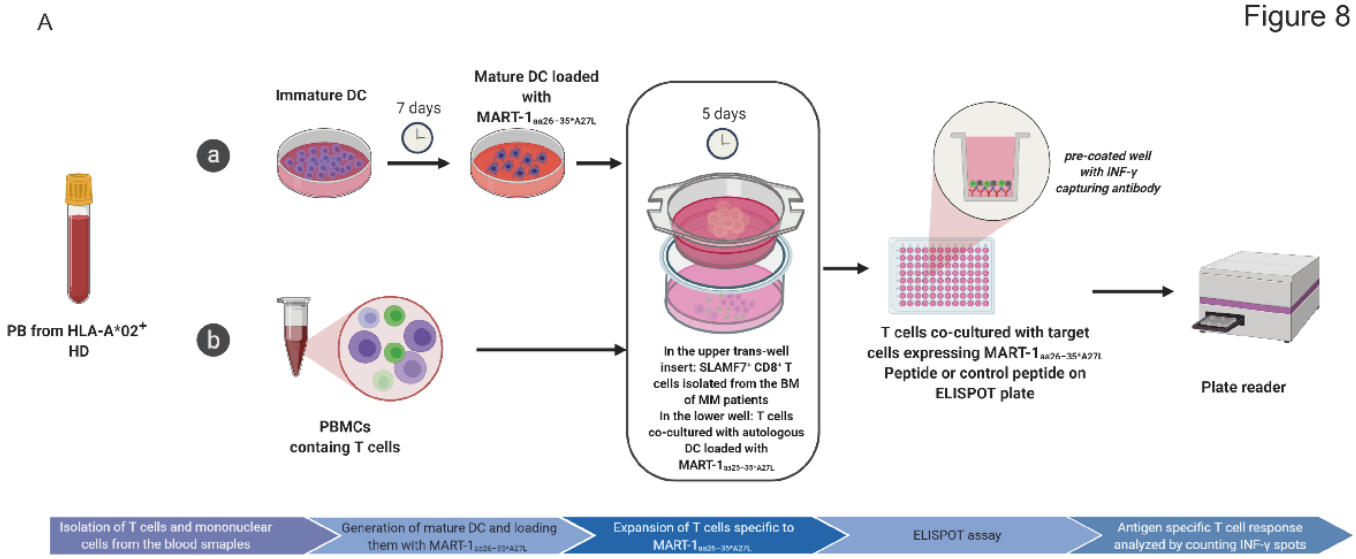
A
Immature DC
7 days
Mature DC loaded with MART-1aa26−35*A27L
a
b
PB from HLA-A*02+ HD
PBMCs containg T cells
5 days
In the upper trans-well insert: SLAMF7+ CD8+ T cells isolated from the BM of MM patients
In the lower well: T cells co-cultured with autologous DC loaded with MART-1aa26−35*A27L
pre-coated well with INF-γ capturing antibody
T cells co-cultured with target cells expressing MART-1aa26−35*A27L Peptide or control peptide on ELISPOT plate
Plate reader
Isolation of T cells and mononuclear cells from the blood smaples
Generation of mature DC and loading them with MART-1aa26−35*A27L
Expansion of T cells specific to MART-1aa26−35*A27L
ELISPOT assay
Antigen specific T cell response analyzed by counting INF-γ spots

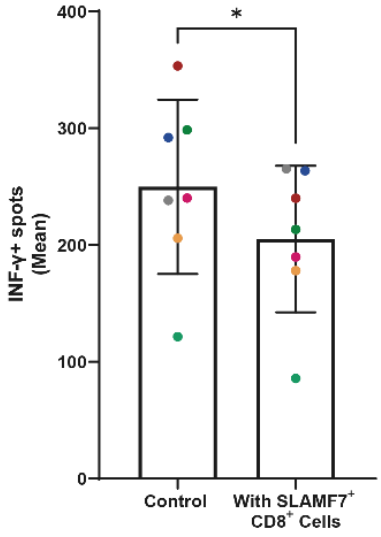
B
INF-γ+ spots (Mean)
400
300
200
100
0
*
Control
With SLAMF7+ CD8+ Cells

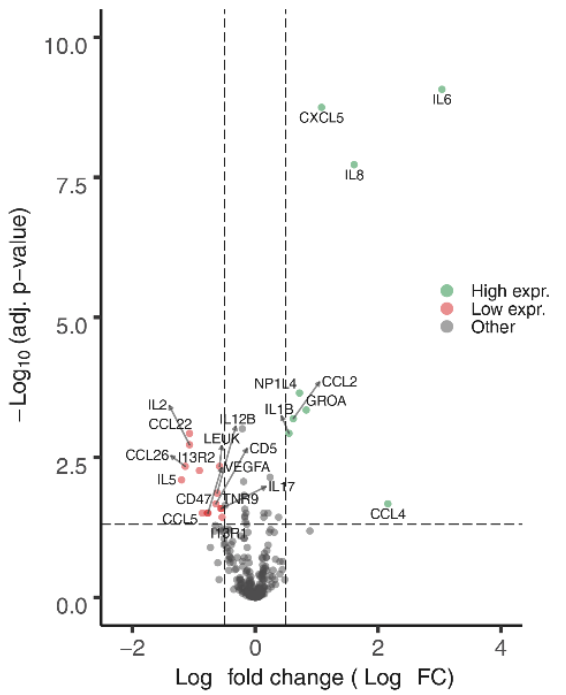
C
10.0
7.5
5.0
2.5
0.0
−Log10 (adj. p−value)
−2
0
2
4
Log fold change (Log FC)
High expr.
Low expr.
Other
IL6
CXCL5
IL8
NP1L4
CCL2
GROA
IL1B
IL2
CCL22
IL12B
LEUK
CD5
CCL26
I13R2
VEGFA
IL5
IL17
CD47
TNR9
CCL5
I13R1
CCL4

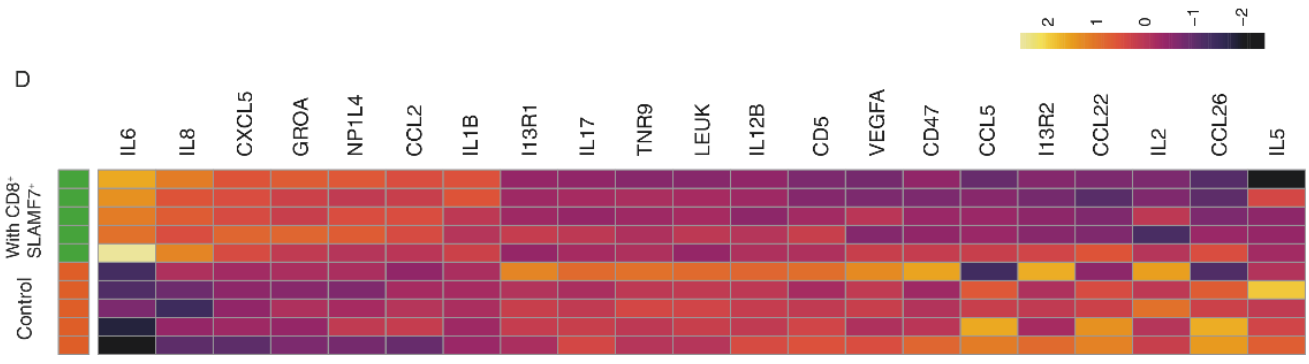
D
2
1
0
−1
−2
IL6
IL8
CXCL5
GROA
NP1L4
CCL2
IL1B
I13R1
IL17
TNR9
LEUK
IL12B
CD5
VEGFA
CD47
CCL5
I13R2
CCL22
IL2
CCL26
IL5
With CD8+ SLAMF7+
Control

Figure 8. Antigen-specific T cell response assessment and cytokine screening (adapted from my written and experimental contribution to (Awwad et al., 2021)):

(A) Schematic diagram explaining the steps for using MART-$1_{aa26-35*A27L}$-specific T cells to test the antigen-specific T cell response with or without SLAMF7^{+}CD8^{+} T cells. **(B)** Scatter plot with bars showing the effect of adding CD8^{+} SLAMF7^{+} T cells from the BM of patients newly diagnosed with MM during the expansion of HD antigen-specific T cells (p=0.038, n=7). **(C)** Volcano plot showing the differentially expressed proteins in the supernatants of T cell cultures from (B), Green dots represent proteins differentially upregulated in the CD8^{+} SLAMF7^{+} T cell-containing cell cultures, and red dots represent proteins differentially upregulated in the control cell cultures (n=5). **(D)** Heatmap showing the top differentially expressed proteins.

Differences between groups were compared using the Mann-Whitney test; $*p < 0.05$, $**p < 0.01$, and $***p < 0.001$.

The bar plots show the mean value with the standard deviation.

SLAMF7$_{low}$ patients, i.e., patients with SLAMF7^{+} CD8^{+} T cell abundances lower than the median SLAMF7^{+} CD8^{+} T cell frequency of all patients. By comparing the number of IFN-γ dots (representing the killing efficiency of T cells), patients in the SLAMF7low group showed significantly more dots than those in the SLAMF7high group, highlighting a stronger antigen-specific T cell response in patients with a low SLAMF7+ CD8+ T cell abundance (p=0.01, Figure 9).

Figure 9

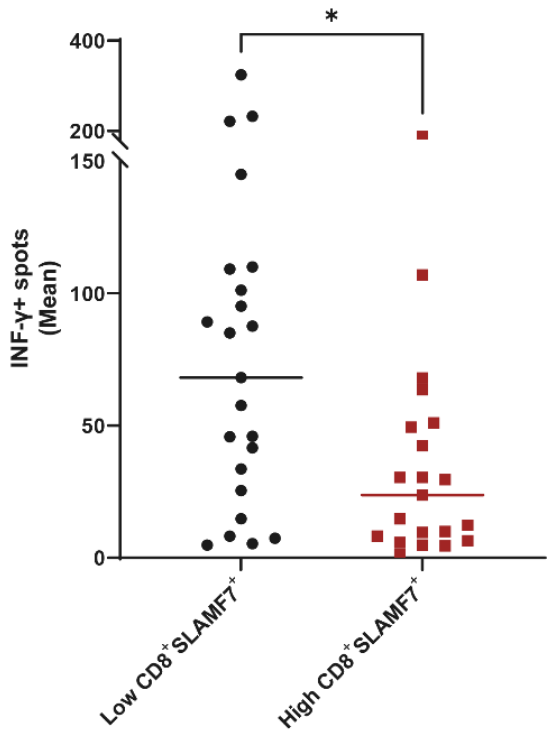

Figure 9. Effect of CD8^{+} SLAMF7^{+} T cell abundance in myeloma patients on the antigen-specific T cell response and cytokines (adapted from my written and experimental contribution to (Awwad et al., 2021)):

Scatter plots showing the effect of CD8^{+} SLAMF7^{+} T cell abundance on the T cell response (each dot represents the mean number of IFN-γ spots of one patient) (p=0.01, n=45).

Differences between groups were compared using the Mann-Whitney test; $*p < 0.05$, $**p < 0.01$, and $***p < 0.001$.

3.2.3. Knock-out Analyses of SLAMF7 Expression in CD8$^+$ T cells

Adapted from my written and experimental contribution to (Awwad et al., 2021):

I then sought to check if SLAMF7 plays a role in the exhaustion of those T cells or whether it is just a marker associated with the cellular phenotype. To test this hypothesis, I established a CRISPR-Cas9 knockout model in T cells (see section 2.11). I validated the knockout using flow cytometry analysis to confirm the decrease in SLAMF7 expression (Figure 10A). Afterward, I incubated the cells for 7 days to allow proper maturation and enhance activation of exhaustion pathways in the cells. Control cells transfected with scrambled gRNA were also cultured under the same conditions. I then used flow cytometry to analyse the expression levels of different maturation markers, including CD28 and CD57, to evaluate the Treg cell phenotype markers CD25, CD27, CD45RA and CD62L to quantify cellular activation and differentiation. I also analysed the expression of different exhaustion surface markers, such as PD-1, LAG-3, and TIGIT, that were upregulated on the surface of SLAMF7$^+$ CD8$^+$ T cells (section 3.1.2). In addition, I performed intranuclear staining to quantify transcription factors that are associated with exhaustion or late differentiation states, such as TOX and T-bet.

The results clearly showed that there was no significant difference between SLAMF7 knockout cells and scramble cells regarding maturation markers or exhaustion markers (Figure 10B & C).

I decided to assess whether SLAMF7 knockout might change cytokine secretion. Thus, I performed another experiment in which I incubated SLAMF7 knockout and control (scrambled) cells for 2 days in serum-free culture medium and then collected the supernatants. I measured the levels of vital cytokines for T cells in the supernatants using ELISA. I analysed the level of IL-2 as an activation cytokine, IFN-γ and granzyme B as cytotoxic effector proteins, and IL-10, as previous work has shown that IL-10 is a vital cytokine for the differentiation of CD8$^+$ Treg cells (Filaci et al., 2007; Plaumann et al., 2018). The results also showed no significant difference between SLAMF7 knockout and scrambled samples (Figure 10D). Overall, those experiments pointed out that SLAMF7 is very unlikely to initiate a specific phenotype in CD8$^+$ T cells; rather, it is likely to be a marker that is upregulated during exhaustion.

Figure 10

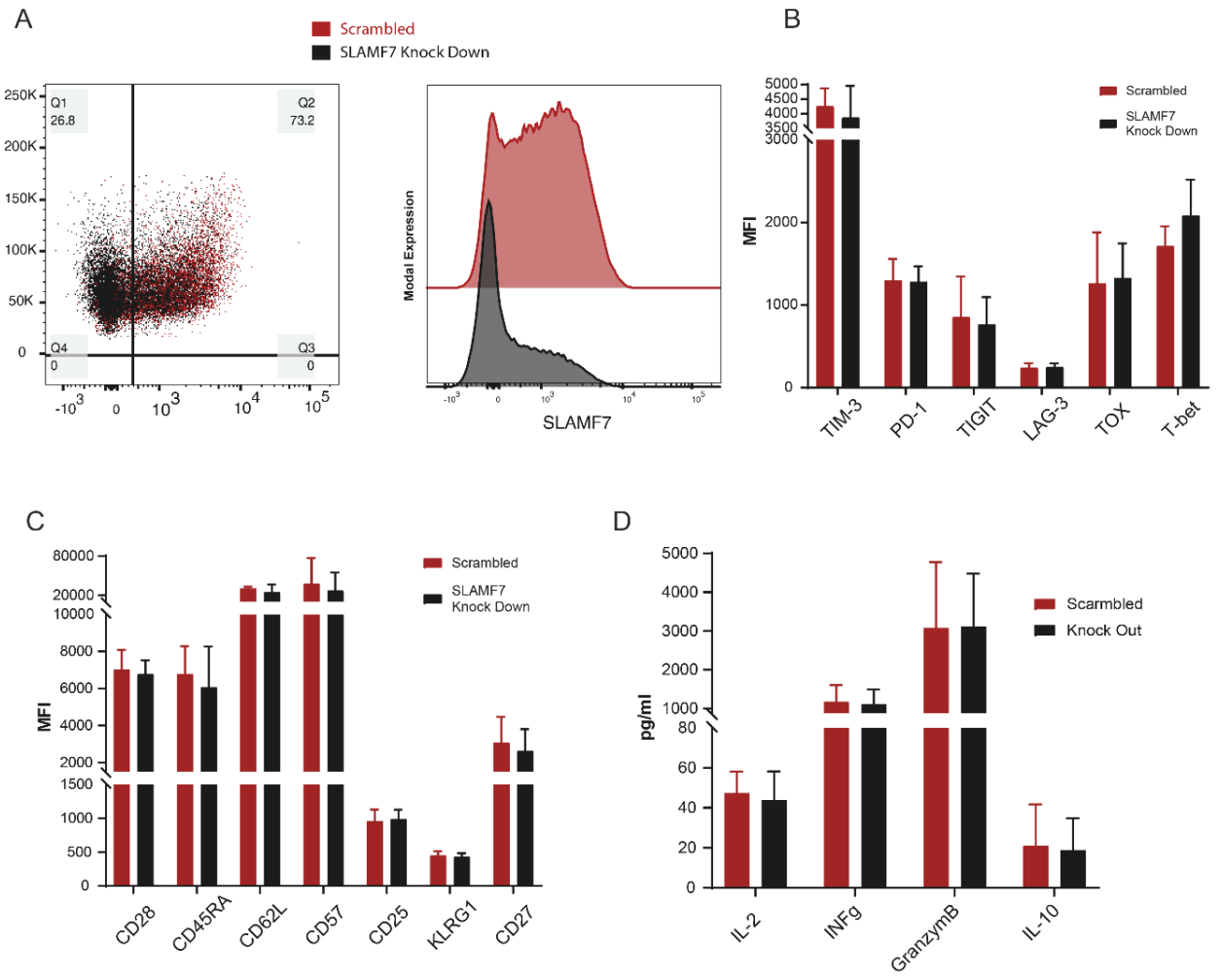

Figure 10. Knock-out analyses of SLAMF7 expression in CD8⁺ (adapted from my written and experimental contribution to (Awwad et al., 2021)):

(A) Dot plot (left) and histogram (right) showing SLAMF7 expression on CD8⁺ T cells in scrambled and knockout cells, **(B)** Bar graph showing the effect of SLAMF7 knockout on the expression of exhaustion markers (n=4). **(C)** Bar graph showing the effect of SLAMF7 knockout on the expression of maturation markers (n=4). **(D)** Bar graph showing the effect of SLAMF7 knockout on the secretion of vital cytokines and immune proteins (n=4).

Differences between groups were evaluated using Student's t-test; ⁎p < 0.05, ⁎⁎p < 0.01, and ⁎⁎⁎p < 0.001. The bar plots show the mean value with the standard deviation.

3.3. Effect of Anti-SLAMF7 Therapy in Myeloma Patients

3.3.1. $CD8^+$ $SLAMF7^+$ T Cell Abundance at Different Time Points During Therapy

Adapted from my written and experimental contribution to (Awwad et al., 2021):

With the previous results in mind, I then decided to explore the effect of elotuzumab on $SLAMF7^+$ $CD8^+$ T cells in patients with MM. GMMG-HD6 clinical trial (NCT02495922), a phase III trial, evaluated the effect of adding elotuzumab to VRD induction/consolidation therapy and lenalidomide maintenance therapy in patients with newly diagnosed MM. The study centres recruited 564 patients, and patients were randomized for induction therapy into two study arms: Study arm A, in which patients received 4 cycles of VRD as induction therapy (21 days per cycle); and study arm B, in which patients received 4 cycles of VRD and elotuzumab (10 mg/kg on days 1, 8 and 15 in induction cycles 1 and 2 and on days 1 and 11 in induction cycles 3 and 4) as induction therapy. I then measured the $SLAMF7^+$ $CD8^+$ T cell abundance in the patients before and after induction therapy with or without elotuzumab. By doing so, I aimed to compare the immunophenotype of patients who received elotuzumab therapy to that of patients who did not receive it. I analysed 265 patients (Table 3); for 140 patients, I obtained a proper measurement for $SLAMF7^+$ expression both before induction therapy (T1) and after induction therapy (T2). The 146 patients included 75 patients from study arm A and 71 patients from study arm B. After the analyses, I cooperated with Axel Benner from the Division of Biostatistics, German Cancer Research Center, and he helped me choose the right statistical method and data visualization figure. Axel Benner also prepared the tables detailing patient characteristics.

I first compared the abundance of $SLAMF7^+$ $CD8^+$ T cells at T1 and T2 in each study arm. Interestingly, I observed a decrease in the abundance of $SLAMF7^+$ $CD8^+$ T cells in both study arms after induction therapy. For study arm A, the decrease was slight, although significant (Figure 11A & B); however, the decrease in study arm B was very strong, with almost the majority of patients dramatically losing the $SLAMF7^+$ $CD8^+$ T cell population (Figure 11C & D). I then compared the abundance of $SLAMF7^+$ $CD8^+$ T cells at T2 between study arm A and study arm B. I found that the abundance at T2 in study arm B was

significantly less than that in study arm A, indicating a direct effect of elotuzumab on those T cells (Figure 11E).

Table 3: Characteristics of patients involved in the assessment of SAMF7-expressing cell abundance (adapted from my written and experimental contribution to (Awwad et al., 2021)):

Characteristics		Study arm A		Study arm B		All	
Age	Median (years; range)	59 (41 -70); 1 missing		59 (33-70)		59 (33 - 70); 1	
		n	(%)	n	(%)	n	(%)
Sex *p = 0.81*	Female	66	47.5	57	45.2	123	46.4
	Male	73	52.5	69	54.8	142	53.6
Heavy chain type *p = 0.66*	IgA	23	16.6	22	17.5	45	17.0
	IgG	90	64.8	79	62.7	169	63.8
	Other (IgM, IgD, IgE)	0	0.0	2	1.6	2	0.8
	None	26	18.7	23	18.2	49	18.5
Light chain type *p = 0.70*	Kappa	91	65.5	79	62.7	170	64.2
	Lambda	48	34.5	47	37.3	95	35.9
ISS[a] *p = 0.52*	I	56	40.3	59	46.8	115	43.4
	II	49	35.2	42	33.3	91	34.3
	III	34	24.5	25	19.8	59	22.3
Cytogenetic risk group[b] *p = 0.88*	0	73	65.2	67	67.0	140	66.0
	1	39	34.8	33	33.0	72	34.0
	missing	27		26		53	

a) ISS, international staging system

b) Cytogenetic high-risk group: the presence of del17p and/or t(4;14) or t(14;16)

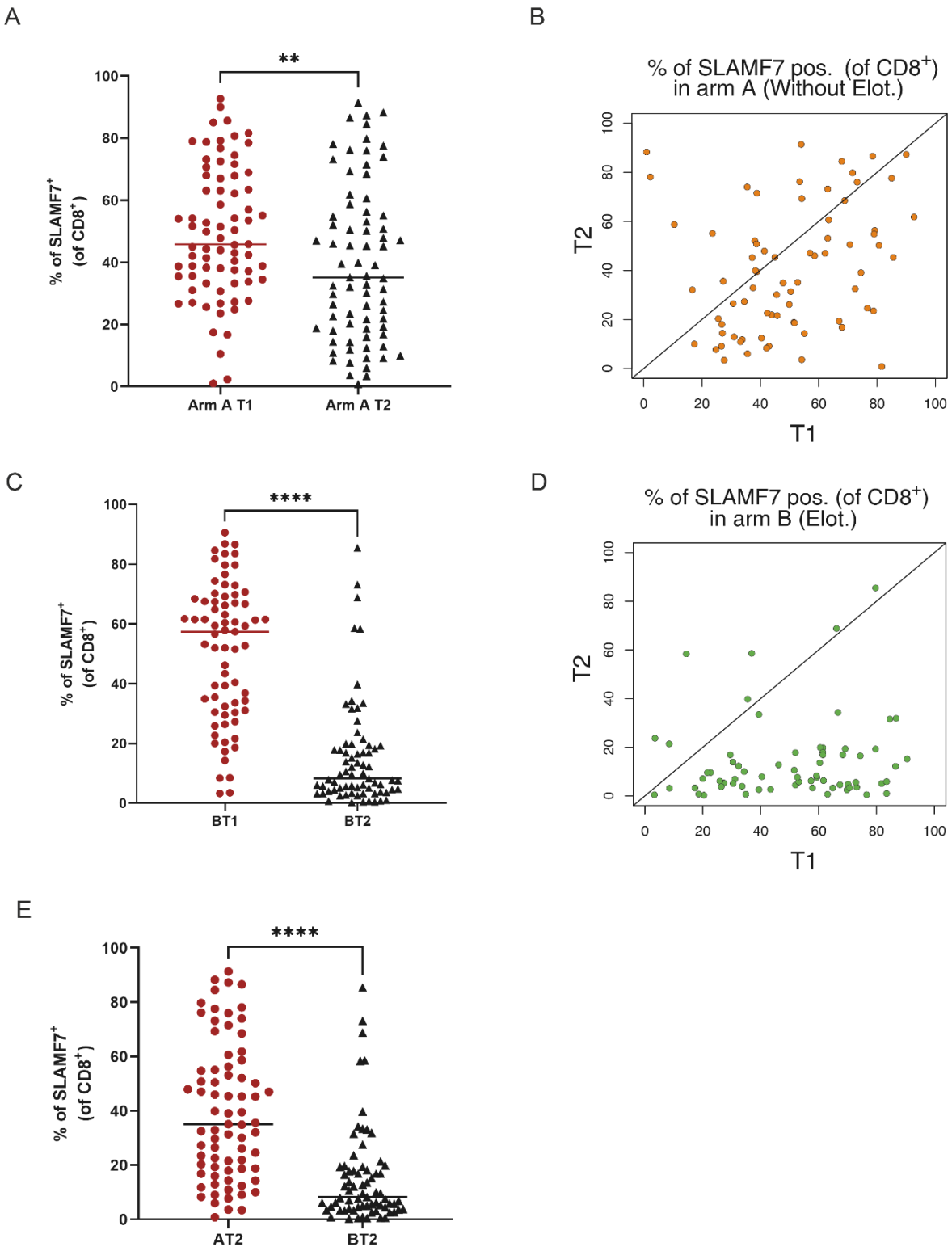

Figure 11. CD8⁺ SLAMF7⁺ T cell abundance at different time points during elotuzumab therapy (adapted from my written and experimental contribution to (Awwad et al., 2021)):

(A&B) Scatter plots showing the effect of induction therapy without elotuzumab on the abundance of SLAMF7⁺ CD8⁺ T cells in arm A (n=75). **(C&D)** Scatter plots showing the effect of induction therapy with elotuzumab on the abundance of SLAMF7⁺ CD8⁺ T cells in arm B (n=71). **(E)** Scatter plot showing the difference between the abundance of SLAMF7⁺ CD8⁺ T cells between patients who received elotuzumab (left, dark red circles) and patients who did not receive elotuzumab (right, black triangles) (n=75 and 71, respectively).

*Differences between groups were evaluated using Student's t-test; *p < 0.05, **p < 0.01, ***p < 0.001, and ****p < 0.0001.*

3.3.2. Comparison to Other SLAMF7-expressing Cells

Adapted from my written and experimental contribution to (Awwad et al., 2021):

To explore whether this decrease in SLAMF7$^+$ CD8$^+$ T cell abundance was caused by cellular depletion or merely a change in the expression of SLAMF7 due to cellular differentiation or receptor internalization, I sought to explore the abundance of CD8$^+$ Treg cells. As described in section 3.1.2, CD8$^+$ Treg cells specifically upregulate SLAMF7 and make up the majority of SLAMF7$^+$ CD8$^+$ T cells. Thus, I analysed the abundance of CD8$^+$ Treg cells at T1 and T2 in both arms A and B, I was able to retrospectively analyse samples from 45 patients. Of them, 22 were in arm A, and 23 were in arm B. I analysed the data together with Axel Benner, and the data showed that there was no significant change in the abundance of CD8$^+$ Treg cells in treated patients within arm A (Figure 12A & B). However, I found a strong significant decrease in the abundance of CD8$^+$ Treg cells in arm B patients who received elotuzumab (Figure 12C & D).

I then decided to assess the effect of elotuzumab therapy on other cells that express SLAMF7 to evaluate whether there is a general depletion mechanism that involves SLAMF7-expressing compartments. Therefore, I analysed the abundance of NK cells in the different study arms at T1 and T2. Again, I was able to perform NK cell analyses for 42 patients retrospectively. Of the patients, 20 were in arm A, and 22 were in arm B. Together with Axel Benner, I analysed the data and found that patients treated in study arm A had no difference in NK cell abundance before and after induction therapy (Figure 12E & F). A decreasing trend in the abundance of NK cells was observed in patients treated within study arm B, although it was not significant (Figure 12G & H).

From these data, I was able to show that elotuzumab targets SLAMF7-expressing CD8$^+$ Treg cells and that their abundance is dramatically decreased after induction therapy containing elotuzumab. A new question was then raised regarding the fate of those cells after elotuzumab therapy. I hypothesized that the SLAMF7-expressing CD8$^+$ T cells might be affected in the following ways:

- Activated by elotuzumab, therefore becoming reactivated and regaining a functional phenotype.
- Depleted by any antibody-dependent mechanism, e.g., ADCC or ADCP.

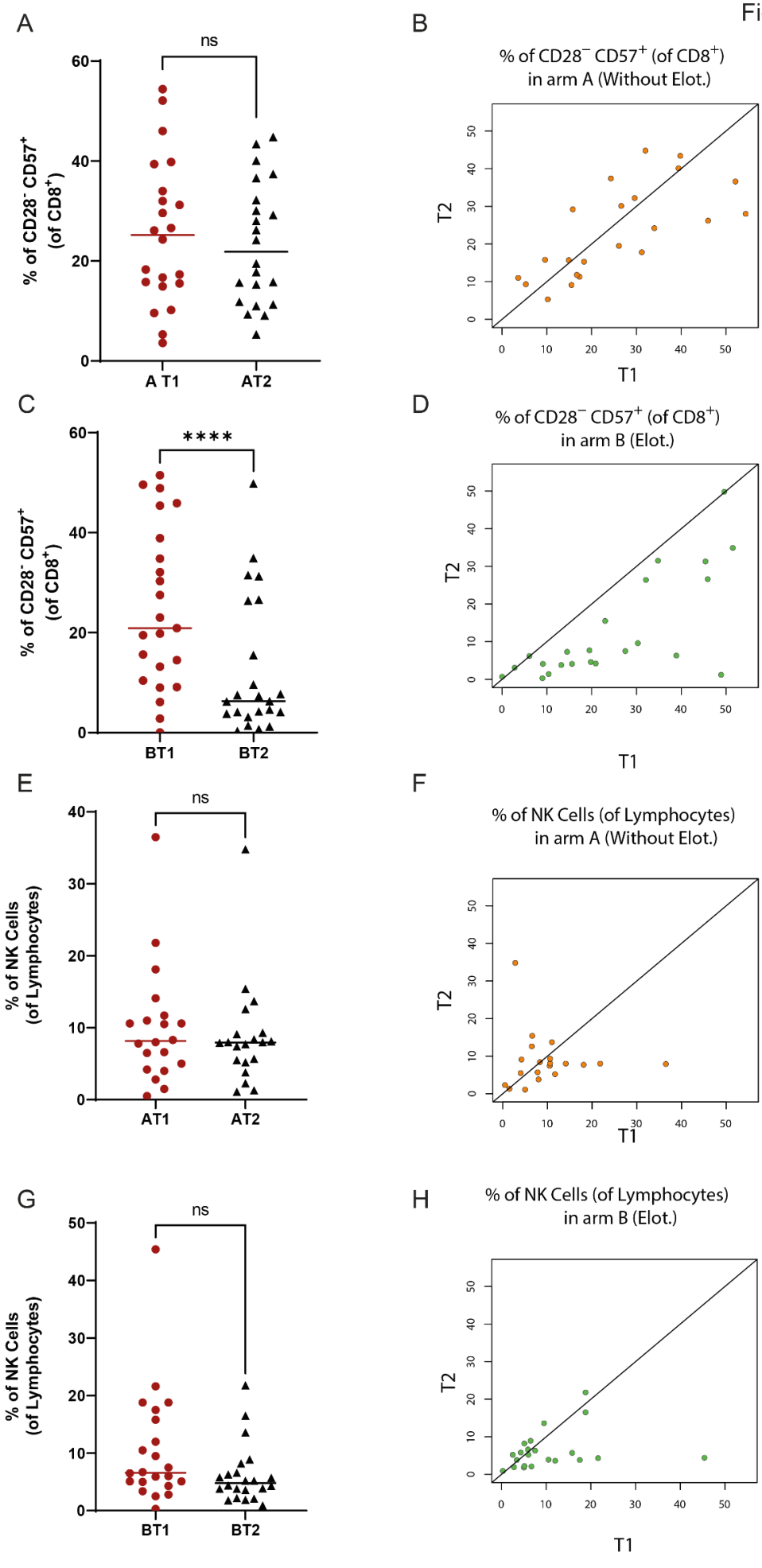
A
ns
% of CD28- CD57+ (of CD8+)
A T1
AT2
B
% of CD28− CD57+ (of CD8+) in arm A (Without Elot.)
T2
T1
C
****
% of CD28- CD57+ (of CD8+)
BT1
BT2
D
% of CD28− CD57+ (of CD8+) in arm B (Elot.)
T2
T1
E
ns
% of NK Cells (of Lymphocytes)
AT1
AT2
F
% of NK Cells (of Lymphocytes) in arm A (Without Elot.)
T2
T1
G
ns
% of NK Cells (of Lymphocytes)
BT1
BT2
H
% of NK Cells (of Lymphocytes) in arm B (Elot.)
T2
T1

Figure 12. $CD8^+$ $SLAMF7^+$ T cell abundance in different SLAMF7-expressing cells (adapted from my written and experimental contribution in (Awwad et al., 2021)):
(A&B) Scatter plots showing the effect of induction therapy without elotuzumab on the abundance of $CD8^+$ Treg cells in arm A (n=22). **(C&D)** Scatter plots showing the effect of induction therapy with elotuzumab on the abundance of $CD8^+$ Treg cells in arm B (n=23). **(E&F**) Scatter plots showing the effect of induction therapy without elotuzumab on the abundance of NK cells in arm A (n=20). **(G&H)** Bar graph (C) and scatter plot (D) showing the effect of induction therapy with elotuzumab on the abundance of NK cells in arm B (n=22).
Differences between groups were evaluated using Student's t-test; $*p < 0.05$, $**p < 0.01$, $***p < 0.001$, and $****p < 0.0001$.

3.3.3. EAT-2 Expression and *In Vitro* Activation Analyses

Adapted from my written and experimental contribution to (Awwad et al., 2021):

In this experiment, I examined the possibility that elotuzumab activates SLAMF7-expressing T cells. I hypothesized that such a mechanism could be achieved by a similar downstream pathway that involves the EAT-2 protein, as described in 1.3.4. Therefore, I decided to assess whether EAT-2 is expressed by $SLAMF7^+$ $CD8^+$ T cells. Therefore, I first checked the RNA sequencing data from section 3.1.3 and compared the relative expression of the SH2D1B gene, which encodes the EAT-2 protein. I also analysed the protein level using intracellular flow cytometry staining analysis. From the RNA sequencing data, I found that while there was almost no detectable gene expression in $CD8^+$ $SLAMF7^-$ T cells, the expression of SH2D1B was detectable in all $SLAMF7^+CD8^+$ samples (Figure 13A). The flow cytometry analysis also confirmed the high expression of EAT-2 protein in $SLAMF7^+$ $CD8^+$ T cells in comparison to $SLAMF7^-CD8^+$ T cells (Figure 13B).

Having confirmed that EAT-2 is expressed in $SLAMF7^+$ $CD8^+$ T cells, I then decided to explore whether elotuzumab can activate SLAMF7-expressing T cells. Therefore, I incubated $CD8^+$ T cells isolated from the BM of 4 different patients newly diagnosed with MM with 100 µg/ml elotuzumab or PBS as a control for 48 h. Afterward, I analysed the secretion of vital cytokines including Granzyme B, INF-γ, IL-2, and perforin using ELISA. The results showed that there was no significant change in the secretion of cytokines except for a slight decrease in IFN-γ in the elotuzumab group, indicating that activation by elotuzumab is very unlikely (Figure 13C).

Figure 13

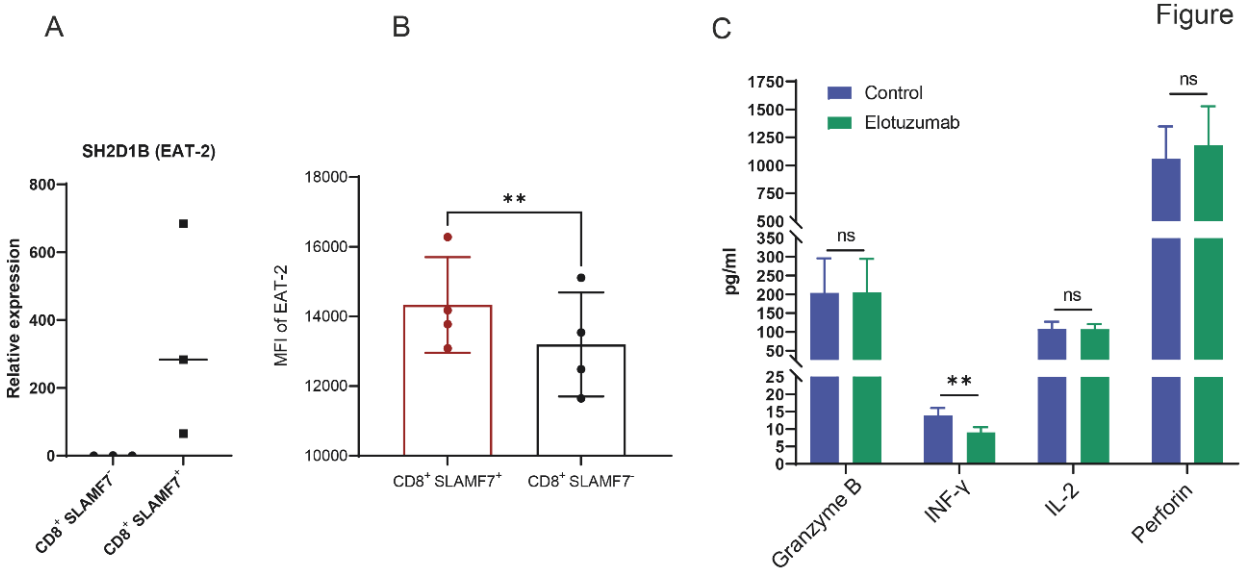

Figure 13. EAT-2 expression and in vitro activation analyses (adapted from my written and experimental contribution to (Awwad et al., 2021)):

(A) Scatter plot showing the effect on the relative RNA expression of the SH2D1B gene (n=3). **(B)** Scatter plot with bars showing the mean fluorescence intensity (MFI) of the EAT-2 protein (n=4) **(C)** Bar plot showing the cytokine secretion levels from $CD8^+$ T cells with or without elotuzumab treatment.

Differences between groups were evaluated using Student's t-test; $*p < 0.05$, $**p < 0.01$, and $***p < 0.001$. The bar plots show the mean value with the standard deviation.

3.4. Deciphering a Novel Mechanism Underlying the Effects of Elotuzumab on T cells

3.4.1. Antibody-dependent Cellular Phagocytosis of SLAMF7$^+$ T Cells Mediated by Elotuzumab

Adapted from my written and experimental contribution to (Awwad et al., 2021):

Based on the previous findings, I realized that elotuzumab leads to the depletion of SLAMF7-expressing T cells; however, I was not able to determine the mechanism by which elotuzumab can achieve this. I hypothesized that SLAMF7$^+$ CD8$^+$ T cells might be eliminated by an ADCP process. Therefore, I cooperated with Dr. Heiko Bruns at the University Hospital Erlangen to test potential phagocytosis. I sorted the T cells from different donors into SLAMF7+/- CD8$^+$ T cells. I also prepared frozen vials with live PBMCs from the same donors. Then, I shipped the sorted cells and PBMCs to Dr. Bruns to perform the phagocytosis assay. Dr. Bruns co-incubated macrophages generated from HDs with sorted autologous SLAMF7$^+$ or SLAMF7$^-$ T cells, which were pre-labelled with cell proliferation dye (CPD), at an effector:target (E:T) ratio of 1:1 in the presence or absence of elotuzumab (10 µg/ml) or control IgG1 antibody for 24 h. To distinguish between phagocytosed CPD-positive T cells and free T cells, Dr. Bruns counterstained macrophages with an anti-CD11b antibody and analysed them by flow cytometry and confocal microscopy.

Interestingly, by analysing the results, I found that elotuzumab caused strong ADCP of SLAMF7$^+$ T cells but not SLAMF7$^-$ T cells, with no observed effect of the control IgG1 antibody (Figure 14A, B and C). The phagocytosis assays showed that elotuzumab induced ADCP of SLAMF7-expressing CD8$^+$ cells.

To confirm that ADCP is the mechanism by which SLAMF7$^+$ CD8$^+$ T cells are depleted, I sought to test this finding in a mouse model. Therefore, I cooperated with Dr. Hakim Echchannaoui from the University Medical Center of Johannes Gutenberg University. Dr. Echchannaoui and I used an NSG mouse model, as NSG mice lack all T, B and NK cells. Mice were injected subcutaneously with the NCI-H929 myeloma cell line. After 7 days, tumour antigen TCR-redirected human CD8$^+$ T cells were adoptively transferred intravenously, and most of these cells expressed SLAMF7. Mice were subdivided into two groups: the *elotuzumab group* received 200 µg elotuzumab on days 10, 17, and 21, and the

control group received only PBS.As soon as the tumour size reached 1 cm^3, mice were sacrificed, and TILs were isolated from freshly extracted tumours and analysed by flow cytometry (the detailed protocol is provided in section 2.10; Figure 14D).

Dr. Echchannaoui and I then analysed the percentage of TILs and compared elotuzumab to the control group to determine whether elotuzumab induced the phagocytosis of TCR-specific SLAMF7$^+$ CD8$^+$ T cells via murine macrophages. The analyses clearly showed that mice in the Elotuzumab group had significantly fewer TILs, indicating a similar depletion mechanism even in the absence of other effector cells (Figure 14E).

3.4.2. Exploring a Potential Role of Natural Killer Cells in the Depletion of SLAMF7$^+$ CD8$^+$ T Cells

Adapted from my written and experimental contribution to (Awwad et al., 2021):

I then sought to check whether NK cells might also play a role in the depletion of SLAMF7$^+$ CD8$^+$ T cells via ADCC. Although the mouse model that lacked NK cells showed strong depletion, one could argue that NK cells might play a similar role. Therefore, I designed an experiment to explore this theory. I enriched the Treg cell population from CD8$^+$ T cells using MACS. I then enriched NK cells using the MACS approach as well from the same donors. Afterward, I co-cultured SLAMF7-expressing CD8$^+$ T cells with autologous NK cells at varying concentrations of elotuzumab (50, 100 or 200 µg/ml) or control with only PBS. To test ADCC in those cells, I used annexin/PI staining to quantify early apoptosis and cell death and assessed the samples by flow cytometry.

The analysis showed no significant increase in cellular apoptosis in the elotuzumab group (Figure 15A), indicating that NK-dependent ADCC is very unlikely.

With the current data showing the elimination of SLAMF7$^+$ CD8$^+$ T cells due to elotuzumab therapy, I wondered why a strong decrease in NK cells was not observed (section 3.3.2) although they also express the SLAMF7 receptor. In other words, why did elotuzumab selectively eliminate Treg cells and not NK cells?

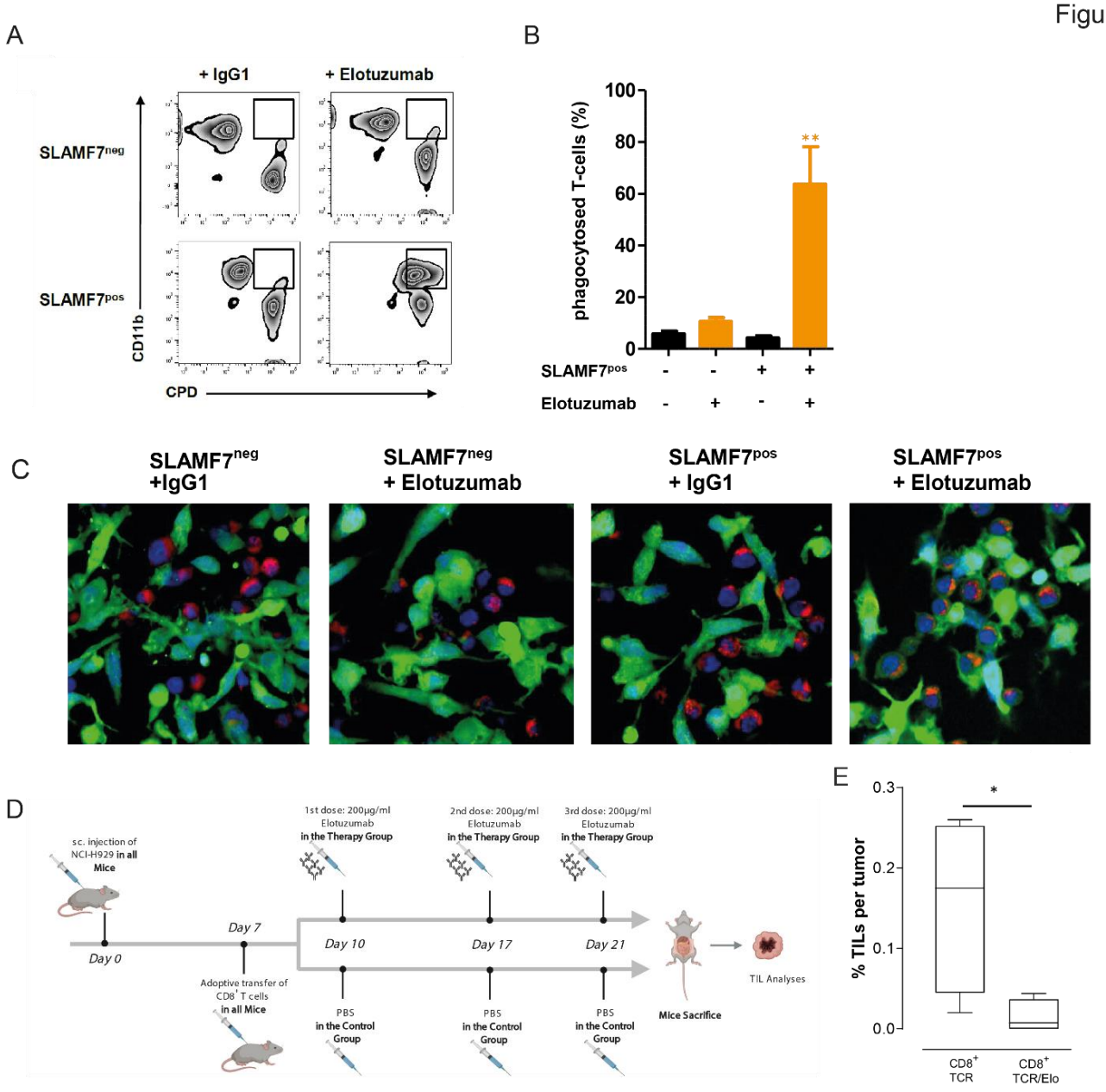

Figure 14. Antibody-dependent cellular phagocytosis of SLAMF7⁺ T cells mediated by elotuzumab (adapted from my written and experimental contribution to (Awwad et al., 2021)):

(A) Macrophages were co-incubated with autologous CPD-labelled T cells (E:T ratio=1:1) in the presence or absence of elotuzumab (10 µg/ml) or control IgG1 antibody for 24 h. To distinguish between phagocytosed CPD-positive T cells and free T cells, macrophages were counterstained with an anti-CD11b antibody and analysed by flow cytometry. **(B)** Bar graph showing the mean percentage of phagocytosed T cells ($CD11b^+$ and CPD^+) from 6 independent experiments. **(C)** CPD-labelled T cells (red) were added to autologous macrophages (stained with CFSE, green) as effectors at an E/T ratio of 1:1 in the presence or absence of elotuzumab or control IgG1 antibody (10 µg/ml). Samples were counterstained with DAPI (blue). After 2 h, phagocytosis was analysed by confocal microscopy at 630X. Scale bar: 10 µm. **(D)** Schematic diagram describing the mouse model experiment. **(E)** Bar graph showing the mean percentage of $CD8^+$ T cells per tumour treated with or without elotuzumab therapy in 4 different mice.

Differences between groups were evaluated using Student's t-test; $*p < 0.05$, $**p < 0.01$, and $***p < 0.001$. Bar plots are showing the mean value with standard deviation.

Therefore, I hypothesized that ADCP should depend on the frequency of cells expressing the marker, so I retrospectively examined the differences in the proportions of $CD8^+$ T cells and NK cells expressing SLAMF7 from previous experiments. Moreover, I assessed the expression level of CD47, which is a phagocytosis-inhibiting ('don't eat me') marker (Kojima et al., 2016; Ridler, 2017), on both $CD8^+$ T cells and NK cells.

Data for the proportion of NK cells expressing SLAMF7 from 42 patients and for the proportion of $CD8^+$ T cells expressing SLAMF7 from 146 patients showed that the frequency of NK cells expressing SLAMF7 was significantly lower than that of $CD8^+$ T cells (Figure 15B). Almost 60% of the patients analysed showed less than 10% SLAMF7-expressing NK cells in the total NK cell compartment, while only 4% of patients analysed showed less than 10% SLAMF7-expressing $CD8^+$ T cells in the $CD8^+$ T cell compartment. Thus, a big difference can be seen in terms of SLAMF7 expression between the two cell types with the NK cells expressing less SLAMF7, so it is reasonable that a partial depletion of these cells might not be very apparent.

By analysing CD47, I found that NK cells strongly express CD47. In comparison to $CD8^+$ T cells, the MFI of CD47 for NK cells was significantly higher, indicating a potential mechanism by which NK cells escape the elotuzumab-induced ADCP by macrophages (Figure 15C).

3.4.3. Correlation of Clinical Outcomes with SLAMF7 Expression

From the above transcriptomic and immunophenotypic data and *in vivo* results, I identified increased expression of exhaustion markers on $SLAMF7^+CD8^+$ cells that were depleted by elotuzumab therapy. Therefore, I next sought to investigate whether SLAMF7 expression on $CD8^+$ cells at the time of diagnosis might have clinical prognostic value or predictive value regarding treatment with elotuzumab. Based on the percentage of $CD8^+$ cells expressing SLAMF7, I divided patients into quartiles, where Q4 represented the highest quartile of patients in terms of SLAMF7 expression on $CD8^+$ cells. I then compared the clinical outcomes from the induction therapy according to response criteria, as previously described (Kumar et al., 2016), between the different groups (Q4 vs Q1-3) of patients in study arm A and patients in study arm B.

Figure 15

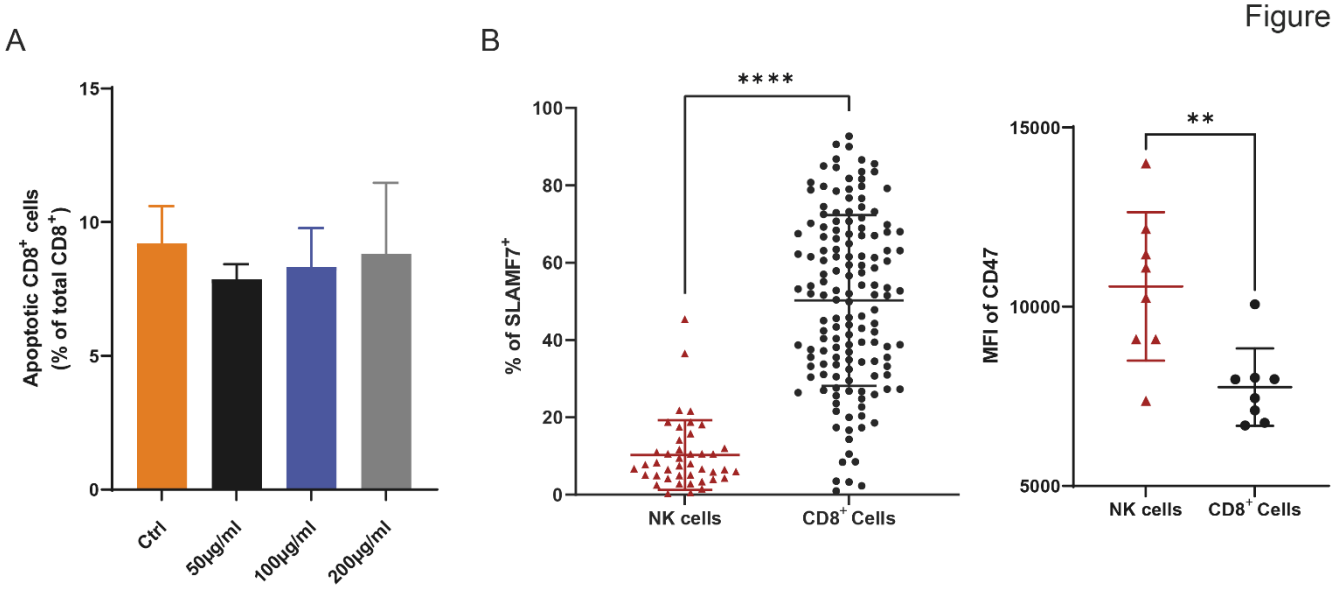

Figure 15. Exploring a potential role of natural killer cells in the depletion of SLAMF7$^+$CD8$^+$ cells (adapted from my written and experimental contribution to (Awwad et al., 2021)):
(A) Bar graph showing the percentage of CD8$^+$ T cells stained positive for annexin or PI (apoptotic or dead cells) in the presence of 0, 50, 100, or 200 µg/ml elotuzumab (n=4). **(B)** Scatter plot showing the percentage of cells expressing SLAMF7 from NK cells (red trianges) or CD8$^+$ T cells (black circles) with each dot representing one patient (for NK cells, n=42, for CD8$^+$ T cells, n=146). **(C)** Scatter plot showing the CD47 MFI of NK cells (red trainges) and CD8$^+$ T cells (black circles) with each dot representing one patient (n=8). *Differences between groups were evaluated using Student's t-test; $*p < 0.05$, $**p < 0.01$, $***p < 0.001$, and $****p < 0.0001$. The bar plots show the mean value with the standard deviation.*

Although the data did not show a significant difference between different groups, I observed a trend for more therapeutic benefit from elotuzumab induction therapy for patients in Q4 (who had a high percentage of SLAMF7$^+$CD8$^+$ cells). While 62.8% of patients in Q4 in study arm A achieved a complete response (CR), near complete response (nCR) or very good partial response (VGPR), 74.2% of patients in Q4 in study arm B achieved a CR, nCR or VGPR after induction therapy, revealing an 11.35% difference. When I compared Q1-3 patients in study arms A and B, the difference was only 6.24%, with 58.65% of patients achieving a CR, nCR or VGPR in study arm A, and 64.89% of patients in study arm B achieving a CR, nCR or VGPR (Figure 16A).

I then checked whether SLAMF7 expression on CD8$^+$ cells correlated with cytogenetic risk groups. Patients with deletion of 17p13 and/or the t(4;14) translocation or gain of 1q21 (>3 copies) were considered to have high risk

(Neben et al., 2012), while the rest were considered to have standard risk. I compared SLAMF7 expression between high- and standard-risk patients and found no significant difference (Figure 16B). I also compared the SLAMF7 expression on $CD8^+$ cells between different myeloma stages (Palumbo et al., 2015) and found no significant difference (Figure 16C).

Taken together, these data suggest that there might be a correlation between SLAMF7 expression levels on $CD8^+$ cells and the benefit of elotuzumab administration during induction therapy that is independent of the risk group or the disease stage.

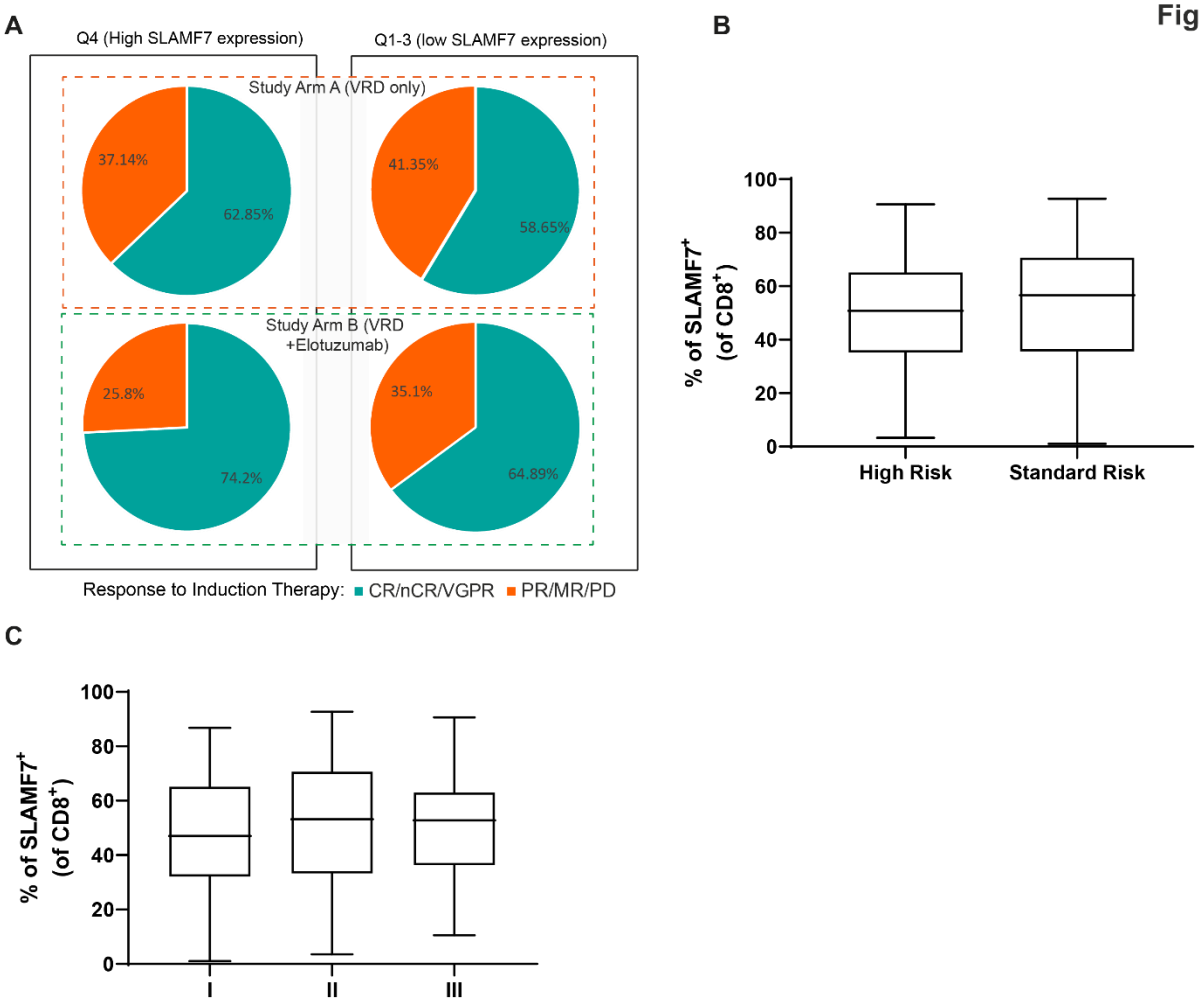

Figure 16. Correlation of clinical outcomes with SLAMF7 expression

(A) 2D pie charts describing the correlation between SLAMF7 expression on $CD8^+$ T cells and response to induction therapy with or without elotuzumab. **(B)** Difference in SLAMF7 expression on $CD8^+$ T cells between patients classified with high-risk and standard-risk myeloma according to cytogenetic aberrations. **(C)** Difference in SLAMF7 expression on $CD8^+$ T cells between patients classified as MM stage I, II or III according to the ISS.

Differences between groups were evaluated using Student's t-test; $*p < 0.05$, $**p < 0.01$, $***p < 0.001$, and $****p < 0.0001$. The bar plots show the mean value with the standard deviation.

4. Discussion

4.1. Characterizing SLAMF7-expressing Cells: Exhausted or Senescent Phenotype?

Cancer immunotherapy is currently one of the most promising treatments for solid and haematological tumours. Patients with melanoma, lung and bladder cancer, and B cell neoplasms, among others, are routinely treated with immunotherapies and have substantial responses compared with those treated with classical therapeutics (Pan et al., 2020). Equally important, the discovery of new immune checkpoints is paving the way for the development of novel immunotherapeutics that should eventually increase both the tumour types and patients eligible for immunotherapy. While current checkpoint inhibitors focus on exhausted T cells, little is known about T cell senescence markers (section 1.1.3.2).

In my work, I focused on the SLAMF7 protein and provided a new understanding of its specific expression patterns. I was able to show that SLAMF7 is highly expressed on the surface of both exhausted and senescent $CD8^+$ T cells. I confirmed this expression pattern by showing a clear correlation of SLAMF7 levels with other described exhaustion and senescence markers, providing a new understanding of SLAMF7 behaviour. I performed transcriptomic analyses to delineate the different signatures of SLAMF7-expressing cells in comparison to SLAMF7 negative T cells and found that have very different transcriptomic state, a finding that highlights the considerable difference between the two cellular phenotypes.

MM, as one of the most common haematological malignancies (Kazandjian, 2016), has been shown to be immunotherapy resistant, with standard PD-1 blockade seeming to induce a weak response (Rosenblatt and Avigan, 2017; Ishida, 2018; Ribrag et al., 2019). One potential reason could be a potential different tumour escape mechanism in MM. Therefore, the identification of new checkpoints for immunosuppression in the MM microenvironment should help overcome these obstacles. My colleagues and other researchers have identified $CD8^+$ $CD28^-$ $CD57^+$ T cells as suppressive $CD8^+$ Treg cells in MM. The level of these cells was associated with the immune response against tumour-specific

antigens and subsequent tumour growth (Filaci et al., 2007; Plaumann et al., 2018). I found that SLAMF7 was highly upregulated on the surface of these cells, a finding that provides evidence that SLAMF7 is a potential immune checkpoint target for MM as well as other tumours that have an increased $CD8^+$ Treg cells. In addition, in another set of analyses to determine the gene sets enriched in $SLAMF7^+$ $CD8^+$ T cells, I found high levels of genes responsible for the upregulation of IL-6. This is a striking finding, as IL-6 is involved in the pathogenesis of MM as well as many other tumours (Matthes et al., 2016; Masjedi et al., 2018; Chonov et al., 2019; Toyoshima et al., 2019).

The upregulation of SLAMF7 on the surface of both exhausted and senescent T cells raises the question of the exact phenotype of SLAMF7-expressing T cells. Exhaustion and senescence are two distinct states that feature different cell behaviours (Akbar and Henson, 2011). In my analyses, RNA sequencing and flow cytometry experiments showed that SLAMF7 was highly upregulated in both states. In particular, the RNA sequencing showed that not all exhaustion markers were upregulated in SLAMF7-expressing T cells, and the same was true for senescence markers; thus, more analyses that use a single-cell sequencing approach could help provide further information.

From another perspective, the identification of senescence-specific immune markers that can be used to target senescent cells is a direction for the development of cancer immunotherapy. Using combined therapy to simultaneously target both cell types might provide a synergistic outcome and counteract tumour evolution during the immunotherapy process.

Of note, the knockout of SLAMF7 in $CD8^+$ T cells did not appear to impact the differentiation or the expression of exhaustion markers. This is a critical finding that indicates that, while being a marker associated with dysfunctional T cells, SLAMF7 does not play a role in programming a unique dysfunctional transcriptional state. One could argue, however, that the incubation time of T cells in this experiment was not long enough to induce an exhaustion phenotype and that the knockout should have been tested in a chronic infection mouse model such as lymphocytic choriomeningitis mammarenavirus-infected mice. (Sandu et al., 2020). Although this is a reasonable argument, I believe that with a sensitive approach such as flow cytometry, one can detect very minor changes

in the abundances of different cell populations; thus, even a small change should have been detectable in my analyses

Specific details in my study should be kept in mind. I focused all my experiments on SLAMF7-expressing T cells from MM patients, and other haematological malignancies and solid tumour microenvironments have not been tested. Although $CD8^+$ Treg cells have been previously described in other tumours (Huff et al., 2019), my findings were not validated in broader tumour models. The main reason for such a limitation was the difficulty of obtaining samples from different departments and institutions and the process of establishing a new ethical approval protocol for human samples, a process that could take years. However, future cooperation with respective research groups that have the ability to perform similar experiments on different tumour models is planned.

4.2. SLAMF7 Expression in Patients and the Tumour-specific T Cell Response

Another strength of this study is the connection between basic cellular research and functional as well as clinical research. This work contributed to the knowledge of the role of $CD8^+$ Treg cells in tumour immunology and the suppression of cytotoxic T cells in patients with MM. The data derived from utilization of SLAMF7-expressing T cells in an antigen-specific tumour model, which provided clear evidence that $SLAMF7^+$ $CD8^+$ T cells can exert immunosuppressive effects on cytotoxic T cells, have underlined the importance of these cells in the tumour microenvironment in MM patients. Moreover, the antigen-specific model in which I tested the suppression capacity of $SLAMF7^+$ $CD8^+$ T cells is a natural model that mimics the biological antigen-specific response to tumour antigens. The model includes generation of mature DCs that are loaded with the MART-$1_{aa26\text{-}35*A27L}$ peptide; of note, T cells specific for this peptide cross react with myeloma cells (Christensen et al., 2009). Such preloaded DCs are then used to train autologous T cells in a similar way to antigen-specific expansion in lymphoid tissues *in vivo*. During the generation of MART-$1_{aa26\text{-}35*A27L}$-specific T cells, $SLAMF7^+$ $CD8^+$ T cells were added to a transwell insert to avoid cell-cell contact. The presence of $SLAMF7^+$ $CD8^+$ T cells during antigen generation helped us identify their role in suppressing both the proliferation and maturation of antigen-specific T cells. The paired comparison

between the same T cells generated in the presence or absence of SLAMF7$^+$ CD8$^+$ T cells provided a very accurate way to evaluate the effect of those cells.

In line with previous evidence about the role of IL-6 in promoting tumour growth and the value of targeting it, cytokine screening in the antigen-specific T cell model confirmed the high level of IL-6 secreted by SLAMF7$^+$ CD8$^+$ T cells. The rationale of targeting IL-6 in MM was proposed as early as 1991, and this strategy has been tested in different clinical trials, but the outcomes have not been very promising (Matthes et al., 2016). The source of IL-6 is debated; some reports have shown that MM cells express IL-6 RNA and protein (Hata et al., 1993; Qi et al., 2015), while others have shown that only the myeloid compartment can produce IL-6 in the BM (Portier et al., 1991). The data I showed from two different experimental sets provide strong evidence that SLAMF7$^+$ CD8$^+$ T cells are a source of IL-6 and that targeting these cells might overcome the need to use IL-6 antagonists. The cytokine screening also provided more information about the activation state of T cells generated in the presence of SLAMF7$^+$ CD8$^+$ T cells, with the generated T cells exhibiting less IL-2 secretion. This is a very important finding that can be considered for future therapeutics targeting the IL-6 axis in MM and other tumours.

The lack of cell sorting and individual cytokine screening is also a weakness in the experimental design. While it is reasonable to think that SLAMF7$^+$ CD8$^+$ T cells are a source of IL-6, as they are the only population that is not present in the control group, other cells could contribute to IL-6 production through a paracrine mechanism. It is possible, although unlikely, that SLAMF7$^+$ CD8$^+$ T cells induce other cell populations in the medium to secrete IL-6.

A core finding of this dissertation is that elotuzumab eliminates SLAMF7$^+$ CD8$^+$ T cells via ADCP. The phagocytosis of a specific population of T cells might be a promising new approach for the development of next-generation immunotherapy. Eliminating senescent suppressor Treg cells such as SLAMF7$^+$ CD8$^+$ CD28$^-$ CD57$^+$ T cells via administration of elotuzumab in MM patients is a novel approach for overcoming immune escape. One question that my study could not answer is why only CD8$^+$ Treg cells were downregulated after elotuzumab-based induction therapy, while other exhausted T cells with upregulated SLAMF7 were not. A reason might be that some cells are more

susceptible to phagocytosis than others, as I observed in the analysis of NK cells and CD47 expression (Section 3.4.2). Another question that should be explored in future studies is how the elimination of these SLAMF7$^+$ CD8$^+$ T cells affects the T cell phenotype in the tumour microenvironment. It is reasonable to hypothesize that such elimination will have a favourable effect on T cell function and cytotoxicity, although a clear investigation is still required.

Although it has been previously described that NK cells are capable of eliminating T cells (Cerboni et al., 2007; Nielsen et al., 2012), my experiments showed that NK cells did not play a role in the elimination of SLAMF7$^+$ CD8$^+$ T cells treated with elotuzumab. Considering that elotuzumab binds to NK cells through FcγRIIIA, the results of such experiments were not justified.

4.3. From Bench to Bedside: Translational Impact?

Data after induction therapy from the GMMG-HD6 trial (NCT02495922), in which patients with newly diagnosed MM were randomized to receive induction therapy in the form of either 4 cycles of VRD only or 4 cycles of VRD and elotuzumab, suggest that patients who have high SLAMF7 expression on their CD8$^+$ T cells could gain a more beneficial effect from VRD plus elotuzumab induction therapy than patients with low SLAMF7 expression. The data were not significant, and a clear correlation was not observed. Although SLAMF7 expression was correlated with TIGIT expression in patients with MM and a higher level of TIGIT, i.e., a higher level of SLAMF7 expression, was associated with better clinical outcomes (Minnie et al., 2018), I did not find a similar clinical correlation in the analysed patient cohorts. It is also reasonable to hypothesize that a higher level of CD8$^+$ Treg cells should have a clinical meaning. Despite the slight trend observed, the detailed clinical analyses did not yield a clear understanding of the effect of SLAMF7 expression on T cells at a clinical level. The main reason, however, could be the very good response most of the patients achieved after induction therapy. More than 65% of the patients achieved CR, nCR, or VGPR. Hence, analysing clinical data after induction therapy is not the best option. A follow-up plan in which the correlation between PFS and SLAMF7 expression will be assessed is being planned.

The significant decrease in SLAMF7^{+} CD8^{+} T cells in patients who did not receive elotuzumab is an interesting observation that might also contribute to the lack of observed clinical correlation between SLAMF7 expression and clinical outcomes. Another explanation could also be that lenalidomide therapy enhances T cell activation *in vivo (Lee et al., 2011; Krämer et al., 2016)* which could overcome the high level of SLAMF7^{+} CD8^{+} T cells in patients.

5. Summary

Despite recent advances in drug development for cancer immunotherapy, only two monoclonal antibodies have been approved for the treatment of multiple myeloma, among them is elotuzumab, an anti-SLAMF7 antibody. Its mechanism of action has previously been only partly described in terms of NK cell activation and direct antibody dependent cellular cytotoxicity; however, the effect of elotuzumab on T cells has not yet been studied. Therefore, I sought to examine whether SLAMF7 is expressed on T cells, its function in T cells, and the effect of elotuzumab binding to T cells in patients with MM.

I analysed SLAMF7 expression on T cells from patients with MM before and after induction therapy with or without elotuzumab. I also utilized the CRISPR-Cas9 knockout model of SLAMF7 to examine its function and RNA transcriptomic sequencing approach. Moreover, I performed extensive immunological functional analyses to study the effect of the abundance of $SLAMF7^+$ T cells and the immune response on tumour cells.

In the first study, I found that SLAMF7 was expressed on T cells, especially on $CD8^+$ T cells. $CD4^+$ T cells showed modest expression. Thus, I further investigated the immunophenotype of $SLAMF7^+$ $CD8^+$ T cells and found that these cells showed a similar phenotype to $CD8^+$ $CD28^-$ $CD57^+$ T cells, a subpopulation previously described by a colleague to exert immunosuppressive capacity to promote tumour growth. Moreover, I found that they expressed high levels of exhaustion markers, indicating that they had an exhausted phenotype as well. Using CRISPR Cas9 knockout model in T cells, I found that there was no significant difference between SLAMF7 knockout and control T cells, suggesting that SLAMF7 is a marker for dysfunction and not an initiator of exhaustion in T cells.

ELISPOT functional assay with T cell from patients showed that patients with a high frequency of $CD8^+$ T cells exhibit weaker anti-tumour cytotoxic activity. Adding $SLAMF7^+$ $CD8^+$ T cells from myeloma patients suppressed the antigen-specific T cell response of healthy donors T cells in my analyses. Clinically, I found a strong decrease in $SLAMF7^+$ $CD8^+$ T cells after induction therapy in patients who received elotuzumab. Therefore, I hypothesized that elotuzumab might induce antibody dependent cellular phagocytosis a of $SLAMF7^+$ $CD8^+$ T

cells. In cooperation with Heiko Bruns at Erlangen University, I found that the majority of SLAMF7^{+} CD8^{+} T cells were phagocytosed by autologous phagocytes after adding elotuzumab *in vitro*. To confirm the finding *in vivo*, Hakim Echchannaoui at Mainz University and used a similar approach in a myeloma mouse model, and we observed consistent finding. After confirming the cells` depletion mechanism, I also checked for a possible role for natural killer cells in the elimination of T cells but found no evidence. Given these findings, I then investigated how Natural killer cells escape phagocytosis despite expressing SLAMF7 by analysing CD47, which is a phagocytosis-inhibiting ('don't eat me') marker, on natural killer cells and comparing it to the expression on T cells. Comparatively, natural killer cells expressed much higher level of CD47 than T cells, highlighting a potential survival advantage against elotuzumab-induced phagocytosis.

In summary, I have shed new light on a key mechanism of action of an anti-SLAMF7 antibody against immunosuppressive CD8^{+} T cells. Previously, anti-SLAMF7 antibodies were thought to act by targeting myeloma cells directly or by bringing together NK cells and myeloma cells. The findings detailed in my work provide evidence for another therapeutic mechanism. This mechanism, together with the clinical findings, provide a novel potential immune target for the future immunotherapy approaches.

I published the results as a first author in Leukemia Journal, Nature Publishing Group, in February 2021 (https://doi.org/10.1038/s41375-021-01172-x)

6. References

Abel, A.M., Yang, C., Thakar, M.S., and Malarkannan, S. (2018). Natural Killer Cells: Development, Maturation, and Clinical Utilization. Frontiers in immunology *9*, 1869.

Akbar, A.N., and Henson, S.M. (2011). Are senescence and exhaustion intertwined or unrelated processes that compromise immunity? Nature reviews. Immunology *11*, 289-295.

Alard, E., Butnariu, A.-B., Grillo, M., Kirkham, C., Zinovkin, D.A., Newnham, L., Macciochi, J., and Pranjol, M.Z.I. (2020). Advances in Anti-Cancer Immunotherapy: Car-T Cell, Checkpoint Inhibitors, Dendritic Cell Vaccines, and Oncolytic Viruses, and Emerging Cellular and Molecular Targets. Cancers *12*.

Alfaleh, M.A., Alsaab, H.O., Mahmoud, A.B., Alkayyal, A.A., Jones, M.L., Mahler, S.M., and Hashem, A.M. (2020). Phage Display Derived Monoclonal Antibodies: From Bench to Bedside. Frontiers in immunology *11*, 1986.

Awwad, M.H.S., Mahmoud, A., Bruns, H., Echchannaoui, H., Kriegsmann, K., Lutz, R., Raab, M.S., Bertsch, U., Munder, M., and Jauch, A., et al. (2021). Selective elimination of immunosuppressive T cells in patients with multiple myeloma. Leukemia.

Blass, E., and Ott, P.A. (2021). Advances in the development of personalized neoantigen-based therapeutic cancer vaccines. Nature reviews. Clinical oncology *18*, 215-229.

Boehm, T., and Bleul, C.C. (2007). The evolutionary history of lymphoid organs. Nature immunology *8*, 131-135.

Boles, K.S., and Mathew, P.A. (2001). Molecular cloning of CS1, a novel human natural killer cell receptor belonging to the CD2 subset of the immunoglobulin superfamily. Immunogenetics *52*, 302-307.

Boles, K.S., Stepp, S.E., Bennett, M., Kumar, V., and Mathew, P.A. (2001). 2B4 (CD244) and CS1: novel members of the CD2 subset of the immunoglobulin superfamily molecules expressed on natural killer cells and other leukocytes. Immunological reviews *181*, 234-249.

Bonilla, F.A., and Oettgen, H.C. (2010). Adaptive immunity. The Journal of allergy and clinical immunology *125*, S33-40.

Brenchley, J.M., Karandikar, N.J., Betts, M.R., Ambrozak, D.R., Hill, B.J., Crotty, L.E., Casazza, J.P., Kuruppu, J., Migueles, S.A., and Connors, M., et al. (2003). Expression of CD57 defines replicative senescence and antigen-induced apoptotic death of CD8+ T cells. Blood *101*, 2711-2720.

Buettner, M., and Lochner, M. (2016). Development and Function of Secondary and Tertiary Lymphoid Organs in the Small Intestine and the Colon. Frontiers in immunology *7*, 342.

Campbell, K.S., Cohen, A.D., and Pazina, T. (2018). Mechanisms of NK Cell Activation and Clinical Activity of the Therapeutic SLAMF7 Antibody, Elotuzumab in Multiple Myeloma. Frontiers in immunology *9*, 2551.

Cerboni, C., Zingoni, A., Cippitelli, M., Piccoli, M., Frati, L., and Santoni, A. (2007). Antigen-activated human T lymphocytes express cell-surface NKG2D ligands via an ATM/ATR-dependent mechanism and become susceptible to autologous NK- cell lysis. Blood *110*, 606-615.

Chim, C.S., Kumar, S.K., Orlowski, R.Z., Cook, G., Richardson, P.G., Gertz, M.A., Giralt, S., Mateos, M.V., Leleu, X., and Anderson, K.C. (2018). Management of relapsed and refractory multiple myeloma: novel agents, antibodies, immunotherapies and beyond. Leukemia *32*, 252-262.

Chonov, D.C., Ignatova, M.M.K., Ananiev, J.R., and Gulubova, M.V. (2019). IL-6 Activities in the Tumour Microenvironment. Part 1. Open access Macedonian journal of medical sciences *7*, 2391-2398.

Chou, J.P., and Effros, R.B. (2013). T cell replicative senescence in human aging. Current pharmaceutical design *19*, 1680-1698.

Christensen, O., Lupu, A., Schmidt, S., Condomines, M., Belle, S., Maier, A., Hose, D., Neuber, B., Moos, M., and Kleist, C., et al. (2009). Melan-A/MART1 analog peptide triggers anti-myeloma T-cells through crossreactivity with HM1.24. Journal of immunotherapy (Hagerstown, Md. : 1997) *32*, 613-621.

Courtney, A.H., Lo, W.-L., and Weiss, A. (2018). TCR Signaling: Mechanisms of Initiation and Propagation. Trends in biochemical sciences *43*, 108-123.

Danilova, N. (2012). The evolution of adaptive immunity. Advances in experimental medicine and biology *738*, 218-235.

Darvin, P., Toor, S.M., Sasidharan Nair, V., and Elkord, E. (2018). Immune checkpoint inhibitors: recent progress and potential biomarkers. Experimental & molecular medicine *50*, 1-11.

DeLuca, D.S., Levin, J.Z., Sivachenko, A., Fennell, T., Nazaire, M.-D., Williams, C., Reich, M., Winckler, W., and Getz, G. (2012). RNA-SeQC: RNA-seq metrics for quality control and process optimization. Bioinformatics (Oxford, England) *28*, 1530-1532.

Dimopoulos, M.A., Dytfeld, D., Grosicki, S., Moreau, P., Takezako, N., Hori, M., Leleu, X., LeBlanc, R., Suzuki, K., and Raab, M.S., et al. (2018). Elotuzumab plus Pomalidomide and Dexamethasone for Multiple Myeloma. The New England journal of medicine *379*, 1811-1822.

Dimopoulos, M.A., Kastritis, E., Rosinol, L., Bladé, J., and Ludwig, H. (2008). Pathogenesis and treatment of renal failure in multiple myeloma. Leukemia *22*, 1485-1493.

Dimopoulos, M.A., Lonial, S., White, D., Moreau, P., Palumbo, A., San-Miguel, J., Shpilberg, O., Anderson, K., Grosicki, S., and Spicka, I., et al. (2017). Elotuzumab plus lenalidomide/dexamethasone for relapsed or refractory multiple myeloma: ELOQUENT-2 follow-up and post-hoc analyses on progression-free survival and tumour growth. British journal of haematology *178*, 896-905.

Dobin, A., Davis, C.A., Schlesinger, F., Drenkow, J., Zaleski, C., Jha, S., Batut, P., Chaisson, M., and Gingeras, T.R. (2013). STAR: ultrafast universal RNA-seq aligner. Bioinformatics (Oxford, England) *29*, 15-21.

Echchannaoui, H., Petschenka, J., Ferreira, E.A., Hauptrock, B., Lotz-Jenne, C., Voss, R.-H., and Theobald, M. (2018). A Potent Tumor-Reactive p53-Specific Single-Chain TCR without On- or Off-Target Autoimmunity In Vivo. Molecular Therapy *27*, 261-271.

Feins, S., Kong, W., Williams, E.F., Milone, M.C., and Fraietta, J.A. (2019). An introduction to chimeric antigen receptor (CAR) T-cell immunotherapy for human cancer. American journal of hematology *94*, S3-S9.

Filaci, G., Fenoglio, D., Fravega, M., Ansaldo, G., Borgonovo, G., Traverso, P., Villaggio, B., Ferrera, A., Kunkl, A., and Rizzi, M., et al. (2007). CD8+ CD28- T regulatory lymphocytes inhibiting T cell proliferative and cytotoxic functions infiltrate human cancers. The Journal of Immunology *179*, 4323-4334.

Filaci, G., Fravega, M., Fenoglio, D., Rizzi, M., Negrini, S., Viggiani, R., and Indiveri, F. (2004). Non-antigen specific CD8+ T suppressor lymphocytes. Clinical and experimental medicine *4*, 86-92.

Gadó, K., Domján, G., Hegyesi, H., and Falus, A. (2000). Role of INTERLEUKIN-6 in the pathogenesis of multiple myeloma. Cell biology international *24*, 195-209.

Granzow, M., Hegenbart, U., Hinderhofer, K., Hose, D., Seckinger, A., Bochtler, T., Hemminki, K., Goldschmidt, H., Schönland, S.O., and Jauch, A. (2017). Novel recurrent chromosomal aberrations detected in clonal plasma cells of light chain amyloidosis patients show potential adverse prognostic effect: first results from a genome-wide copy number array analysis. Haematologica *102*, 1281-1290.

Haen, S.P., Löffler, M.W., Rammensee, H.-G., and Brossart, P. (2020). Towards new horizons: characterization, classification and implications of the tumour antigenic repertoire. Nature reviews. Clinical oncology *17*, 595-610.

Hajicek, N., and Sondek, J. (2020). Structural basis for the activation of PLC-gamma isozymes by phosphorylation and cancer-associated mutations.

Haslam, A., and Prasad, V. (2019). Estimation of the Percentage of US Patients With Cancer Who Are Eligible for and Respond to Checkpoint Inhibitor Immunotherapy Drugs. JAMA network open *2*, e192535.

Hata, H., Xiao, H., Petrucci, M.T., Woodliff, J., Chang, R., and Epstein, J. (1993). Interleukin-6 gene expression in multiple myeloma: a characteristic of immature tumor cells. Blood *81*, 3357-3364.

Heffner, M., and Fearon, D.T. (2007). Loss of T cell receptor-induced Bmi-1 in the KLRG1(+) senescent CD8(+) T lymphocyte. Proceedings of the National Academy of Sciences of the United States of America *104*, 13414-13419.

Henson, S.M., and Akbar, A.N. (2009). KLRG1--more than a marker for T cell senescence. Age (Dordrecht, Netherlands) *31*, 285-291.

Herrero, A.B., García-Gómez, A., Garayoa, M., Corchete, L.A., Hernández, J.M., San Miguel, J., and Gutierrez, N.C. (2016). Effects of IL-8 Up-Regulation on Cell Survival and Osteoclastogenesis in Multiple Myeloma. The American journal of pathology *186*, 2171-2182.

Hodi, F.S., O'Day, S.J., McDermott, D.F., Weber, R.W., Sosman, J.A., Haanen, J.B., Gonzalez, R., Robert, C., Schadendorf, D., and Hassel, J.C., et al. (2010). Improved survival with ipilimumab in patients with metastatic melanoma. The New England journal of medicine *363*, 711-723.

Hsi, E.D., Steinle, R., Balasa, B., Szmania, S., Draksharapu, A., Shum, B.P., Huseni, M., Powers, D., Nanisetti, A., and Zhang, Y., et al. (2008). CS1, a potential new therapeutic antibody target for the treatment of multiple myeloma. Clinical cancer research : an official journal of the American Association for Cancer Research *14*, 2775-2784.

Huff, W.X., Kwon, J.H., Henriquez, M., Fetcko, K., and Dey, M. (2019). The Evolving Role of CD8+CD28- Immunosenescent T Cells in Cancer Immunology. International journal of molecular sciences *20*.

Hundemer, M., Schmidt, S., Condomines, M., Lupu, A., Hose, D., Moos, M., Cremer, F., Kleist, C., Terness, P., and Belle, S., et al. (2006). Identification of a new HLA-A2-restricted T-cell epitope within HM1.24 as immunotherapy target for multiple myeloma. Experimental hematology *34*, 486-496.

Huse, M. (2009). The T-cell-receptor signaling network. Journal of cell science *122*, 1269-1273.

Hwang, J.-R., Byeon, Y., Kim, D., and Park, S.-G. (2020). Recent insights of T cell receptor-mediated signaling pathways for T cell activation and development. Experimental & molecular medicine *52*, 750-761.

Ishida, T. (2018). Therapeutic antibodies for multiple myeloma. Japanese journal of clinical oncology *48*, 957-963.

Jelinek, T., Paiva, B., and Hajek, R. (2018). Update on PD-1/PD-L1 Inhibitors in Multiple Myeloma. Frontiers in immunology *9*, 2431.

Jiang, W., He, Y., He, W., Wu, G., Zhou, X., Sheng, Q., Zhong, W., Lu, Y., Ding, Y., and Lu, Q., et al. (2020). Exhausted CD8+T Cells in the Tumor Immune Microenvironment: New Pathways to Therapy. Frontiers in immunology *11*, 622509.

Jin, L., and Harrison, S.C. (2002). Crystal Structure of human calcineurin complexed with cyclosporin A and human cyclophilin.

Kazandjian, D. (2016). Multiple myeloma epidemiology and survival: A unique malignancy. Seminars in oncology *43*, 676-681.

Khan, O., Giles, J.R., McDonald, S., Manne, S., Ngiow, S.F., Patel, K.P., Werner, M.T., Huang, A.C., Alexander, K.A., and Wu, J.E., et al. (2019). TOX transcriptionally and epigenetically programs CD8+ T cell exhaustion. Nature *571*, 211-218.

Köhler, G., and Milstein, C. (1975). Continuous cultures of fused cells secreting antibody of predefined specificity. Nature *256*, 495-497.

Kojima, Y., Volkmer, J.-P., McKenna, K., Civelek, M., Lusis, A.J., Miller, C.L., Direnzo, D., Nanda, V., Ye, J., and Connolly, A.J., et al. (2016). CD47-blocking antibodies restore phagocytosis and prevent atherosclerosis. Nature *536*, 86-90.

Krämer, I., Engelhardt, M., Fichtner, S., Neuber, B., Medenhoff, S., Bertsch, U., Hillengass, J., Raab, M.-S., Hose, D., and Ho, A.D., et al. (2016). Lenalidomide enhances myeloma-specific T-cell responses in vivo and in vitro. Oncoimmunology *5*, e1139662.

Krejcik, J., Casneuf, T., Nijhof, I.S., Verbist, B., Bald, J., Plesner, T., Syed, K., Liu, K., van de Donk, N.W.C.J., and Weiss, B.M., et al. (2016). Daratumumab depletes CD38+ immune regulatory cells, promotes T-cell expansion, and skews T-cell repertoire in multiple myeloma. Blood *128*, 384-394.

Krönke, J., Kuchenbauer, F., Kull, M., Teleanu, V., Bullinger, L., Bunjes, D., Greiner, A., Kolmus, S., Köpff, S., and Schreder, M., et al. (2017). IKZF1 expression is a prognostic marker in newly diagnosed standard-risk multiple myeloma treated with lenalidomide and intensive chemotherapy: a study of the German Myeloma Study Group (DSMM). Leukemia *31*, 1363-1367.

Kuehl, W.M., and Bergsagel, P.L. (2002). Multiple myeloma: evolving genetic events and host interactions. Nature reviews. Cancer *2*, 175-187.

Kumar, S., Paiva, B., Anderson, K.C., Durie, B., Landgren, O., Moreau, P., Munshi, N., Lonial, S., Bladé, J., and Mateos, M.-V., et al. (2016). International Myeloma Working Group consensus criteria for response and minimal residual disease assessment in multiple myeloma. The Lancet Oncology *17*, e328-e346.

Kurdi, A.T., Glavey, S.V., Bezman, N.A., Jhatakia, A., Guerriero, J.L., Manier, S., Moschetta, M., Mishima, Y., Roccaro, A., and Detappe, A., et al. (2018). Antibody-Dependent Cellular Phagocytosis by Macrophages is a Novel Mechanism of Action of Elotuzumab. Molecular cancer therapeutics *17*, 1454-1463.

Kyle, R.A., Gertz, M.A., Witzig, T.E., Lust, J.A., Lacy, M.Q., Dispenzieri, A., Fonseca, R., Rajkumar, S.V., Offord, J.R., and Larson, D.R., et al. (2003). Review of 1027 patients with newly diagnosed multiple myeloma. Mayo Clinic proceedings *78*, 21-33.

Larson, R.C., and Maus, M.V. (2021). Recent advances and discoveries in the mechanisms and functions of CAR T cells. Nature reviews. Cancer *21*, 145-161.

Lee, B.-N., Gao, H., Cohen, E.N., Badoux, X., Wierda, W.G., Estrov, Z., Faderl, S.H., Keating, M.J., Ferrajoli, A., and Reuben, J.M. (2011). Treatment

with lenalidomide modulates T-cell immunophenotype and cytokine production in patients with chronic lymphocytic leukemia. Cancer *117*, 3999-4008.

Lee, L.X., Toskic, D., Ma, X., Zhou, P., Kugelmass, A., Fogaren, T., and Comenzo, R.L. (2018). Senescent CD8+ T Cells in Myeloma Patients: Implications for Cellular Therapies. Blood *132*, 5688.

Li, H., Handsaker, B., Wysoker, A., Fennell, T., Ruan, J., Homer, N., Marth, G., Abecasis, G., and Durbin, R. (2009). The Sequence Alignment/Map format and SAMtools. Bioinformatics (Oxford, England) *25*, 2078-2079.

Li, H., Wu, K., Tao, K., Chen, L., Zheng, Q., Lu, X., Liu, J., Shi, L., Liu, C., and Wang, G., et al. (2012). Tim-3/galectin-9 signaling pathway mediates T-cell dysfunction and predicts poor prognosis in patients with hepatitis B virus-associated hepatocellular carcinoma. Hepatology (Baltimore, Md.) *56*, 1342-1351.

Li, X., Shao, C., Shi, Y., and Han, W. (2018). Lessons learned from the blockade of immune checkpoints in cancer immunotherapy. Journal of hematology & oncology *11*, 31.

Liao, Y., Smyth, G.K., and Shi, W. (2014). featureCounts: an efficient general purpose program for assigning sequence reads to genomic features. Bioinformatics (Oxford, England) *30*, 923-930.

Liberzon, A., Birger, C., Thorvaldsdóttir, H., Ghandi, M., Mesirov, J.P., and Tamayo, P. (2015). The Molecular Signatures Database (MSigDB) hallmark gene set collection. Cell systems *1*, 417-425.

Lipson, E.J., and Drake, C.G. (2011). Ipilimumab: an anti-CTLA-4 antibody for metastatic melanoma. Clinical cancer research : an official journal of the American Association for Cancer Research *17*, 6958-6962.

Lonial, S., Dimopoulos, M.A., Weisel, K., White, D., Moreau, P., Mateos, M.-V., San-Miguel, J., Anderson, K.C., Shpilberg, O., and Grosicki, S., et al. (2018). Extended 5-y follow-up (FU) of phase 3 ELOQUENT-2 study of elotuzumab + lenalidomide/dexamethasone (ELd) vs Ld in relapsed/refractory multiple myeloma (RRMM). JCO *36*, 8040.

Love, M.I., Huber, W., and Anders, S. (2014). Moderated estimation of fold change and dispersion for RNA-seq data with DESeq2. Genome biology *15*, 550.

Luis Munoz-Erazo, Janet L. Rhodes, Valentine C. Marion, and Roslyn A. Kemp (2020). Tertiary lymphoid structures in cancer – considerations for patient prognosis. Cell Mol Immunol *17*, 570-575.

Malaer, J.D., and Mathew, P.A. (2017). CS1 (SLAMF7, CD319) is an effective immunotherapeutic target for multiple myeloma. American journal of cancer research *7*, 1637-1641.

Marshall, J.S., Warrington, R., Watson, W., and Kim, H.L. (2018). An introduction to immunology and immunopathology. Allergy, asthma, and clinical immunology : official journal of the Canadian Society of Allergy and Clinical Immunology *14*, 49.

Martinez, G.J., Pereira, R.M., Äijö, T., Kim, E.Y., Marangoni, F., Pipkin, M.E., Togher, S., Heissmeyer, V., Zhang, Y.C., and Crotty, S., et al. (2015). The transcription factor NFAT promotes exhaustion of activated $CD8^+$ T cells. Immunity *42*, 265-278.

Masjedi, A., Hashemi, V., Hojjat-Farsangi, M., Ghalamfarsa, G., Azizi, G., Yousefi, M., and Jadidi-Niaragh, F. (2018). The significant role of interleukin-6 and its signaling pathway in the immunopathogenesis and treatment of breast cancer. Biomedicine & pharmacotherapy = Biomedecine & pharmacotherapie *108*, 1415-1424.

Mateos, M.-V., Dimopoulos, M.A., Cavo, M., Suzuki, K., Jakubowiak, A., Knop, S., Doyen, C., Lucio, P., Nagy, Z., and Kaplan, P., et al. (2018). Daratumumab plus Bortezomib, Melphalan, and Prednisone for Untreated Myeloma. The New England journal of medicine *378*, 518-528.

Matsuzaki, J., Gnjatic, S., Mhawech-Fauceglia, P., Beck, A., Miller, A., Tsuji, T., Eppolito, C., Qian, F., Lele, S., and Shrikant, P., et al. (2010). Tumor-infiltrating NY-ESO-1-specific CD8+ T cells are negatively regulated by LAG-3 and PD-1 in human ovarian cancer. Proceedings of the National Academy of Sciences of the United States of America *107*, 7875-7880.

Matthes, T., Manfroi, B., and Huard, B. (2016). Revisiting IL-6 antagonism in multiple myeloma. Critical reviews in oncology/hematology *105*, 1-4.

Minnie, S.A., Kuns, R.D., Gartlan, K.H., Zhang, P., Wilkinson, A.N., Samson, L., Guillerey, C., Engwerda, C., MacDonald, K.P.A., and Smyth, M.J., et al. (2018). Myeloma escape after stem cell transplantation is a consequence of T-cell exhaustion and is prevented by TIGIT blockade. Blood *132*, 1675-1688.

Mittelbrunn, M., and Kroemer, G. (2021). Hallmarks of T cell aging. Nature immunology.

Mognol, G.P., Spreafico, R., Wong, V., Scott-Browne, J.P., Togher, S., Hoffmann, A., Hogan, P.G., Rao, A., and Trifari, S. (2017). Exhaustion-associated regulatory regions in CD8+ tumor-infiltrating T cells. Proceedings of the National Academy of Sciences of the United States of America *114*, E2776-E2785.

Mullard, A. (2021). FDA approves 100th monoclonal antibody product. Nature reviews. Drug discovery.

Neben, K., Lokhorst, H.M., Jauch, A., Bertsch, U., Hielscher, T., van der Holt, B., Salwender, H., Blau, I.W., Weisel, K., and Pfreundschuh, M., et al. (2012). Administration of bortezomib before and after autologous stem cell transplantation improves outcome in multiple myeloma patients with deletion 17p. Blood *119*, 940-948.

Neefjes, J., Jongsma, M.L.M., Paul, P., and Bakke, O. (2011). Towards a systems understanding of MHC class I and MHC class II antigen presentation. Nature reviews. Immunology *11*, 823-836.

Netea, M.G., Schlitzer, A., Placek, K., Joosten, L.A.B., and Schultze, J.L. (2019). Innate and Adaptive Immune Memory: an Evolutionary Continuum in the Host's Response to Pathogens. Cell host & microbe *25*, 13-26.

Neuber, B., Dai, J., Waraich, W.A., Awwad, M.H.S., Engelhardt, M., Schmitt, M., Medenhoff, S., Witzens-Harig, M., Ho, A.D., and Goldschmidt, H., et al. (2017). Lenalidomide overcomes the immunosuppression of regulatory CD8+CD28- T-cells. Oncotarget *8*, 98200-98214.

Nielsen, N., Ødum, N., Ursø, B., Lanier, L.L., and Spee, P. (2012). Cytotoxicity of CD56(bright) NK cells towards autologous activated CD4+ T cells is mediated through NKG2D, LFA-1 and TRAIL and dampened via CD94/NKG2A. PloS one *7*, e31959.

Nishida, H., and Yamada, T. (2019). Monoclonal Antibody Therapies in Multiple Myeloma: A Challenge to Develop Novel Targets. Journal of oncology *2019*, 6084012.

O'Connell, P., Pepelyayeva, Y., Blake, M.K., Hyslop, S., Crawford, R.B., Rizzo, M.D., Pereira-Hicks, C., Godbehere, S., Dale, L., and Gulick, P., et al. (2019). SLAMF7 Is a Critical Negative Regulator of IFN-α-Mediated CXCL10 Production in Chronic HIV Infection. Journal of immunology (Baltimore, Md. : 1950) *202*, 228-238.

O'Donnell, J.S., Teng, M.W.L., and Smyth, M.J. (2019). Cancer immunoediting and resistance to T cell-based immunotherapy. Nature reviews. Clinical oncology *16*, 151-167.

Okada, T.S. and Kondoh, H. (1986). Commitment and instability in cell differentiation. [8th conference held by the Yamada Science Foundation [1985]) (Orlando: Academic Press).

Palumbo, A., Avet-Loiseau, H., Oliva, S., Lokhorst, H.M., Goldschmidt, H., Rosinol, L., Richardson, P., Caltagirone, S., Lahuerta, J.J., and Facon, T., et al. (2015). Revised International Staging System for Multiple Myeloma: A Report From International Myeloma Working Group. Journal of clinical oncology : official journal of the American Society of Clinical Oncology *33*, 2863-2869.

Pan, C., Liu, H., Robins, E., Song, W., Liu, D., Li, Z., and Zheng, L. (2020). Next-generation immuno-oncology agents: current momentum shifts in cancer immunotherapy. Journal of hematology & oncology *13*, 29.

Paul, S., and Schaefer, B.C. (2013). A new look at T cell receptor signaling to nuclear factor-κB. Trends in immunology *34*, 269-281.

Pawelec, G. (2019). Is There a Positive Side to T Cell Exhaustion? Frontiers in immunology *10*, 111.

Pazina, T., James, A.M., MacFarlane, A.W., Bezman, N.A., Henning, K.A., Bee, C., Graziano, R.F., Robbins, M.D., Cohen, A.D., and Campbell, K.S. (2017). The anti-SLAMF7 antibody elotuzumab mediates NK cell activation through both CD16-dependent and -independent mechanisms. Oncoimmunology *6*, e1339853.

Plaumann, J., Engelhardt, M., Awwad, M.H.S., Echchannaoui, H., Amman, E., Raab, M.S., Hillengass, J., Halama, N., Neuber, B., and Müller-Tidow, C., et al. (2018). IL-10 inducible CD8+ regulatory T-cells are enriched in patients with multiple myeloma and impact the generation of antigen-specific T-cells. Cancer immunology, immunotherapy : CII *67*, 1695-1707.

Portier, M., Rajzbaum, G., Zhang, X.G., Attal, M., Rusalen, C., Wijdenes, J., Mannoni, P., Maraninchi, D., Piechaczyk, M., and Bataille, R. (1991). In vivo interleukin 6 gene expression in the tumoral environment in multiple myeloma. European journal of immunology *21*, 1759-1762.

Punt, J., Stranford, S.A., Jones, P.P., and Owen, J.A. (C 2019). Immunology (New York: Macmillan education).

Qi, C., Tian, S., Wang, J., Ma, H., Qian, K., and Zhang, X. (2015). Co-expression of CD40/CD40L on XG1 multiple myeloma cells promotes IL-6 autocrine function. Cancer Investigation *33*, 6-15.

Raza, S., Safyan, R.A., and Lentzsch, S. (2017). Immunomodulatory Drugs (IMiDs) in Multiple Myeloma. Current cancer drug targets *17*, 846-857.

Redoglia, V., Boccadoro, M., Battaglio, S., Dianzani, U., Massaia, M., and Pileri, A. (1990). Multiple myeloma: altered CD4/CD8 ratio in bone marrow. Haematologica *75*, 129-131.

Ribrag, V., Avigan, D.E., Green, D.J., Wise-Draper, T., Posada, J.G., Vij, R., Zhu, Y., Farooqui, M.Z.H., Marinello, P., and Siegel, D.S. (2019). Phase 1b trial of pembrolizumab monotherapy for relapsed/refractory multiple myeloma: KEYNOTE-013. British journal of haematology *186*, e41-e44.

Richardson, P.G., Beksaç, M., Špička, I., and Mikhael, J. (2020). Isatuximab for the treatment of relapsed/refractory multiple myeloma. Expert opinion on biological therapy *20*, 1395-1404.

Ridler, C. (2017). Neuro-oncology: CD47 antibody helps phagocytes fight paediatric cancer. Nature reviews. Neurology *13*, 258-259.

Rio, D.C., Ares, M., Hannon, G.J., and Nilsen, T.W. (2010). Purification of RNA using TRIzol (TRI reagent). Cold Spring Harbor protocols *2010*, pdb.prot5439.

Robert, C. (2020). A decade of immune-checkpoint inhibitors in cancer therapy. Nature communications *11*, 3801.

Rosenblatt, J., and Avigan, D. (2017). Targeting the PD-1/PD-L1 axis in multiple myeloma: a dream or a reality? Blood *129*, 275-279.

Sandu, I., Cerletti, D., Claassen, M., and Oxenius, A. (2020). Exhausted CD8+ T cells exhibit low and strongly inhibited TCR signaling during chronic LCMV infection. Nature communications *11*, 4454.

Schreiber, R.D., Old, L.J., and Smyth, M.J. (2011). Cancer immunoediting: integrating immunity's roles in cancer suppression and promotion. Science (New York, N.Y.) *331*, 1565-1570.

Sekine, T., Perez-Potti, A., Nguyen, S., Gorin, J.-B., Wu, V.H., Gostick, E., Llewellyn-Lacey, S., Hammer, Q., Falck-Jones, S., and Vangeti, S., et al. (2020). TOX is expressed by exhausted and polyfunctional human effector memory CD8+ T cells. Science immunology *5*.

Shi, G., Han, J., Liu, G., Hao, Y., Ma, Y., Li, T., Wu, X., Zhang, H., Liu, Y., and Wang, B., et al. (2014). Expansion of activated regulatory T cells by myeloid-specific chemokines via an alternative pathway in CSF of bacterial meningitis patients. European journal of immunology *44*, 420-430.

Silverstein, A.M. (1982). Development of the concept of immunologic specificity, I. Cellular Immunology *67*, 396-409.

Strioga, M., Pasukoniene, V., and Characiejus, D. (2011). CD8+ CD28- and CD8+ CD57+ T cells and their role in health and disease. Immunology *134*, 17-32.

Subramanian, A., Tamayo, P., Mootha, V.K., Mukherjee, S., Ebert, B.L., Gillette, M.A., Paulovich, A., Pomeroy, S.L., Golub, T.R., and Lander, E.S., et al. (2005). Gene set enrichment analysis: a knowledge-based approach for interpreting genome-wide expression profiles. Proceedings of the National Academy of Sciences of the United States of America *102*, 15545-15550.

Subramanian, N., Torabi-Parizi, P., Gottschalk, R.A., Germain, R.N., and Dutta, B. (2015). Network representations of immune system complexity. Wiley interdisciplinary reviews. Systems biology and medicine *7*, 13-38.

Suen, H., Brown, R., Yang, S., Weatherburn, C., Ho, P.J., Woodland, N., Nassif, N., Barbaro, P., Bryant, C., and Hart, D., et al. (2016). Multiple myeloma causes clonal T-cell immunosenescence: identification of potential novel targets for promoting tumour immunity and implications for checkpoint blockade. Leukemia *30*, 1716-1724.

Tai, Y.-T., Soydan, E., Song, W., Fulciniti, M., Kim, K., Hong, F., Li, X.-F., Burger, P., Rumizen, M.J., and Nahar, S., et al. (2009). CS1 promotes multiple myeloma cell adhesion, clonogenic growth, and tumorigenicity via c-maf-mediated interactions with bone marrow stromal cells. Blood *113*, 4309-4318.

Takeuchi, K., Roehrl, M.H., Sun, Z.Y., and Wagner, G. (2007). Structure of the calcineurin-NFAT complex.

Tarasov, A., Vilella, A.J., Cuppen, E., Nijman, I.J., and Prins, P. (2015). Sambamba: fast processing of NGS alignment formats. Bioinformatics (Oxford, England) *31*, 2032-2034.

Toyoshima, Y., Kitamura, H., Xiang, H., Ohno, Y., Homma, S., Kawamura, H., Takahashi, N., Kamiyama, T., Tanino, M., and Taketomi, A. (2019). IL6 Modulates the Immune Status of the Tumor Microenvironment to Facilitate Metastatic Colonization of Colorectal Cancer Cells. Cancer immunology research *7*, 1944-1957.

Vaddepally, R.K., Kharel, P., Pandey, R., Garje, R., and Chandra, A.B. (2020). Review of Indications of FDA-Approved Immune Checkpoint Inhibitors per NCCN Guidelines with the Level of Evidence. Cancers *12*.

Vermi, W., Micheletti, A., Finotti, G., Tecchio, C., Calzetti, F., Costa, S., Bugatti, M., Calza, S., Agostinelli, C., and Pileri, S., et al. (2018). slan+ Monocytes and Macrophages Mediate CD20-Dependent B-cell Lymphoma Elimination via ADCC and ADCP. Cancer research *78*, 3544-3559.

Vesely, M.D., Kershaw, M.H., Schreiber, R.D., and Smyth, M.J. (2011). Natural innate and adaptive immunity to cancer. Annual review of immunology *29*, 235-271.

Waldman, A.D., Fritz, J.M., and Lenardo, M.J. (2020). A guide to cancer immunotherapy: from T cell basic science to clinical practice. Nature reviews. Immunology *20*, 651-668.

Weiner, L.M., Surana, R., and Wang, S. (2010). Monoclonal antibodies: versatile platforms for cancer immunotherapy. Nature reviews. Immunology *10*, 317-327.

Wherry, E.J., and Kurachi, M. (2015). Molecular and cellular insights into T cell exhaustion. Nature reviews. Immunology *15*, 486-499.

Wieczorek, M., Abualrous, E.T., Sticht, J., Álvaro-Benito, M., Stolzenberg, S., Noé, F., and Freund, C. (2017). Major Histocompatibility Complex (MHC) Class I and MHC Class II Proteins: Conformational Plasticity in Antigen Presentation. Frontiers in immunology *8*, 292.

Willenbacher, W., Willenbacher, E., Zelle-Rieser, C., Biedermann, R., Weger, R., Jöhrer, K., and Brunner, A. (2016). Bone marrow microenvironmental CD4 + and CD8 + lymphocyte infiltration patterns define overall- and progression free survival in standard risk multiple myeloma--an analysis from the Austrian Myeloma Registry. Leukemia & lymphoma *57*, 1478-1481.

Yu, G., Wang, L.-G., Han, Y., and He, Q.-Y. (2012). clusterProfiler: an R package for comparing biological themes among gene clusters. Omics : a journal of integrative biology *16*, 284-287.

Zelle-Rieser, C., Thangavadivel, S., Biedermann, R., Brunner, A., Stoitzner, P., Willenbacher, E., Greil, R., and Jöhrer, K. (2016). T cells in multiple myeloma display features of exhaustion and senescence at the tumor site. Journal of hematology & oncology *9*, 116.

Zhao, Y., Shao, Q., and Peng, G. (2020). Exhaustion and senescence: two crucial dysfunctional states of T cells in the tumor microenvironment. Cellular & molecular immunology *17*, 27-35.

Zhu, A., Ibrahim, J.G., and Love, M.I. (2018). Heavy-tailed prior distributions for sequence count data: removing the noise and preserving large differences. Bioinformatics (Oxford, England).

Zhu, X., Kim, J.L., Rose, P.E., Stover, D.R., and Toledo, L.M. (2000). CRYSTAL STRUCTURE OF THE LYMPHOCYTE-SPECIFIC KINASE LCK IN COMPLEX WITH STAUROSPORINE.

7. Personal Contribution to Data Acquisition & Personal Publications

This project was intellectually planned and developed by me and my supervisor Prof. Dr. Michael Hundemer, some experiments have been performed in cooperation with other internal and external collaborators. I alone conducted the experimental and evaluation of the data acquired in sections: 3.1.2, 3.2.2, 3.2.3, 3.3.3, 3.4.2, 3.4.3. I, with technical assistance from Sergej Medenhoff, Michael Benn, Larissa Schönhoff, Lena Richards, and clinical statistics support from Axel Benner, performed the experimental part and evaluation of the data of the following sections: 3.1.1, 3.3.1, 3.3.2. I cooperated with Heiko Bruns for the phagocytosis assay and Hakim Echchannaoui for the mouse model to perform the experimental part and evaluation of the data included in section 3.4.1. I cooperated with Abdelrahman Mahmoud to perform the data processing of RNA sequencing analyses, after the data acquirement in the DKFZ Genomics core facility, in section 3.1.3. I alone performed the experimental part and evaluation of the data included in section 3.2.1, however, the screening assay was acquired at Sciomics GmBH.

Of note, all patients` samples that have been used throughout the study were provided by the GMMG study group. The HD6 clinical, which is a randomized phase III clinical trial to study the effect of elotuzumab, was totally managed and organized by the GMMG groups without any contribution from my side. I received the samples and the clinical outcomes from the GMMG to perform my analyses and experiments related to the project.

The work included in this dissertation have already been published in the following articles:

Awwad, M.H.S., Mahmoud, A., Bruns, H., Echchannaoui, H., Kriegsmann, K., Lutz, R., Raab, M.S., Bertsch, U., Munder, M., and Jauch, A., et al. (2021). **Selective elimination of immunosuppressive T cells in patients with multiple myeloma**. Leukemia Journal.

The article is based on the results in sections: 3.1.1, 3.1.2, 3.1.3, 3.2.1, 3.2.2, 3.2.3, 3.3.1, 3.3.2, 3.3.3, 3.4.1, and 3.4.2. My experimental contribution to this

publication is the same as described previously for each respective section, my contribution to the preparation of the manuscript includes writing the manuscript, the manuscript's composition, including the introduction, the material and methods section after receiving the detailed protocols from external collaborators, results section, and the discussion section.

Further personal publications:

Legscha KJ, Antunes Ferreira E, Chamoun A, Lang A, **Awwad MHS**, Ton GNHQ, Galetzka D, Guezguez B, Hundemer M, Bourdon JC, Munder M, Theobald M, Echchannaoui H (2021). **Δ133p53α enhances metabolic and cellular fitness of TCR-engineered T cells and promotes superior antitumor immunity**. Journal of Immunotherapy of Cancer.

Mougiakakos D, Bach C, Böttcher M, Beier F, Röhner L, Stoll A, Rehli M, Gebhard C, Lischer C, Eberhardt M, Vera J, Büttner-Herold M, Bitterer K, Balzer H, Leffler M, Jitschin S, Hundemer M, **Awwad MHS**, Busch M, Stenger S, Völkl S, Schütz C, Krönke J, Mackensen A, Bruns H. (2021) **The IKZF1-IRF4/IRF5 Axis Controls Polarization of Myeloma-Associated Macrophages.** Cancer Immunol Research Journal

Kriegsmann K, Hundemer M, Hofmeister-Mielke N, Reichert P, Manta CP, **Awwad MHS**, Sauer S, Bertsch U, Besemer B, Fenk R, Hänel M, Munder M, Weisel KC, Blau IW, Neubauer A, Müller-Tidow C, Raab MS, Goldschmidt H, Huhn S, (2020) **Comparison of NGS and MFC Methods: Key Metrics in Multiple Myeloma MRD Assessment.** Cancers Journal

Kriegsmann K, Baertsch MA, **Awwad MHS**, Merz M, Hose D, Seckinger A, Jauch A, Becker N, Benner A, Raab MS, Hillengass J, Bertsch U, Dürig J, Salwender HJ, Hänel M, Fenk R, Munder M, Weisel K, Müller-Tidow C, Goldschmidt H, Hundemer M. (2019) **Cereblon-binding proteins expression levels correlate with hyperdiploidy in newly diagnosed multiple myeloma patients.** Blood Cancer Journal

Awwad MHS, Kriegsmann K, Plaumann J, Benn M, Hillengass J, Raab MS, Bertsch U, Munder M, Weisel K, Salwender HJ, Hänel M, Fenk R, Dürig J, Müller-Tidow C, Goldschmidt H, Hundemer M. (2018) The prognostic and predictive value of IKZF1 and IKZF3 expression in T-cells in patients with multiple myeloma. Oncoimmunology Journal

Plaumann J, Engelhardt M, **Awwad MHS**, Echchannaoui H, Amman E, Raab MS, Hillengass J, Halama N, Neuber B, Müller-Tidow C, Goldschmidt H, Hundemer M. (2018) **IL-10 inducible CD8+ regulatory T-cells are enriched in patients with multiple myeloma and impact the generation of antigen-specific T-cells.** Cancer Immunol Immunotherapy Journal

Kriegsmann K, Dittrich T, Neuber B, **Awwad MHS**, Hegenbart U, Goldschmidt H, Hillengass J, Hose D, Seckinger A, Müller-Tidow C, Ho AD, Schönland S, Hundemer M. (2018) **Quantification of number of CD38 sites on bone marrow plasma cells in patients with light chain amyloidosis and smoldering multiple myeloma.** Cytometry B Clinical Cytometry Journal

Neuber B, Dai J, Waraich WA, **Awwad MHS**, Engelhardt M, Schmitt M, Medenhoff S, Witzens-Harig M, Ho AD, Goldschmidt H, Hundemer M. (2017) **Lenalidomide overcomes the immunosuppression of regulatory CD8+CD28- T-cells.** Oncotarget Journal

Zusammenfassung

Trotz der Fortschritte in der immuntherapeutischen Entwicklung sind bisher nur zwei monoklonale Antikörper für die Behandlung des Multiplen Myeloms zugelassen. Einer davon ist Elotuzumab, ein spezifischer Antikörper der gegen SLAMF7. Der Wirkmechanismus von Elotuzumab ist bisher nur teilweise beschrieben, zum einen zeigt sich eine direkte zelluläre Zytotoxizität des Antikörpers gegen Zellen des Multiplen Myeloms, zum anderen eine Modulation von „natürlichen Killer Zellen“. Die Wirkung von Elotuzumab auf T-Zellen, die ebenfalls auf ihrer Oberfläche SLAMF7 exprimieren, wurde bisher nicht analysiert. Ziel meiner Arbeit war zu untersuchen, auf welchen T-Zell Populationen SLAMF7 exprimiert wird, seine Funktion in T-Zellen zu beschreiben und den Einfluss von Elotuzumab auf T-Zellen bei Patienten mit Multiplem Myelom zu demonstrieren.

Ich analysierte die SLAMF7-Expression auf T-Zellen von Patienten mit Multiplem Myelom vor und nach einer Induktionschemotherapie mit oder ohne Elotuzumab. Desweitern verwendeten wir ein SLAMF7 CRISPR-Cas9-Knock-out-Modell, um dessen Funktion zusammen mit einem Hochdurchsatz-RNA-Transkriptom-Sequenzierungsansatz zu analysieren. Darüber hinaus habe ich umfangreiche immunologische Funktionsanalysen durchgeführt, um den Einfluss von SLAMF7-positiven T-Zellen bezüglich der Immunantwort auf Zellen des Multiplen Myeloms zu untersuchen.

Als erstes Ergebnis stellte ich fest, dass SLAMF7 auf T-Zellen, insbesondere auf $CD8^+$ T-Zellen, exprimiert wurde, CD4+ T-Zellen zeigten dagegen nur eine geringe Expression. In weitergehenden Untersuchungen des Immunphänotyp von $SLAMF7^+$ $CD8^+$ T-Zellen fand ich heraus, dass diese Zellen einen ähnlichen Phänotyp wie $CD8^+$ $CD28^-$ $CD57^+$ T-Zellen aufweisen, eine Subpopulation, die bereits als immunsuppressiv in der Literatur beschrieben wurde. Den suppressiven Charakter dieser Zellpopulation konnte ich molekularbiologisch mittels RNA-Sequenzierung weiter bestätigen.

ELISPOT-Assays mit T-Zellen von Patienten mit einer hohen und niedrigen Frequenz von $SLAMF7^+$ $CD8^+$ T-Zellen zeigten, dass Patienten mit einer hohen Frequenz von $SLAMF7^+$ $CD8^+$ T-Zellen eine schwächere zytotoxische Aktivität

haben. In einem weiteren Experiment, bei dem ich T-Zellen von gesunden Spendern in An- oder Abwesenheit von SLAMF7$^+$ CD8$^+$ T-Zellen, die aus Myelom-Patienten isoliert wurden, kultivierte, stellte ich fest, dass die Zugabe von SLAMF7$^+$ CD8$^+$ T-Zellen die antigenspezifische T-Zellantwort unterdrückte. Dieses Ergebnis bestätigte den immunsuppressiven Charakter dieser T-Zellen. Mittels Analysen der SLAMF7-Expression aus dem peripheren Blut der Patienten vor und nach einer Induktionstherapie mit oder ohne Elotuzumab innerhalb der GMMG HD7 Studie konnte ich zeigen, dass eine starke Abnahme der Anzahl der SLAMF7$^+$ CD8$^+$ T-Zellen nach der Induktionstherapie bei Patienten die Elotuzumab erhielten, auftritt.

In Zusammenarbeit mit Heiko Bruns von der Universität Erlangen fanden wir heraus, dass die Mehrheit der SLAMF7$^+$ CD8$^+$ T-Zellen nach Zugabe von Elotuzumab *in vitro* von autologen Makrophagen phagozytiert wurde. Um diesen Befund *in vivo* zu bestätigen, haben Hakim Echchannaoui von der Universität Mainz und ich einen ähnlichen Ansatz in einem Myelom-Mausmodell durchgeführt. Nach der Injektion von SLAMF7$^+$ CD8$^+$ T-Zellen, die gegen den in diesen Mäusen etablierten Tumorklon des Multiplen Myeloms gerichtet waren, zeigten die Mäuse, die Elotuzumab erhielten, weniger tumorinfiltrierende SLAMF7$^+$ CD8$^+$ T-Zellen. Das bestätigte, dass auch in diesem Versuchsaufbau diese Zellen durch Elotuzumab wurden.

Meine Arbeit wirft ein neues Licht auf den immunologischen Wirkmechanismus des Anti-SLAMF7-Antikörpers Elotuzumab. Bisher ging man davon aus, dass der Anti-SLAMF7-Antikörper nur dann wirkt, wenn er direkt auf Myelomzellen abzielt oder wenn er „natürliche Killer-Zellen“ moduliert. Die in meiner Arbeit dargelegten Befunde sprechen für einen weiteren therapeutischen Mechanismus, der die Elimination von immunsuppressive T-Zellen betrifft. Dieser Mechanismus könnte für immuntherapeutische Ansätze, nicht nur beim Multiplen Myelom, sondern auch bei anderen Tumorentitäten von Bedeutung sein.

Appendices

List of Upregulated Genes: SLAMF7^{+} vs SLAMF7^{-}

Gene	Log2FoldChange	*p*adj	Description
SERPINA1	17.07146463	1.63E-06	serpin peptidase inhibitor, clade A (alpha-1 antiproteinase, antitrypsin), member 1 [Source:HGNC Symbol;Acc:8941]
S100A12	15.35268158	5.79E-05	S100 calcium binding protein A12 [Source:HGNC Symbol;Acc:10489]
B3GNT7	13.79944682	1.79E-18	UDP-GlcNAc:betaGal beta-1,3-N-acetylglucosaminyltransferase 7 [Source:HGNC Symbol;Acc:18811]
FPR1	13.78510117	9.57E-05	formyl peptide receptor 1 [Source:HGNC Symbol;Acc:3826]
LILRB2	13.56814201	0.000181943	leukocyte immunoglobulin-like receptor, subfamily B (with TM and ITIM domains), member 2 [Source:HGNC Symbol;Acc:6606]
TREM1	13.50634182	0.000108176	triggering receptor expressed on myeloid cells 1 [Source:HGNC Symbol;Acc:17760]
IL1RN	13.2958462	1.59E-05	interleukin 1 receptor antagonist [Source:HGNC Symbol;Acc:6000]
MPEG1	13.23639441	0.000149181	macrophage expressed 1 [Source:HGNC Symbol;Acc:29619]
IL1B	12.67850084	2.02E-10	interleukin 1, beta [Source:HGNC Symbol;Acc:5992]
LILRA3	12.58685464	0.000343032	leukocyte immunoglobulin-like receptor, subfamily A (without TM domain), member 3 [Source:HGNC Symbol;Acc:6604]
CCR1	12.58085515	6.80E-06	chemokine (C-C motif) receptor 1 [Source:HGNC Symbol;Acc:1602]
MNDA	12.48234088	0.000193837	myeloid cell nuclear differentiation antigen [Source:HGNC Symbol;Acc:7183]
SLC1A7	12.31708078	1.36E-07	solute carrier family 1 (glutamate transporter), member 7 [Source:HGNC Symbol;Acc:10945]
KIR3DX1	12.15436741	1.65E-14	killer cell immunoglobulin-like receptor, three domains, X1 [Source:HGNC Symbol;Acc:25043]
SYK	12.10181103	0.000343332	spleen tyrosine kinase [Source:HGNC Symbol;Acc:11491]
IL8	12.04733286	2.34E-05	interleukin 8 [Source:HGNC Symbol;Acc:6025]
KIR2DL3	11.95383963	2.71E-14	killer cell immunoglobulin-like receptor, two domains, long cytoplasmic tail, 3 [Source:HGNC Symbol;Acc:6331]
CD93	11.95015813	1.54E-06	CD93 molecule [Source:HGNC Symbol;Acc:15855]
KIR3DL1	11.89824393	4.10E-05	killer cell immunoglobulin-like receptor, three domains, long cytoplasmic tail, 1 [Source:HGNC Symbol;Acc:6338]
APOBEC3A	11.86964885	6.08E-06	apolipoprotein B mRNA editing enzyme, catalytic polypeptide-like 3A [Source:HGNC Symbol;Acc:17343]
CD300LF	11.85403042	0.00024319	CD300 molecule-like family member f [Source:HGNC Symbol;Acc:29883]
THBD	11.84187147	4.19E-05	thrombomodulin [Source:HGNC Symbol;Acc:11784]
MSR1	11.82538859	0.001915805	macrophage scavenger receptor 1 [Source:HGNC Symbol;Acc:7376]
S100A8	11.72559157	2.28E-09	S100 calcium binding protein A8 [Source:HGNC Symbol;Acc:10498]
CD86	11.68638615	3.86E-05	CD86 molecule [Source:HGNC Symbol;Acc:1705]
VCAN	11.62916111	3.61E-07	versican [Source:HGNC Symbol;Acc:2464]
CD300LB	11.61073747	8.97E-05	CD300 molecule-like family member b [Source:HGNC Symbol;Acc:30811]
GPR141	11.58957849	2.02E-13	G protein-coupled receptor 141 [Source:HGNC Symbol;Acc:19997]
FCGR2A	11.58858922	3.88E-06	Fc fragment of IgG, low affinity IIa, receptor (CD32) [Source:HGNC Symbol;Acc:3616]
ITGAX	11.51020161	6.68E-11	integrin, alpha X (complement component 3 receptor 4 subunit) [Source:HGNC Symbol;Acc:6152]
HNMT	11.42933608	0.000335321	histamine N-methyltransferase [Source:HGNC Symbol;Acc:5028]
LRRC25	11.41537466	0.00011945	leucine rich repeat containing 25 [Source:HGNC Symbol;Acc:29806]
LILRB1	11.2806627	4.58E-17	leukocyte immunoglobulin-like receptor, subfamily B (with TM and ITIM domains), member 1 [Source:HGNC Symbol;Acc:6605]
SDC2	11.27550337	0.002764851	syndecan 2 [Source:HGNC Symbol;Acc:10659]
CPVL	11.2320864	4.26E-07	carboxypeptidase, vitellogenic-like [Source:HGNC Symbol;Acc:14399]
PRSS30P	11.17522181	4.40E-11	protease, serine, 30, pseudogene [Source:HGNC Symbol;Acc:28753]
GPR153	11.07986909	3.91E-11	G protein-coupled receptor 153 [Source:HGNC Symbol;Acc:23618]
MEF2C	10.89853178	0.000481238	myocyte enhancer factor 2C [Source:HGNC Symbol;Acc:6996]
KLRC2	10.84919404	1.13E-17	killer cell lectin-like receptor subfamily C, member 2 [Source:HGNC Symbol;Acc:6375]

KYNU	10.5894133	0.000407392	kynureninase [Source:HGNC Symbol;Acc:6469]
NFAM1	10.481808	0.000815113	NFAT activating protein with ITAM motif 1 [Source:HGNC Symbol;Acc:29872]
PID1	10.47553194	0.002957953	phosphotyrosine interaction domain containing 1 [Source:HGNC Symbol;Acc:26084]
B3GAT1	10.38728064	3.80E-14	beta-1,3-glucuronyltransferase 1 (glucuronosyltransferase P) [Source:HGNC Symbol;Acc:921]
FCN1	10.3872558	2.23E-06	ficolin (collagen/fibrinogen domain containing) 1 [Source:HGNC Symbol;Acc:3623]
CHST15	10.38623532	0.000599797	carbohydrate (N-acetylgalactosamine 4-sulfate 6-O) sulfotransferase 15 [Source:HGNC Symbol;Acc:18137]
RAB31	10.3719091	1.94E-05	RAB31, member RAS oncogene family [Source:HGNC Symbol;Acc:9771]
ST14	10.36334057	0.001747855	suppression of tumorigenicity 14 (colon carcinoma) [Source:HGNC Symbol;Acc:11344]
OLR1	10.31949025	0.002721399	oxidized low density lipoprotein (lectin-like) receptor 1 [Source:HGNC Symbol;Acc:8133]
PDGFRB	10.22499007	2.56E-10	platelet-derived growth factor receptor, beta polypeptide [Source:HGNC Symbol;Acc:8804]
MAFB	10.21677103	0.000135715	v-maf avian musculoaponeurotic fibrosarcoma oncogene homolog B [Source:HGNC Symbol;Acc:6408]
ADRB1	10.12195615	4.89E-09	adrenoceptor beta 1 [Source:HGNC Symbol;Acc:285]
SIGLEC14	10.10552484	0.000571418	sialic acid binding Ig-like lectin 14 [Source:HGNC Symbol;Acc:32926]
NME8	10.00270039	8.41E-13	NME/NM23 family member 8 [Source:HGNC Symbol;Acc:16473]
LYZ	9.986935196	8.10E-09	lysozyme [Source:HGNC Symbol;Acc:6740]
KIR2DL4	9.955935478	2.11E-07	killer cell immunoglobulin-like receptor, two domains, long cytoplasmic tail, 4 [Source:HGNC Symbol;Acc:6332]
MS4A7	9.852344781	0.000105382	membrane-spanning 4-domains, subfamily A, member 7 [Source:HGNC Symbol;Acc:13378]
SH2D1B	9.78443818	6.82E-11	SH2 domain containing 1B [Source:HGNC Symbol;Acc:30416]
CXCL3	9.776589866	0.000210514	chemokine (C-X-C motif) ligand 3 [Source:HGNC Symbol;Acc:4604]
ANPEP	9.754683635	0.000444534	alanyl (membrane) aminopeptidase [Source:HGNC Symbol;Acc:500]
FXYD6	9.712386419	2.40E-06	FXYD domain containing ion transport regulator 6 [Source:HGNC Symbol;Acc:4030]
PMP22	9.683976045	0.001590729	peripheral myelin protein 22 [Source:HGNC Symbol;Acc:9118]
CST3	9.552689301	1.38E-05	cystatin C [Source:HGNC Symbol;Acc:2475]
HSPA6	9.516927923	1.41E-07	heat shock 70kDa protein 6 (HSP70B') [Source:HGNC Symbol;Acc:5239]
CLEC7A	9.457901434	0.000592681	C-type lectin domain family 7, member A [Source:HGNC Symbol;Acc:14558]
AQP9	9.447930446	0.00021338	aquaporin 9 [Source:HGNC Symbol;Acc:643]
RCVRN	9.348890738	1.00E-06	recoverin [Source:HGNC Symbol;Acc:9937]
EFNA5	9.329615199	4.77E-08	ephrin-A5 [Source:HGNC Symbol;Acc:3225]
TNNI2	9.312996614	0.000201874	troponin I type 2 (skeletal, fast) [Source:HGNC Symbol;Acc:11946]
MET	9.310698883	0.005489354	met proto-oncogene [Source:HGNC Symbol;Acc:7029]
LMO2	9.232013742	1.08E-08	LIM domain only 2 (rhombotin-like 1) [Source:HGNC Symbol;Acc:6642]
TNS1	9.216184016	4.73E-06	tensin 1 [Source:HGNC Symbol;Acc:11973]
PLAU	9.169396124	5.60E-06	plasminogen activator, urokinase [Source:HGNC Symbol;Acc:9052]
PLXDC2	9.127941581	0.000173941	plexin domain containing 2 [Source:HGNC Symbol;Acc:21013]
MLC1	9.055447068	4.38E-11	megalencephalic leukoencephalopathy with subcortical cysts 1 [Source:HGNC Symbol;Acc:17082]
SLC22A18AS	9.047877472	3.77E-05	solute carrier family 22 (organic cation transporter), member 18 antisense [Source:HGNC Symbol;Acc:10965]
FCGR2C	8.959163722	5.04E-10	Fc fragment of IgG, low affinity IIc, receptor for (CD32) (gene/pseudogene) [Source:HGNC Symbol;Acc:15626]
LGALS2	8.934312791	0.000793812	lectin, galactoside-binding, soluble, 2 [Source:HGNC Symbol;Acc:6562]
SCD5	8.925311441	1.73E-06	stearoyl-CoA desaturase 5 [Source:HGNC Symbol;Acc:21088]
SGCD	8.904565775	4.32E-05	sarcoglycan, delta (35kDa dystrophin-associated glycoprotein) [Source:HGNC Symbol;Acc:10807]
FFAR2	8.894983519	9.22E-05	free fatty acid receptor 2 [Source:HGNC Symbol;Acc:4501]
SPRY2	8.892026311	1.21E-09	sprouty homolog 2 (Drosophila) [Source:HGNC Symbol;Acc:11270]
S100A9	8.890072642	2.53E-06	S100 calcium binding protein A9 [Source:HGNC Symbol;Acc:10499]
KLRD1	8.82349762	1.58E-46	killer cell lectin-like receptor subfamily D, member 1 [Source:HGNC Symbol;Acc:6378]
FCGR3A	8.822726754	1.82E-05	Fc fragment of IgG, low affinity IIIa, receptor (CD16a) [Source:HGNC Symbol;Acc:3619]

FCGR1B	8.79522621	4.11E-05	Fc fragment of IgG, high affinity Ib, receptor (CD64) [Source:HGNC Symbol;Acc:3614]
GZMB	8.746744058	1.31E-29	granzyme B (granzyme 2, cytotoxic T-lymphocyte-associated serine esterase 1) [Source:HGNC Symbol;Acc:4709]
LGALS12	8.729352727	7.16E-05	lectin, galactoside-binding, soluble, 12 [Source:HGNC Symbol;Acc:15788]
HOXA10	8.720456332	1.52E-06	homeobox A10 [Source:HGNC Symbol;Acc:5100]
CYP1B1	8.692130257	0.000710413	cytochrome P450, family 1, subfamily B, polypeptide 1 [Source:HGNC Symbol;Acc:2597]
CXCL2	8.653270788	0.000122815	chemokine (C-X-C motif) ligand 2 [Source:HGNC Symbol;Acc:4603]
PTGS1	8.626757933	0.00139757	prostaglandin-endoperoxide synthase 1 (prostaglandin G/H synthase and cyclooxygenase) [Source:HGNC Symbol;Acc:9604]
PF4V1	8.540089024	0.000236251	platelet factor 4 variant 1 [Source:HGNC Symbol;Acc:8862]
KIR2DS4	8.511761388	6.05E-12	killer cell immunoglobulin-like receptor, two domains, short cytoplasmic tail, 4 [Source:HGNC Symbol;Acc:6336]
CSF3R	8.462602642	0.000183508	colony stimulating factor 3 receptor (granulocyte) [Source:HGNC Symbol;Acc:2439]
ASCL2	8.425799123	2.51E-05	achaete-scute family bHLH transcription factor 2 [Source:HGNC Symbol;Acc:739]
SIRPA	8.413892617	0.001196773	signal-regulatory protein alpha [Source:HGNC Symbol;Acc:9662]
TYROBP	8.404036396	3.56E-28	TYRO protein tyrosine kinase binding protein [Source:HGNC Symbol;Acc:12449]
AC068580.6	8.39282167	0.000179671	
FGR	8.370706643	4.51E-19	feline Gardner-Rasheed sarcoma viral oncogene homolog [Source:HGNC Symbol;Acc:3697]
PLA2G7	8.337375793	0.00011653	phospholipase A2, group VII (platelet-activating factor acetylhydrolase, plasma) [Source:HGNC Symbol;Acc:9040]
TMEM158	8.23907985	0.010607313	transmembrane protein 158 (gene/pseudogene) [Source:HGNC Symbol;Acc:30293]
LIM2	8.228155303	4.19E-05	lens intrinsic membrane protein 2, 19kDa [Source:HGNC Symbol;Acc:6610]
APOA2	8.213447443	0.00033024	apolipoprotein A-II [Source:HGNC Symbol;Acc:601]
LAMB3	8.194072648	1.07E-06	laminin, beta 3 [Source:HGNC Symbol;Acc:6490]
FAM20C	8.170993327	0.002335446	family with sequence similarity 20, member C [Source:HGNC Symbol;Acc:22140]
CSF2RA	8.096501101	0.00029985	colony stimulating factor 2 receptor, alpha, low-affinity (granulocyte-macrophage) [Source:HGNC Symbol;Acc:2435]
FAM49A	8.083848725	3.25E-31	family with sequence similarity 49, member A [Source:HGNC Symbol;Acc:25373]
KIR2DP1	8.078322544	0.000164464	killer cell immunoglobulin-like receptor, two domains, pseudogene 1 [Source:HGNC Symbol;Acc:16344]
C5AR2	8.077384329	0.000251521	complement component 5a receptor 2 [Source:HGNC Symbol;Acc:4527]
SETBP1	8.063202019	3.49E-32	SET binding protein 1 [Source:HGNC Symbol;Acc:15573]
AC069363.1	8.062905297	1.05E-07	
CATSPER1	7.973228258	0.000613604	cation channel, sperm associated 1 [Source:HGNC Symbol;Acc:17116]
CCDC149	7.9564015	0.000359557	coiled-coil domain containing 149 [Source:HGNC Symbol;Acc:25405]
AC104809.4	7.94372182	0.000526469	
PRSS23	7.884511217	2.07E-25	protease, serine, 23 [Source:HGNC Symbol;Acc:14370]
AC011747.3	7.879135083	0.000441926	
LRRK1	7.805800838	0.000351386	leucine-rich repeat kinase 1 [Source:HGNC Symbol;Acc:18608]
RBM47	7.794748197	0.000648987	RNA binding motif protein 47 [Source:HGNC Symbol;Acc:30358]
CXCR1	7.792742659	0.000107089	chemokine (C-X-C motif) receptor 1 [Source:HGNC Symbol;Acc:6026]
FGFBP2	7.778465017	5.08E-48	fibroblast growth factor binding protein 2 [Source:HGNC Symbol;Acc:29451]
CMKLR1	7.7746477	1.73E-07	chemokine-like receptor 1 [Source:HGNC Symbol;Acc:2121]
RETN	7.76928432	0.001467808	resistin [Source:HGNC Symbol;Acc:20389]
SORT1	7.760079949	5.95E-05	sortilin 1 [Source:HGNC Symbol;Acc:11186]
HMOX1	7.753567647	5.60E-07	heme oxygenase (decycling) 1 [Source:HGNC Symbol;Acc:5013]
CCL4L2	7.704963243	5.36E-11	chemokine (C-C motif) ligand 4-like 2 [Source:HGNC Symbol;Acc:24066]
PDGFD	7.669801702	1.29E-07	platelet derived growth factor D [Source:HGNC Symbol;Acc:30620]
CES1	7.657523644	0.011248465	carboxylesterase 1 [Source:HGNC Symbol;Acc:1863]
AC017104.6	7.621976699	1.59E-07	

BIRC7	7.572185806	1.65E-06	baculoviral IAP repeat containing 7 [Source:HGNC Symbol;Acc:13702]
HSPA7	7.493124867	3.99E-09	heat shock 70kDa protein 7 (HSP70B) [Source:HGNC Symbol;Acc:5240]
SPRED1	7.41935953	0.000251521	sprouty-related, EVH1 domain containing 1 [Source:HGNC Symbol;Acc:20249]
JDP2	7.415582475	0.001286529	Jun dimerization protein 2 [Source:HGNC Symbol;Acc:17546]
ALDH3B1	7.399076577	0.001570988	aldehyde dehydrogenase 3 family, member B1 [Source:HGNC Symbol;Acc:410]
KIFC3	7.398431826	3.21E-09	kinesin family member C3 [Source:HGNC Symbol;Acc:6326]
STAB1	7.393592428	0.000111754	stabilin 1 [Source:HGNC Symbol;Acc:18628]
FOXA3	7.353521475	0.000208051	forkhead box A3 [Source:HGNC Symbol;Acc:5023]
C3orf65	7.309815366	0.001112607	chromosome 3 open reading frame 65 [Source:HGNC Symbol;Acc:32674]
EREG	7.307614578	0.001766248	epiregulin [Source:HGNC Symbol;Acc:3443]
S1PR3	7.307447949	3.82E-05	sphingosine-1-phosphate receptor 3 [Source:HGNC Symbol;Acc:3167]
CCDC89	7.280974733	0.000257749	coiled-coil domain containing 89 [Source:HGNC Symbol;Acc:26762]
MT1DP	7.271385496	0.000370554	metallothionein 1D, pseudogene [Source:HGNC Symbol;Acc:7396]
MERTK	7.235704043	0.001768005	c-mer proto-oncogene tyrosine kinase [Source:HGNC Symbol;Acc:7027]
FCAR	7.190054233	0.002057521	Fc fragment of IgA, receptor for [Source:HGNC Symbol;Acc:3608]
CDA	7.18551144	0.000150855	cytidine deaminase [Source:HGNC Symbol;Acc:1712]
FCER1G	7.181421602	3.25E-05	Fc fragment of IgE, high affinity I, receptor for; gamma polypeptide [Source:HGNC Symbol;Acc:3611]
PIK3AP1	7.162331126	7.09E-31	phosphoinositide-3-kinase adaptor protein 1 [Source:HGNC Symbol;Acc:30034]
GPR56	7.153567807	3.98E-17	G protein-coupled receptor 56 [Source:HGNC Symbol;Acc:4512]
FCGR2B	7.143111887	0.000493858	Fc fragment of IgG, low affinity IIb, receptor (CD32) [Source:HGNC Symbol;Acc:3618]
TBC1D12	7.133685853	0.002595006	TBC1 domain family, member 12 [Source:HGNC Symbol;Acc:29082]
CCL4L1	7.11412696	0.001268679	chemokine (C-C motif) ligand 4-like 1 [Source:HGNC Symbol;Acc:10631]
PCDH1	7.095288986	6.11E-13	protocadherin 1 [Source:HGNC Symbol;Acc:8655]
KRT86	7.090373929	2.76E-05	keratin 86 [Source:HGNC Symbol;Acc:6463]
LYN	7.088875471	4.14E-19	v-yes-1 Yamaguchi sarcoma viral related oncogene homolog [Source:HGNC Symbol;Acc:6735]
S1PR5	7.054016345	1.32E-23	sphingosine-1-phosphate receptor 5 [Source:HGNC Symbol;Acc:14299]
NKG7	7.027061707	7.09E-31	natural killer cell group 7 sequence [Source:HGNC Symbol;Acc:7830]
CYP4F22	7.021958469	0.002583286	cytochrome P450, family 4, subfamily F, polypeptide 22 [Source:HGNC Symbol;Acc:26820]
ETV1	7.008710026	0.001460989	ets variant 1 [Source:HGNC Symbol;Acc:3490]
KCNE1	6.967093762	0.001449437	potassium voltage-gated channel, Isk-related family, member 1 [Source:HGNC Symbol;Acc:6240]
IGJ	6.907089604	0.00347612	immunoglobulin J polypeptide, linker protein for immunoglobulin alpha and mu polypeptides [Source:HGNC Symbol;Acc:5713]
HCAR2	6.904461721	0.003197469	hydroxycarboxylic acid receptor 2 [Source:HGNC Symbol;Acc:24827]
TNS3	6.902110244	0.00242697	tensin 3 [Source:HGNC Symbol;Acc:21616]
CCL3	6.878491385	1.58E-22	chemokine (C-C motif) ligand 3 [Source:HGNC Symbol;Acc:10627]
CSTA	6.84382251	0.005959539	cystatin A (stefin A) [Source:HGNC Symbol;Acc:2481]
AP000695.6	6.815245052	0.005187961	
HHEX	6.808550646	1.19E-11	hematopoietically expressed homeobox [Source:HGNC Symbol;Acc:4901]
SEMA6B	6.790016	0.00042231	sema domain, transmembrane domain (TM), and cytoplasmic domain, (semaphorin) 6B [Source:HGNC Symbol;Acc:10739]
TRPM4	6.776907301	0.002764851	transient receptor potential cation channel, subfamily M, member 4 [Source:HGNC Symbol;Acc:17993]
AC009951.2	6.745363038	2.88E-10	
CXXC11	6.728667865	0.002579872	CXXC finger protein 11 [Source:HGNC Symbol;Acc:26585]
GZMH	6.722685452	8.27E-20	granzyme H (cathepsin G-like 2, protein h-CCPX) [Source:HGNC Symbol;Acc:4710]
RGS9	6.720409774	9.22E-23	regulator of G-protein signaling 9 [Source:HGNC Symbol;Acc:10004]
PTRF	6.709847293	0.004283807	polymerase I and transcript release factor [Source:HGNC Symbol;Acc:9688]
IL1RL2	6.705137859	9.96E-07	interleukin 1 receptor-like 2 [Source:HGNC Symbol;Acc:5999]

PLXNB2	6.688767171	0.001581184	plexin B2 [Source:HGNC Symbol;Acc:9104]
FRMPD3	6.650297506	3.24E-18	FERM and PDZ domain containing 3 [Source:HGNC Symbol;Acc:29382]
NMUR1	6.579493625	1.77E-13	neuromedin U receptor 1 [Source:HGNC Symbol;Acc:4518]
UCN2	6.571302291	0.003601284	urocortin 2 [Source:HGNC Symbol;Acc:18414]
NLRP12	6.556979799	0.000421092	NLR family, pyrin domain containing 12 [Source:HGNC Symbol;Acc:22938]
BNC2	6.556332288	1.79E-11	basonuclin 2 [Source:HGNC Symbol;Acc:30988]
IL1R2	6.53421422	1.02E-07	interleukin 1 receptor, type II [Source:HGNC Symbol;Acc:5994]
PLEK	6.524027627	8.91E-16	pleckstrin [Source:HGNC Symbol;Acc:9070]
RN7SL798P	6.486054526	0.002579872	RNA, 7SL, cytoplasmic 798, pseudogene [Source:HGNC Symbol;Acc:46814]
TFCP2L1	6.476544268	3.64E-09	transcription factor CP2-like 1 [Source:HGNC Symbol;Acc:17925]
DTNA	6.464319208	0.006832924	dystrobrevin, alpha [Source:HGNC Symbol;Acc:3057]
SLC9A3R2	6.456408276	0.002403732	solute carrier family 9, subfamily A (NHE3, cation proton antiporter 3), member 3 regulator 2 [Source:HGNC Symbol;Acc:11076]
MS4A6A	6.450983081	0.000390454	membrane-spanning 4-domains, subfamily A, member 6A [Source:HGNC Symbol;Acc:13375]
NUAK1	6.429018779	1.77E-12	NUAK family, SNF1-like kinase, 1 [Source:HGNC Symbol;Acc:14311]
XCL2	6.42668446	7.18E-19	chemokine (C motif) ligand 2 [Source:HGNC Symbol;Acc:10646]
CCL4	6.420964655	7.58E-16	chemokine (C-C motif) ligand 4 [Source:HGNC Symbol;Acc:10630]
GPR97	6.412526519	2.25E-12	G protein-coupled receptor 97 [Source:HGNC Symbol;Acc:13728]
CEBPD	6.401371047	0.002579872	CCAAT/enhancer binding protein (C/EBP), delta [Source:HGNC Symbol;Acc:1835]
VCAM1	6.380466648	6.57E-09	vascular cell adhesion molecule 1 [Source:HGNC Symbol;Acc:12663]
P2RX1	6.29328026	0.000371001	purinergic receptor P2X, ligand-gated ion channel, 1 [Source:HGNC Symbol;Acc:8533]
VMO1	6.270508654	0.000444199	vitelline membrane outer layer 1 homolog (chicken) [Source:HGNC Symbol;Acc:30387]
VEGFA	6.266380646	1.24E-09	vascular endothelial growth factor A [Source:HGNC Symbol;Acc:12680]
HP	6.260629177	1.42E-05	haptoglobin [Source:HGNC Symbol;Acc:5141]
C9orf47	6.241368823	0.011096143	chromosome 9 open reading frame 47 [Source:HGNC Symbol;Acc:23669]
ARHGEF28	6.229701635	1.64E-07	Rho guanine nucleotide exchange factor (GEF) 28 [Source:HGNC Symbol;Acc:30322]
ANGPTL2	6.21083359	0.003749718	angiopoietin-like 2 [Source:HGNC Symbol;Acc:490]
INHBA	6.208807783	0.001301062	inhibin, beta A [Source:HGNC Symbol;Acc:6066]
TRGV8	6.206497558	0.000989185	T cell receptor gamma variable 8 [Source:HGNC Symbol;Acc:12294]
HBQ1	6.20249568	0.01277726	hemoglobin, theta 1 [Source:HGNC Symbol;Acc:4833]
MS4A14	6.192069256	0.010862542	membrane-spanning 4-domains, subfamily A, member 14 [Source:HGNC Symbol;Acc:30706]
AC064874.1	6.174797392	0.009715987	Uncharacterized protein [Source:UniProtKB/TrEMBL;Acc:B8ZZ52]
C9orf139	6.140820165	0.011594212	chromosome 9 open reading frame 139 [Source:HGNC Symbol;Acc:31426]
MEG3	6.137887633	2.56E-05	maternally expressed 3 (non-protein coding) [Source:HGNC Symbol;Acc:14575]
DYSF	6.133849738	9.84E-10	dysferlin [Source:HGNC Symbol;Acc:3097]
GNLY	6.129332883	2.19E-37	granulysin [Source:HGNC Symbol;Acc:4414]
CXXC5	6.107679301	5.35E-11	CXXC finger protein 5 [Source:HGNC Symbol;Acc:26943]
PLCG2	6.094458126	6.53E-22	phospholipase C, gamma 2 (phosphatidylinositol-specific) [Source:HGNC Symbol;Acc:9066]
AC009495.2	6.092606142	1.12E-08	
SCHIP1	6.087853194	0.000929734	schwannomin interacting protein 1 [Source:HGNC Symbol;Acc:15678]
VSTM1	6.085419661	0.001636192	V-set and transmembrane domain containing 1 [Source:HGNC Symbol;Acc:29455]
VIPR2	6.081565611	3.40E-05	vasoactive intestinal peptide receptor 2 [Source:HGNC Symbol;Acc:12695]
TMEM176B	6.080817691	0.005312987	transmembrane protein 176B [Source:HGNC Symbol;Acc:29596]
HK3	6.078538567	0.003350243	hexokinase 3 (white cell) [Source:HGNC Symbol;Acc:4925]
SIGLEC17P	6.077284418	1.72E-08	sialic acid binding Ig-like lectin 17, pseudogene [Source:HGNC Symbol;Acc:15604]
OSBPL5	6.069451374	6.00E-23	oxysterol binding protein-like 5 [Source:HGNC Symbol;Acc:16392]
PANX2	6.064671295	0.001235585	pannexin 2 [Source:HGNC Symbol;Acc:8600]

PRLR	6.012150496	0.012996884	prolactin receptor [Source:HGNC Symbol;Acc:9446]
LINC00883	6.010797206	2.65E-05	long intergenic non-protein coding RNA 883 [Source:HGNC Symbol;Acc:48569]
KRT18P16	6.000215145	0.014898737	keratin 18 pseudogene 16 [Source:HGNC Symbol;Acc:33384]
SLAMF7	5.997037418	6.94E-19	SLAM family member 7 [Source:HGNC Symbol;Acc:21394]
KLRC3	5.994303469	1.54E-09	killer cell lectin-like receptor subfamily C, member 3 [Source:HGNC Symbol;Acc:6376]
EDNRB	5.977407841	0.016320563	endothelin receptor type B [Source:HGNC Symbol;Acc:3180]
MYO3B	5.964074702	3.53E-07	myosin IIIB [Source:HGNC Symbol;Acc:15576]
COPZ2	5.953927093	2.70E-05	coatomer protein complex, subunit zeta 2 [Source:HGNC Symbol;Acc:19356]
TMTC1	5.953031484	0.001272202	transmembrane and tetratricopeptide repeat containing 1 [Source:HGNC Symbol;Acc:24099]
ITGAM	5.951496887	4.98E-44	integrin, alpha M (complement component 3 receptor 3 subunit) [Source:HGNC Symbol;Acc:6149]
LINC00384	5.951099425	0.0004814	long intergenic non-protein coding RNA 384 [Source:HGNC Symbol;Acc:42711]
GDF15	5.938408476	0.010301674	growth differentiation factor 15 [Source:HGNC Symbol;Acc:30142]
AC005932.1	5.93515489	0.01428356	
FCRL6	5.926831503	7.77E-24	Fc receptor-like 6 [Source:HGNC Symbol;Acc:31910]
RIN2	5.886775806	0.004126187	Ras and Rab interactor 2 [Source:HGNC Symbol;Acc:18750]
C1orf21	5.871266423	7.89E-05	chromosome 1 open reading frame 21 [Source:HGNC Symbol;Acc:15494]
SLCO4C1	5.867143959	8.32E-13	solute carrier organic anion transporter family, member 4C1 [Source:HGNC Symbol;Acc:23612]
TRGV7	5.854109573	1.01E-06	T cell receptor gamma variable 7 (pseudogene) [Source:HGNC Symbol;Acc:12293]
PTAFR	5.834383412	0.000329376	platelet-activating factor receptor [Source:HGNC Symbol;Acc:9582]
AC004540.5	5.803820526	0.017555993	
LGR6	5.759645101	5.72E-14	leucine-rich repeat containing G protein-coupled receptor 6 [Source:HGNC Symbol;Acc:19719]
HIC1	5.735621727	0.005869184	hypermethylated in cancer 1 [Source:HGNC Symbol;Acc:4909]
VNN1	5.728121534	0.016870924	vanin 1 [Source:HGNC Symbol;Acc:12705]
COBLL1	5.718757896	0.017117937	cordon-bleu WH2 repeat protein-like 1 [Source:HGNC Symbol;Acc:23571]
NAPSB	5.716601319	0.004458226	napsin B aspartic peptidase, pseudogene [Source:HGNC Symbol;Acc:13396]
LRFN2	5.710783806	0.012189634	leucine rich repeat and fibronectin type III domain containing 2 [Source:HGNC Symbol;Acc:21226]
PAQR4	5.700008963	0.009401429	progestin and adipoQ receptor family member IV [Source:HGNC Symbol;Acc:26386]
LINC00484	5.685265888	1.68E-06	long intergenic non-protein coding RNA 484 [Source:HGNC Symbol;Acc:27862]
NCR1	5.664522735	7.34E-12	natural cytotoxicity triggering receptor 1 [Source:HGNC Symbol;Acc:6731]
ZNF683	5.664505288	1.13E-16	zinc finger protein 683 [Source:HGNC Symbol;Acc:28495]
KIF7	5.662600848	0.003343745	kinesin family member 7 [Source:HGNC Symbol;Acc:30497]
GTSE1	5.638170854	1.98E-15	G-2 and S-phase expressed 1 [Source:HGNC Symbol;Acc:13698]
C15orf38	5.63445299	0.018012483	chromosome 15 open reading frame 38 [Source:HGNC Symbol;Acc:28782]
MN1	5.630959428	3.06E-08	meningioma (disrupted in balanced translocation) 1 [Source:HGNC Symbol;Acc:7180]
ZEB2	5.617811351	3.07E-18	zinc finger E-box binding homeobox 2 [Source:HGNC Symbol;Acc:14881]
AL391421.1	5.591639486	0.018506548	Uncharacterized protein; cDNA FLJ43696 fis, clone TBAES2007964 [Source:UniProtKB/TrEMBL;Acc:Q6ZUH9]
FAM129B	5.560347492	3.33E-06	family with sequence similarity 129, member B [Source:HGNC Symbol;Acc:25282]
SH3RF2	5.539880727	0.000227969	SH3 domain containing ring finger 2 [Source:HGNC Symbol;Acc:26299]
GAS7	5.536928977	1.14E-15	growth arrest-specific 7 [Source:HGNC Symbol;Acc:4169]
SATB2	5.532081926	1.06E-05	SATB homeobox 2 [Source:HGNC Symbol;Acc:21637]
NCAM1	5.512093723	1.43E-10	neural cell adhesion molecule 1 [Source:HGNC Symbol;Acc:7656]
AC092580.2	5.483395991	0.013900071	
SMKR1	5.48132768	0.014966484	small lysine-rich protein 1 [Source:HGNC Symbol;Acc:43561]
EMR3	5.46597425	0.001982303	egf-like module containing, mucin-like, hormone receptor-like 3 [Source:HGNC Symbol;Acc:23647]
C5AR1	5.465120859	0.001005477	complement component 5a receptor 1 [Source:HGNC Symbol;Acc:1338]
AC108448.2	5.457085166	8.29E-12	

MMP17	5.447225867	0.015471455	matrix metallopeptidase 17 (membrane-inserted) [Source:HGNC Symbol;Acc:7163]
CFD	5.441205158	0.002544123	complement factor D (adipsin) [Source:HGNC Symbol;Acc:2771]
PROK2	5.426879541	8.86E-13	prokineticin 2 [Source:HGNC Symbol;Acc:18455]
HBEGF	5.425606934	0.001481299	heparin-binding EGF-like growth factor [Source:HGNC Symbol;Acc:3059]
LGALS9B	5.425323679	0.003838227	lectin, galactoside-binding, soluble, 9B [Source:HGNC Symbol;Acc:24842]
AC009951.1	5.418707926	2.13E-18	
MYOF	5.389101972	0.003326841	myoferlin [Source:HGNC Symbol;Acc:3656]
MATK	5.363130872	5.55E-16	megakaryocyte-associated tyrosine kinase [Source:HGNC Symbol;Acc:6906]
PYGL	5.355382641	0.006376925	phosphorylase, glycogen, liver [Source:HGNC Symbol;Acc:9725]
SLC4A4	5.35306388	2.35E-09	solute carrier family 4 (sodium bicarbonate cotransporter), member 4 [Source:HGNC Symbol;Acc:11030]
SRC	5.332236228	4.54E-08	v-src avian sarcoma (Schmidt-Ruppin A-2) viral oncogene homolog [Source:HGNC Symbol;Acc:11283]
PADI2	5.330449308	0.003807699	peptidyl arginine deiminase, type II [Source:HGNC Symbol;Acc:18341]
EOMES	5.319268533	3.09E-34	eomesodermin [Source:HGNC Symbol;Acc:3372]
SPHK1	5.312693334	1.66E-09	sphingosine kinase 1 [Source:HGNC Symbol;Acc:11240]
TNFSF13	5.308696601	0.000100932	tumor necrosis factor (ligand) superfamily, member 13 [Source:HGNC Symbol;Acc:11928]
ZNF385A	5.292773934	1.40E-10	zinc finger protein 385A [Source:HGNC Symbol;Acc:17521]
HOXB9	5.283447204	0.005297181	homeobox B9 [Source:HGNC Symbol;Acc:5120]
FAM72A	5.255511114	0.002525813	family with sequence similarity 72, member A [Source:HGNC Symbol;Acc:24044]
KCNJ5	5.232665734	0.018362686	potassium inwardly-rectifying channel, subfamily J, member 5 [Source:HGNC Symbol;Acc:6266]
GOLIM4	5.232548434	2.13E-18	golgi integral membrane protein 4 [Source:HGNC Symbol;Acc:15448]
TCERG1L	5.227056052	3.12E-05	transcription elongation regulator 1-like [Source:HGNC Symbol;Acc:23533]
AGAP1	5.204002588	4.16E-16	ArfGAP with GTPase domain, ankyrin repeat and PH domain 1 [Source:HGNC Symbol;Acc:16922]
CD8A	5.196251803	1.14E-19	CD8a molecule [Source:HGNC Symbol;Acc:1706]
PSCA	5.163817407	0.006267695	prostate stem cell antigen [Source:HGNC Symbol;Acc:9500]
EIF2S2P3	5.154965667	0.002033462	eukaryotic translation initiation factor 2, subunit 2 beta pseudogene 3 [Source:HGNC Symbol;Acc:31664]
PIK3R3	5.146311923	4.16E-16	phosphoinositide-3-kinase, regulatory subunit 3 (gamma) [Source:HGNC Symbol;Acc:8981]
AC015969.3	5.140795967	0.020451575	
NLRP7	5.125743828	0.000137303	NLR family, pyrin domain containing 7 [Source:HGNC Symbol;Acc:22947]
RORB	5.103682512	0.005116751	RAR-related orphan receptor B [Source:HGNC Symbol;Acc:10259]
CLDND2	5.094928926	5.20E-10	claudin domain containing 2 [Source:HGNC Symbol;Acc:28511]
FHAD1	5.084179114	4.58E-10	forkhead-associated (FHA) phosphopeptide binding domain 1 [Source:HGNC Symbol;Acc:29408]
IQSEC2	5.081463269	1.66E-05	IQ motif and Sec7 domain 2 [Source:HGNC Symbol;Acc:29059]
AC004840.9	5.080135655	8.95E-10	
LINC00163	5.078261104	0.007525086	long intergenic non-protein coding RNA 163 [Source:HGNC Symbol;Acc:33165]
IL19	5.0708284	0.002506491	interleukin 19 [Source:HGNC Symbol;Acc:5990]
LTBP1	5.070599592	0.000702795	latent transforming growth factor beta binding protein 1 [Source:HGNC Symbol;Acc:6714]
SLC47A1	5.070170372	0.000363049	solute carrier family 47 (multidrug and toxin extrusion), member 1 [Source:HGNC Symbol;Acc:25588]
BASP1	5.068931206	0.01137019	brain abundant, membrane attached signal protein 1 [Source:HGNC Symbol;Acc:957]
CX3CR1	5.059848937	1.85E-07	chemokine (C-X3-C motif) receptor 1 [Source:HGNC Symbol;Acc:2558]
GAS2L1	5.059474595	0.000694979	growth arrest-specific 2 like 1 [Source:HGNC Symbol;Acc:16955]
THBS1	5.058413081	0.00050966	thrombospondin 1 [Source:HGNC Symbol;Acc:11785]
LYNX1	5.008180579	0.004281332	Ly6/neurotoxin 1 [Source:HGNC Symbol;Acc:29604]
AC051649.12	4.98420181	0.024441914	
EMR2	4.964011751	1.97E-06	egf-like module containing, mucin-like, hormone receptor-like 2 [Source:HGNC Symbol;Acc:3337]
SIGLEC10	4.944294923	0.005664777	sialic acid binding Ig-like lectin 10 [Source:HGNC Symbol;Acc:15620]

ZDHHC1	4.937968552	0.00888021	zinc finger, DHHC-type containing 1 [Source:HGNC Symbol;Acc:17916]
LAG3	4.937631226	9.39E-18	lymphocyte-activation gene 3 [Source:HGNC Symbol;Acc:6476]
SLC11A1	4.918080877	0.000677254	solute carrier family 11 (proton-coupled divalent metal ion transporter), member 1 [Source:HGNC Symbol;Acc:10907]
CCL5	4.917242907	4.75E-26	chemokine (C-C motif) ligand 5 [Source:HGNC Symbol;Acc:10632]
IRX5	4.882215444	0.006366797	iroquois homeobox 5 [Source:HGNC Symbol;Acc:14361]
AC011747.7	4.879842918	0.006225226	
C15orf48	4.872376101	1.13E-06	chromosome 15 open reading frame 48 [Source:HGNC Symbol;Acc:29898]
AC092316.2	4.866726151	6.00E-07	
FPR3	4.856103816	0.002444331	formyl peptide receptor 3 [Source:HGNC Symbol;Acc:3828]
RNA5SP498	4.849406841	0.010461235	RNA, 5S ribosomal pseudogene 498 [Source:HGNC Symbol;Acc:43398]
CD14	4.841332358	0.000755154	CD14 molecule [Source:HGNC Symbol;Acc:1628]
CRYBA4	4.830280426	0.009865385	crystallin, beta A4 [Source:HGNC Symbol;Acc:2396]
SYN1	4.82778471	2.29E-05	synapsin I [Source:HGNC Symbol;Acc:11494]
ZNF703	4.80152574	3.15E-08	zinc finger protein 703 [Source:HGNC Symbol;Acc:25883]
CDKN1C	4.797259018	6.83E-09	cyclin-dependent kinase inhibitor 1C (p57, Kip2) [Source:HGNC Symbol;Acc:1786]
GFPT2	4.768314899	1.06E-11	glutamine-fructose-6-phosphate transaminase 2 [Source:HGNC Symbol;Acc:4242]
RASSF4	4.753820193	1.98E-08	Ras association (RalGDS/AF-6) domain family member 4 [Source:HGNC Symbol;Acc:20793]
TBKBP1	4.737987679	5.84E-29	TBK1 binding protein 1 [Source:HGNC Symbol;Acc:30140]
C2orf62	4.724816008	0.000289842	chromosome 2 open reading frame 62 [Source:HGNC Symbol;Acc:25062]
TMEM92	4.720463636	0.001797451	transmembrane protein 92 [Source:HGNC Symbol;Acc:26579]
SCARNA23	4.719789394	7.80E-05	small Cajal body-specific RNA 23 [Source:HGNC Symbol;Acc:32581]
MGLL	4.707792145	0.00306307	monoglyceride lipase [Source:HGNC Symbol;Acc:17038]
CTSD	4.701306432	1.40E-06	cathepsin D [Source:HGNC Symbol;Acc:2529]
PIF1	4.701273695	2.39E-07	PIF1 5'-to-3' DNA helicase [Source:HGNC Symbol;Acc:26220]
PODN	4.694448187	0.002669909	podocan [Source:HGNC Symbol;Acc:23174]
NXPH4	4.690559531	5.99E-07	neurexophilin 4 [Source:HGNC Symbol;Acc:8078]
SLC7A11	4.666701408	0.000299329	solute carrier family 7 (anionic amino acid transporter light chain, xc- system), member 11 [Source:HGNC Symbol;Acc:11059]
FGD2	4.660686662	1.43E-05	FYVE, RhoGEF and PH domain containing 2 [Source:HGNC Symbol;Acc:3664]
HNRNPA3P2	4.658199666	6.36E-16	heterogeneous nuclear ribonucleoprotein A3 pseudogene 2 [Source:HGNC Symbol;Acc:16605]
C9orf66	4.64206849	4.63E-06	chromosome 9 open reading frame 66 [Source:HGNC Symbol;Acc:26436]
OSR2	4.617104214	2.11E-07	odd-skipped related transciption factor 2 [Source:HGNC Symbol;Acc:15830]
NRGN	4.613355705	2.76E-05	neurogranin (protein kinase C substrate, RC3) [Source:HGNC Symbol;Acc:8000]
ARHGAP24	4.606147876	0.004219938	Rho GTPase activating protein 24 [Source:HGNC Symbol;Acc:25361]
DOCK5	4.591500254	7.62E-12	dedicator of cytokinesis 5 [Source:HGNC Symbol;Acc:23476]
FASLG	4.587899771	2.83E-10	Fas ligand (TNF superfamily, member 6) [Source:HGNC Symbol;Acc:11936]
C19orf59	4.587661566	0.004192195	chromosome 19 open reading frame 59 [Source:HGNC Symbol;Acc:27291]
GPR114	4.58105223	3.85E-13	G protein-coupled receptor 114 [Source:HGNC Symbol;Acc:19010]
TTC38	4.564539871	2.94E-19	tetratricopeptide repeat domain 38 [Source:HGNC Symbol;Acc:26082]
LCNL1	4.55603758	0.000176989	lipocalin-like 1 [Source:HGNC Symbol;Acc:34436]
MEIS2	4.553783212	0.000178247	Meis homeobox 2 [Source:HGNC Symbol;Acc:7001]
DLX2	4.551898626	0.000996229	distal-less homeobox 2 [Source:HGNC Symbol;Acc:2915]
ACHE	4.549539918	1.52E-06	acetylcholinesterase (Yt blood group) [Source:HGNC Symbol;Acc:108]
VENTX	4.54683592	0.017231739	VENT homeobox [Source:HGNC Symbol;Acc:13639]
RNF135	4.53807324	2.58E-07	ring finger protein 135 [Source:HGNC Symbol;Acc:21158]
DTHD1	4.531663846	1.52E-08	death domain containing 1 [Source:HGNC Symbol;Acc:37261]
MIR642A	4.514278655	0.001004645	microRNA 642a [Source:HGNC Symbol;Acc:32898]

RIN1	4.510050778	0.00807523	Ras and Rab interactor 1 [Source:HGNC Symbol;Acc:18749]
RN7SL204P	4.500052319	0.003462883	RNA, 7SL, cytoplasmic 204, pseudogene [Source:HGNC Symbol;Acc:46220]
DDAH2	4.491282142	3.03E-07	dimethylarginine dimethylaminohydrolase 2 [Source:HGNC Symbol;Acc:2716]
CNR2	4.470025104	2.16E-08	cannabinoid receptor 2 (macrophage) [Source:HGNC Symbol;Acc:2160]
BTK	4.46149081	0.000105382	Bruton agammaglobulinemia tyrosine kinase [Source:HGNC Symbol;Acc:1133]
PLEKHO2	4.457150256	2.13E-10	pleckstrin homology domain containing, family O member 2 [Source:HGNC Symbol;Acc:30026]
AC000003.2	4.449500486	8.97E-06	CDNA FLJ25865 fis, clone CBR01927 [Source:UniProtKB/TrEMBL;Acc:Q8N7A4]
TST	4.448582076	0.004630767	thiosulfate sulfurtransferase (rhodanese) [Source:HGNC Symbol;Acc:12388]
NDST1	4.439148154	7.73E-05	N-deacetylase/N-sulfotransferase (heparan glucosaminyl) 1 [Source:HGNC Symbol;Acc:7680]
ADAP2	4.421433299	0.014824609	ArfGAP with dual PH domains 2 [Source:HGNC Symbol;Acc:16487]
FCGR3B	4.414354845	0.010284224	Fc fragment of IgG, low affinity IIIb, receptor (CD16b) [Source:HGNC Symbol;Acc:3620]
SDS	4.395870223	1.76E-05	serine dehydratase [Source:HGNC Symbol;Acc:10691]
DRAXIN	4.385980839	0.0002311	dorsal inhibitory axon guidance protein [Source:HGNC Symbol;Acc:25054]
ALDH1A2	4.362418299	0.002579872	aldehyde dehydrogenase 1 family, member A2 [Source:HGNC Symbol;Acc:15472]
RHOU	4.348116419	1.45E-05	ras homolog family member U [Source:HGNC Symbol;Acc:17794]
AK4	4.336382071	0.004916573	adenylate kinase 4 [Source:HGNC Symbol;Acc:363]
PTGDS	4.328851371	1.79E-20	prostaglandin D2 synthase 21kDa (brain) [Source:HGNC Symbol;Acc:9592]
METRNL	4.321216612	1.79E-20	meteorin, glial cell differentiation regulator-like [Source:HGNC Symbol;Acc:27584]
AC005083.1	4.319007627	0.018606313	
AGPAT2	4.313769832	6.65E-05	1-acylglycerol-3-phosphate O-acyltransferase 2 [Source:HGNC Symbol;Acc:325]
ACOX2	4.312592703	0.005312079	acyl-CoA oxidase 2, branched chain [Source:HGNC Symbol;Acc:120]
NCF1C	4.294279485	0.005270147	neutrophil cytosolic factor 1C pseudogene [Source:HGNC Symbol;Acc:32523]
LILRA6	4.288966661	0.000595702	leukocyte immunoglobulin-like receptor, subfamily A (with TM domain), member 6 [Source:HGNC Symbol;Acc:15495]
C6orf25	4.265111028	0.006224229	chromosome 6 open reading frame 25 [Source:HGNC Symbol;Acc:13937]
METTL7A	4.262548155	5.60E-07	methyltransferase like 7A [Source:HGNC Symbol;Acc:24550]
MRAS	4.259985227	0.000605109	muscle RAS oncogene homolog [Source:HGNC Symbol;Acc:7227]
PTMS	4.241654481	2.38E-07	parathymosin [Source:HGNC Symbol;Acc:9629]
TBX21	4.225623304	5.46E-22	T-box 21 [Source:HGNC Symbol;Acc:11599]
OSCAR	4.221727279	2.23E-05	osteoclast associated, immunoglobulin-like receptor [Source:HGNC Symbol;Acc:29960]
KIF19	4.219149759	6.25E-09	kinesin family member 19 [Source:HGNC Symbol;Acc:26735]
GSC	4.213247977	0.001650554	goosecoid homeobox [Source:HGNC Symbol;Acc:4612]
LOXL3	4.209933644	0.001728249	lysyl oxidase-like 3 [Source:HGNC Symbol;Acc:13869]
TPST2	4.18638034	1.85E-13	tyrosylprotein sulfotransferase 2 [Source:HGNC Symbol;Acc:12021]
PLBD1	4.180099136	0.000105382	phospholipase B domain containing 1 [Source:HGNC Symbol;Acc:26215]
KCNB1	4.180078455	0.018986672	potassium voltage-gated channel, Shab-related subfamily, member 1 [Source:HGNC Symbol;Acc:6231]
PRF1	4.166545434	1.65E-23	perforin 1 (pore forming protein) [Source:HGNC Symbol;Acc:9360]
Mrz 01	4.157155112	0.000193837	membrane-associated ring finger (C3HC4) 1, E3 ubiquitin protein ligase [Source:HGNC Symbol;Acc:26077]
TRIB1	4.14451904	1.75E-05	tribbles pseudokinase 1 [Source:HGNC Symbol;Acc:16891]
TGFBI	4.14269596	0.005302632	transforming growth factor, beta-induced, 68kDa [Source:HGNC Symbol;Acc:11771]
NTNG2	4.124637812	2.29E-10	netrin G2 [Source:HGNC Symbol;Acc:14288]
ABI3	4.121784472	3.85E-13	ABI family, member 3 [Source:HGNC Symbol;Acc:29859]
SOX13	4.11230484	5.28E-09	SRY (sex determining region Y)-box 13 [Source:HGNC Symbol;Acc:11192]
TNFRSF21	4.105079553	0.017609587	tumor necrosis factor receptor superfamily, member 21 [Source:HGNC Symbol;Acc:13469]
CEBPB	4.097643964	2.30E-05	CCAAT/enhancer binding protein (C/EBP), beta [Source:HGNC Symbol;Acc:1834]
CHST12	4.096193688	3.11E-20	carbohydrate (chondroitin 4) sulfotransferase 12 [Source:HGNC Symbol;Acc:17423]

MIB2	4.091424099	6.52E-19	mindbomb E3 ubiquitin protein ligase 2 [Source:HGNC Symbol;Acc:30577]
AC019221.4	4.084381161	0.000404148	
PDLIM7	4.068726693	7.89E-06	PDZ and LIM domain 7 (enigma) [Source:HGNC Symbol;Acc:22958]
ATP8B4	4.066777535	0.000694979	ATPase, class I, type 8B, member 4 [Source:HGNC Symbol;Acc:13536]
ODF3B	4.065817001	0.000121384	outer dense fiber of sperm tails 3B [Source:HGNC Symbol;Acc:34388]
DPYSL3	4.062076552	0.014189529	dihydropyrimidinase-like 3 [Source:HGNC Symbol;Acc:3015]
DOCK4	4.061105831	0.000548512	dedicator of cytokinesis 4 [Source:HGNC Symbol;Acc:19192]
SAPCD2	4.035155386	0.010955722	suppressor APC domain containing 2 [Source:HGNC Symbol;Acc:28055]
CD8B	4.027365403	1.12E-19	CD8b molecule [Source:HGNC Symbol;Acc:1707]
SPON2	4.017436839	2.41E-24	spondin 2, extracellular matrix protein [Source:HGNC Symbol;Acc:11253]
TMEM176A	4.015156596	0.018145461	transmembrane protein 176A [Source:HGNC Symbol;Acc:24930]
KLRC1	4.012936541	0.010036158	killer cell lectin-like receptor subfamily C, member 1 [Source:HGNC Symbol;Acc:6374]
FZD4	4.009266083	0.010705897	frizzled family receptor 4 [Source:HGNC Symbol;Acc:4042]
TRGV2	4.004935363	2.29E-10	T cell receptor gamma variable 2 [Source:HGNC Symbol;Acc:12287]
NR6A1	3.995056762	0.014002699	nuclear receptor subfamily 6, group A, member 1 [Source:HGNC Symbol;Acc:7985]
F2R	3.989503285	4.54E-07	coagulation factor II (thrombin) receptor [Source:HGNC Symbol;Acc:3537]
LANCL3	3.975215559	0.004834236	LanC lantibiotic synthetase component C-like 3 (bacterial) [Source:HGNC Symbol;Acc:24767]
LRG1	3.974652295	0.014220406	leucine-rich alpha-2-glycoprotein 1 [Source:HGNC Symbol;Acc:29480]
C19orf38	3.968345522	0.007265999	chromosome 19 open reading frame 38 [Source:HGNC Symbol;Acc:34073]
CD160	3.964013252	2.26E-06	CD160 molecule [Source:HGNC Symbol;Acc:17013]
PDLIM1	3.962602924	1.12E-07	PDZ and LIM domain 1 [Source:HGNC Symbol;Acc:2067]
CST7	3.953396937	1.58E-22	cystatin F (leukocystatin) [Source:HGNC Symbol;Acc:2479]
PRR5L	3.9520412	1.58E-16	proline rich 5 like [Source:HGNC Symbol;Acc:25878]
AIF1	3.937235458	0.014958098	allograft inflammatory factor 1 [Source:HGNC Symbol;Acc:352]
RN7SL381P	3.936431665	0.000151348	RNA, 7SL, cytoplasmic 381, pseudogene [Source:HGNC Symbol;Acc:46397]
TTYH3	3.93510358	0.000289831	tweety family member 3 [Source:HGNC Symbol;Acc:22222]
SIGLEC9	3.925399981	6.42E-12	sialic acid binding Ig-like lectin 9 [Source:HGNC Symbol;Acc:10878]
NEIL3	3.922722903	0.001163094	nei endonuclease VIII-like 3 (E. coli) [Source:HGNC Symbol;Acc:24573]
SDPR	3.917644732	0.000395663	serum deprivation response [Source:HGNC Symbol;Acc:10690]
CLEC1B	3.915327549	0.010288284	C-type lectin domain family 1, member B [Source:HGNC Symbol;Acc:24356]
OR2B11	3.911767495	0.023894939	olfactory receptor, family 2, subfamily B, member 11 [Source:HGNC Symbol;Acc:31249]
IFI30	3.910275929	0.010742395	interferon, gamma-inducible protein 30 [Source:HGNC Symbol;Acc:5398]
GLB1L2	3.908362582	6.49E-09	galactosidase, beta 1-like 2 [Source:HGNC Symbol;Acc:25129]
MLTK	3.906648038	4.48E-06	Mitogen-activated protein kinase kinase kinase MLT [Source:UniProtKB/Swiss-Prot;Acc:Q9NYL2]
AP000462.1	3.898624472	0.002024696	
KLF4	3.897214941	0.012262594	Kruppel-like factor 4 (gut) [Source:HGNC Symbol;Acc:6348]
CBFA2T3	3.890777143	0.011555621	core-binding factor, runt domain, alpha subunit 2; translocated to, 3 [Source:HGNC Symbol;Acc:1537]
EIF4EBP1	3.885871866	3.59E-14	eukaryotic translation initiation factor 4E binding protein 1 [Source:HGNC Symbol;Acc:3288]
APOBR	3.880571976	3.18E-08	apolipoprotein B receptor [Source:HGNC Symbol;Acc:24087]
ADM	3.880392844	0.000142668	adrenomedullin [Source:HGNC Symbol;Acc:259]
MXRA7	3.872174513	8.16E-12	matrix-remodelling associated 7 [Source:HGNC Symbol;Acc:7541]
IGF2BP2	3.865176151	8.03E-05	insulin-like growth factor 2 mRNA binding protein 2 [Source:HGNC Symbol;Acc:28867]
JAKMIP1	3.858008369	1.18E-07	janus kinase and microtubule interacting protein 1 [Source:HGNC Symbol;Acc:26460]
UBA52P6	3.853859887	3.93E-07	ubiquitin A-52 residue ribosomal protein fusion product 1 pseudogene 6 [Source:HGNC Symbol;Acc:36763]
LRRC16B	3.850757595	3.19E-09	leucine rich repeat containing 16B [Source:HGNC Symbol;Acc:20272]
SH3BP2	3.840999267	1.51E-06	SH3-domain binding protein 2 [Source:HGNC Symbol;Acc:10825]

ADAM28	3.836527388	2.23E-09	ADAM metallopeptidase domain 28 [Source:HGNC Symbol;Acc:206]
SRGAP2B	3.831679433	2.72E-05	SLIT-ROBO Rho GTPase activating protein 2B [Source:HGNC Symbol;Acc:35237]
STYK1	3.815050108	9.01E-05	serine/threonine/tyrosine kinase 1 [Source:HGNC Symbol;Acc:18889]
ITGAD	3.809544465	0.020368533	integrin, alpha D [Source:HGNC Symbol;Acc:6146]
TRGV9	3.80262395	1.54E-06	T cell receptor gamma variable 9 [Source:HGNC Symbol;Acc:12295]
HBA1	3.800642752	0.007702945	hemoglobin, alpha 1 [Source:HGNC Symbol;Acc:4823]
F13A1	3.788328186	0.017555993	coagulation factor XIII, A1 polypeptide [Source:HGNC Symbol;Acc:3531]
TNFSF9	3.779021705	8.90E-06	tumor necrosis factor (ligand) superfamily, member 9 [Source:HGNC Symbol;Acc:11939]
CD63	3.775457571	4.63E-07	CD63 molecule [Source:HGNC Symbol;Acc:1692]
TRGV1	3.74759841	0.002544123	T cell receptor gamma variable 1 (non-functional) [Source:HGNC Symbol;Acc:12284]
CMC1	3.744125821	2.60E-14	C-x(9)-C motif containing 1 [Source:HGNC Symbol;Acc:28783]
GRN	3.734350925	4.78E-05	granulin [Source:HGNC Symbol;Acc:4601]
TRGC2	3.730940604	4.00E-18	T cell receptor gamma constant 2 [Source:HGNC Symbol;Acc:12276]
SHB	3.721445981	5.82E-05	Src homology 2 domain containing adaptor protein B [Source:HGNC Symbol;Acc:10838]
DNAJC28	3.711879986	0.00162899	DnaJ (Hsp40) homolog, subfamily C, member 28 [Source:HGNC Symbol;Acc:1297]
NANOS3	3.707048486	0.002710235	nanos homolog 3 (Drosophila) [Source:HGNC Symbol;Acc:22048]
LINC00937	3.704724139	0.000782157	long intergenic non-protein coding RNA 937 [Source:HGNC Symbol;Acc:48629]
KLRF1	3.702962624	1.35E-10	killer cell lectin-like receptor subfamily F, member 1 [Source:HGNC Symbol;Acc:13342]
SGMS2	3.69893861	0.005892226	sphingomyelin synthase 2 [Source:HGNC Symbol;Acc:28395]
SLC2A8	3.696967955	1.89E-15	solute carrier family 2 (facilitated glucose transporter), member 8 [Source:HGNC Symbol;Acc:13812]
TNFRSF12A	3.685586234	2.43E-05	tumor necrosis factor receptor superfamily, member 12A [Source:HGNC Symbol;Acc:18152]
HOTAIRM1	3.683302212	1.77E-06	HOXA transcript antisense RNA, myeloid-specific 1 [Source:HGNC Symbol;Acc:37117]
TMCC3	3.678395869	8.94E-18	transmembrane and coiled-coil domain family 3 [Source:HGNC Symbol;Acc:29199]
MON1A	3.678088954	1.74E-07	MON1 secretory trafficking family member A [Source:HGNC Symbol;Acc:28207]
CLIC3	3.674404964	0.00251422	chloride intracellular channel 3 [Source:HGNC Symbol;Acc:2064]
IER3	3.666375389	3.94E-08	immediate early response 3 [Source:HGNC Symbol;Acc:5392]
ANKRD9	3.666148787	0.00278304	ankyrin repeat domain 9 [Source:HGNC Symbol;Acc:20096]
SERTAD3	3.660201546	6.38E-18	SERTA domain containing 3 [Source:HGNC Symbol;Acc:17931]
BAIAP2	3.659525549	2.80E-05	BAI1-associated protein 2 [Source:HGNC Symbol;Acc:947]
APBB2	3.658338974	0.02159699	amyloid beta (A4) precursor protein-binding, family B, member 2 [Source:HGNC Symbol;Acc:582]
LLGL2	3.654317951	5.60E-20	lethal giant larvae homolog 2 (Drosophila) [Source:HGNC Symbol;Acc:6629]
CTBP2	3.643725449	1.28E-06	C-terminal binding protein 2 [Source:HGNC Symbol;Acc:2495]
GPR27	3.642866197	1.01E-06	G protein-coupled receptor 27 [Source:HGNC Symbol;Acc:4482]
TOR2A	3.63287365	2.05E-11	torsin family 2, member A [Source:HGNC Symbol;Acc:11996]
VSTM2B	3.62187705	0.025089625	V-set and transmembrane domain containing 2B [Source:HGNC Symbol;Acc:33595]
CEP78	3.618746514	1.84E-13	centrosomal protein 78kDa [Source:HGNC Symbol;Acc:25740]
CNTLN	3.617051166	0.003532004	centlein, centrosomal protein [Source:HGNC Symbol;Acc:23432]
EFHD2	3.615709611	3.00E-10	EF-hand domain family, member D2 [Source:HGNC Symbol;Acc:28670]
MYO6	3.609967678	9.03E-11	myosin VI [Source:HGNC Symbol;Acc:7605]
TRIO	3.606818613	1.49E-07	trio Rho guanine nucleotide exchange factor [Source:HGNC Symbol;Acc:12303]
MAP3K8	3.599877123	7.49E-06	mitogen-activated protein kinase kinase kinase 8 [Source:HGNC Symbol;Acc:6860]
AL589739.1	3.58433774	2.87E-05	Uncharacterized protein [Source:UniProtKB/TrEMBL;Acc:M0QY59]
EPHX4	3.584330121	5.98E-05	epoxide hydrolase 4 [Source:HGNC Symbol;Acc:23758]
ZG16B	3.57748135	0.010576675	zymogen granule protein 16B [Source:HGNC Symbol;Acc:30456]
CMIP	3.568251162	1.48E-14	c-Maf inducing protein [Source:HGNC Symbol;Acc:24319]
MYCL	3.563970039	0.03369778	v-myc avian myelocytomatosis viral oncogene lung carcinoma derived homolog [Source:HGNC Symbol;Acc:7555]

ALDH2	3.563670661	0.000895181	aldehyde dehydrogenase 2 family (mitochondrial) [Source:HGNC Symbol;Acc:404]
PRKAR2B	3.562771528	0.000263764	protein kinase, cAMP-dependent, regulatory, type II, beta [Source:HGNC Symbol;Acc:9392]
DOCK6	3.559404254	0.000212875	dedicator of cytokinesis 6 [Source:HGNC Symbol;Acc:19189]
ARHGEF12	3.558787293	1.55E-15	Rho guanine nucleotide exchange factor (GEF) 12 [Source:HGNC Symbol;Acc:14193]
LST1	3.555404841	0.010747969	leukocyte specific transcript 1 [Source:HGNC Symbol;Acc:14189]
LILRB3	3.551562719	0.000427257	leukocyte immunoglobulin-like receptor, subfamily B (with TM and ITIM domains), member 3 [Source:HGNC Symbol;Acc:6607]
RGAG4	3.549348755	0.000554348	retrotransposon gag domain containing 4 [Source:HGNC Symbol;Acc:29430]
AC015849.2	3.547396958	0.001043005	
CD244	3.537473245	1.13E-11	CD244 molecule, natural killer cell receptor 2B4 [Source:HGNC Symbol;Acc:18171]
ZBTB7B	3.535685045	4.09E-05	zinc finger and BTB domain containing 7B [Source:HGNC Symbol;Acc:18668]
IFITM3	3.535120433	0.011635083	interferon induced transmembrane protein 3 [Source:HGNC Symbol;Acc:5414]
TMEM63C	3.524792406	6.60E-05	transmembrane protein 63C [Source:HGNC Symbol;Acc:23787]
MGAT1	3.524378795	5.17E-11	mannosyl (alpha-1,3-)-glycoprotein beta-1,2-N-acetylglucosaminyltransferase [Source:HGNC Symbol;Acc:7044]
MYO1F	3.522901176	7.94E-25	myosin IF [Source:HGNC Symbol;Acc:7600]
BCAT1	3.516274144	0.003951035	branched chain amino-acid transaminase 1, cytosolic [Source:HGNC Symbol;Acc:976]
DPRXP4	3.515038922	0.005411745	divergent-paired related homeobox pseudogene 4 [Source:HGNC Symbol;Acc:32170]
AUTS2	3.512837363	4.30E-14	autism susceptibility candidate 2 [Source:HGNC Symbol;Acc:14262]
SLC43A2	3.512597148	4.57E-05	solute carrier family 43 (amino acid system L transporter), member 2 [Source:HGNC Symbol;Acc:23087]
KIF5A	3.510044519	0.00151053	kinesin family member 5A [Source:HGNC Symbol;Acc:6323]
ADRB2	3.500425014	4.06E-14	adrenoceptor beta 2, surface [Source:HGNC Symbol;Acc:286]
GNGT2	3.497931015	2.70E-06	guanine nucleotide binding protein (G protein), gamma transducing activity polypeptide 2 [Source:HGNC Symbol;Acc:4412]
GM2A	3.490552118	8.38E-05	GM2 ganglioside activator [Source:HGNC Symbol;Acc:4367]
LRP1	3.488239942	0.00031303	low density lipoprotein receptor-related protein 1 [Source:HGNC Symbol;Acc:6692]
CDKN2A	3.477843158	9.50E-05	cyclin-dependent kinase inhibitor 2A [Source:HGNC Symbol;Acc:1787]
FCHO2	3.474220082	2.55E-08	FCH domain only 2 [Source:HGNC Symbol;Acc:25180]
SLC22A4	3.470830801	0.000333264	solute carrier family 22 (organic cation/zwitterion transporter), member 4 [Source:HGNC Symbol;Acc:10968]
KLHL4	3.465070485	0.035528985	kelch-like family member 4 [Source:HGNC Symbol;Acc:6355]
GSN	3.461898721	7.23E-08	gelsolin [Source:HGNC Symbol;Acc:4620]
EGR4	3.459122606	0.02820723	early growth response 4 [Source:HGNC Symbol;Acc:3241]
AP000695.4	3.45856877	0.006994391	
FBN2	3.456052678	0.026417642	fibrillin 2 [Source:HGNC Symbol;Acc:3604]
MMP19	3.455404033	0.027482159	matrix metallopeptidase 19 [Source:HGNC Symbol;Acc:7165]
GATA6	3.454676218	0.000966369	GATA binding protein 6 [Source:HGNC Symbol;Acc:4174]
PTPN12	3.445525221	4.34E-17	protein tyrosine phosphatase, non-receptor type 12 [Source:HGNC Symbol;Acc:9645]
CARD9	3.433066083	0.026091663	caspase recruitment domain family, member 9 [Source:HGNC Symbol;Acc:16391]
FMN1	3.426282996	0.003431146	formin 1 [Source:HGNC Symbol;Acc:3768]
LPCAT1	3.425544578	1.71E-13	lysophosphatidylcholine acyltransferase 1 [Source:HGNC Symbol;Acc:25718]
FGD4	3.409465291	0.003087469	FYVE, RhoGEF and PH domain containing 4 [Source:HGNC Symbol;Acc:19125]
GZMA	3.399648095	4.00E-10	granzyme A (granzyme 1, cytotoxic T-lymphocyte-associated serine esterase 3) [Source:HGNC Symbol;Acc:4708]
CAMK2N1	3.395588809	2.79E-10	calcium/calmodulin-dependent protein kinase II inhibitor 1 [Source:HGNC Symbol;Acc:24190]
FLVCR2	3.390703106	0.001365212	feline leukemia virus subgroup C cellular receptor family, member 2 [Source:HGNC Symbol;Acc:20105]
RGS3	3.380534482	3.07E-09	regulator of G-protein signaling 3 [Source:HGNC Symbol;Acc:9999]
SMCO4	3.377376338	0.01461745	single-pass membrane protein with coiled-coil domains 4 [Source:HGNC Symbol;Acc:24810]
NCEH1	3.37374686	0.000135604	neutral cholesterol ester hydrolase 1 [Source:HGNC Symbol;Acc:29260]

ATP1A3	3.371469313	5.90E-12	ATPase, Na+/K+ transporting, alpha 3 polypeptide [Source:HGNC Symbol;Acc:801]
RPS27AP2	3.365481413	0.03253348	ribosomal protein S27a pseudogene 2 [Source:HGNC Symbol;Acc:16572]
FBLN2	3.363569939	0.018080841	fibulin 2 [Source:HGNC Symbol;Acc:3601]
PDGFC	3.362386489	0.034013661	platelet derived growth factor C [Source:HGNC Symbol;Acc:8801]
DAB2	3.354517356	0.002605085	Dab, mitogen-responsive phosphoprotein, homolog 2 (Drosophila) [Source:HGNC Symbol;Acc:2662]
ZNF296	3.346452871	1.52E-06	zinc finger protein 296 [Source:HGNC Symbol;Acc:15981]
IGFBP6	3.3409989	0.017015784	insulin-like growth factor binding protein 6 [Source:HGNC Symbol;Acc:5475]
HEY1	3.333998513	0.019500276	hes-related family bHLH transcription factor with YRPW motif 1 [Source:HGNC Symbol;Acc:4880]
TRIM36	3.322710804	0.010223488	tripartite motif containing 36 [Source:HGNC Symbol;Acc:16280]
PHACTR1	3.320153785	0.00011119	phosphatase and actin regulator 1 [Source:HGNC Symbol;Acc:20990]
TOR4A	3.317524704	0.000437374	torsin family 4, member A [Source:HGNC Symbol;Acc:25981]
SF3A3P1	3.313010473	0.008241419	splicing factor 3a, subunit 3 pseudogene 1 [Source:HGNC Symbol;Acc:16576]
PLOD1	3.309065273	1.76E-08	procollagen-lysine, 2-oxoglutarate 5-dioxygenase 1 [Source:HGNC Symbol;Acc:9081]
C8G	3.303650263	0.000817937	complement component 8, gamma polypeptide [Source:HGNC Symbol;Acc:1354]
AC092580.4	3.300533374	1.76E-08	
CACNA2D2	3.296954943	9.79E-07	calcium channel, voltage-dependent, alpha 2/delta subunit 2 [Source:HGNC Symbol;Acc:1400]
RPS6KA4	3.296319377	6.14E-05	ribosomal protein S6 kinase, 90kDa, polypeptide 4 [Source:HGNC Symbol;Acc:10433]
GAB1	3.295921341	0.023291978	GRB2-associated binding protein 1 [Source:HGNC Symbol;Acc:4066]
ZMIZ1	3.291080494	2.44E-05	zinc finger, MIZ-type containing 1 [Source:HGNC Symbol;Acc:16493]
NRARP	3.289102808	0.00473787	NOTCH-regulated ankyrin repeat protein [Source:HGNC Symbol;Acc:33843]
GRINA	3.28593704	1.95E-05	glutamate receptor, ionotropic, N-methyl D-aspartate-associated protein 1 (glutamate binding) [Source:HGNC Symbol;Acc:4589]
GAB3	3.27899519	4.60E-12	GRB2-associated binding protein 3 [Source:HGNC Symbol;Acc:17515]
EVA1B	3.274863251	0.017771527	eva-1 homolog B (C. elegans) [Source:HGNC Symbol;Acc:25558]
MAP2K3	3.2696349	2.00E-09	mitogen-activated protein kinase kinase 3 [Source:HGNC Symbol;Acc:6843]
FAM179A	3.268043522	1.84E-09	family with sequence similarity 179, member A [Source:HGNC Symbol;Acc:33715]
PHOSPHO1	3.266421083	0.000110183	phosphatase, orphan 1 [Source:HGNC Symbol;Acc:16815]
AC011816.1	3.260991237	0.010040105	
MARCKSL1	3.24991515	4.72E-05	MARCKS-like 1 [Source:HGNC Symbol;Acc:7142]
XPNPEP2	3.244321989	0.000215228	X-prolyl aminopeptidase (aminopeptidase P) 2, membrane-bound [Source:HGNC Symbol;Acc:12823]
NFIB	3.244149666	0.033235101	nuclear factor I/B [Source:HGNC Symbol;Acc:7785]
ITPRIPL2	3.238428289	0.000205163	inositol 1,4,5-trisphosphate receptor interacting protein-like 2 [Source:HGNC Symbol;Acc:27257]
FBP1	3.234907682	0.001799115	fructose-1,6-bisphosphatase 1 [Source:HGNC Symbol;Acc:3606]
MEFV	3.232540227	0.00599692	Mediterranean fever [Source:HGNC Symbol;Acc:6998]
LGALS1	3.229935528	8.37E-08	lectin, galactoside-binding, soluble, 1 [Source:HGNC Symbol;Acc:6561]
APOBEC3G	3.228231917	2.75E-08	apolipoprotein B mRNA editing enzyme, catalytic polypeptide-like 3G [Source:HGNC Symbol;Acc:17357]
PTGER2	3.227821173	0.000203504	prostaglandin E receptor 2 (subtype EP2), 53kDa [Source:HGNC Symbol;Acc:9594]
IGLC3	3.223750871	0.037906025	immunoglobulin lambda constant 3 (Kern-Oz+ marker) [Source:HGNC Symbol;Acc:5857]
MVB12B	3.221343847	1.14E-19	multivesicular body subunit 12B [Source:HGNC Symbol;Acc:23368]
SLC2A6	3.218293307	0.000239895	solute carrier family 2 (facilitated glucose transporter), member 6 [Source:HGNC Symbol;Acc:11011]
PDZD4	3.209014865	5.28E-09	PDZ domain containing 4 [Source:HGNC Symbol;Acc:21167]
MYBL1	3.204991778	5.12E-12	v-myb avian myeloblastosis viral oncogene homolog-like 1 [Source:HGNC Symbol;Acc:7547]
CKB	3.20339126	8.95E-05	creatine kinase, brain [Source:HGNC Symbol;Acc:1991]
ADAP1	3.199111588	1.26E-05	ArfGAP with dual PH domains 1 [Source:HGNC Symbol;Acc:16486]
MPST	3.193153497	1.67E-05	mercaptopyruvate sulfurtransferase [Source:HGNC Symbol;Acc:7223]
ATL1	3.188950407	0.000147688	atlastin GTPase 1 [Source:HGNC Symbol;Acc:11231]

C4orf48	3.185175691	0.000117331	chromosome 4 open reading frame 48 [Source:HGNC Symbol;Acc:34437]
ABHD17C	3.181414784	2.15E-06	abhydrolase domain containing 17C [Source:HGNC Symbol;Acc:26925]
PARD6G	3.181235942	0.000328639	par-6 family cell polarity regulator gamma [Source:HGNC Symbol;Acc:16076]
SH3GL1P2	3.180813058	0.005665399	SH3-domain GRB2-like 1 pseudogene 2 [Source:HGNC Symbol;Acc:10836]
DLX4	3.177541578	0.024876537	distal-less homeobox 4 [Source:HGNC Symbol;Acc:2917]
TTC16	3.177138209	7.63E-05	tetratricopeptide repeat domain 16 [Source:HGNC Symbol;Acc:26536]
ARSD	3.17613186	6.01E-05	arylsulfatase D [Source:HGNC Symbol;Acc:717]
C11orf95	3.175630932	6.06E-05	chromosome 11 open reading frame 95 [Source:HGNC Symbol;Acc:28449]
IGSF6	3.168296799	0.000310417	immunoglobulin superfamily, member 6 [Source:HGNC Symbol;Acc:5953]
TESC	3.1671877	3.68E-06	tescalcin [Source:HGNC Symbol;Acc:26065]
GAS1	3.166898238	0.009340268	growth arrest-specific 1 [Source:HGNC Symbol;Acc:4165]
PF4	3.1628463	0.024888096	platelet factor 4 [Source:HGNC Symbol;Acc:8861]
PEG10	3.162252039	0.000471178	paternally expressed 10 [Source:HGNC Symbol;Acc:14005]
FAM109A	3.160888755	0.002707012	family with sequence similarity 109, member A [Source:HGNC Symbol;Acc:26509]
MIR27A	3.157822538	0.009287694	microRNA 27a [Source:HGNC Symbol;Acc:31613]
HOXA1	3.149730441	7.70E-07	homeobox A1 [Source:HGNC Symbol;Acc:5099]
RGS12	3.145417647	1.69E-05	regulator of G-protein signaling 12 [Source:HGNC Symbol;Acc:9994]
ARHGAP23	3.140183162	0.035707354	Rho GTPase activating protein 23 [Source:HGNC Symbol;Acc:29293]
TMCC2	3.138270151	0.003061725	transmembrane and coiled-coil domain family 2 [Source:HGNC Symbol;Acc:24239]
IQGAP3	3.137845303	0.020684804	IQ motif containing GTPase activating protein 3 [Source:HGNC Symbol;Acc:20669]
RAB13	3.127958184	0.027860642	RAB13, member RAS oncogene family [Source:HGNC Symbol;Acc:9762]
ARL11	3.118125198	0.02158724	ADP-ribosylation factor-like 11 [Source:HGNC Symbol;Acc:24046]
PLA2G16	3.116356703	2.62E-10	phospholipase A2, group XVI [Source:HGNC Symbol;Acc:17825]
KRT8P48	3.113433245	0.003159648	keratin 8 pseudogene 48 [Source:HGNC Symbol;Acc:48344]
C17orf66	3.113252433	0.001300362	chromosome 17 open reading frame 66 [Source:HGNC Symbol;Acc:26548]
AMOT	3.104684532	7.19E-05	angiomotin [Source:HGNC Symbol;Acc:17810]
NCF1	3.09776246	0.017462505	neutrophil cytosolic factor 1 [Source:HGNC Symbol;Acc:7660]
FAM53B	3.097480515	1.08E-12	family with sequence similarity 53, member B [Source:HGNC Symbol;Acc:28968]
LATS2	3.096815442	2.65E-06	large tumor suppressor kinase 2 [Source:HGNC Symbol;Acc:6515]
COL6A2	3.096783501	6.76E-09	collagen, type VI, alpha 2 [Source:HGNC Symbol;Acc:2212]
AC147651.3	3.096709816	0.037610208	
MIR548AC	3.091897747	0.014835847	microRNA 548ac [Source:HGNC Symbol;Acc:41626]
SCRG1	3.09143706	0.003591175	stimulator of chondrogenesis 1 [Source:HGNC Symbol;Acc:17036]
AC092316.1	3.086655393	0.036810954	
OPRL1	3.084910374	0.008127042	opiate receptor-like 1 [Source:HGNC Symbol;Acc:8155]
CTIF	3.08233898	0.002458357	CBP80/20-dependent translation initiation factor [Source:HGNC Symbol;Acc:23925]
POU3F1	3.0817587	0.000985726	POU class 3 homeobox 1 [Source:HGNC Symbol;Acc:9214]
RALB	3.081047495	2.14E-05	v-ral simian leukemia viral oncogene homolog B [Source:HGNC Symbol;Acc:9840]
HSPA4L	3.079124273	0.016055608	heat shock 70kDa protein 4-like [Source:HGNC Symbol;Acc:17041]
LCN2	3.078573751	0.032604922	lipocalin 2 [Source:HGNC Symbol;Acc:6526]
SYNGR1	3.061678096	3.76E-06	synaptogyrin 1 [Source:HGNC Symbol;Acc:11498]
CHST10	3.060921347	1.87E-08	carbohydrate sulfotransferase 10 [Source:HGNC Symbol;Acc:19650]
SCARF1	3.056468784	0.004573996	scavenger receptor class F, member 1 [Source:HGNC Symbol;Acc:16820]
FGL2	3.050449217	0.000267442	fibrinogen-like 2 [Source:HGNC Symbol;Acc:3696]
GSE1	3.045525788	3.09E-20	Gse1 coiled-coil protein [Source:HGNC Symbol;Acc:28979]
ADAMTS10	3.041566894	2.57E-12	ADAM metallopeptidase with thrombospondin type 1 motif, 10 [Source:HGNC Symbol;Acc:13201]

RN7SL21P	3.029108247	0.038083768	RNA, 7SL, cytoplasmic 21, pseudogene [Source:HGNC Symbol;Acc:46037]
LUCAT1	3.013211594	5.70E-05	lung cancer associated transcript 1 (non-protein coding) [Source:HGNC Symbol;Acc:48498]
AC139100.3	3.01066135	0.013587336	
DMKN	3.005930482	0.002784107	dermokine [Source:HGNC Symbol;Acc:25063]
C3AR1	3.002719153	0.001476824	complement component 3a receptor 1 [Source:HGNC Symbol;Acc:1319]
CHST2	2.994139591	0.000512445	carbohydrate (N-acetylglucosamine-6-O) sulfotransferase 2 [Source:HGNC Symbol;Acc:1970]
IFNG	2.991158753	1.63E-05	interferon, gamma [Source:HGNC Symbol;Acc:5438]
CRTAM	2.987706488	2.83E-10	cytotoxic and regulatory T cell molecule [Source:HGNC Symbol;Acc:24313]
BCL11A	2.984742782	0.010984192	B-cell CLL/lymphoma 11A (zinc finger protein) [Source:HGNC Symbol;Acc:13221]
LSM3P2	2.982997425	0.008608939	LSM3 pseudogene 2 [Source:HGNC Symbol;Acc:44347]
RRAD	2.982426926	0.005731518	Ras-related associated with diabetes [Source:HGNC Symbol;Acc:10446]
SBK1	2.979552849	1.70E-06	SH3 domain binding kinase 1 [Source:HGNC Symbol;Acc:17699]
ZNF467	2.976369085	0.006334095	zinc finger protein 467 [Source:HGNC Symbol;Acc:23154]
ASPDH	2.97098701	0.025547623	aspartate dehydrogenase domain containing [Source:HGNC Symbol;Acc:33856]
F3	2.96737486	0.010008644	coagulation factor III (thromboplastin, tissue factor) [Source:HGNC Symbol;Acc:3541]
LINC00936	2.957125272	5.03E-05	long intergenic non-protein coding RNA 936 [Source:HGNC Symbol;Acc:27883]
GPX1	2.954352497	0.001025268	glutathione peroxidase 1 [Source:HGNC Symbol;Acc:4553]
CBX4	2.954116919	2.86E-05	chromobox homolog 4 [Source:HGNC Symbol;Acc:1554]
BLVRB	2.939027175	1.33E-09	biliverdin reductase B (flavin reductase (NADPH)) [Source:HGNC Symbol;Acc:1063]
NACC2	2.937067292	0.000417548	NACC family member 2, BEN and BTB (POZ) domain containing [Source:HGNC Symbol;Acc:23846]
C16orf95	2.935942897	0.013589545	chromosome 16 open reading frame 95 [Source:HGNC Symbol;Acc:40033]
GNB2	2.931567419	1.00E-06	guanine nucleotide binding protein (G protein), beta polypeptide 2 [Source:HGNC Symbol;Acc:4398]
SPDEF	2.931135915	0.004970147	SAM pointed domain containing ETS transcription factor [Source:HGNC Symbol;Acc:17257]
ASCL5	2.929853087	0.04590456	achaete-scute family bHLH transcription factor 5 [Source:HGNC Symbol;Acc:33169]
MPO	2.926950854	0.021944377	myeloperoxidase [Source:HGNC Symbol;Acc:7218]
IRAK3	2.924039588	0.02912124	interleukin-1 receptor-associated kinase 3 [Source:HGNC Symbol;Acc:17020]
ARAP3	2.91939855	4.26E-07	ArfGAP with RhoGAP domain, ankyrin repeat and PH domain 3 [Source:HGNC Symbol;Acc:24097]
ENC1	2.917241303	8.35E-09	ectodermal-neural cortex 1 (with BTB domain) [Source:HGNC Symbol;Acc:3345]
SSBP4	2.916192108	3.49E-05	single stranded DNA binding protein 4 [Source:HGNC Symbol;Acc:15676]
CTNNA1	2.9088566	1.02E-05	catenin (cadherin-associated protein), alpha 1, 102kDa [Source:HGNC Symbol;Acc:2509]
PLCB3	2.906034454	0.000154595	phospholipase C, beta 3 (phosphatidylinositol-specific) [Source:HGNC Symbol;Acc:9056]
NAP1L4P1	2.905089844	4.11E-05	nucleosome assembly protein 1-like 4 pseudogene 1 [Source:HGNC Symbol;Acc:39740]
ODF3L1	2.902060257	0.031309026	outer dense fiber of sperm tails 3-like 1 [Source:HGNC Symbol;Acc:28735]
OSBPL7	2.895135352	4.97E-11	oxysterol binding protein-like 7 [Source:HGNC Symbol;Acc:16387]
ZBTB7A	2.894641033	1.68E-06	zinc finger and BTB domain containing 7A [Source:HGNC Symbol;Acc:18078]
TSHZ3	2.891926393	0.007400772	teashirt zinc finger homeobox 3 [Source:HGNC Symbol;Acc:30700]
MIR23A	2.884969512	0.019387784	microRNA 23a [Source:HGNC Symbol;Acc:31605]
FEZ1	2.88481701	0.010036158	fasciculation and elongation protein zeta 1 (zygin I) [Source:HGNC Symbol;Acc:3659]
FAM110A	2.884530336	6.77E-05	family with sequence similarity 110, member A [Source:HGNC Symbol;Acc:16188]
ZCCHC24	2.88015479	5.02E-07	zinc finger, CCHC domain containing 24 [Source:HGNC Symbol;Acc:26911]
FBN3	2.878087227	0.013778845	fibrillin 3 [Source:HGNC Symbol;Acc:18794]
C17orf59	2.873377599	2.71E-06	chromosome 17 open reading frame 59 [Source:HGNC Symbol;Acc:25939]
CIITA	2.861766465	0.000172046	class II, major histocompatibility complex, transactivator [Source:HGNC Symbol;Acc:7067]
C2orf48	2.85930336	0.015167503	chromosome 2 open reading frame 48 [Source:HGNC Symbol;Acc:26322]
SAMD3	2.85752193	1.77E-13	sterile alpha motif domain containing 3 [Source:HGNC Symbol;Acc:21574]

RRBP1	2.854545302	6.23E-10	ribosome binding protein 1 [Source:HGNC Symbol;Acc:10448]
PVRL2	2.852187794	0.030221447	poliovirus receptor-related 2 (herpesvirus entry mediator B) [Source:HGNC Symbol;Acc:9707]
N4BP3	2.850879915	1.71E-06	NEDD4 binding protein 3 [Source:HGNC Symbol;Acc:29852]
CLCF1	2.84726723	9.89E-10	cardiotrophin-like cytokine factor 1 [Source:HGNC Symbol;Acc:17412]
BMF	2.84587627	1.57E-06	Bcl2 modifying factor [Source:HGNC Symbol;Acc:24132]
ADAM32	2.841381885	0.027811404	ADAM metallopeptidase domain 32 [Source:HGNC Symbol;Acc:15479]
AC144831.1	2.841032714	0.004283807	
SPECC1	2.83602586	3.51E-09	sperm antigen with calponin homology and coiled-coil domains 1 [Source:HGNC Symbol;Acc:30615]
ASGR1	2.835183282	0.012409258	asialoglycoprotein receptor 1 [Source:HGNC Symbol;Acc:742]
DAPK2	2.833199076	3.15E-05	death-associated protein kinase 2 [Source:HGNC Symbol;Acc:2675]
QSOX1	2.828964559	1.70E-06	quiescin Q6 sulfhydryl oxidase 1 [Source:HGNC Symbol;Acc:9756]
AC007278.3	2.824436899	0.000305273	
RAB27B	2.814377687	1.15E-08	RAB27B, member RAS oncogene family [Source:HGNC Symbol;Acc:9767]
DMWD	2.812547978	1.18E-06	dystrophia myotonica, WD repeat containing [Source:HGNC Symbol;Acc:2936]
C1orf177	2.807292522	0.037541604	chromosome 1 open reading frame 177 [Source:HGNC Symbol;Acc:26854]
IRF5	2.804797997	0.002053925	interferon regulatory factor 5 [Source:HGNC Symbol;Acc:6120]
CCDC71L	2.804316113	0.000116695	coiled-coil domain containing 71-like [Source:HGNC Symbol;Acc:26685]
CHN2	2.803491979	7.66E-08	chimerin 2 [Source:HGNC Symbol;Acc:1944]
DGKQ	2.79836672	7.66E-11	diacylglycerol kinase, theta 110kDa [Source:HGNC Symbol;Acc:2856]
SOGA1	2.79226914	0.012622833	suppressor of glucose, autophagy associated 1 [Source:HGNC Symbol;Acc:16111]
PPM1L	2.787696948	0.000694979	protein phosphatase, Mg2+/Mn2+ dependent, 1L [Source:HGNC Symbol;Acc:16381]
C12orf75	2.787661362	8.54E-07	chromosome 12 open reading frame 75 [Source:HGNC Symbol;Acc:35164]
BFSP1	2.772529712	0.000314532	beaded filament structural protein 1, filensin [Source:HGNC Symbol;Acc:1040]
IL27	2.771209656	0.024903063	interleukin 27 [Source:HGNC Symbol;Acc:19157]
MT1E	2.77091608	5.73E-06	metallothionein 1E [Source:HGNC Symbol;Acc:7397]
CD300A	2.765773255	5.28E-08	CD300a molecule [Source:HGNC Symbol;Acc:19319]
RCAN2	2.765449636	0.024865961	regulator of calcineurin 2 [Source:HGNC Symbol;Acc:3041]
RN7SL280P	2.762115804	0.008127042	RNA, 7SL, cytoplasmic 280, pseudogene [Source:HGNC Symbol;Acc:46296]
PAFAH2	2.762014576	3.99E-07	platelet-activating factor acetylhydrolase 2, 40kDa [Source:HGNC Symbol;Acc:8579]
RXRA	2.759448255	2.86E-05	retinoid X receptor, alpha [Source:HGNC Symbol;Acc:10477]
SDHAF1	2.751580362	0.000147688	succinate dehydrogenase complex assembly factor 1 [Source:HGNC Symbol;Acc:33867]
PHLDA2	2.749280879	0.020747546	pleckstrin homology-like domain, family A, member 2 [Source:HGNC Symbol;Acc:12385]
SGCE	2.748728387	0.017555993	sarcoglycan, epsilon [Source:HGNC Symbol;Acc:10808]
CTSW	2.742165012	0.001057205	cathepsin W [Source:HGNC Symbol;Acc:2546]
MIR142	2.741706659	3.03E-06	microRNA 142 [Source:HGNC Symbol;Acc:31529]
GGH	2.737638634	3.39E-05	gamma-glutamyl hydrolase (conjugase, folylpolygammaglutamyl hydrolase) [Source:HGNC Symbol;Acc:4248]
CALML6	2.73601935	0.048798046	calmodulin-like 6 [Source:HGNC Symbol;Acc:24193]
FABP5P7	2.733794074	0.020661667	fatty acid binding protein 5 pseudogene 7 [Source:HGNC Symbol;Acc:31070]
CORO1C	2.732265776	7.15E-06	coronin, actin binding protein, 1C [Source:HGNC Symbol;Acc:2254]
B4GALT5	2.729054742	3.28E-08	UDP-Gal:betaGlcNAc beta 1,4- galactosyltransferase, polypeptide 5 [Source:HGNC Symbol;Acc:928]
TCF4	2.72849412	0.001327215	transcription factor 4 [Source:HGNC Symbol;Acc:11634]
FOSL1	2.726817502	0.00058574	FOS-like antigen 1 [Source:HGNC Symbol;Acc:13718]
IL12A	2.724368882	4.84E-05	interleukin 12A (natural killer cell stimulatory factor 1, cytotoxic lymphocyte maturation factor 1, p35) [Source:HGNC Symbol;Acc:5969]
ST3GAL4	2.723052283	1.18E-07	ST3 beta-galactoside alpha-2,3-sialyltransferase 4 [Source:HGNC Symbol;Acc:10864]
EHD3	2.718249934	0.003614198	EH-domain containing 3 [Source:HGNC Symbol;Acc:3244]

ZNF787	2.713268339	0.002633242	zinc finger protein 787 [Source:HGNC Symbol;Acc:26998]
C10orf128	2.711646027	2.62E-07	chromosome 10 open reading frame 128 [Source:HGNC Symbol;Acc:27274]
LINC00537	2.70994819	0.002579872	long intergenic non-protein coding RNA 537 [Source:HGNC Symbol;Acc:43654]
HES6	2.709611837	4.40E-06	hes family bHLH transcription factor 6 [Source:HGNC Symbol;Acc:18254]
HOPX	2.706369118	1.49E-08	HOP homeobox [Source:HGNC Symbol;Acc:24961]
SLC15A4	2.706290638	1.89E-13	solute carrier family 15 (oligopeptide transporter), member 4 [Source:HGNC Symbol;Acc:23090]
SWAP70	2.704704961	1.91E-05	SWAP switching B-cell complex 70kDa subunit [Source:HGNC Symbol;Acc:17070]
C20orf24	2.702374278	5.31E-06	chromosome 20 open reading frame 24 [Source:HGNC Symbol;Acc:15870]
XCL1	2.701297605	1.42E-05	chemokine (C motif) ligand 1 [Source:HGNC Symbol;Acc:10645]
MAN1A1	2.693863067	3.80E-06	mannosidase, alpha, class 1A, member 1 [Source:HGNC Symbol;Acc:6821]
AC015849.14	2.69313474	0.01071374	
DENND3	2.692913394	1.59E-08	DENN/MADD domain containing 3 [Source:HGNC Symbol;Acc:29134]
ORM2	2.688608236	3.86E-06	orosomucoid 2 [Source:HGNC Symbol;Acc:8499]
RUSC2	2.687008445	0.016854123	RUN and SH3 domain containing 2 [Source:HGNC Symbol;Acc:23625]
S100A10	2.686424866	0.000809891	S100 calcium binding protein A10 [Source:HGNC Symbol;Acc:10487]
TYMP	2.686243538	0.00352933	thymidine phosphorylase [Source:HGNC Symbol;Acc:3148]
ADRBK2	2.684802505	0.002053925	adrenergic, beta, receptor kinase 2 [Source:HGNC Symbol;Acc:290]
SMTN	2.672551798	0.000694979	smoothelin [Source:HGNC Symbol;Acc:11126]
TRPV3	2.667613211	0.03428842	transient receptor potential cation channel, subfamily V, member 3 [Source:HGNC Symbol;Acc:18084]
MARK4	2.665849839	4.26E-10	MAP/microtubule affinity-regulating kinase 4 [Source:HGNC Symbol;Acc:13538]
AC103828.1	2.665701598	8.20E-06	
ENPP5	2.657684941	0.021129997	ectonucleotide pyrophosphatase/phosphodiesterase 5 (putative) [Source:HGNC Symbol;Acc:13717]
FAM72D	2.656500192	0.046066984	family with sequence similarity 72, member D [Source:HGNC Symbol;Acc:33593]
ENG	2.651251938	0.000298662	endoglin [Source:HGNC Symbol;Acc:3349]
CADM1	2.645611214	2.71E-05	cell adhesion molecule 1 [Source:HGNC Symbol;Acc:5951]
DPF3	2.64556081	0.00773601	D4, zinc and double PHD fingers, family 3 [Source:HGNC Symbol;Acc:17427]
CISH	2.645048046	5.48E-08	cytokine inducible SH2-containing protein [Source:HGNC Symbol;Acc:1984]
SIPA1	2.643958793	1.42E-06	signal-induced proliferation-associated 1 [Source:HGNC Symbol;Acc:10885]
PPP2R2B	2.643451671	3.38E-10	protein phosphatase 2, regulatory subunit B, beta [Source:HGNC Symbol;Acc:9305]
CLUH	2.642997843	1.65E-05	clustered mitochondria (cluA/CLU1) homolog [Source:HGNC Symbol;Acc:29094]
OGFRL1	2.64285739	5.60E-07	opioid growth factor receptor-like 1 [Source:HGNC Symbol;Acc:21378]
HOXB7	2.638950471	0.001139904	homeobox B7 [Source:HGNC Symbol;Acc:5118]
PPP1R14B	2.637061867	0.001293872	protein phosphatase 1, regulatory (inhibitor) subunit 14B [Source:HGNC Symbol;Acc:9057]
HPSE	2.635906121	0.001026193	heparanase [Source:HGNC Symbol;Acc:5164]
LYAR	2.631108371	7.82E-14	Ly1 antibody reactive [Source:HGNC Symbol;Acc:26021]
GPR35	2.628468288	0.006489734	G protein-coupled receptor 35 [Source:HGNC Symbol;Acc:4492]
BCL2L2	2.624827526	0.00884334	BCL2-like 2 [Source:HGNC Symbol;Acc:995]
AC016586.1	2.624379158	1.60E-10	
SCO2	2.623916998	0.004082887	SCO2 cytochrome c oxidase assembly protein [Source:HGNC Symbol;Acc:10604]
KIF14	2.620060154	0.011174443	kinesin family member 14 [Source:HGNC Symbol;Acc:19181]
LGALS3	2.619243198	0.00489686	lectin, galactoside-binding, soluble, 3 [Source:HGNC Symbol;Acc:6563]
C11orf84	2.616762756	1.85E-05	chromosome 11 open reading frame 84 [Source:HGNC Symbol;Acc:25115]
RAPGEF2	2.613028113	1.40E-06	Rap guanine nucleotide exchange factor (GEF) 2 [Source:HGNC Symbol;Acc:16854]
DFNB31	2.612104439	6.11E-10	deafness, autosomal recessive 31 [Source:HGNC Symbol;Acc:16361]
NCF1B	2.611300355	0.010111625	neutrophil cytosolic factor 1B pseudogene [Source:HGNC Symbol;Acc:32522]
SH3BP1	2.610100321	0.000300735	SH3-domain binding protein 1 [Source:HGNC Symbol;Acc:10824]

UBE2M	2.607262251	5.62E-05	ubiquitin-conjugating enzyme E2M [Source:HGNC Symbol;Acc:12491]
ADAM15	2.60636502	0.001015601	ADAM metallopeptidase domain 15 [Source:HGNC Symbol;Acc:193]
GALNT3	2.605193336	4.61E-06	UDP-N-acetyl-alpha-D-galactosamine: polypeptide N-acetylgalactosaminyltransferase 3 (GalNAc-T3) [Source:HGNC Symbol;Acc:4125]
ANG	2.604224791	0.013959423	angiogenin, ribonuclease, RNase A family, 5 [Source:HGNC Symbol;Acc:483]
LINC01023	2.601223317	0.004802759	long intergenic non-protein coding RNA 1023 [Source:HGNC Symbol;Acc:49004]
DBN1	2.597649962	0.002275189	drebrin 1 [Source:HGNC Symbol;Acc:2695]
PLEKHG1	2.597523382	0.003067708	pleckstrin homology domain containing, family G (with RhoGef domain) member 1 [Source:HGNC Symbol;Acc:20884]
UBXN10	2.59654403	0.001728669	UBX domain protein 10 [Source:HGNC Symbol;Acc:26354]
ZSCAN20	2.594861761	0.021655546	zinc finger and SCAN domain containing 20 [Source:HGNC Symbol;Acc:13093]
SLA2	2.592858894	8.03E-05	Src-like-adaptor 2 [Source:HGNC Symbol;Acc:17329]
SESN2	2.59144439	3.40E-12	sestrin 2 [Source:HGNC Symbol;Acc:20746]
ARID3A	2.568162201	9.26E-06	AT rich interactive domain 3A (BRIGHT-like) [Source:HGNC Symbol;Acc:3031]
SNX18	2.567276551	0.000111631	sorting nexin 18 [Source:HGNC Symbol;Acc:19245]
TSPAN33	2.56461845	0.005617019	tetraspanin 33 [Source:HGNC Symbol;Acc:28743]
PLEKHA5	2.563993662	1.75E-10	pleckstrin homology domain containing, family A member 5 [Source:HGNC Symbol;Acc:30036]
IGFBP7	2.562340514	0.001590226	insulin-like growth factor binding protein 7 [Source:HGNC Symbol;Acc:5476]
APOBEC3H	2.558041445	3.91E-06	apolipoprotein B mRNA editing enzyme, catalytic polypeptide-like 3H [Source:HGNC Symbol;Acc:24100]
SPTBN4	2.556036212	1.68E-06	spectrin, beta, non-erythrocytic 4 [Source:HGNC Symbol;Acc:14896]
YPEL1	2.554615221	0.00030548	yippee-like 1 (Drosophila) [Source:HGNC Symbol;Acc:12845]
GPX1P1	2.550012045	0.01518414	glutathione peroxidase pseudogene 1 [Source:HGNC Symbol;Acc:4560]
CUEDC1	2.548469355	0.045557124	CUE domain containing 1 [Source:HGNC Symbol;Acc:31350]
DMXL2	2.543691422	0.003010146	Dmx-like 2 [Source:HGNC Symbol;Acc:2938]
DMPK	2.54218908	1.80E-06	dystrophia myotonica-protein kinase [Source:HGNC Symbol;Acc:2933]
PFN1P1	2.541443999	0.026451413	profilin 1 pseudogene 1 [Source:HGNC Symbol;Acc:42989]
HDGF	2.537770101	1.69E-08	hepatoma-derived growth factor [Source:HGNC Symbol;Acc:4856]
MYPOP	2.534057893	0.000625989	Myb-related transcription factor, partner of profilin [Source:HGNC Symbol;Acc:20178]
AIRN	2.523619032	0.012698828	antisense of IGF2R non-protein coding RNA [Source:HGNC Symbol;Acc:34515]
SYTL2	2.521034038	6.36E-07	synaptotagmin-like 2 [Source:HGNC Symbol;Acc:15585]
LASP1	2.520644442	1.40E-11	LIM and SH3 protein 1 [Source:HGNC Symbol;Acc:6513]
AP000640.10	2.519599278	0.049413176	
KIR3DL2	2.51765881	7.19E-05	Uncharacterized protein [Source:UniProtKB/TrEMBL;Acc:A8MVX7]
TUBB6	2.517284492	0.039815983	tubulin, beta 6 class V [Source:HGNC Symbol;Acc:20776]
RAB4A	2.509916118	3.56E-05	RAB4A, member RAS oncogene family [Source:HGNC Symbol;Acc:9781]
QPRT	2.505644271	0.005093458	quinolinate phosphoribosyltransferase [Source:HGNC Symbol;Acc:9755]
GIPR	2.504769373	0.000166117	gastric inhibitory polypeptide receptor [Source:HGNC Symbol;Acc:4271]
SLC9A3R1	2.503754271	2.52E-12	solute carrier family 9, subfamily A (NHE3, cation proton antiporter 3), member 3 regulator 1 [Source:HGNC Symbol;Acc:11075]
SAP30	2.499103887	2.77E-05	Sin3A-associated protein, 30kDa [Source:HGNC Symbol;Acc:10532]
ABCD1	2.497593398	0.00853203	ATP-binding cassette, sub-family D (ALD), member 1 [Source:HGNC Symbol;Acc:61]
PLSCR1	2.492961448	0.000793651	phospholipid scramblase 1 [Source:HGNC Symbol;Acc:9092]
PLAGL1	2.488185862	0.001252168	pleiomorphic adenoma gene-like 1 [Source:HGNC Symbol;Acc:9046]
FOXD2	2.48730748	0.000148288	forkhead box D2 [Source:HGNC Symbol;Acc:3803]
COPRS	2.485825294	0.001727986	coordinator of PRMT5, differentiation stimulator [Source:HGNC Symbol;Acc:28848]
CACNB3	2.484037012	3.72E-07	calcium channel, voltage-dependent, beta 3 subunit [Source:HGNC Symbol;Acc:1403]
AOAH	2.480224882	1.41E-06	acyloxyacyl hydrolase (neutrophil) [Source:HGNC Symbol;Acc:548]
MUC12	2.478534074	0.002304545	mucin 12, cell surface associated [Source:HGNC Symbol;Acc:7510]

SLC14A2	2.476263127	0.030267363	solute carrier family 14 (urea transporter), member 2 [Source:HGNC Symbol;Acc:10919]
COTL1	2.474270835	0.002606059	coactosin-like 1 (Dictyostelium) [Source:HGNC Symbol;Acc:18304]
ABLIM2	2.474047626	2.72E-05	actin binding LIM protein family, member 2 [Source:HGNC Symbol;Acc:19195]
TRGV10	2.473323405	6.14E-05	T cell receptor gamma variable 10 (non-functional) [Source:HGNC Symbol;Acc:12285]
RN7SL288P	2.471830222	0.003306068	RNA, 7SL, cytoplasmic 288, pseudogene [Source:HGNC Symbol;Acc:46304]
TAF4	2.468530729	4.25E-08	TAF4 RNA polymerase II, TATA box binding protein (TBP)-associated factor, 135kDa [Source:HGNC Symbol;Acc:11537]
ZNF618	2.46597823	0.001001232	zinc finger protein 618 [Source:HGNC Symbol;Acc:29416]
GFOD1	2.465117914	0.000469966	glucose-fructose oxidoreductase domain containing 1 [Source:HGNC Symbol;Acc:21096]
LRRC45	2.464592487	0.01621298	leucine rich repeat containing 45 [Source:HGNC Symbol;Acc:28302]
HAMP	2.464049159	0.003122311	hepcidin antimicrobial peptide [Source:HGNC Symbol;Acc:15598]
AC068522.4	2.463914481	0.002946306	
ZNF668	2.463682069	0.000499579	zinc finger protein 668 [Source:HGNC Symbol;Acc:25821]
TP53I11	2.461049886	4.71E-05	tumor protein p53 inducible protein 11 [Source:HGNC Symbol;Acc:16842]
MSC	2.45960182	1.17E-08	musculin [Source:HGNC Symbol;Acc:7321]
IER5L	2.456731613	0.003903326	immediate early response 5-like [Source:HGNC Symbol;Acc:23679]
PTGES	2.454111546	0.043395337	prostaglandin E synthase [Source:HGNC Symbol;Acc:9599]
CSF1R	2.450982177	1.40E-05	colony stimulating factor 1 receptor [Source:HGNC Symbol;Acc:2433]
LY86	2.446909327	0.039374618	lymphocyte antigen 86 [Source:HGNC Symbol;Acc:16837]
PADI6	2.446769524	0.040654185	peptidyl arginine deiminase, type VI [Source:HGNC Symbol;Acc:20449]
UBALD1	2.443708617	0.000271829	UBA-like domain containing 1 [Source:HGNC Symbol;Acc:29576]
RHOC	2.44197277	7.51E-07	ras homolog family member C [Source:HGNC Symbol;Acc:669]
PYCARD	2.441726291	0.005661369	PYD and CARD domain containing [Source:HGNC Symbol;Acc:16608]
HMG20B	2.439402267	0.000592304	high mobility group 20B [Source:HGNC Symbol;Acc:5002]
AKNA	2.436540171	1.51E-13	AT-hook transcription factor [Source:HGNC Symbol;Acc:24108]
PPIF	2.434777086	0.001333107	peptidylprolyl isomerase F [Source:HGNC Symbol;Acc:9259]
LCN12	2.434432484	0.027860642	lipocalin 12 [Source:HGNC Symbol;Acc:28733]
C12orf39	2.434173484	0.034942794	chromosome 12 open reading frame 39 [Source:HGNC Symbol;Acc:28139]
ARPC5L	2.433812522	7.09E-09	actin related protein 2/3 complex, subunit 5-like [Source:HGNC Symbol;Acc:23366]
TMEM200A	2.433102055	0.01133503	transmembrane protein 200A [Source:HGNC Symbol;Acc:21075]
GBGT1	2.432602644	0.045475988	globoside alpha-1,3-N-acetylgalactosaminyltransferase 1 [Source:HGNC Symbol;Acc:20460]
DSCC1	2.430445043	0.002628267	DNA replication and sister chromatid cohesion 1 [Source:HGNC Symbol;Acc:24453]
NT5C	2.429615529	0.002154922	5', 3'-nucleotidase, cytosolic [Source:HGNC Symbol;Acc:17144]
PCAT6	2.427440436	0.033313596	prostate cancer associated transcript 6 (non-protein coding) [Source:HGNC Symbol;Acc:43714]
NRSN2	2.425622066	0.000402525	neurensin 2 [Source:HGNC Symbol;Acc:16229]
AC078852.2	2.423823576	0.040479667	
PKN1	2.423822877	9.41E-05	protein kinase N1 [Source:HGNC Symbol;Acc:9405]
SEMA3F	2.423153645	0.020290012	sema domain, immunoglobulin domain (Ig), short basic domain, secreted, (semaphorin) 3F [Source:HGNC Symbol;Acc:10728]
NAT14	2.421923074	0.00377631	N-acetyltransferase 14 (GCN5-related, putative) [Source:HGNC Symbol;Acc:28918]
CYP27A1	2.416792676	0.026658359	cytochrome P450, family 27, subfamily A, polypeptide 1 [Source:HGNC Symbol;Acc:2605]
SLC27A3	2.415778077	2.64E-05	solute carrier family 27 (fatty acid transporter), member 3 [Source:HGNC Symbol;Acc:10997]
AUNIP	2.415327773	0.015524094	aurora kinase A and ninein interacting protein [Source:HGNC Symbol;Acc:28363]
RPS12P26	2.413397166	0.011221923	ribosomal protein S12 pseudogene 26 [Source:HGNC Symbol;Acc:36320]
TNFRSF1A	2.411120145	0.000515524	tumor necrosis factor receptor superfamily, member 1A [Source:HGNC Symbol;Acc:11916]
IMPA2	2.410808739	0.010856377	inositol(myo)-1(or 4)-monophosphatase 2 [Source:HGNC Symbol;Acc:6051]
UBE2D1	2.40988941	0.001558863	ubiquitin-conjugating enzyme E2D 1 [Source:HGNC Symbol;Acc:12474]

TBC1D10B	2.407803367	3.47E-05	TBC1 domain family, member 10B [Source:HGNC Symbol;Acc:24510]
MBOAT7	2.404512855	0.000126431	membrane bound O-acyltransferase domain containing 7 [Source:HGNC Symbol;Acc:15505]
RPL30P13	2.403262232	0.010245809	ribosomal protein L30 pseudogene 13 [Source:HGNC Symbol;Acc:36280]
SCN3B	2.403067758	0.024657881	sodium channel, voltage-gated, type III, beta subunit [Source:HGNC Symbol;Acc:20665]
USP28	2.400820679	5.46E-06	ubiquitin specific peptidase 28 [Source:HGNC Symbol;Acc:12625]
IGHM	2.400717264	0.025482033	immunoglobulin heavy constant mu [Source:HGNC Symbol;Acc:5541]
PDE2A	2.397979305	1.98E-07	phosphodiesterase 2A, cGMP-stimulated [Source:HGNC Symbol;Acc:8777]
FAM171B	2.397886575	0.031536311	family with sequence similarity 171, member B [Source:HGNC Symbol;Acc:29412]
KIF13A	2.391589781	0.016764781	kinesin family member 13A [Source:HGNC Symbol;Acc:14566]
AHDC1	2.387268582	1.01E-06	AT hook, DNA binding motif, containing 1 [Source:HGNC Symbol;Acc:25230]
LSM14B	2.387078384	7.60E-10	LSM14B, SCD6 homolog B (S. cerevisiae) [Source:HGNC Symbol;Acc:15887]
OCEL1	2.386744979	0.000735262	occludin/ELL domain containing 1 [Source:HGNC Symbol;Acc:26221]
TPRA1	2.380550465	0.000928729	transmembrane protein, adipocyte asscociated 1 [Source:HGNC Symbol;Acc:30413]
CHMP4B	2.376394869	0.000943744	charged multivesicular body protein 4B [Source:HGNC Symbol;Acc:16171]
VPS37D	2.372210571	0.0354133	vacuolar protein sorting 37 homolog D (S. cerevisiae) [Source:HGNC Symbol;Acc:18287]
DDN	2.372183425	0.002669909	dendrin [Source:HGNC Symbol;Acc:24458]
MEX3D	2.371289595	0.021476985	mex-3 RNA binding family member D [Source:HGNC Symbol;Acc:16734]
RAP1GAP2	2.37098357	1.07E-07	RAP1 GTPase activating protein 2 [Source:HGNC Symbol;Acc:29176]
ABCA2	2.366389305	3.45E-08	ATP-binding cassette, sub-family A (ABC1), member 2 [Source:HGNC Symbol;Acc:32]
RABL6	2.364324755	0.000657227	RAB, member RAS oncogene family-like 6 [Source:HGNC Symbol;Acc:24703]
FABP5	2.36382024	0.003010146	fatty acid binding protein 5 (psoriasis-associated) [Source:HGNC Symbol;Acc:3560]
FAM222A	2.35838913	0.001849829	family with sequence similarity 222, member A [Source:HGNC Symbol;Acc:25915]
LAT2	2.357781595	2.29E-08	linker for activation of T cells family, member 2 [Source:HGNC Symbol;Acc:12749]
UNC93B1	2.356648343	0.007236746	unc-93 homolog B1 (C. elegans) [Source:HGNC Symbol;Acc:13481]
PLXND1	2.351834824	4.04E-06	plexin D1 [Source:HGNC Symbol;Acc:9107]
RDH10	2.348508156	2.15E-07	retinol dehydrogenase 10 (all-trans) [Source:HGNC Symbol;Acc:19975]
KLRK1	2.346949114	0.000490914	killer cell lectin-like receptor subfamily K, member 1 [Source:HGNC Symbol;Acc:18788]
TNIP3	2.342549465	9.72E-06	TNFAIP3 interacting protein 3 [Source:HGNC Symbol;Acc:19315]
HAVCR2	2.341975372	0.002637781	hepatitis A virus cellular receptor 2 [Source:HGNC Symbol;Acc:18437]
HRAS	2.338824357	0.000881176	Harvey rat sarcoma viral oncogene homolog [Source:HGNC Symbol;Acc:5173]
ADAM8	2.334412326	1.42E-06	ADAM metallopeptidase domain 8 [Source:HGNC Symbol;Acc:215]
FLNA	2.332149283	1.11E-06	filamin A, alpha [Source:HGNC Symbol;Acc:3754]
CLMN	2.330742097	0.010031501	calmin (calponin-like, transmembrane) [Source:HGNC Symbol;Acc:19972]
CDK18	2.330348538	0.036034133	cyclin-dependent kinase 18 [Source:HGNC Symbol;Acc:8751]
S100A4	2.329507321	0.000660519	S100 calcium binding protein A4 [Source:HGNC Symbol;Acc:10494]
S100A2	2.329152211	0.03428842	S100 calcium binding protein A2 [Source:HGNC Symbol;Acc:10492]
EGR2	2.328083184	0.002183778	early growth response 2 [Source:HGNC Symbol;Acc:3239]
SERPINE1	2.32796522	0.004034598	serpin peptidase inhibitor, clade E (nexin, plasminogen activator inhibitor type 1), member 1 [Source:HGNC Symbol;Acc:8583]
S100A6	2.327326475	5.89E-05	S100 calcium binding protein A6 [Source:HGNC Symbol;Acc:10496]
PALLD	2.321093542	0.005198613	palladin, cytoskeletal associated protein [Source:HGNC Symbol;Acc:17068]
AC007365.3	2.320987865	0.035810222	
PPP1R16A	2.320949295	0.00513786	protein phosphatase 1, regulatory subunit 16A [Source:HGNC Symbol;Acc:14941]
VAV3	2.318406871	4.85E-07	vav 3 guanine nucleotide exchange factor [Source:HGNC Symbol;Acc:12659]
C17orf58	2.31263952	0.000283463	chromosome 17 open reading frame 58 [Source:HGNC Symbol;Acc:27568]
PRRG4	2.310908412	0.034633769	proline rich Gla (G-carboxyglutamic acid) 4 (transmembrane) [Source:HGNC Symbol;Acc:30799]

CXXC4	2.309621923	0.023975273	CXXC finger protein 4 [Source:HGNC Symbol;Acc:24593]
TMEM170B	2.308165246	0.004347008	transmembrane protein 170B [Source:HGNC Symbol;Acc:34244]
FAM26F	2.304449603	0.031953988	family with sequence similarity 26, member F [Source:HGNC Symbol;Acc:33391]
TSEN54	2.301972299	6.14E-08	TSEN54 tRNA splicing endonuclease subunit [Source:HGNC Symbol;Acc:27561]
HCN3	2.30175746	0.000762102	hyperpolarization activated cyclic nucleotide-gated potassium channel 3 [Source:HGNC Symbol;Acc:19183]
CLSPN	2.301232271	0.000658335	claspin [Source:HGNC Symbol;Acc:19715]
RAB20	2.300902835	0.024815583	RAB20, member RAS oncogene family [Source:HGNC Symbol;Acc:18260]
NACC1	2.300369825	0.000293647	nucleus accumbens associated 1, BEN and BTB (POZ) domain containing [Source:HGNC Symbol;Acc:20967]
ABHD12	2.299803034	0.00011653	abhydrolase domain containing 12 [Source:HGNC Symbol;Acc:15868]
ZFHX3	2.29907606	0.028437737	zinc finger homeobox 3 [Source:HGNC Symbol;Acc:777]
MXD4	2.298171476	3.72E-07	MAX dimerization protein 4 [Source:HGNC Symbol;Acc:13906]
C1orf61	2.296663523	7.32E-06	chromosome 1 open reading frame 61 [Source:HGNC Symbol;Acc:30780]
COL7A1	2.290585286	0.005078459	collagen, type VII, alpha 1 [Source:HGNC Symbol;Acc:2214]
CISD3	2.289393396	0.000936385	CDGSH iron sulfur domain 3 [Source:HGNC Symbol;Acc:27578]
MCOLN2	2.286082019	4.00E-08	mucolipin 2 [Source:HGNC Symbol;Acc:13357]
PRDM8	2.283571742	0.005119429	PR domain containing 8 [Source:HGNC Symbol;Acc:13993]
KIF21A	2.282901728	9.35E-07	kinesin family member 21A [Source:HGNC Symbol;Acc:19349]
DGKZP1	2.280253354	0.027828348	diacylglycerol kinase, zeta pseudogene 1 [Source:HGNC Symbol;Acc:39263]
RN7SL589P	2.279991904	0.003621891	RNA, 7SL, cytoplasmic 589, pseudogene [Source:HGNC Symbol;Acc:46605]
KLRG1	2.27949412	1.47E-05	killer cell lectin-like receptor subfamily G, member 1 [Source:HGNC Symbol;Acc:6380]
AC012358.8	2.276204594	0.007540881	
OTOF	2.276091026	0.000736981	otoferlin [Source:HGNC Symbol;Acc:8515]
CCDC85B	2.268345439	0.001479149	coiled-coil domain containing 85B [Source:HGNC Symbol;Acc:24926]
MELK	2.267955098	0.006657275	maternal embryonic leucine zipper kinase [Source:HGNC Symbol;Acc:16870]
PATL2	2.266297124	4.86E-08	protein associated with topoisomerase II homolog 2 (yeast) [Source:HGNC Symbol;Acc:33630]
TNFRSF1B	2.261612703	5.45E-06	tumor necrosis factor receptor superfamily, member 1B [Source:HGNC Symbol;Acc:11917]
LINC00299	2.261545945	0.000167217	long intergenic non-protein coding RNA 299 [Source:HGNC Symbol;Acc:27940]
EHD1	2.261348844	6.11E-06	EH-domain containing 1 [Source:HGNC Symbol;Acc:3242]
SIPA1L2	2.260959213	0.01190181	signal-induced proliferation-associated 1 like 2 [Source:HGNC Symbol;Acc:23800]
PLXNB1	2.257408048	0.007750519	plexin B1 [Source:HGNC Symbol;Acc:9103]
LIMK1	2.256498395	1.68E-05	LIM domain kinase 1 [Source:HGNC Symbol;Acc:6613]
RN7SL368P	2.254019586	0.025538376	RNA, 7SL, cytoplasmic 368, pseudogene [Source:HGNC Symbol;Acc:46384]
TSC22D4	2.25115441	5.99E-07	TSC22 domain family, member 4 [Source:HGNC Symbol;Acc:21696]
RNF187	2.250137769	0.00017693	ring finger protein 187 [Source:HGNC Symbol;Acc:27146]
JSRP1	2.248287192	0.027036298	junctional sarcoplasmic reticulum protein 1 [Source:HGNC Symbol;Acc:24963]
TLR6	2.246318012	0.003244626	toll-like receptor 6 [Source:HGNC Symbol;Acc:16711]
GFI1	2.245798768	6.74E-08	growth factor independent 1 transcription repressor [Source:HGNC Symbol;Acc:4237]
MFSD10	2.245743789	1.64E-05	major facilitator superfamily domain containing 10 [Source:HGNC Symbol;Acc:16894]
ARMC5	2.24448018	0.00130924	armadillo repeat containing 5 [Source:HGNC Symbol;Acc:25781]
HIP1	2.244351397	5.25E-05	huntingtin interacting protein 1 [Source:HGNC Symbol;Acc:4913]
ZBP1	2.23843354	1.14E-08	Z-DNA binding protein 1 [Source:HGNC Symbol;Acc:16176]
MICALCL	2.238131414	0.012758212	MICAL C-terminal like [Source:HGNC Symbol;Acc:25933]
PHLDA1	2.236358036	0.007644087	pleckstrin homology-like domain, family A, member 1 [Source:HGNC Symbol;Acc:8933]
BATF3	2.235701068	0.030659078	basic leucine zipper transcription factor, ATF-like 3 [Source:HGNC Symbol;Acc:28915]
SDF2L1	2.233586845	0.000180102	stromal cell-derived factor 2-like 1 [Source:HGNC Symbol;Acc:10676]
NUMBL	2.230481085	0.003772319	numb homolog (Drosophila)-like [Source:HGNC Symbol;Acc:8061]

A2M	2.226167634	0.00029321	alpha-2-macroglobulin [Source:HGNC Symbol;Acc:7]
KIRREL3	2.225235269	0.029462702	kin of IRRE like 3 (Drosophila) [Source:HGNC Symbol;Acc:23204]
GINS1	2.22507947	0.046088228	GINS complex subunit 1 (Psf1 homolog) [Source:HGNC Symbol;Acc:28980]
RHOB	2.223549485	7.19E-05	ras homolog family member B [Source:HGNC Symbol;Acc:668]
APOBEC3C	2.222771944	1.91E-06	apolipoprotein B mRNA editing enzyme, catalytic polypeptide-like 3C [Source:HGNC Symbol;Acc:17353]
GPX3	2.221153301	0.008683964	glutathione peroxidase 3 (plasma) [Source:HGNC Symbol;Acc:4555]
FCRL3	2.220782745	0.011942639	Fc receptor-like 3 [Source:HGNC Symbol;Acc:18506]
NAB2	2.215217763	0.003672218	NGFI-A binding protein 2 (EGR1 binding protein 2) [Source:HGNC Symbol;Acc:7627]
G6PD	2.213354886	8.43E-06	glucose-6-phosphate dehydrogenase [Source:HGNC Symbol;Acc:4057]
C9orf142	2.209697972	1.76E-06	chromosome 9 open reading frame 142 [Source:HGNC Symbol;Acc:27849]
CDC34	2.208522488	0.000502474	cell division cycle 34 [Source:HGNC Symbol;Acc:1734]
IL5RA	2.203832436	0.004994886	interleukin 5 receptor, alpha [Source:HGNC Symbol;Acc:6017]
MCTP2	2.201539332	1.49E-07	multiple C2 domains, transmembrane 2 [Source:HGNC Symbol;Acc:25636]
RGS19	2.2015043	0.001973048	regulator of G-protein signaling 19 [Source:HGNC Symbol;Acc:13735]
CCDC78	2.200870154	0.007156958	coiled-coil domain containing 78 [Source:HGNC Symbol;Acc:14153]
GIT1	2.200156984	3.79E-07	G protein-coupled receptor kinase interacting ArfGAP 1 [Source:HGNC Symbol;Acc:4272]
MAP1S	2.199810964	0.000245133	microtubule-associated protein 1S [Source:HGNC Symbol;Acc:15715]
RAB11FIP5	2.196004615	4.79E-06	RAB11 family interacting protein 5 (class I) [Source:HGNC Symbol;Acc:24845]
RHOQ	2.191283052	0.000361255	ras homolog family member Q [Source:HGNC Symbol;Acc:17736]
NCS1	2.190455563	0.001376693	neuronal calcium sensor 1 [Source:HGNC Symbol;Acc:3953]
UAP1L1	2.189383064	0.000299559	UDP-N-acteylglucosamine pyrophosphorylase 1-like 1 [Source:HGNC Symbol;Acc:28082]
EEF1DP3	2.18772203	0.0002311	eukaryotic translation elongation factor 1 delta pseudogene 3 [Source:HGNC Symbol;Acc:30486]
AL591806.1	2.18383268	0.003310932	Uncharacterized protein [Source:UniProtKB/TrEMBL;Acc:M0QZM2]
PCTP	2.180203377	0.000274129	phosphatidylcholine transfer protein [Source:HGNC Symbol;Acc:8752]
FBXW5	2.17960045	0.000579994	F-box and WD repeat domain containing 5 [Source:HGNC Symbol;Acc:13613]
CCDC88B	2.175766498	0.00235067	coiled-coil domain containing 88B [Source:HGNC Symbol;Acc:26757]
MOB3B	2.170232159	0.015483681	MOB kinase activator 3B [Source:HGNC Symbol;Acc:23825]
DNMBP	2.167902097	6.72E-07	dynamin binding protein [Source:HGNC Symbol;Acc:30373]
JAZF1	2.165275403	1.50E-05	JAZF zinc finger 1 [Source:HGNC Symbol;Acc:28917]
PARP10	2.165188311	0.012262378	poly (ADP-ribose) polymerase family, member 10 [Source:HGNC Symbol;Acc:25895]
NHSL1	2.160160333	0.041899402	NHS-like 1 [Source:HGNC Symbol;Acc:21021]
ITPK1	2.159303257	0.00031303	inositol-tetrakisphosphate 1-kinase [Source:HGNC Symbol;Acc:6177]
KIF15	2.15728638	0.015288853	kinesin family member 15 [Source:HGNC Symbol;Acc:17273]
HTATSF1P2	2.153786696	0.026952917	HIV-1 Tat specific factor 1 pseudogene 2 [Source:HGNC Symbol;Acc:38586]
RNF166	2.153579879	9.58E-07	ring finger protein 166 [Source:HGNC Symbol;Acc:28856]
TRGV5P	2.152664483	0.023208232	T cell receptor gamma variable 5P (pseudogene) [Source:HGNC Symbol;Acc:12291]
CDHR1	2.152021333	0.012821937	cadherin-related family member 1 [Source:HGNC Symbol;Acc:14550]
RPL32P1	2.148550414	0.004994886	ribosomal protein L32 pseudogene 1 [Source:HGNC Symbol;Acc:10339]
IFNL1	2.147492517	0.010110313	interferon, lambda 1 [Source:HGNC Symbol;Acc:18363]
TRGC1	2.146216075	0.00178455	T cell receptor gamma constant 1 [Source:HGNC Symbol;Acc:12275]
SYNE1	2.146177757	2.34E-07	spectrin repeat containing, nuclear envelope 1 [Source:HGNC Symbol;Acc:17089]
GFER	2.145151915	0.000183508	growth factor, augmenter of liver regeneration [Source:HGNC Symbol;Acc:4236]
WDR41	2.144981695	2.27E-08	WD repeat domain 41 [Source:HGNC Symbol;Acc:25601]
HRASLS2	2.142043236	0.01318446	HRAS-like suppressor 2 [Source:HGNC Symbol;Acc:17824]
ZNF35	2.139184712	0.001292892	zinc finger protein 35 [Source:HGNC Symbol;Acc:13099]
CALHM2	2.138736322	0.001879175	calcium homeostasis modulator 2 [Source:HGNC Symbol;Acc:23493]

PCGF6	2.135064305	1.08E-05	polycomb group ring finger 6 [Source:HGNC Symbol;Acc:21156]
ANKRD35	2.132358715	0.034372915	ankyrin repeat domain 35 [Source:HGNC Symbol;Acc:26323]
AP2A1	2.131257604	9.72E-06	adaptor-related protein complex 2, alpha 1 subunit [Source:HGNC Symbol;Acc:561]
ATG2A	2.126904495	2.73E-06	autophagy related 2A [Source:HGNC Symbol;Acc:29028]
ARHGAP26	2.126432064	3.92E-08	Rho GTPase activating protein 26 [Source:HGNC Symbol;Acc:17073]
CABLES1	2.125936523	0.037362973	Cdk5 and Abl enzyme substrate 1 [Source:HGNC Symbol;Acc:25097]
SKAP2	2.124043958	9.53E-05	src kinase associated phosphoprotein 2 [Source:HGNC Symbol;Acc:15687]
MFI2	2.123352912	0.049563318	antigen p97 (melanoma associated) identified by monoclonal antibodies 133.2 and 96.5 [Source:HGNC Symbol;Acc:7037]
LINC00092	2.122978082	0.049136691	long intergenic non-protein coding RNA 92 [Source:HGNC Symbol;Acc:31408]
KCP	2.121429985	0.01557908	kielin/chordin-like protein [Source:HGNC Symbol;Acc:17585]
NAGS	2.119726079	0.019470246	N-acetylglutamate synthase [Source:HGNC Symbol;Acc:17996]
AC114730.3	2.11915825	0.027615311	
ZNF710	2.118875166	0.002797821	zinc finger protein 710 [Source:HGNC Symbol;Acc:25352]
PNPLA6	2.114915591	0.001704689	patatin-like phospholipase domain containing 6 [Source:HGNC Symbol;Acc:16268]
CPEB3	2.11410573	0.000296273	cytoplasmic polyadenylation element binding protein 3 [Source:HGNC Symbol;Acc:21746]
ASB2	2.113558966	0.001813485	ankyrin repeat and SOCS box containing 2 [Source:HGNC Symbol;Acc:16012]
EPN1	2.113114262	0.001189493	epsin 1 [Source:HGNC Symbol;Acc:21604]
CD302	2.107906258	0.016904294	CD302 molecule [Source:HGNC Symbol;Acc:30843]
FAM214B	2.104186587	0.001292531	family with sequence similarity 214, member B [Source:HGNC Symbol;Acc:25666]
MIR26B	2.090186509	0.040171187	microRNA 26b [Source:HGNC Symbol;Acc:31612]
CTSS	2.088551835	0.003529612	cathepsin S [Source:HGNC Symbol;Acc:2545]
SIRT2	2.08659015	9.40E-08	sirtuin 2 [Source:HGNC Symbol;Acc:10886]
LENG9	2.083378137	0.033994587	leukocyte receptor cluster (LRC) member 9 [Source:HGNC Symbol;Acc:16306]
TRGJP2	2.082575457	0.049739467	T cell receptor gamma joining P2 [Source:HGNC Symbol;Acc:12281]
MAP1LC3B2	2.073560412	0.047483085	microtubule-associated protein 1 light chain 3 beta 2 [Source:HGNC Symbol;Acc:34390]
CRIM1	2.072333718	0.00024319	cysteine rich transmembrane BMP regulator 1 (chordin-like) [Source:HGNC Symbol;Acc:2359]
ANKDD1A	2.071444808	4.18E-06	ankyrin repeat and death domain containing 1A [Source:HGNC Symbol;Acc:28002]
FPGS	2.069347187	0.001189493	folylpolyglutamate synthase [Source:HGNC Symbol;Acc:3824]
SNX8	2.065005593	0.004976699	sorting nexin 8 [Source:HGNC Symbol;Acc:14972]
SNAPC2	2.064760401	0.000282589	small nuclear RNA activating complex, polypeptide 2, 45kDa [Source:HGNC Symbol;Acc:11135]
FCGRT	2.062179824	0.022891278	Fc fragment of IgG, receptor, transporter, alpha [Source:HGNC Symbol;Acc:3621]
EHBP1L1	2.060747595	0.003851196	EH domain binding protein 1-like 1 [Source:HGNC Symbol;Acc:30682]
ADPRH	2.058772979	0.021501872	ADP-ribosylarginine hydrolase [Source:HGNC Symbol;Acc:269]
TKTL1	2.055694289	0.005621811	transketolase-like 1 [Source:HGNC Symbol;Acc:11835]
PPP1R18	2.053280069	0.000551207	protein phosphatase 1, regulatory subunit 18 [Source:HGNC Symbol;Acc:29413]
NCOR2	2.052516024	4.70E-05	nuclear receptor corepressor 2 [Source:HGNC Symbol;Acc:7673]
DLG5	2.050606485	0.000447656	discs, large homolog 5 (Drosophila) [Source:HGNC Symbol;Acc:2904]
TRPM2	2.050552812	0.043928284	transient receptor potential cation channel, subfamily M, member 2 [Source:HGNC Symbol;Acc:12339]
SULF2	2.049888076	0.006307059	sulfatase 2 [Source:HGNC Symbol;Acc:20392]
PRR5	2.049235783	0.000962231	proline rich 5 (renal) [Source:HGNC Symbol;Acc:31682]
SH3BP5	2.049023073	1.58E-05	SH3-domain binding protein 5 (BTK-associated) [Source:HGNC Symbol;Acc:10827]
ACAP3	2.047179903	0.00583244	ArfGAP with coiled-coil, ankyrin repeat and PH domains 3 [Source:HGNC Symbol;Acc:16754]
FAM89B	2.046368568	0.01190181	family with sequence similarity 89, member B [Source:HGNC Symbol;Acc:16708]
PTPRCAP	2.043415111	0.000703655	protein tyrosine phosphatase, receptor type, C-associated protein [Source:HGNC Symbol;Acc:9667]
NRROS	2.042062063	0.000824724	negative regulator of reactive oxygen species [Source:HGNC Symbol;Acc:24613]

TMCO3	2.040931646	0.001131177	transmembrane and coiled-coil domains 3 [Source:HGNC Symbol;Acc:20329]
ACTN4	2.040235045	2.03E-06	actinin, alpha 4 [Source:HGNC Symbol;Acc:166]
MVD	2.039119024	0.000339713	mevalonate (diphospho) decarboxylase [Source:HGNC Symbol;Acc:7529]
SRGAP2	2.033220571	0.001615197	SLIT-ROBO Rho GTPase activating protein 2 [Source:HGNC Symbol;Acc:19751]
ZNF322	2.033030369	0.029977953	zinc finger protein 322 [Source:HGNC Symbol;Acc:23640]
NDUFB7	2.032408263	5.93E-05	NADH dehydrogenase (ubiquinone) 1 beta subcomplex, 7, 18kDa [Source:HGNC Symbol;Acc:7702]
PVRL1	2.031544212	0.000805533	poliovirus receptor-related 1 (herpesvirus entry mediator C) [Source:HGNC Symbol;Acc:9706]
SPN	2.031375908	0.000345706	sialophorin [Source:HGNC Symbol;Acc:11249]
ZNF541	2.030855892	2.62E-05	zinc finger protein 541 [Source:HGNC Symbol;Acc:25294]
CDC42EP3	2.03060018	8.81E-06	CDC42 effector protein (Rho GTPase binding) 3 [Source:HGNC Symbol;Acc:16943]
MYRF	2.028700244	0.010288284	myelin regulatory factor [Source:HGNC Symbol;Acc:1181]
MS4A1	2.028432765	0.010680306	membrane-spanning 4-domains, subfamily A, member 1 [Source:HGNC Symbol;Acc:7315]
MYO9B	2.028385596	2.53E-05	myosin IXB [Source:HGNC Symbol;Acc:7609]
REEP4	2.027273063	3.25E-06	receptor accessory protein 4 [Source:HGNC Symbol;Acc:26176]
BCL2A1	2.023783084	0.009709209	BCL2-related protein A1 [Source:HGNC Symbol;Acc:991]
SPIRE1	2.023718585	0.004958716	spire-type actin nucleation factor 1 [Source:HGNC Symbol;Acc:30622]
MB21D1	2.021558351	0.000458168	Mab-21 domain containing 1 [Source:HGNC Symbol;Acc:21367]
ZNF524	2.020272459	0.023686109	zinc finger protein 524 [Source:HGNC Symbol;Acc:28322]
APLP2	2.019659573	0.000711078	amyloid beta (A4) precursor-like protein 2 [Source:HGNC Symbol;Acc:598]
NANOGP4	2.016844834	0.026724857	Nanog homeobox pseudogene 4 [Source:HGNC Symbol;Acc:23102]
ARHGAP30	2.015091416	0.0029945	Rho GTPase activating protein 30 [Source:HGNC Symbol;Acc:27414]
GLTSCR1	2.013954857	0.002713665	glioma tumor suppressor candidate region gene 1 [Source:HGNC Symbol;Acc:4332]
PTPRE	2.013694322	1.15E-05	protein tyrosine phosphatase, receptor type, E [Source:HGNC Symbol;Acc:9669]
TMEM147	2.013567668	7.12E-05	transmembrane protein 147 [Source:HGNC Symbol;Acc:30414]
ALYREF	2.01117422	0.002373363	Aly/REF export factor [Source:HGNC Symbol;Acc:19071]
HMGN1P8	2.009805648	0.027533429	high mobility group nucleosome binding domain 1 pseudogene 8 [Source:HGNC Symbol;Acc:39351]
SMAD5	2.008430771	1.99E-05	SMAD family member 5 [Source:HGNC Symbol;Acc:6771]
AP000487.5	2.00740501	0.018027749	
KCNK5	2.005360045	0.046951733	potassium channel, subfamily K, member 5 [Source:HGNC Symbol;Acc:6280]
CTTNBP2NL	2.004708108	0.049760999	CTTNBP2 N-terminal like [Source:HGNC Symbol;Acc:25330]
MAFF	2.003787788	0.005731518	v-maf avian musculoaponeurotic fibrosarcoma oncogene homolog F [Source:HGNC Symbol;Acc:6780]
AC092620.2	2.002876183	6.40E-05	
NBEAL2	2.002038724	3.30E-05	neurobeachin-like 2 [Source:HGNC Symbol;Acc:31928]
PDE4A	2.001604324	0.00186348	phosphodiesterase 4A, cAMP-specific [Source:HGNC Symbol;Acc:8780]
GK5	2.001319657	5.10E-05	glycerol kinase 5 (putative) [Source:HGNC Symbol;Acc:28635]

List of Downregulated Genes: SLAMF7^{+} vs SLAMF7^{-}

Gene	Log2FoldChange	*p*adj	Description
C10orf35	-2.001164556	0.012262378	chromosome 10 open reading frame 35 [Source:HGNC Symbol;Acc:23519]
INF2	-2.003213069	0.018212047	inverted formin, FH2 and WH2 domain containing [Source:HGNC Symbol;Acc:23791]
TRAV6	-2.00697901	0.006687071	T cell receptor alpha variable 6 [Source:HGNC Symbol;Acc:12144]
TSPYL5	-2.011041829	0.041693321	TSPY-like 5 [Source:HGNC Symbol;Acc:29367]
MAGI3	-2.014077399	0.006577364	membrane associated guanylate kinase, WW and PDZ domain containing 3 [Source:HGNC Symbol;Acc:29647]
ZWINT	-2.017592205	0.000226173	ZW10 interacting kinetochore protein [Source:HGNC Symbol;Acc:13195]
SLC30A7	-2.020597529	0.000122023	solute carrier family 30 (zinc transporter), member 7 [Source:HGNC Symbol;Acc:19306]
MBOAT1	-2.027562175	3.06E-07	membrane bound O-acyltransferase domain containing 1 [Source:HGNC Symbol;Acc:21579]
SIRPG	-2.038073153	0.008413468	signal-regulatory protein gamma [Source:HGNC Symbol;Acc:15757]
SDK1	-2.040939715	0.041965538	sidekick cell adhesion molecule 1 [Source:HGNC Symbol;Acc:19307]
AF001548.5	-2.048437243	0.000957056	
FRMD3	-2.049503969	0.015257244	FERM domain containing 3 [Source:HGNC Symbol;Acc:24125]
EEF1A1P38	-2.051092796	0.012352356	eukaryotic translation elongation factor 1 alpha 1 pseudogene 38 [Source:HGNC Symbol;Acc:37916]
SPTBN1	-2.051200438	6.11E-06	spectrin, beta, non-erythrocytic 1 [Source:HGNC Symbol;Acc:11275]
TRAV4	-2.051621449	0.003391237	T cell receptor alpha variable 4 [Source:HGNC Symbol;Acc:12140]
SAMHD1	-2.051711335	1.34E-05	SAM domain and HD domain 1 [Source:HGNC Symbol;Acc:15925]
ZNF550	-2.051947918	0.00014959	zinc finger protein 550 [Source:HGNC Symbol;Acc:28643]
EPX	-2.05358421	0.03537118	eosinophil peroxidase [Source:HGNC Symbol;Acc:3423]
TMEM177	-2.055040417	0.00346378	transmembrane protein 177 [Source:HGNC Symbol;Acc:28143]
ZNF439	-2.059977967	0.012794756	zinc finger protein 439 [Source:HGNC Symbol;Acc:20873]
CLUHP3	-2.060211793	0.000231711	clustered mitochondria (cluA/CLU1) homolog pseudogene 3 [Source:HGNC Symbol;Acc:28447]
AC004017.1	-2.061232133	0.016581576	Uncharacterized protein [Source:UniProtKB/TrEMBL;Acc:M0R3E0]
ZNF542	-2.061602759	9.93E-05	zinc finger protein 542 [Source:HGNC Symbol;Acc:25393]
INSL3	-2.067519373	0.000419324	insulin-like 3 (Leydig cell) [Source:HGNC Symbol;Acc:6086]
USP10	-2.070149057	2.11E-07	ubiquitin specific peptidase 10 [Source:HGNC Symbol;Acc:12608]
LRRN2	-2.071792547	0.018728668	leucine rich repeat neuronal 2 [Source:HGNC Symbol;Acc:16914]
OCLM	-2.074747763	0.001386414	oculomedin [Source:HGNC Symbol;Acc:8103]
AC009948.5	-2.074891024	1.50E-05	
FOXP1	-2.082120279	9.13E-09	forkhead box P1 [Source:HGNC Symbol;Acc:3823]
SRSF6	-2.08401284	2.24E-06	serine/arginine-rich splicing factor 6 [Source:HGNC Symbol;Acc:10788]
EEF1A1P29	-2.086974489	0.032045555	eukaryotic translation elongation factor 1 alpha 1 pseudogene 29 [Source:HGNC Symbol;Acc:37904]
HYAL3	-2.087485772	0.003618079	hyaluronoglucosaminidase 3 [Source:HGNC Symbol;Acc:5322]
FNBP1L	-2.095146479	0.040449753	formin binding protein 1-like [Source:HGNC Symbol;Acc:20851]
ZNF773	-2.096367824	5.55E-05	zinc finger protein 773 [Source:HGNC Symbol;Acc:30487]
SLAMF1	-2.100867892	3.47E-05	signaling lymphocytic activation molecule family member 1 [Source:HGNC Symbol;Acc:10903]
TSPAN15	-2.106483818	0.034013539	tetraspanin 15 [Source:HGNC Symbol;Acc:23298]
ZFR2	-2.10930701	0.008958451	zinc finger RNA binding protein 2 [Source:HGNC Symbol;Acc:29189]
OXNAD1	-2.109435297	2.15E-10	oxidoreductase NAD-binding domain containing 1 [Source:HGNC Symbol;Acc:25128]
PWAR6	-2.111401994	0.032606099	Prader Willi/Angelman region RNA 6 [Source:HGNC Symbol;Acc:49129]
P2RY10	-2.112972838	1.88E-06	purinergic receptor P2Y, G-protein coupled, 10 [Source:HGNC Symbol;Acc:19906]
NECAP2	-2.113324623	7.76E-10	NECAP endocytosis associated 2 [Source:HGNC Symbol;Acc:25528]
DST	-2.116487505	0.000805599	dystonin [Source:HGNC Symbol;Acc:1090]
SPG20	-2.118138665	0.000168265	spastic paraplegia 20 (Troyer syndrome) [Source:HGNC Symbol;Acc:18514]

SMC1B	-2.122813543	0.001791284	structural maintenance of chromosomes 1B [Source:HGNC Symbol;Acc:11112]
KRT72	-2.122870254	0.005300538	keratin 72 [Source:HGNC Symbol;Acc:28932]
PHLDB3	-2.123919762	9.11E-07	pleckstrin homology-like domain, family B, member 3 [Source:HGNC Symbol;Acc:30499]
EIF4EBP3	-2.126286077	0.005947181	eukaryotic translation initiation factor 4E binding protein 3 [Source:HGNC Symbol;Acc:3290]
GPX2	-2.12865401	0.005191296	glutathione peroxidase 2 (gastrointestinal) [Source:HGNC Symbol;Acc:4554]
AC061992.2	-2.138372177	0.006816198	
ZP1	-2.140363889	0.04732746	zona pellucida glycoprotein 1 (sperm receptor) [Source:HGNC Symbol;Acc:13187]
C17orf72	-2.142819677	4.42E-06	chromosome 17 open reading frame 72 [Source:HGNC Symbol;Acc:25673]
ACBD4	-2.14329791	0.000193837	acyl-CoA binding domain containing 4 [Source:HGNC Symbol;Acc:23337]
VSIG10	-2.144805124	0.001572098	V-set and immunoglobulin domain containing 10 [Source:HGNC Symbol;Acc:26078]
FAM60A	-2.150033353	1.08E-09	family with sequence similarity 60, member A [Source:HGNC Symbol;Acc:30702]
VWA5A	-2.152544552	0.002000908	von Willebrand factor A domain containing 5A [Source:HGNC Symbol;Acc:6658]
ALG14	-2.154459487	0.000278825	ALG14, UDP-N-acetylglucosaminyltransferase subunit [Source:HGNC Symbol;Acc:28287]
C12orf65	-2.156402136	8.03E-05	chromosome 12 open reading frame 65 [Source:HGNC Symbol;Acc:26784]
EEF2K	-2.16007903	0.000297756	eukaryotic elongation factor-2 kinase [Source:HGNC Symbol;Acc:24615]
CUBN	-2.161643027	0.008620849	cubilin (intrinsic factor-cobalamin receptor) [Source:HGNC Symbol;Acc:2548]
RPL17P40	-2.163842083	0.012911645	ribosomal protein L17 pseudogene 40 [Source:HGNC Symbol;Acc:36672]
CNKSR2	-2.165821705	0.00608692	connector enhancer of kinase suppressor of Ras 2 [Source:HGNC Symbol;Acc:19701]
BEX4	-2.166342562	7.74E-08	brain expressed, X-linked 4 [Source:HGNC Symbol;Acc:25475]
AC109333.10	-2.171669354	0.034039448	
ZNF814	-2.172431794	1.81E-07	zinc finger protein 814 [Source:HGNC Symbol;Acc:33258]
PLEKHG4	-2.178717864	0.004950697	pleckstrin homology domain containing, family G (with RhoGef domain) member 4 [Source:HGNC Symbol;Acc:24501]
TTC3P1	-2.183746578	0.002942564	tetratricopeptide repeat domain 3 pseudogene 1 [Source:HGNC Symbol;Acc:23318]
ACP6	-2.188157943	5.03E-05	acid phosphatase 6, lysophosphatidic [Source:HGNC Symbol;Acc:29609]
TCF7	-2.188768949	1.90E-05	transcription factor 7 (T-cell specific, HMG-box) [Source:HGNC Symbol;Acc:11639]
C1orf172	-2.189976929	0.005330683	chromosome 1 open reading frame 172 [Source:HGNC Symbol;Acc:26624]
PITPNM2	-2.192903552	0.000317413	phosphatidylinositol transfer protein, membrane-associated 2 [Source:HGNC Symbol;Acc:21044]
PAIP2B	-2.195729127	0.020986839	poly(A) binding protein interacting protein 2B [Source:HGNC Symbol;Acc:29200]
TRAJ57	-2.197918254	0.036079611	T cell receptor alpha joining 57 [Source:HGNC Symbol;Acc:12089]
ZNF844	-2.201563651	0.00301192	zinc finger protein 844 [Source:HGNC Symbol;Acc:25932]
ANKRD18EP	-2.211362963	0.006362832	ankyrin repeat domain 18E, pseudogene [Source:HGNC Symbol;Acc:43609]
ACSL6	-2.213567176	2.17E-06	acyl-CoA synthetase long-chain family member 6 [Source:HGNC Symbol;Acc:16496]
ZNF546	-2.216447012	0.012252915	zinc finger protein 546 [Source:HGNC Symbol;Acc:28671]
LMO7	-2.223124347	0.003988864	LIM domain 7 [Source:HGNC Symbol;Acc:6646]
SNX9	-2.229724914	0.000406401	sorting nexin 9 [Source:HGNC Symbol;Acc:14973]
ZNF813	-2.230202256	1.14E-05	zinc finger protein 813 [Source:HGNC Symbol;Acc:33257]
EGLN3	-2.231099172	0.045198098	egl-9 family hypoxia-inducible factor 3 [Source:HGNC Symbol;Acc:14661]
COL1A1	-2.239689786	0.000418437	collagen, type I, alpha 1 [Source:HGNC Symbol;Acc:2197]
AGMAT	-2.241814109	0.010276024	agmatine ureohydrolase (agmatinase) [Source:HGNC Symbol;Acc:18407]
MCOLN3	-2.242448893	0.022546835	mucolipin 3 [Source:HGNC Symbol;Acc:13358]
ZBTB25	-2.24901844	2.48E-07	zinc finger and BTB domain containing 25 [Source:HGNC Symbol;Acc:13112]
KCTD21	-2.250305479	0.00824888	potassium channel tetramerization domain containing 21 [Source:HGNC Symbol;Acc:27452]
CDS1	-2.250880198	0.013688642	CDP-diacylglycerol synthase (phosphatidate cytidylyltransferase) 1 [Source:HGNC Symbol;Acc:1800]
PARK2	-2.25246892	0.008766028	parkin RBR E3 ubiquitin protein ligase [Source:HGNC Symbol;Acc:8607]
BIRC3	-2.260068201	7.94E-11	baculoviral IAP repeat containing 3 [Source:HGNC Symbol;Acc:591]
TUB	-2.262903527	0.01436664	tubby bipartite transcription factor [Source:HGNC Symbol;Acc:12406]

ZNF93	-2.263605597	0.000444521	zinc finger protein 93 [Source:HGNC Symbol;Acc:13169]
LINC00899	-2.268937287	0.005403656	long intergenic non-protein coding RNA 899 [Source:HGNC Symbol;Acc:48583]
TMEM30B	-2.273228964	0.000407436	transmembrane protein 30B [Source:HGNC Symbol;Acc:27254]
ADAM19	-2.286336315	0.004732691	ADAM metallopeptidase domain 19 [Source:HGNC Symbol;Acc:197]
ZNF256	-2.29543393	0.006510531	zinc finger protein 256 [Source:HGNC Symbol;Acc:13049]
IL12RB2	-2.295858645	0.000112153	interleukin 12 receptor, beta 2 [Source:HGNC Symbol;Acc:5972]
ADAMTS17	-2.296073937	3.29E-05	ADAM metallopeptidase with thrombospondin type 1 motif, 17 [Source:HGNC Symbol;Acc:17109]
SGTB	-2.296285468	3.77E-09	small glutamine-rich tetratricopeptide repeat (TPR)-containing, beta [Source:HGNC Symbol;Acc:23567]
BEX2	-2.298072873	1.28E-09	brain expressed X-linked 2 [Source:HGNC Symbol;Acc:30933]
ICAM2	-2.302426241	5.22E-10	intercellular adhesion molecule 2 [Source:HGNC Symbol;Acc:5345]
ZNF677	-2.313035671	0.001149349	zinc finger protein 677 [Source:HGNC Symbol;Acc:28730]
FAM86FP	-2.314839557	0.042103663	family with sequence similarity 86, member F, pseudogene [Source:HGNC Symbol;Acc:42357]
RHOH	-2.316440503	5.26E-08	ras homolog family member H [Source:HGNC Symbol;Acc:686]
PIK3IP1	-2.325754482	2.48E-06	phosphoinositide-3-kinase interacting protein 1 [Source:HGNC Symbol;Acc:24942]
LPIN3	-2.328324235	0.030150236	lipin 3 [Source:HGNC Symbol;Acc:14451]
SEC14L2	-2.330798727	6.26E-07	SEC14-like 2 (S. cerevisiae) [Source:HGNC Symbol;Acc:10699]
LIMS2	-2.344633137	0.018745203	LIM and senescent cell antigen-like domains 2 [Source:HGNC Symbol;Acc:16084]
ALPK1	-2.346093101	0.002505679	alpha-kinase 1 [Source:HGNC Symbol;Acc:20917]
ABCC2	-2.349898651	0.004947691	ATP-binding cassette, sub-family C (CFTR/MRP), member 2 [Source:HGNC Symbol;Acc:53]
ZNF287	-2.353752541	2.48E-06	zinc finger protein 287 [Source:HGNC Symbol;Acc:13502]
WDR89	-2.35827597	2.64E-05	WD repeat domain 89 [Source:HGNC Symbol;Acc:20489]
IPCEF1	-2.360575132	3.98E-08	interaction protein for cytohesin exchange factors 1 [Source:HGNC Symbol;Acc:21204]
PIM2	-2.36928037	7.38E-08	pim-2 oncogene [Source:HGNC Symbol;Acc:8987]
KRT2	-2.369604079	0.010976168	keratin 2 [Source:HGNC Symbol;Acc:6439]
RPL18P10	-2.374578265	0.000116949	ribosomal protein L18 pseudogene 10 [Source:HGNC Symbol;Acc:35957]
AP3M2	-2.377061983	9.38E-10	adaptor-related protein complex 3, mu 2 subunit [Source:HGNC Symbol;Acc:570]
AC002128.5	-2.378355774	0.008946029	
LMLN	-2.378866003	0.000509826	leishmanolysin-like (metallopeptidase M8 family) [Source:HGNC Symbol;Acc:15991]
THTPA	-2.387928022	8.16E-05	thiamine triphosphatase [Source:HGNC Symbol;Acc:18987]
ZC3H12D	-2.391695346	5.96E-08	zinc finger CCCH-type containing 12D [Source:HGNC Symbol;Acc:21175]
AC144521.1	-2.397605788	0.000933578	
DGKA	-2.398273867	1.18E-08	diacylglycerol kinase, alpha 80kDa [Source:HGNC Symbol;Acc:2849]
C4orf32	-2.399135781	0.000339713	chromosome 4 open reading frame 32 [Source:HGNC Symbol;Acc:26813]
ABCA6	-2.403707931	0.037354018	ATP-binding cassette, sub-family A (ABC1), member 6 [Source:HGNC Symbol;Acc:36]
DUSP16	-2.407609256	3.92E-08	dual specificity phosphatase 16 [Source:HGNC Symbol;Acc:17909]
C14orf64	-2.408597019	1.43E-05	chromosome 14 open reading frame 64 [Source:HGNC Symbol;Acc:20111]
Y_RNA	-2.411058607	0.031852949	Y RNA [Source:RFAM;Acc:RF00019]
RTKN2	-2.416919836	0.016252301	rhotekin 2 [Source:HGNC Symbol;Acc:19364]
SMARCA1	-2.427925383	0.048049806	SWI/SNF related, matrix associated, actin dependent regulator of chromatin, subfamily a, member 1 [Source:HGNC Symbol;Acc:11097]
METAP1D	-2.429121191	4.98E-05	methionyl aminopeptidase type 1D (mitochondrial) [Source:HGNC Symbol;Acc:32583]
TUBA3E	-2.435297165	0.028086044	tubulin, alpha 3e [Source:HGNC Symbol;Acc:20765]
FAM213A	-2.438975861	1.21E-05	family with sequence similarity 213, member A [Source:HGNC Symbol;Acc:28651]
USP51	-2.442434522	1.07E-05	ubiquitin specific peptidase 51 [Source:HGNC Symbol;Acc:23086]
U4	-2.443210515	0.01317454	U4 spliceosomal RNA [Source:RFAM;Acc:RF00015]
BEST4	-2.444701193	9.01E-06	bestrophin 4 [Source:HGNC Symbol;Acc:17106]
SEC14L3	-2.447713399	0.002024122	SEC14-like 3 (S. cerevisiae) [Source:HGNC Symbol;Acc:18655]

AK5	-2.449783442	0.000577871	adenylate kinase 5 [Source:HGNC Symbol;Acc:365]
ZNF776	-2.45060669	2.10E-10	zinc finger protein 776 [Source:HGNC Symbol;Acc:26765]
C4orf26	-2.469184906	0.012043268	chromosome 4 open reading frame 26 [Source:HGNC Symbol;Acc:26300]
OR52N4	-2.46977614	0.045081784	olfactory receptor, family 52, subfamily N, member 4 (gene/pseudogene) [Source:HGNC Symbol;Acc:15230]
HN1L	-2.470146421	0.006983154	hematological and neurological expressed 1-like [Source:HGNC Symbol;Acc:14137]
TIMD4	-2.477981302	0.017731402	T-cell immunoglobulin and mucin domain containing 4 [Source:HGNC Symbol;Acc:25132]
SLC8B1	-2.478613155	1.55E-09	solute carrier family 8 (sodium/lithium/calcium exchanger), member B1 [Source:HGNC Symbol;Acc:26175]
SATB1	-2.486885023	3.04E-09	SATB homeobox 1 [Source:HGNC Symbol;Acc:10541]
TMIGD2	-2.491475711	0.038414527	transmembrane and immunoglobulin domain containing 2 [Source:HGNC Symbol;Acc:28324]
SOAT2	-2.494242738	0.044662726	sterol O-acyltransferase 2 [Source:HGNC Symbol;Acc:11178]
ZNF606	-2.495356428	5.59E-05	zinc finger protein 606 [Source:HGNC Symbol;Acc:25879]
TMEM173	-2.496745789	1.96E-09	transmembrane protein 173 [Source:HGNC Symbol;Acc:27962]
ZFP30	-2.507386962	0.00024319	ZFP30 zinc finger protein [Source:HGNC Symbol;Acc:29555]
RFX3	-2.51021621	5.55E-08	regulatory factor X, 3 (influences HLA class II expression) [Source:HGNC Symbol;Acc:9984]
TRAV35	-2.511309876	0.02801683	T cell receptor alpha variable 35 [Source:HGNC Symbol;Acc:12134]
ZDHHC11B	-2.514042035	4.02E-05	zinc finger, DHHC-type containing 11B [Source:HGNC Symbol;Acc:32962]
TNK1	-2.516617017	0.00029321	tyrosine kinase, non-receptor, 1 [Source:HGNC Symbol;Acc:11940]
MKRN3	-2.517178305	0.021168407	makorin ring finger protein 3 [Source:HGNC Symbol;Acc:7114]
ZDHHC11	-2.520394411	0.003161915	zinc finger, DHHC-type containing 11 [Source:HGNC Symbol;Acc:19158]
BACH2	-2.521168499	1.02E-06	BTB and CNC homology 1, basic leucine zipper transcription factor 2 [Source:HGNC Symbol;Acc:14078]
RPS15AP24	-2.521918669	3.56E-05	ribosomal protein S15a pseudogene 24 [Source:HGNC Symbol;Acc:36174]
AC020571.3	-2.52223901	0.004020243	
DHRS3	-2.522832843	4.26E-10	dehydrogenase/reductase (SDR family) member 3 [Source:HGNC Symbol;Acc:17693]
ZNF331	-2.523377271	1.63E-11	zinc finger protein 331 [Source:HGNC Symbol;Acc:15489]
ZNF154	-2.532307894	4.54E-07	zinc finger protein 154 [Source:HGNC Symbol;Acc:12939]
RAPGEF6	-2.533243822	4.79E-06	Rap guanine nucleotide exchange factor (GEF) 6 [Source:HGNC Symbol;Acc:20655]
POLR3E	-2.534116132	5.57E-10	polymerase (RNA) III (DNA directed) polypeptide E (80kD) [Source:HGNC Symbol;Acc:30347]
TNNC1	-2.536526155	0.004054246	troponin C type 1 (slow) [Source:HGNC Symbol;Acc:11943]
ZNF540	-2.537871211	2.87E-05	zinc finger protein 540 [Source:HGNC Symbol;Acc:25331]
FAM124B	-2.553268554	0.030480542	family with sequence similarity 124B [Source:HGNC Symbol;Acc:26224]
NBPF15	-2.55976512	2.05E-06	neuroblastoma breakpoint family, member 15 [Source:HGNC Symbol;Acc:28791]
RPL7L1P12	-2.562190141	0.025027726	ribosomal protein L7-like 1 pseudogene 12 [Source:HGNC Symbol;Acc:39811]
RPL21P121	-2.567488038	0.013634152	ribosomal protein L21 pseudogene 121 [Source:HGNC Symbol;Acc:36429]
IL6ST	-2.568891713	7.10E-12	interleukin 6 signal transducer (gp130, oncostatin M receptor) [Source:HGNC Symbol;Acc:6021]
CAMK4	-2.582285471	7.34E-12	calcium/calmodulin-dependent protein kinase IV [Source:HGNC Symbol;Acc:1464]
TTN	-2.593689105	1.64E-06	titin [Source:HGNC Symbol;Acc:12403]
HID1	-2.594130503	0.000612869	HID1 domain containing [Source:HGNC Symbol;Acc:15736]
ZNF483	-2.598701738	5.98E-08	zinc finger protein 483 [Source:HGNC Symbol;Acc:23384]
RPS6P16	-2.603531871	0.012043268	ribosomal protein S6 pseudogene 16 [Source:HGNC Symbol;Acc:35668]
RASGRF2	-2.608968139	0.000394321	Ras protein-specific guanine nucleotide-releasing factor 2 [Source:HGNC Symbol;Acc:9876]
C1orf95	-2.611784469	0.010457226	chromosome 1 open reading frame 95 [Source:HGNC Symbol;Acc:30491]
PHBP9	-2.615441817	2.42E-06	prohibitin pseudogene 9 [Source:HGNC Symbol;Acc:39288]
ARMCX2	-2.61736583	0.032239274	armadillo repeat containing, X-linked 2 [Source:HGNC Symbol;Acc:16869]
SNED1	-2.622367807	3.77E-10	sushi, nidogen and EGF-like domains 1 [Source:HGNC Symbol;Acc:24696]
TNFAIP8	-2.623018203	1.79E-09	tumor necrosis factor, alpha-induced protein 8 [Source:HGNC Symbol;Acc:17260]
ZNF577	-2.623807523	2.30E-07	zinc finger protein 577 [Source:HGNC Symbol;Acc:28673]

AP001205.1	-2.632597246	2.79E-05	
AC093110.3	-2.634723743	0.006641748	
SVILP1	-2.643832297	0.009937301	supervillin pseudogene 1 [Source:HGNC Symbol;Acc:44959]
MIR378I	-2.64698182	6.96E-05	microRNA 378i [Source:HGNC Symbol;Acc:41620]
CSGALNACT1	-2.648125259	1.51E-08	chondroitin sulfate N-acetylgalactosaminyltransferase 1 [Source:HGNC Symbol;Acc:24290]
ZNF665	-2.65668965	0.000397836	zinc finger protein 665 [Source:HGNC Symbol;Acc:25885]
EEF1A1P19	-2.658715295	0.000197529	eukaryotic translation elongation factor 1 alpha 1 pseudogene 19 [Source:HGNC Symbol;Acc:37892]
TIAM1	-2.663896983	0.001868999	T-cell lymphoma invasion and metastasis 1 [Source:HGNC Symbol;Acc:11805]
PLLP	-2.669184957	0.008534686	plasmolipin [Source:HGNC Symbol;Acc:18553]
TRPC1	-2.694731511	3.29E-05	transient receptor potential cation channel, subfamily C, member 1 [Source:HGNC Symbol;Acc:12333]
IL7R	-2.69894256	2.45E-10	interleukin 7 receptor [Source:HGNC Symbol;Acc:6024]
ID3	-2.699700192	5.30E-12	inhibitor of DNA binding 3, dominant negative helix-loop-helix protein [Source:HGNC Symbol;Acc:5362]
AC018892.9	-2.703832191	0.008411175	
GEM	-2.712022091	7.23E-05	GTP binding protein overexpressed in skeletal muscle [Source:HGNC Symbol;Acc:4234]
AE000661.37	-2.712383931	0.00406918	
ACE	-2.716663978	0.012591955	angiotensin I converting enzyme [Source:HGNC Symbol;Acc:2707]
TRAJ55	-2.719654604	0.009572553	T cell receptor alpha joining 55 (pseudogene) [Source:HGNC Symbol;Acc:12087]
DFNB59	-2.731990685	0.002814112	deafness, autosomal recessive 59 [Source:HGNC Symbol;Acc:29502]
RNF157	-2.733907169	0.000180149	ring finger protein 157 [Source:HGNC Symbol;Acc:29402]
LINC00511	-2.734552433	0.023292593	long intergenic non-protein coding RNA 511 [Source:HGNC Symbol;Acc:43564]
AFF3	-2.735277433	0.005665399	AF4/FMR2 family, member 3 [Source:HGNC Symbol;Acc:6473]
PIFO	-2.739917102	0.045234416	primary cilia formation [Source:HGNC Symbol;Acc:27009]
CXCR5	-2.750067554	0.000312366	chemokine (C-X-C motif) receptor 5 [Source:HGNC Symbol;Acc:1060]
ACER1	-2.751991327	0.001172345	alkaline ceramidase 1 [Source:HGNC Symbol;Acc:18356]
SEMA6A	-2.756316063	0.0051785	sema domain, transmembrane domain (TM), and cytoplasmic domain, (semaphorin) 6A [Source:HGNC Symbol;Acc:10738]
PLCL1	-2.757109109	4.95E-05	phospholipase C-like 1 [Source:HGNC Symbol;Acc:9063]
DISC1	-2.757568207	1.52E-06	disrupted in schizophrenia 1 [Source:HGNC Symbol;Acc:2888]
TRAT1	-2.76260517	6.74E-08	T cell receptor associated transmembrane adaptor 1 [Source:HGNC Symbol;Acc:30698]
ZNF492	-2.772522782	0.006577364	zinc finger protein 492 [Source:HGNC Symbol;Acc:23707]
AGPAT5	-2.775733281	8.53E-12	1-acylglycerol-3-phosphate O-acyltransferase 5 [Source:HGNC Symbol;Acc:20886]
HAPLN3	-2.775911091	0.001892073	hyaluronan and proteoglycan link protein 3 [Source:HGNC Symbol;Acc:21446]
ZNF518B	-2.781729328	1.14E-11	zinc finger protein 518B [Source:HGNC Symbol;Acc:29365]
TMEM25	-2.792378722	0.000205403	transmembrane protein 25 [Source:HGNC Symbol;Acc:25890]
MYC	-2.799110267	1.60E-05	v-myc avian myelocytomatosis viral oncogene homolog [Source:HGNC Symbol;Acc:7553]
SLC22A23	-2.806972268	0.000991907	solute carrier family 22, member 23 [Source:HGNC Symbol;Acc:21106]
FBLN5	-2.807563086	0.000393414	fibulin 5 [Source:HGNC Symbol;Acc:3602]
EPHX2	-2.810096327	0.000437374	epoxide hydrolase 2, cytoplasmic [Source:HGNC Symbol;Acc:3402]
ZNF839P1	-2.814592456	0.013506367	zinc finger protein 839 pseudogene 1 [Source:HGNC Symbol;Acc:38455]
TAF4B	-2.814931049	5.68E-07	TAF4b RNA polymerase II, TATA box binding protein (TBP)-associated factor, 105kDa [Source:HGNC Symbol;Acc:11538]
FAM174B	-2.819412614	7.39E-07	family with sequence similarity 174, member B [Source:HGNC Symbol;Acc:34339]
RN7SKP110	-2.824415317	0.000144586	RNA, 7SK small nuclear pseudogene 110 [Source:HGNC Symbol;Acc:45834]
EXPH5	-2.825143936	0.000694979	exophilin 5 [Source:HGNC Symbol;Acc:30578]
TRAV27	-2.830368431	0.000866683	T cell receptor alpha variable 27 [Source:HGNC Symbol;Acc:12125]
METTL15P1	-2.830475934	0.007971028	methyltransferase like 15 pseudogene 1 [Source:HGNC Symbol;Acc:31926]
DHX9P1	-2.831492643	0.002954514	DEAH (Asp-Glu-Ala-His) box polypeptide 9 pseudogene 1 [Source:HGNC Symbol;Acc:2751]

EEF1A1P14	-2.844557659	0.008230278	eukaryotic translation elongation factor 1 alpha 1 pseudogene 14 [Source:HGNC Symbol;Acc:3197]
TRAJ46	-2.86134269	0.00435375	T cell receptor alpha joining 46 [Source:HGNC Symbol;Acc:12077]
CEACAM1	-2.864234552	0.002288466	carcinoembryonic antigen-related cell adhesion molecule 1 (biliary glycoprotein) [Source:HGNC Symbol;Acc:1814]
SLC44A5	-2.872931107	0.00953883	solute carrier family 44, member 5 [Source:HGNC Symbol;Acc:28524]
ATP13A4	-2.87653583	0.020248548	ATPase type 13A4 [Source:HGNC Symbol;Acc:25422]
SETD7	-2.877547766	1.44E-11	SET domain containing (lysine methyltransferase) 7 [Source:HGNC Symbol;Acc:30412]
HABP4	-2.877659149	1.03E-12	hyaluronan binding protein 4 [Source:HGNC Symbol;Acc:17062]
EEF1A1P12	-2.879037507	4.57E-05	eukaryotic translation elongation factor 1 alpha 1 pseudogene 12 [Source:HGNC Symbol;Acc:3195]
NMNAT3	-2.87952701	0.012401518	nicotinamide nucleotide adenylyltransferase 3 [Source:HGNC Symbol;Acc:20989]
ZNF165	-2.880240513	1.48E-07	zinc finger protein 165 [Source:HGNC Symbol;Acc:12953]
ZNF140	-2.890680137	4.46E-07	zinc finger protein 140 [Source:HGNC Symbol;Acc:12925]
TSPAN18	-2.897827532	0.001460989	tetraspanin 18 [Source:HGNC Symbol;Acc:20660]
SDR42E1	-2.900846987	6.68E-07	short chain dehydrogenase/reductase family 42E, member 1 [Source:HGNC Symbol;Acc:29834]
SC5D	-2.904957506	5.65E-17	sterol-C5-desaturase [Source:HGNC Symbol;Acc:10547]
TNFRSF25	-2.91890758	2.15E-07	tumor necrosis factor receptor superfamily, member 25 [Source:HGNC Symbol;Acc:11910]
ZBTB16	-2.920969305	8.27E-06	zinc finger and BTB domain containing 16 [Source:HGNC Symbol;Acc:12930]
ZNF274	-2.922047944	6.02E-09	zinc finger protein 274 [Source:HGNC Symbol;Acc:13068]
MIR4458HG	-2.929121744	0.003010883	MIR4458 host gene (non-protein coding) [Source:HGNC Symbol;Acc:49008]
KCTD3	-2.943802226	0.008102449	potassium channel tetramerization domain containing 3 [Source:HGNC Symbol;Acc:21305]
KLHL31	-2.944843335	0.042631355	kelch-like family member 31 [Source:HGNC Symbol;Acc:21353]
OBSCN	-2.94610713	6.38E-07	obscurin, cytoskeletal calmodulin and titin-interacting RhoGEF [Source:HGNC Symbol;Acc:15719]
FAIM3	-2.947953824	1.06E-11	Fas apoptotic inhibitory molecule 3 [Source:HGNC Symbol;Acc:14315]
ZNF705E	-2.948992503	0.008491769	zinc finger protein 705E [Source:HGNC Symbol;Acc:33203]
OCM	-2.953133759	0.000690652	oncomodulin [Source:HGNC Symbol;Acc:8105]
AC004837.5	-2.963773014	0.001887198	
LRRC16A	-2.967611032	0.000686698	leucine rich repeat containing 16A [Source:HGNC Symbol;Acc:21581]
PCSK5	-2.975374008	0.000268309	proprotein convertase subtilisin/kexin type 5 [Source:HGNC Symbol;Acc:8747]
EEF1A1P8	-2.977938863	0.029000094	eukaryotic translation elongation factor 1 alpha 1 pseudogene 8 [Source:HGNC Symbol;Acc:3203]
KRT18P34	-2.979207302	0.018431278	keratin 18 pseudogene 34 [Source:HGNC Symbol;Acc:33403]
AXIN2	-2.97958341	0.000254828	axin 2 [Source:HGNC Symbol;Acc:904]
IL24	-2.982772681	4.18E-08	interleukin 24 [Source:HGNC Symbol;Acc:11346]
CNN3	-2.984193929	1.32E-05	calponin 3, acidic [Source:HGNC Symbol;Acc:2157]
ZNF891	-2.986883338	4.17E-05	zinc finger protein 891 [Source:HGNC Symbol;Acc:38709]
EEF1A1P16	-2.995152701	0.018131969	eukaryotic translation elongation factor 1 alpha 1 pseudogene 16 [Source:HGNC Symbol;Acc:37889]
FOXP3	-3.00113789	2.76E-05	forkhead box P3 [Source:HGNC Symbol;Acc:6106]
AL162458.1	-3.009958954	0.041899402	
ESPN	-3.013694766	0.035193285	espin [Source:HGNC Symbol;Acc:13281]
AC005237.4	-3.019445831	0.012824773	
PRKG2	-3.024429535	0.008051159	protein kinase, cGMP-dependent, type II [Source:HGNC Symbol;Acc:9416]
RPS6KL1	-3.024535017	4.28E-06	ribosomal protein S6 kinase-like 1 [Source:HGNC Symbol;Acc:20222]
PKIA	-3.035133419	0.002713665	protein kinase (cAMP-dependent, catalytic) inhibitor alpha [Source:HGNC Symbol;Acc:9017]
RAB25	-3.037482723	0.006576488	RAB25, member RAS oncogene family [Source:HGNC Symbol;Acc:18238]
KLF7	-3.039126141	1.04E-14	Kruppel-like factor 7 (ubiquitous) [Source:HGNC Symbol;Acc:6350]
CUX2	-3.040739453	0.023502716	cut-like homeobox 2 [Source:HGNC Symbol;Acc:19347]
MBOAT4	-3.04739017	3.21E-09	membrane bound O-acyltransferase domain containing 4 [Source:HGNC Symbol;Acc:32311]

PDE9A	-3.049819799	0.003011167	phosphodiesterase 9A [Source:HGNC Symbol;Acc:8795]
ZNF10	-3.05211406	1.06E-11	zinc finger protein 10 [Source:HGNC Symbol;Acc:12879]
KLHL3	-3.073531754	5.44E-09	kelch-like family member 3 [Source:HGNC Symbol;Acc:6354]
AC110926.4	-3.083290198	0.039185509	
TNFSF8	-3.087262565	9.84E-08	tumor necrosis factor (ligand) superfamily, member 8 [Source:HGNC Symbol;Acc:11938]
DISP1	-3.105234967	0.015483681	dispatched homolog 1 (Drosophila) [Source:HGNC Symbol;Acc:19711]
DKK4	-3.129735852	0.015674837	dickkopf WNT signaling pathway inhibitor 4 [Source:HGNC Symbol;Acc:2894]
RFESD	-3.133723745	0.000154595	Rieske (Fe-S) domain containing [Source:HGNC Symbol;Acc:29587]
SLC4A5	-3.136175338	6.09E-06	solute carrier family 4 (sodium bicarbonate cotransporter), member 5 [Source:HGNC Symbol;Acc:18168]
PAK3	-3.139009685	7.53E-05	p21 protein (Cdc42/Rac)-activated kinase 3 [Source:HGNC Symbol;Acc:8592]
MICU3	-3.141420189	0.001592438	mitochondrial calcium uptake family, member 3 [Source:HGNC Symbol;Acc:27820]
GPRASP1	-3.187951887	1.42E-06	G protein-coupled receptor associated sorting protein 1 [Source:HGNC Symbol;Acc:24834]
PLAT	-3.197330284	3.26E-05	plasminogen activator, tissue [Source:HGNC Symbol;Acc:9051]
SERINC5	-3.218111052	4.05E-11	serine incorporator 5 [Source:HGNC Symbol;Acc:18825]
RN7SL180P	-3.238129116	0.032037637	RNA, 7SL, cytoplasmic 180, pseudogene [Source:HGNC Symbol;Acc:46196]
FHL1	-3.239798988	1.48E-08	four and a half LIM domains 1 [Source:HGNC Symbol;Acc:3702]
TTC28	-3.245264782	0.001292892	tetratricopeptide repeat domain 28 [Source:HGNC Symbol;Acc:29179]
GRAP	-3.248045882	0.000206797	GRB2-related adaptor protein [Source:HGNC Symbol;Acc:4562]
WNK3	-3.249495801	0.035992597	WNK lysine deficient protein kinase 3 [Source:HGNC Symbol;Acc:14543]
ANK3	-3.256018151	2.27E-05	ankyrin 3, node of Ranvier (ankyrin G) [Source:HGNC Symbol;Acc:494]
FST	-3.262474102	0.000470527	follistatin [Source:HGNC Symbol;Acc:3971]
TDRD12	-3.279442481	0.024893098	tudor domain containing 12 [Source:HGNC Symbol;Acc:25044]
AKR1C1	-3.282838696	0.003327804	aldo-keto reductase family 1, member C1 [Source:HGNC Symbol;Acc:384]
CCDC141	-3.29130962	5.22E-05	coiled-coil domain containing 141 [Source:HGNC Symbol;Acc:26821]
PTK2	-3.292222597	1.08E-08	protein tyrosine kinase 2 [Source:HGNC Symbol;Acc:9611]
AC002331.1	-3.293391411	0.03833634	
SNTG2	-3.301877772	0.020035218	syntrophin, gamma 2 [Source:HGNC Symbol;Acc:13741]
LTB	-3.304078061	1.18E-11	lymphotoxin beta (TNF superfamily, member 3) [Source:HGNC Symbol;Acc:6711]
SH3YL1	-3.310825459	1.83E-08	SH3 and SYLF domain containing 1 [Source:HGNC Symbol;Acc:29546]
ALDH5A1	-3.322986626	5.93E-05	aldehyde dehydrogenase 5 family, member A1 [Source:HGNC Symbol;Acc:408]
AC022182.1	-3.325657312	9.68E-06	
FBXL16	-3.328780895	0.00149884	F-box and leucine-rich repeat protein 16 [Source:HGNC Symbol;Acc:14150]
SPTLC1P1	-3.333153464	0.000661563	serine palmitoyltransferase, long chain base subunit 1 pseudogene 1 [Source:HGNC Symbol;Acc:39668]
ICOS	-3.341015033	9.99E-13	inducible T-cell co-stimulator [Source:HGNC Symbol;Acc:5351]
IL23A	-3.345000279	6.21E-07	interleukin 23, alpha subunit p19 [Source:HGNC Symbol;Acc:15488]
PASK	-3.351080778	9.68E-25	PAS domain containing serine/threonine kinase [Source:HGNC Symbol;Acc:17270]
TRABD2A	-3.35507554	1.38E-07	TraB domain containing 2A [Source:HGNC Symbol;Acc:27013]
DNAH6	-3.35867582	3.86E-06	dynein, axonemal, heavy chain 6 [Source:HGNC Symbol;Acc:2951]
GIMAP8	-3.36032411	3.04E-08	GTPase, IMAP family member 8 [Source:HGNC Symbol;Acc:21792]
TLDC2	-3.360919921	7.68E-11	TBC/LysM-associated domain containing 2 [Source:HGNC Symbol;Acc:16112]
CDH3	-3.360984854	0.005689368	cadherin 3, type 1, P-cadherin (placental) [Source:HGNC Symbol;Acc:1762]
NEDD4L	-3.378930328	1.60E-10	neural precursor cell expressed, developmentally down-regulated 4-like, E3 ubiquitin protein ligase [Source:HGNC Symbol;Acc:7728]
APOD	-3.397847553	0.03483619	apolipoprotein D [Source:HGNC Symbol;Acc:612]
ZEB1	-3.39874465	1.27E-13	zinc finger E-box binding homeobox 1 [Source:HGNC Symbol;Acc:11642]
FSIP2	-3.403455425	0.030038044	fibrous sheath interacting protein 2 [Source:HGNC Symbol;Acc:21675]
GCSAM	-3.416757907	0.000277893	germinal center-associated, signaling and motility [Source:HGNC Symbol;Acc:20253]

AC135983.2	-3.428723255	0.033347312	Protein LOC100996413 [Source:UniProtKB/TrEMBL;Acc:M0R198]
SULT1B1	-3.438574102	8.03E-05	sulfotransferase family, cytosolic, 1B, member 1 [Source:HGNC Symbol;Acc:17845]
ABCG2	-3.478461093	0.000293303	ATP-binding cassette, sub-family G (WHITE), member 2 [Source:HGNC Symbol;Acc:74]
MEGF6	-3.478740192	2.64E-05	multiple EGF-like-domains 6 [Source:HGNC Symbol;Acc:3232]
ZC4H2	-3.484416652	4.16E-05	zinc finger, C4H2 domain containing [Source:HGNC Symbol;Acc:24931]
HPCAL4	-3.488131655	7.49E-09	hippocalcin like 4 [Source:HGNC Symbol;Acc:18212]
INADL	-3.507201797	3.73E-10	InaD-like (Drosophila) [Source:HGNC Symbol;Acc:28881]
PTGR1	-3.508522427	0.00160755	prostaglandin reductase 1 [Source:HGNC Symbol;Acc:18429]
INPP4B	-3.509687243	1.60E-08	inositol polyphosphate-4-phosphatase, type II, 105kDa [Source:HGNC Symbol;Acc:6075]
MCAM	-3.516263927	5.94E-06	melanoma cell adhesion molecule [Source:HGNC Symbol;Acc:6934]
AC008063.2	-3.532032068	0.005717258	
GCNT4	-3.534027859	1.32E-05	glucosaminyl (N-acetyl) transferase 4, core 2 [Source:HGNC Symbol;Acc:17973]
PVT1	-3.534641783	3.45E-14	Pvt1 oncogene (non-protein coding) [Source:HGNC Symbol;Acc:9709]
SGK2	-3.552665207	0.01339709	serum/glucocorticoid regulated kinase 2 [Source:HGNC Symbol;Acc:13900]
ZNF462	-3.567688779	0.016252301	zinc finger protein 462 [Source:HGNC Symbol;Acc:21684]
PBX1	-3.569699478	0.042850927	pre-B-cell leukemia homeobox 1 [Source:HGNC Symbol;Acc:8632]
NBPF13P	-3.570635386	0.004940351	neuroblastoma breakpoint family, member 13, pseudogene [Source:HGNC Symbol;Acc:31995]
CRIP2	-3.571089279	2.47E-06	cysteine-rich protein 2 [Source:HGNC Symbol;Acc:2361]
ARMCX4	-3.579656918	8.61E-07	armadillo repeat containing, X-linked 4 [Source:HGNC Symbol;Acc:28615]
FBXO15	-3.582566229	0.030030816	F-box protein 15 [Source:HGNC Symbol;Acc:13617]
FAM134B	-3.584987288	4.70E-05	family with sequence similarity 134, member B [Source:HGNC Symbol;Acc:25964]
LAMP3	-3.597841151	2.77E-06	lysosomal-associated membrane protein 3 [Source:HGNC Symbol;Acc:14582]
SUSD3	-3.604271419	1.69E-06	sushi domain containing 3 [Source:HGNC Symbol;Acc:28391]
PLAG1	-3.622004441	1.19E-05	pleiomorphic adenoma gene 1 [Source:HGNC Symbol;Acc:9045]
CYSLTR1	-3.626324906	1.07E-06	cysteinyl leukotriene receptor 1 [Source:HGNC Symbol;Acc:17451]
GP5	-3.641615131	0.00047542	glycoprotein V (platelet) [Source:HGNC Symbol;Acc:4443]
SPTLC3	-3.645348437	0.008285783	serine palmitoyltransferase, long chain base subunit 3 [Source:HGNC Symbol;Acc:16253]
CD27	-3.648694674	5.91E-13	CD27 molecule [Source:HGNC Symbol;Acc:11922]
GSTM2	-3.666615897	6.50E-14	glutathione S-transferase mu 2 (muscle) [Source:HGNC Symbol;Acc:4634]
HOOK1	-3.668291569	3.83E-12	hook microtubule-tethering protein 1 [Source:HGNC Symbol;Acc:19884]
ZNF347	-3.670238722	5.55E-05	zinc finger protein 347 [Source:HGNC Symbol;Acc:16447]
ZNF300	-3.677020764	1.49E-06	zinc finger protein 300 [Source:HGNC Symbol;Acc:13091]
LINC00315	-3.688784408	0.010288284	long intergenic non-protein coding RNA 315 [Source:HGNC Symbol;Acc:16621]
NGFRAP1	-3.708581337	8.96E-08	nerve growth factor receptor (TNFRSF16) associated protein 1 [Source:HGNC Symbol;Acc:13388]
AQP3	-3.728647553	3.76E-08	aquaporin 3 (Gill blood group) [Source:HGNC Symbol;Acc:636]
TMEM45B	-3.764897876	7.86E-12	transmembrane protein 45B [Source:HGNC Symbol;Acc:25194]
KANK1	-3.766392328	8.10E-06	KN motif and ankyrin repeat domains 1 [Source:HGNC Symbol;Acc:19309]
WDR64	-3.780521901	0.003255715	WD repeat domain 64 [Source:HGNC Symbol;Acc:26570]
IGF1R	-3.783601286	9.94E-11	insulin-like growth factor 1 receptor [Source:HGNC Symbol;Acc:5465]
C21orf90	-3.792975603	0.039889452	chromosome 21 open reading frame 90 [Source:HGNC Symbol;Acc:16428]
SH2D3A	-3.792992371	2.02E-13	SH2 domain containing 3A [Source:HGNC Symbol;Acc:16885]
CMTM8	-3.794944084	8.70E-05	CKLF-like MARVEL transmembrane domain containing 8 [Source:HGNC Symbol;Acc:19179]
EPHB4	-3.800346747	1.21E-06	EPH receptor B4 [Source:HGNC Symbol;Acc:3395]
ZNF442	-3.827162601	1.43E-05	zinc finger protein 442 [Source:HGNC Symbol;Acc:20877]
GRAPL	-3.836913558	0.039103055	GRB2-related adaptor protein-like [Source:HGNC Symbol;Acc:37240]
AC097713.4	-3.849031215	1.77E-06	

RPL12P18	-3.849426307	8.67E-05	ribosomal protein L12 pseudogene 18 [Source:HGNC Symbol;Acc:36750]
NPAS2	-3.854784249	9.74E-05	neuronal PAS domain protein 2 [Source:HGNC Symbol;Acc:7895]
ANKRD55	-3.871236156	5.24E-05	ankyrin repeat domain 55 [Source:HGNC Symbol;Acc:25681]
CHMP7	-3.899205776	4.12E-18	charged multivesicular body protein 7 [Source:HGNC Symbol;Acc:28439]
RASSF6	-3.916330078	0.022850543	Ras association (RalGDS/AF-6) domain family member 6 [Source:HGNC Symbol;Acc:20796]
RN7SL556P	-3.936897628	0.000592438	RNA, 7SL, cytoplasmic 556, pseudogene [Source:HGNC Symbol;Acc:46572]
TNFRSF10D	-3.960573272	5.44E-09	tumor necrosis factor receptor superfamily, member 10d, decoy with truncated death domain [Source:HGNC Symbol;Acc:11907]
TBC1D4	-3.961142918	1.42E-12	TBC1 domain family, member 4 [Source:HGNC Symbol;Acc:19165]
SLC25A5P5	-3.962954948	0.016021193	solute carrier family 25 (mitochondrial carrier; adenine nucleotide translocator), member 5 pseudogene 5 [Source:HGNC Symbol;Acc:511]
NCMAP	-3.967512912	0.018048366	noncompact myelin associated protein [Source:HGNC Symbol;Acc:29332]
NTRK2	-3.971098214	0.016949068	neurotrophic tyrosine kinase, receptor, type 2 [Source:HGNC Symbol;Acc:8032]
SESN3	-3.979055105	8.92E-28	sestrin 3 [Source:HGNC Symbol;Acc:23060]
RBM20	-3.999991085	0.00332048	RNA binding motif protein 20 [Source:HGNC Symbol;Acc:27424]
ZNF501	-4.00489701	0.000805533	zinc finger protein 501 [Source:HGNC Symbol;Acc:23717]
ITGA6	-4.042835094	1.85E-10	integrin, alpha 6 [Source:HGNC Symbol;Acc:6142]
SLC13A5	-4.05065303	0.014028787	solute carrier family 13 (sodium-dependent citrate transporter), member 5 [Source:HGNC Symbol;Acc:23089]
FAM184A	-4.063360318	4.60E-05	family with sequence similarity 184, member A [Source:HGNC Symbol;Acc:20991]
FRMD7	-4.094407902	0.035992597	FERM domain containing 7 [Source:HGNC Symbol;Acc:8079]
ZNF311	-4.10142046	0.036160451	zinc finger protein 311 [Source:HGNC Symbol;Acc:13847]
CHN1	-4.121664945	2.72E-11	chimerin 1 [Source:HGNC Symbol;Acc:1943]
DCDC1	-4.125753677	0.011842104	doublecortin domain containing 1 [Source:HGNC Symbol;Acc:20625]
ANKK1	-4.156907732	1.60E-07	ankyrin repeat and kinase domain containing 1 [Source:HGNC Symbol;Acc:21027]
ACOT12	-4.160893239	0.033985339	acyl-CoA thioesterase 12 [Source:HGNC Symbol;Acc:24436]
AC023590.1	-4.187986943	0.001142025	Uncharacterized protein[Source:UniProtKB/TrEMBL;Acc:E9PPA6]
DIRC3	-4.196814083	5.99E-07	disrupted in renal carcinoma 3 [Source:HGNC Symbol;Acc:17805]
SLC35F1	-4.202667836	0.012122854	solute carrier family 35, member F1 [Source:HGNC Symbol;Acc:21483]
GPA33	-4.210774199	5.44E-09	glycoprotein A33 (transmembrane) [Source:HGNC Symbol;Acc:4445]
MAL	-4.253408159	0.010288284	mal, T-cell differentiation protein [Source:HGNC Symbol;Acc:6817]
BTLA	-4.255253174	1.48E-13	B and T lymphocyte associated [Source:HGNC Symbol;Acc:21087]
TRAJ52	-4.262920153	0.001066692	T cell receptor alpha joining 52 [Source:HGNC Symbol;Acc:12084]
PPEF1	-4.278748385	0.033457693	protein phosphatase, EF-hand calcium binding domain 1 [Source:HGNC Symbol;Acc:9243]
ZNF418	-4.278814423	3.97E-06	zinc finger protein 418 [Source:HGNC Symbol;Acc:20647]
GIPC3	-4.280706063	0.015275527	GIPC PDZ domain containing family, member 3 [Source:HGNC Symbol;Acc:18183]
FAM172BP	-4.287382736	4.26E-07	family with sequence similarity 172, member B, pseudogene [Source:HGNC Symbol;Acc:34336]
ZNF681	-4.324281927	5.57E-12	zinc finger protein 681 [Source:HGNC Symbol;Acc:26457]
LYPD3	-4.32642065	8.44E-10	LY6/PLAUR domain containing 3 [Source:HGNC Symbol;Acc:24880]
PLXNA4	-4.327859765	3.29E-06	plexin A4 [Source:HGNC Symbol;Acc:9102]
LRRN3	-4.332826029	0.000148108	leucine rich repeat neuronal 3 [Source:HGNC Symbol;Acc:17200]
TXK	-4.334205052	5.17E-19	TXK tyrosine kinase [Source:HGNC Symbol;Acc:12434]
TESPA1	-4.350330288	4.35E-35	thymocyte expressed, positive selection associated 1 [Source:HGNC Symbol;Acc:29109]
PRKCA	-4.353759447	2.19E-37	protein kinase C, alpha [Source:HGNC Symbol;Acc:9393]
HYKK	-4.37985486	0.000331509	hydroxylysine kinase [Source:HGNC Symbol;Acc:34403]
RCAN3	-4.380392196	6.58E-20	RCAN family member 3 [Source:HGNC Symbol;Acc:3042]
PARD3B	-4.389303067	0.002966834	par-3 family cell polarity regulator beta [Source:HGNC Symbol;Acc:14446]
THBS4	-4.389361818	8.27E-06	thrombospondin 4 [Source:HGNC Symbol;Acc:11788]

TRAJ56	-4.399894767	0.003406878	T cell receptor alpha joining 56 [Source:HGNC Symbol;Acc:12088]
RALGPS2	-4.440715301	1.67E-11	Ral GEF with PH domain and SH3 binding motif 2 [Source:HGNC Symbol;Acc:30279]
SCML1	-4.456504339	2.59E-12	sex comb on midleg-like 1 (Drosophila) [Source:HGNC Symbol;Acc:10580]
LEF1	-4.458465455	2.13E-13	lymphoid enhancer-binding factor 1 [Source:HGNC Symbol;Acc:6551]
TRAV3	-4.467738701	3.58E-06	T cell receptor alpha variable 3 (gene/pseudogene) [Source:HGNC Symbol;Acc:12128]
FAM83F	-4.47477421	1.57E-07	family with sequence similarity 83, member F [Source:HGNC Symbol;Acc:25148]
HKDC1	-4.485955824	0.000571513	hexokinase domain containing 1 [Source:HGNC Symbol;Acc:23302]
AC020907.2	-4.527149366	0.027295544	
STAP1	-4.549889085	1.17E-08	signal transducing adaptor family member 1 [Source:HGNC Symbol;Acc:24133]
CASC15	-4.553546546	0.029816319	cancer susceptibility candidate 15 (non-protein coding) [Source:HGNC Symbol;Acc:28245]
ANKRD18A	-4.559647848	2.14E-12	ankyrin repeat domain 18A [Source:HGNC Symbol;Acc:23643]
LTK	-4.573324994	2.92E-07	leukocyte receptor tyrosine kinase [Source:HGNC Symbol;Acc:6721]
MMRN1	-4.587828327	0.027223827	multimerin 1 [Source:HGNC Symbol;Acc:7178]
HLF	-4.593057993	0.0001557	hepatic leukemia factor [Source:HGNC Symbol;Acc:4977]
ZSCAN18	-4.595032582	4.73E-12	zinc finger and SCAN domain containing 18 [Source:HGNC Symbol;Acc:21037]
ZNF471	-4.655514398	0.029189508	zinc finger protein 471 [Source:HGNC Symbol;Acc:23226]
CASP1P2	-4.66846491	0.025897866	caspase 1, apoptosis-related cysteine peptidase pseudogene 2 [Source:HGNC Symbol;Acc:43776]
PI16	-4.669171907	1.32E-06	peptidase inhibitor 16 [Source:HGNC Symbol;Acc:21245]
ALOXE3	-4.702903389	0.000229053	arachidonate lipoxygenase 3 [Source:HGNC Symbol;Acc:13743]
ACVR1C	-4.708888247	1.44E-15	activin A receptor, type IC [Source:HGNC Symbol;Acc:18123]
DBNDD1	-4.734153395	0.000125893	dysbindin (dystrobrevin binding protein 1) domain containing 1 [Source:HGNC Symbol;Acc:28455]
ZDHHC15	-4.774549569	4.23E-05	zinc finger, DHHC-type containing 15 [Source:HGNC Symbol;Acc:20342]
TRAV33	-4.800205546	0.021655546	T cell receptor alpha variable 33 (pseudogene) [Source:HGNC Symbol;Acc:12132]
SLC2A3P4	-4.814926513	0.021129997	solute carrier family 2 (facilitated glucose transporter), member 3 pseudogene 4 [Source:HGNC Symbol;Acc:31076]
AC093642.4	-4.823368692	7.47E-06	
RN7SKP184	-4.832281928	0.021565465	RNA, 7SK small nuclear pseudogene 184 [Source:HGNC Symbol;Acc:45908]
CASC11	-4.835113956	0.021655546	cancer susceptibility candidate 11 (non-protein coding) [Source:HGNC Symbol;Acc:48939]
ZNF563	-4.844486611	3.59E-16	zinc finger protein 563 [Source:HGNC Symbol;Acc:30498]
C1orf51	-4.870524616	2.69E-06	chromosome 1 open reading frame 51 [Source:HGNC Symbol;Acc:25200]
NELL2	-4.880598411	1.93E-15	NEL-like 2 (chicken) [Source:HGNC Symbol;Acc:7751]
NOG	-4.881966028	2.37E-06	noggin [Source:HGNC Symbol;Acc:7866]
CCDC110	-4.88536853	0.020995024	coiled-coil domain containing 110 [Source:HGNC Symbol;Acc:28504]
HNRNPA1P21	-4.888878867	0.003391237	heterogeneous nuclear ribonucleoprotein A1 pseudogene 21 [Source:HGNC Symbol;Acc:39539]
AEBP1	-4.906514115	5.30E-09	AE binding protein 1 [Source:HGNC Symbol;Acc:303]
TRAV39	-4.919708497	0.000860035	T cell receptor alpha variable 39 [Source:HGNC Symbol;Acc:12139]
CCT4P2	-4.932832146	0.001092328	chaperonin containing TCP1, subunit 4 (delta) pseudogene 2 [Source:HGNC Symbol;Acc:35141]
RGMB	-4.945500553	2.52E-13	repulsive guidance molecule family member b [Source:HGNC Symbol;Acc:26896]
GCK	-4.958148891	0.018724865	glucokinase (hexokinase 4) [Source:HGNC Symbol;Acc:4195]
SH3RF3	-5.016799526	1.20E-07	SH3 domain containing ring finger 3 [Source:HGNC Symbol;Acc:24699]
LINC01036	-5.03478782	0.019525237	long intergenic non-protein coding RNA 1036 [Source:HGNC Symbol;Acc:49024]
TSPAN6	-5.058272055	1.12E-06	tetraspanin 6 [Source:HGNC Symbol;Acc:11858]
SCARA3	-5.07161181	0.019945744	scavenger receptor class A, member 3 [Source:HGNC Symbol;Acc:19000]
ZIK1	-5.093637443	2.73E-10	zinc finger protein interacting with K protein 1 [Source:HGNC Symbol;Acc:33104]
CD248	-5.11283094	0.0029106	CD248 molecule, endosialin [Source:HGNC Symbol;Acc:18219]
RN7SL671P	-5.124697201	0.01585122	RNA, 7SL, cytoplasmic 671, pseudogene [Source:HGNC Symbol;Acc:46687]
PKD1L1	-5.206929718	0.000397915	polycystic kidney disease 1 like 1 [Source:HGNC Symbol;Acc:18053]

COL5A2	-5.380071401	0.001368652	collagen, type V, alpha 2 [Source:HGNC Symbol;Acc:2210]
AKAP6	-5.398592036	2.61E-07	A kinase (PRKA) anchor protein 6 [Source:HGNC Symbol;Acc:376]
LINC00470	-5.400079777	0.018080841	long intergenic non-protein coding RNA 470 [Source:HGNC Symbol;Acc:1225]
ZNF704	-5.431064562	0.000210162	zinc finger protein 704 [Source:HGNC Symbol;Acc:32291]
KRT18	-5.475256803	6.20E-08	keratin 18 [Source:HGNC Symbol;Acc:6430]
LDOC1	-5.487045353	9.90E-12	leucine zipper, down-regulated in cancer 1 [Source:HGNC Symbol;Acc:6548]
TRAV22	-5.506506526	4.18E-06	T cell receptor alpha variable 22 [Source:HGNC Symbol;Acc:12119]
ALS2CL	-5.514744517	3.54E-20	ALS2 C-terminal like [Source:HGNC Symbol;Acc:20605]
SDK2	-5.522464903	7.45E-12	sidekick cell adhesion molecule 2 [Source:HGNC Symbol;Acc:19308]
OR52N2	-5.554699616	0.009656421	olfactory receptor, family 52, subfamily N, member 2 [Source:HGNC Symbol;Acc:15228]
RBM11	-5.576102655	6.60E-15	RNA binding motif protein 11 [Source:HGNC Symbol;Acc:9897]
ADTRP	-5.637981393	0.00098612	androgen-dependent TFPI-regulating protein [Source:HGNC Symbol;Acc:21214]
FAM133A	-5.63818364	0.010281709	family with sequence similarity 133, member A [Source:HGNC Symbol;Acc:26748]
SLC16A10	-5.658180405	3.74E-09	solute carrier family 16 (aromatic amino acid transporter), member 10 [Source:HGNC Symbol;Acc:17027]
CXorf58	-5.665678229	0.008059883	chromosome X open reading frame 58 [Source:HGNC Symbol;Acc:26356]
MIR663A	-5.668908603	0.00980151	microRNA 663a [Source:HGNC Symbol;Acc:32919]
TRAV23DV6	-5.682648694	1.43E-05	T cell receptor alpha variable 23/delta variable 6 [Source:HGNC Symbol;Acc:12120]
SOX8	-5.683671842	0.008669496	SRY (sex determining region Y)-box 8 [Source:HGNC Symbol;Acc:11203]
DPPA4	-5.690869862	0.008452182	developmental pluripotency associated 4 [Source:HGNC Symbol;Acc:19200]
AC009312.1	-5.701078976	0.00825416	
RN7SKP9	-5.701538022	0.007570856	RNA, 7SK small nuclear pseudogene 9 [Source:HGNC Symbol;Acc:42627]
DCT	-5.718131401	0.01010622	dopachrome tautomerase [Source:HGNC Symbol;Acc:2709]
LRP6	-5.722301281	1.73E-07	low density lipoprotein receptor-related protein 6 [Source:HGNC Symbol;Acc:6698]
CD40LG	-5.73486698	8.43E-17	CD40 ligand [Source:HGNC Symbol;Acc:11935]
ZFP28	-5.787874218	0.000229568	ZFP28 zinc finger protein [Source:HGNC Symbol;Acc:17801]
KCNA2	-5.808668358	0.008711027	potassium voltage-gated channel, shaker-related subfamily, member 2 [Source:HGNC Symbol;Acc:6220]
OR1X5P	-5.830257044	0.006326803	olfactory receptor, family 1, subfamily X, member 5 pseudogene [Source:HGNC Symbol;Acc:31245]
AC103563.9	-5.86963591	0.006629162	
TRIM2	-5.888763006	1.17E-09	tripartite motif containing 2 [Source:HGNC Symbol;Acc:15974]
TRBV1	-5.913531675	0.005011587	T cell receptor beta variable 1 (pseudogene) [Source:HGNC Symbol;Acc:12176]
CR2	-5.963740349	0.000175337	complement component (3d/Epstein Barr virus) receptor 2 [Source:HGNC Symbol;Acc:2336]
SAMD12	-5.966790004	1.53E-12	sterile alpha motif domain containing 12 [Source:HGNC Symbol;Acc:31750]
TRAV2	-5.977812565	7.86E-12	T cell receptor alpha variable 2 [Source:HGNC Symbol;Acc:12116]
TCEAL2	-6.000343193	0.000974234	transcription elongation factor A (SII)-like 2 [Source:HGNC Symbol;Acc:29818]
SELP	-6.010038156	0.00011653	selectin P (granule membrane protein 140kDa, antigen CD62) [Source:HGNC Symbol;Acc:10721]
SNX18P3	-6.03001368	0.009039369	sorting nexin 18 pseudogene 3 [Source:HGNC Symbol;Acc:39611]
ZNF717	-6.050913713	0.004811036	zinc finger protein 717 [Source:HGNC Symbol;Acc:29448]
TIMM8AP1	-6.097836684	0.003577995	translocase of inner mitochondrial membrane 8 homolog A (yeast) pseudogene 1 [Source:HGNC Symbol;Acc:17802]
FANK1	-6.108811692	0.00778571	fibronectin type III and ankyrin repeat domains 1 [Source:HGNC Symbol;Acc:23527]
CDR1	-6.113425703	0.003450335	cerebellar degeneration-related protein 1, 34kDa [Source:HGNC Symbol;Acc:1798]
LINC00402	-6.120719901	1.03E-08	long intergenic non-protein coding RNA 402 [Source:HGNC Symbol;Acc:42732]
GPR15	-6.142095604	1.84E-09	G protein-coupled receptor 15 [Source:HGNC Symbol;Acc:4469]
SARDH	-6.145528651	1.71E-10	sarcosine dehydrogenase [Source:HGNC Symbol;Acc:10536]
LAMB4	-6.162322022	0.006200564	laminin, beta 4 [Source:HGNC Symbol;Acc:6491]
TNFSF11	-6.181732382	0.003933034	tumor necrosis factor (ligand) superfamily, member 11 [Source:HGNC Symbol;Acc:11926]
DACT1	-6.198975032	0.003369021	dishevelled-binding antagonist of beta-catenin 1 [Source:HGNC Symbol;Acc:17748]

SLC22A17	-6.201952503	2.15E-12	solute carrier family 22, member 17 [Source:HGNC Symbol;Acc:23095]
CACNA1I	-6.227636645	2.54E-24	calcium channel, voltage-dependent, T type, alpha 1I subunit [Source:HGNC Symbol;Acc:1396]
CACHD1	-6.233335112	3.27E-05	cache domain containing 1 [Source:HGNC Symbol;Acc:29314]
ANKRD36BP2	-6.272042338	4.18E-15	ankyrin repeat domain 36B pseudogene 2 [Source:HGNC Symbol;Acc:33607]
AJAP1	-6.373182453	0.003566024	adherens junctions associated protein 1 [Source:HGNC Symbol;Acc:30801]
CCR6	-6.48849908	2.54E-13	chemokine (C-C motif) receptor 6 [Source:HGNC Symbol;Acc:1607]
FHIT	-6.49577273	3.90E-43	fragile histidine triad [Source:HGNC Symbol;Acc:3701]
KRT128P	-6.497917851	0.003327022	keratin 128 pseudogene [Source:HGNC Symbol;Acc:48882]
DPP4	-6.512647259	2.94E-15	dipeptidyl-peptidase 4 [Source:HGNC Symbol;Acc:3009]
KIT	-6.544555054	7.91E-05	v-kit Hardy-Zuckerman 4 feline sarcoma viral oncogene homolog [Source:HGNC Symbol;Acc:6342]
F2RL1	-6.587639484	1.17E-06	coagulation factor II (thrombin) receptor-like 1 [Source:HGNC Symbol;Acc:3538]
ISM1	-6.610020532	7.67E-05	isthmin 1, angiogenesis inhibitor [Source:HGNC Symbol;Acc:16213]
CLIC6	-6.632159894	0.001868999	chloride intracellular channel 6 [Source:HGNC Symbol;Acc:2065]
SLC5A5	-6.666616304	1.35E-12	solute carrier family 5 (sodium/iodide cotransporter), member 5 [Source:HGNC Symbol;Acc:11040]
SELE	-6.709276503	0.00127653	selectin E [Source:HGNC Symbol;Acc:10718]
SLC4A10	-6.749863632	0.000929977	solute carrier family 4, sodium bicarbonate transporter, member 10 [Source:HGNC Symbol;Acc:13811]
CCR8	-6.79770305	2.39E-07	chemokine (C-C motif) receptor 8 [Source:HGNC Symbol;Acc:1609]
MANSC1	-6.828950937	0.002063335	MANSC domain containing 1 [Source:HGNC Symbol;Acc:25505]
AE000658.31	-6.841235339	0.001074785	
MYO16	-6.881510898	0.001529092	myosin XVI [Source:HGNC Symbol;Acc:29822]
FSBP	-6.892709059	0.000895081	fibrinogen silencer binding protein [Source:HGNC Symbol;Acc:43653]
MDS2	-6.918531018	0.000146505	myelodysplastic syndrome 2 translocation associated [Source:HGNC Symbol;Acc:29633]
VSIG1	-6.962157416	3.95E-17	V-set and immunoglobulin domain containing 1 [Source:HGNC Symbol;Acc:28675]
FAAH2	-6.977071874	1.44E-15	fatty acid amide hydrolase 2 [Source:HGNC Symbol;Acc:26440]
KRT18P39	-7.011264571	0.00046823	keratin 18 pseudogene 39 [Source:HGNC Symbol;Acc:33408]
REG4	-7.078714191	0.001087573	regenerating islet-derived family, member 4 [Source:HGNC Symbol;Acc:22977]
SLC40A1	-7.080196737	3.83E-17	solute carrier family 40 (iron-regulated transporter), member 1 [Source:HGNC Symbol;Acc:10909]
GULOP	-7.132835118	0.000340492	gulonolactone (L-) oxidase, pseudogene [Source:HGNC Symbol;Acc:4695]
P2RY14	-7.136744134	0.000763569	purinergic receptor P2Y, G-protein coupled, 14 [Source:HGNC Symbol;Acc:16442]
UBQLNL	-7.238462673	0.000337418	ubiquilin-like [Source:HGNC Symbol;Acc:28294]
ATP5G1P1	-7.29953468	0.000377198	ATP synthase, H+ transporting, mitochondrial Fo complex, subunit C1 (subunit 9) pseudogene 1 [Source:HGNC Symbol;Acc:19815]
RBMS3	-7.328663344	8.20E-07	RNA binding motif, single stranded interacting protein 3 [Source:HGNC Symbol;Acc:13427]
MEOX1	-7.448732755	0.000437374	mesenchyme homeobox 1 [Source:HGNC Symbol;Acc:7013]
CD28	-7.458265068	1.25E-15	CD28 molecule [Source:HGNC Symbol;Acc:1653]
SNORA14	-7.464225146	0.000115434	Small nucleolar RNA SNORA14 [Source:RFAM;Acc:RF00397]
SHISA2	-7.498107254	4.71E-15	shisa family member 2 [Source:HGNC Symbol;Acc:20366]
ADD2	-7.6004555	4.54E-07	adducin 2 (beta) [Source:HGNC Symbol;Acc:244]
SPIN3	-7.714253319	6.02E-05	spindlin family, member 3 [Source:HGNC Symbol;Acc:27272]
ALDH7A1	-7.725023434	0.000320069	aldehyde dehydrogenase 7 family, member A1 [Source:HGNC Symbol;Acc:877]
NBEA	-7.738690725	1.69E-10	neurobeachin [Source:HGNC Symbol;Acc:7648]
IL2RA	-7.782488777	3.39E-25	interleukin 2 receptor, alpha [Source:HGNC Symbol;Acc:6008]
AC103563.8	-7.837925786	3.08E-05	
CCR7	-7.962885673	5.84E-58	chemokine (C-C motif) receptor 7 [Source:HGNC Symbol;Acc:1608]
CLDN1	-7.991408112	0.000257515	claudin 1 [Source:HGNC Symbol;Acc:2032]
RN7SL555P	-7.993852356	2.56E-05	RNA, 7SL, cytoplasmic 555, pseudogene [Source:HGNC Symbol;Acc:46571]
LAMC3	-8.112023773	4.74E-11	laminin, gamma 3 [Source:HGNC Symbol;Acc:6494]

EDA	-8.174201303	1.26E-15	ectodysplasin A [Source:HGNC Symbol;Acc:3157]
EPPK1	-8.290812064	4.33E-06	epiplakin 1 [Source:HGNC Symbol;Acc:15577]
FBLN7	-8.430128176	2.09E-39	fibulin 7 [Source:HGNC Symbol;Acc:26740]
MTHFD1P1	-8.514458517	3.29E-06	methylenetetrahydrofolate dehydrogenase (NADP+ dependent) 1 pseudogene 1 [Source:HGNC Symbol;Acc:7433]
GPR125	-8.566606936	7.22E-06	G protein-coupled receptor 125 [Source:HGNC Symbol;Acc:13839]
CDH1	-8.650876139	2.84E-05	cadherin 1, type 1, E-cadherin (epithelial) [Source:HGNC Symbol;Acc:1748]
OR52N3P	-8.69262246	4.98E-06	olfactory receptor, family 52, subfamily N, member 3 pseudogene [Source:HGNC Symbol;Acc:15229]
ZNF662	-8.881974791	2.15E-06	zinc finger protein 662 [Source:HGNC Symbol;Acc:31930]
CCR4	-8.954944817	1.38E-25	chemokine (C-C motif) receptor 4 [Source:HGNC Symbol;Acc:1605]
ST6GALNAC1	-8.958766509	8.32E-13	ST6 (alpha-N-acetyl-neuraminyl-2,3-beta-galactosyl-1,3)-N-acetylgalactosaminide alpha-2,6-sialyltransferase 1 [Source:HGNC Symbol;Acc:23614]
CD200	-9.02135419	4.70E-28	CD200 molecule [Source:HGNC Symbol;Acc:7203]
RAI2	-9.022347968	4.09E-07	retinoic acid induced 2 [Source:HGNC Symbol;Acc:9835]
KRT18P15	-9.09246948	5.69E-07	keratin 18 pseudogene 15 [Source:HGNC Symbol;Acc:32449]
EMR4P	-9.106801995	1.97E-11	egf-like module containing, mucin-like, hormone receptor-like 4 pseudogene [Source:HGNC Symbol;Acc:19240]
CCR12P	-9.281104051	6.46E-08	chemokine (C-C motif) receptor 12, pseudogene [Source:HGNC Symbol;Acc:39812]
EPGN	-9.283141892	2.15E-07	epithelial mitogen [Source:HGNC Symbol;Acc:17470]
GJB6	-9.308262985	5.34E-07	gap junction protein, beta 6, 30kDa [Source:HGNC Symbol;Acc:4288]
PHF2P2	-9.594658839	1.08E-07	PHD finger protein 2 pseudogene 2 [Source:HGNC Symbol;Acc:38808]
SEMA5A	-9.596647874	1.62E-08	sema domain, seven thrombospondin repeats (type 1 and type 1-like), transmembrane domain (TM) and short cytoplasmic domain, (semaphorin) 5A [Source:HGNC Symbol;Acc:10736]
GREM2	-9.600205879	8.29E-08	gremlin 2, DAN family BMP antagonist [Source:HGNC Symbol;Acc:17655]
GTSCR1	-9.646691114	5.72E-09	Gilles de la Tourette syndrome chromosome region, candidate 1 [Source:HGNC Symbol;Acc:18406]
EDAR	-9.736537069	3.11E-12	ectodysplasin A receptor [Source:HGNC Symbol;Acc:2895]
C14orf132	-9.757881713	1.31E-08	chromosome 14 open reading frame 132 [Source:HGNC Symbol;Acc:20346]
BCL2L14	-9.805958178	7.67E-09	BCL2-like 14 (apoptosis facilitator) [Source:HGNC Symbol;Acc:16657]
TRAV20	-9.834721751	5.30E-09	T cell receptor alpha variable 20 [Source:HGNC Symbol;Acc:12117]
ZNF667	-9.866520648	2.23E-09	zinc finger protein 667 [Source:HGNC Symbol;Acc:28854]
ZNF135	-9.969912581	5.28E-09	zinc finger protein 135 [Source:HGNC Symbol;Acc:12919]
WNT7A	-9.982460053	1.82E-12	wingless-type MMTV integration site family, member 7A [Source:HGNC Symbol;Acc:12786]
ADAM23	-10.38676493	1.98E-10	ADAM metallopeptidase domain 23 [Source:HGNC Symbol;Acc:202]
DSC1	-10.46513881	3.90E-09	desmocollin 1 [Source:HGNC Symbol;Acc:3035]
C4BPB	-10.49809212	2.92E-09	complement component 4 binding protein, beta [Source:HGNC Symbol;Acc:1328]
RORC	-10.52704488	5.29E-10	RAR-related orphan receptor C [Source:HGNC Symbol;Acc:10260]
SIAH3	-10.53429476	3.15E-08	siah E3 ubiquitin protein ligase family member 3 [Source:HGNC Symbol;Acc:30553]
SORCS3	-10.54113041	7.66E-11	sortilin-related VPS10 domain containing receptor 3 [Source:HGNC Symbol;Acc:16699]
BEND5	-10.69096134	1.16E-10	BEN domain containing 5 [Source:HGNC Symbol;Acc:25668]
NRCAM	-10.75595946	5.40E-11	neuronal cell adhesion molecule [Source:HGNC Symbol;Acc:7994]
KRT1	-10.81763328	1.59E-11	keratin 1 [Source:HGNC Symbol;Acc:6412]
FAM153B	-10.87410454	1.31E-16	family with sequence similarity 153, member B [Source:HGNC Symbol;Acc:27323]
FAM153A	-11.00338812	3.54E-17	family with sequence similarity 153, member A [Source:HGNC Symbol;Acc:29940]
DBH	-11.15870174	1.84E-12	dopamine beta-hydroxylase (dopamine beta-monooxygenase) [Source:HGNC Symbol;Acc:2689]
NEFL	-11.36975455	8.15E-13	neurofilament, light polypeptide [Source:HGNC Symbol;Acc:7739]
CA6	-11.84999257	3.25E-14	carbonic anhydrase VI [Source:HGNC Symbol;Acc:1380]
SUSD4	-11.87174752	1.29E-14	sushi domain containing 4 [Source:HGNC Symbol;Acc:25470]
TSHZ2	-15.12800979	2.41E-24	teashirt zinc finger homeobox 2 [Source:HGNC Symbol;Acc:13010]

List of Analyzed Proteins in the Supernatants of Cultures with or without $CD8^+$ $SLAMF7^+$

Full list of all analyzed protein in a High throughput screening of 351 different cytokines and immune proteins in the supernatants of the T cells cultures with/without $CD8^+$ $SLAMF7^+$

ID	Name	uniprot.gene	logFC	AveExpr	P.Value	adj.P.Val
ab1600	CCL22	CCL22	-1.07	15.54	2.24E-05	0.001177684
ab1583	IGKC	IGKC	-0.29	15.53	0.236295445	0.634608968
ab1612	ALBU	ALB	-0.21	15.52	0.381366607	0.777745408
ab1624	S10A8/9	NA	0.45	15.35	0.045353578	0.229384444
ab2782	CD44v2	CD44	-0.65	15.22	0.004291676	0.051779414
ab1584	IGLC1	IGLC1	-0.27	15.21	0.257955442	0.652323236
ab1925	CSF1R	CSF1R	-0.55	15.2	0.005126883	0.058980012
ab1623	CO3	C3	0.05	15.18	0.763341284	0.969849071
ab1132	BTLA	BTLA	-0.15	15.15	0.634860301	0.916799244
ab2700	TLR3	TLR3	-0.18	14.95	0.414418827	0.803323903
ab1059	CXCR5	CXCR5	-0.36	14.94	0.0475808	0.236108499
ab1737	OSTP	SPP1	0.4	14.91	0.101764024	0.382341977
ab1732	HGF	HGF	-0.73	14.89	0.018903718	0.127852402
ab2312	IL8	CXCL8	1.61	14.85	1.08E-10	1.89E-08
ab0993	CD81	CD81	-0.44	14.81	0.040075244	0.210795781
ab1947	I13R2	IL13RA2	-0.91	14.81	0.000144453	0.005427305
ab1402	ITB2	ITGB2	-0.24	14.74	0.298714411	0.690267287
ab2214	ADIPO	ADIPOQ	-0.55	14.74	0.0067693	0.065079603
ab1637	BASI	BSG	-0.52	14.72	0.006954573	0.065323309
ab1448	CD47	CD47	-0.78	14.64	0.001838089	0.031188218
ab1599	CCL26	CCL26	-1.14	14.59	0.000112995	0.004571957
ab2263	IL1A	IL1A	-0.41	14.59	0.03553497	0.194702025
ab1831	IL2RA	IL2RA	-0.05	14.53	0.871651317	0.975520601
ab2129	SLAF8	SLAMF8	-0.13	14.53	0.508084598	0.867277332
ab2176	INHBA	INHBA	0.4	14.51	0.045129172	0.229384444
ab1778	DPP4	DPP4	-0.01	14.5	0.963229552	0.995308645
ab1481	CD99	CD99	-0.29	14.45	0.033908393	0.193519337
ab1725	LIF	LIF	0.13	14.44	0.494831982	0.859827332
ab2455	TNR1B	TNFRSF1B	0.06	14.44	0.75988224	0.968552386
ab2441	IL34	IL34	-0.66	14.4	0.006804901	0.065079603
ab1540	CD44	CD44	-0.12	14.38	0.453326653	0.82284348
ab1215	HMGB1	HMGB1	-0.41	14.37	0.048851265	0.240147342
ab1582	TBB3	TUBB3	-0.39	14.35	0.015980868	0.114095751
ab2374	FGF2	FGF2	-0.31	14.34	0.067980953	0.308258459
ab1781	NRP1	NRP1	0	14.28	0.985949835	0.997245684
ab1940	ANGP4	ANGPT4	0.01	14.27	0.959889567	0.995308645
ab1995	IGF1R	IGF1R	-0.46	14.27	0.020056951	0.130345991
ab1454	ICAM1	ICAM1	-0.14	14.15	0.222940856	0.607600468
ab1453	CD53	CD53	-0.33	14.07	0.073148261	0.31845927

ab2445	TNR16	NGFR	-0.51	14.03	0.011002083	0.0889682
ab1670	CYTL1	CYTL1	-0.07	14.01	0.71082936	0.940025388
ab1529	CD5	CD5	-0.64	13.97	0.000863951	0.021268364
ab1478	TNR6	FAS	-0.39	13.93	0.037390586	0.200688249
ab1524	CD3deg	CD3E	0.06	13.88	0.71385456	0.940025388
ab1634	CEAM5,8	CEACAM5	-0.46	13.87	0.023748029	0.148707899
ab1492	GLPB	GYPB	-0.44	13.77	0.005348397	0.059856525
ab2250	TR13B	TNFRSF13B	-0.19	13.72	0.173633286	0.537241813
ab1028	TNR9	TNFRSF9	-0.56	13.71	0.00119599	0.025824197
ab1817	IL20	IL20	-0.49	13.7	0.014822934	0.109814973
ab2717	IL17	IL17A	-0.55	13.65	0.001227386	0.025824197
ab2391	CCL4	CCL4	2.16	13.64	0.000889551	0.021268364
ab1604	VEGFA	VEGFA	-0.77	13.61	0.00181	0.031188218
ab1731	IL12B	IL12B	-0.62	13.61	0.00048328	0.013729658
ab0987	CCR7	CCR7	-0.24	13.59	0.145214265	0.481387536
ab1459	NCAM1	NCAM1	-0.41	13.56	0.023564313	0.148707899
ab1358	CD3E	CD3E	-0.08	13.54	0.649893284	0.923902344
ab1933	IL22	IL22	0.33	13.54	0.210673345	0.589437124
ab1901	IL2	IL2	-1.07	13.53	3.93E-05	0.001880987
ab1774	CCL24	CCL24	-0.26	13.49	0.345308496	0.73515079
ab2132	SLAF1	SLAMF1	-0.24	13.47	0.222042144	0.607600468
ab1433	GP1BA	GP1BA	-0.1	13.44	0.60937492	0.916799244
ab1471	TFR1	TFRC	0.01	13.43	0.957827304	0.995308645
ab2246	CD166	ALCAM	0.07	13.4	0.716635324	0.940025388
ab1514	PERM	MPO	0.27	13.38	0.201967441	0.574242563
ab2342	ADA17	ADAM17	-0.08	13.38	0.524260421	0.869281146
ab1627	CD14	CD14	-0.59	13.35	0.139709709	0.48001171
ab1117	CTLA4	CTLA4	0.06	13.34	0.663387667	0.929956303
ab2491	SDF1	CXCL12	-0.1	13.33	0.600138148	0.916799244
ab1613	VEGFC	VEGFC	0.06	13.31	0.562769623	0.898940908
ab1842	TIMP1	TIMP1	0.15	13.31	0.25442356	0.652323236
ab2434	IL1RA	IL1RN	0.29	13.3	0.078474725	0.326138749
ab1538	ITA2B (CD41a)	ITGA2B	0.04	13.27	0.78771929	0.975520601
ab1567	ITAV	ITGAV	0.02	13.26	0.895149544	0.977109373
ab2290	BCAM	BCAM	0.33	13.24	0.03930028	0.208807551
ab1553	HLA-I	NA	0.38	13.22	0.002585892	0.036994417
ab1432	ITA2B	ITGA2B	-0.43	13.15	0.080845351	0.327658516
ab1900	FCER2	FCER2	-0.03	13.14	0.767276173	0.972499438
ab2437	CD276	CD276	-0.07	13.11	0.725989533	0.947569464
ab1611	Lactoferin	LTF	-0.35	13.08	0.320195235	0.716692314
ab1794	TR10D	TNFRSF10D	-0.04	13.06	0.679730951	0.93213366
ab1832	UPAR	PLAUR	0.19	13.05	0.022755935	0.145971
ab1885	ONCM	OSM	0.16	13.04	0.065453826	0.302006248
ab1390	AMPN	ANPEP	-0.22	13.01	0.181793899	0.552737518
ab1419	CD27	CD27	0.02	12.99	0.901048052	0.977109373

ab1566	ITA6	ITGA6	0.03	12.97	0.756423124	0.968552386
ab1017	TNFL4	TNFSF4	0.21	12.96	0.324318559	0.716771269
ab1442	CD45RA	PTPRC	-0.05	12.96	0.707350053	0.939560929
ab2515	CXL16	CXCL16	-0.2	12.96	0.060201587	0.280230396
ab2760	CADH2	CDH2	0.02	12.95	0.907655954	0.977109373
ab1546	CD63	CD63	0.28	12.94	0.120396104	0.42789426
ab1565	ITA5	ITGA5	-0.03	12.91	0.856064134	0.975520601
ab2783	CD36	CD36	-0.42	12.9	0.03080352	0.18412104
ab1671	CCL5	CCL5	-0.86	12.86	0.001657302	0.031188218
ab2067	HAVR2	HAVCR2	-0.06	12.85	0.427633756	0.808892945
ab1495	DPB1	HLA-DPB1	-0.3	12.75	0.151920781	0.481387536
ab1378	CD9	CD9	-0.2	12.74	0.296199369	0.690267287
ab1598	CCL20	CCL20	-0.1	12.72	0.164799726	0.512926957
ab1970	I13R1	IL13RA1	-0.54	12.71	0.002602269	0.036994417
ab1944	C163A	CD163	0.19	12.69	0.078270841	0.326138749
ab1991	AREG	AREG	-0.16	12.68	0.39746994	0.788940334
ab1493	HLA-ABC	NA	-0.02	12.67	0.869262239	0.975520601
ab1375	CD8A	CD8A	0.06	12.62	0.693937795	0.939560929
ab1692	CCL7	CCL7	0.13	12.61	0.090016421	0.350730649
ab1345	PRIO	PRNP	-0.24	12.6	0.009405829	0.079677036
ab2674	TNF11	TNFSF11	-0.12	12.6	0.354992614	0.740396194
ab1983	TNFL6	FASLG	-0.16	12.54	0.198944284	0.574242563
ab1753	TGFB2	TGFB2	-0.23	12.5	0.204364284	0.574998857
ab1602	NGF-beta	NGF	0.02	12.46	0.867656722	0.975520601
ab1497	IL6	IL6	3.04	12.45	1.62E-12	8.51E-10
ab1706	IL6RA	IL6R	-0.06	12.42	0.43212722	0.808892945
ab1795	CCL3	CCL3	0.89	12.4	0.006758607	0.065079603
ab1461	LFA3	CD58	0.08	12.36	0.632942379	0.916799244
ab1709	NP1L4	NAP1L4	0.72	12.33	1.71E-06	0.000224372
ab2407	I17RA	IL17RA	-0.05	12.32	0.774659114	0.973684305
ab1473	CD72	CD72	0.15	12.31	0.026173512	0.161967853
ab1681	IL12p70	IL12A	0.04	12.23	0.667020259	0.929967152
ab2431	IL5	IL5	-1.2	12.23	0.000243347	0.008000036
ab1466	LYAM1	SELL	0.25	12.22	0.005588083	0.061236073
ab1752	TNR5	CD40	-0.15	12.19	0.092721499	0.358614033
ab1579	anti-dsDNA	NA	0.23	12.18	0.007640592	0.068792624
ab1224	IL34_MOUSE	Il34	0.26	12.17	0.260433231	0.652323236
ab1711	TN13B	TNFSF13B	-0.19	12.16	0.000275092	0.008511669
ab2150	CCL23	CCL23	0.05	12.16	0.458760931	0.824579234
ab0991	LEUK	SPN	-0.58	12.12	0.000112987	0.004571957
ab2448	CCL17	CCL17	0.48	12.12	0.150057491	0.481387536
ab1765	TNR14	TNFRSF14	-0.18	12.09	0.010613373	0.087228656
ab1420	CD28	CD28	-0.25	12.07	0.127294734	0.4463802
ab2363	CEAM1	CEACAM1	0.13	12.04	0.284434793	0.686296793
ab1384	ITAL	ITGAL	-0.19	12.02	0.271145778	0.672748488

ab1585	CCL19	CCL19	0.11	12.02	0.034456765	0.193519337
ab1111	ENTP1	ENTPD1	-0.61	11.99	0.049382335	0.240510263
ab1536	CR1	CR1	-0.06	11.95	0.643980865	0.921083315
ab1999	LYAM2	SELE	-0.49	11.94	0.000995877	0.022775277
ab1581	DRA	HLA-DRA	-0.09	11.93	0.297146985	0.690267287
ab1943	LYAM3	SELP	0.44	11.92	0.073863177	0.31845927
ab1987	EPCAM	EPCAM	-0.09	11.92	0.50432619	0.866556462
ab1593	IgE	NA	0.07	11.88	0.322959973	0.716771269
ab1371	CD7	CD7	-0.26	11.85	0.146261054	0.481387536
ab1480	4F2	SLC3A2	-0.05	11.84	0.443635158	0.816552575
ab1535	PECA1	PECAM1	0	11.83	0.993289356	0.997245684
ab1488	SELPL	SELPLG	-0.11	11.79	0.327505385	0.717782635
ab1510	IL15	IL15	-0.51	11.79	0.016051493	0.114095751
ab1423	TNR8	TNFRSF8	-0.42	11.78	0.005985349	0.063254786
ab2373	BMP5	BMP5	-0.03	11.78	0.758063431	0.968552386
ab1619	VGFR2	KDR	0	11.77	0.967740418	0.995308645
ab1679	IL36G	IL36G	0.02	11.77	0.790723081	0.975520601
ab1713	ELAF	PI3	-0.09	11.75	0.089188451	0.350097948
ab1690	CCL8	CCL8	0.14	11.68	0.001784473	0.031188218
ab1957	CSF1	CSF1	-0.24	11.64	0.140535748	0.48001171
ab1696	IL16	IL16	0.13	11.63	0.097441752	0.373496709
ab1928	IL4	IL4	0.04	11.63	0.688566437	0.938305559
ab1601	CCL25	CCL25	0.13	11.61	0.08114363	0.327658516
ab1716	IL13	IL13	0.07	11.59	0.414343136	0.803323903
ab1450	ICAM3	ICAM3	-0.09	11.57	0.792945664	0.975520601
ab1828	CXCL5	CXCL5	1.08	11.57	6.80E-12	1.79E-09
ab2435	CCL2	CCL2	0.62	11.57	8.57E-06	0.000644196
ab1405	CD19	CD19	-0.04	11.54	0.732067905	0.950784488
ab2403	IL17C	IL17C	0.15	11.54	0.257160864	0.652323236
ab1426	CD34	CD34	-0.04	11.53	0.423126517	0.808892945
ab1525	CD4	CD4	-0.06	11.51	0.513580486	0.868287631
ab1857	TNR11	TNFRSF11A	-0.37	11.5	0.012956513	0.100222438
ab1561	FCG2A	FCGR2A	0	11.49	0.987162324	0.997245684
ab1632	CEAM1,3,5,6,8	CEACAM1	0	11.48	0.996980131	0.997245684
ab1772	BMP7	BMP7	-0.02	11.46	0.819795892	0.975520601
ab2704	GRN	GRN	-0.09	11.45	0.495299775	0.859827332
ab1367	CD6	CD6	-0.08	11.43	0.678860204	0.93213366
ab1921	TNFB	LTA	0.24	11.43	0.000203822	0.007147359
ab1087	MUC1	MUC1	0.11	11.42	0.570248885	0.902637887
ab2474	ERBB2	ERBB2	-0.05	11.4	0.782886822	0.975520601
ab1415	CD24	CD24	0.1	11.32	0.532786615	0.873039749
ab1532	FCG3A	FCGR3A	-0.1	11.31	0.18698419	0.558827749
ab1543	ITA4	ITGA4	0.13	11.29	0.066481639	0.304081235
ab1356	CD2	CD2	0.11	11.25	0.475569574	0.839428173
ab1439	PTPRC (CD45)	PTPRC	-0.01	11.25	0.857798212	0.975520601

ab1608	HLAG	HLA-G	-0.03	11.25	0.700134266	0.939560929
ab2317	BMP6	BMP6	0	11.25	0.971971063	0.995308645
ab1816	MIF	MIF	0.12	11.24	0.037133593	0.200688249
ab2688	NAMPT	NAMPT	0.12	11.24	0.054726375	0.261691575
ab1446	MCP	CD46	0.14	11.23	0.00251888	0.036994417
ab2332	TNR1A	TNFRSF1A	-0.18	11.21	0.011189383	0.0889682
ab0974	PDCD1	PDCD1	0.1	11.2	0.356122124	0.740396194
ab1203	LAMP1	LAMP1	0.15	11.19	0.505765844	0.866556462
ab1490	MPRI	IGF2R	-0.07	11.19	0.117691006	0.424010061
ab1533	CR2	CR2	0	11.19	0.997245684	0.997245684
ab2004	GROA	CXCL1	0.83	11.18	5.14E-06	0.000450899
ab2720	CEAM5	CEACAM5	0.31	11.18	0.007759718	0.068792624
ab1639	CD69	CD69	-0.01	11.17	0.871662894	0.975520601
ab2227	TNR17	TNFRSF17	0.13	11.17	0.146384718	0.481387536
ab1464	CD59	CD59	-0.01	11.14	0.814527485	0.975520601
ab1830	CD97	CD97	0.03	11.14	0.597805733	0.916799244
ab2503	CXL10	CXCL10	-0.14	11.14	0.085912047	0.339772457
ab1501	PRTN3	PRTN3	-0.18	11.11	0.000572553	0.015058156
ab1841	PLF4	PF4	0.09	11.09	0.409836379	0.803323903
ab1744	KIT	KIT	0.03	11.07	0.630293749	0.916799244
ab1594	CD20	MS4A1	0.06	11.06	0.237202908	0.634608968
ab1733	IL33RA	NA	0.07	11.06	0.199816201	0.574242563
ab1934	TR11B	TNFRSF11B	0.18	11.06	0.034583304	0.193519337
ab1401	CDw17	NA	-0.04	11.04	0.573272725	0.902818722
ab1633	CEAM6	CEACAM6	0	11.04	0.978058727	0.997013353
ab1213	IL33_MOUSE	Il33	0.09	11.03	0.359725206	0.744942749
ab2135	EPCR	PROCR	-0.03	10.98	0.712381566	0.940025388
ab2145	TNR21	TNFRSF21	-0.02	10.93	0.804406641	0.975520601
ab1960	BMP4	BMP4	0.03	10.91	0.527107796	0.869281146
ab2749	IL32	IL32	0.06	10.89	0.531736008	0.873039749
ab1868	TLR2	TLR2	0.03	10.88	0.614760921	0.916799244
ab1878	CCL28	CCL28	-0.13	10.88	0.018584374	0.127852402
ab1388	ITAM	ITGAM	-0.04	10.87	0.599666353	0.916799244
ab2301	TNF14	TNFSF14	0.02	10.87	0.920693591	0.984318758
ab2254	NEP	MME	0.01	10.86	0.935305168	0.989880319
ab1494	HLA-DR	NA	-0.06	10.85	0.631077108	0.916799244
ab1980	FLT3	FLT3	0.02	10.85	0.830550911	0.975520601
ab1491	GLPA	GYPA	-0.17	10.83	0.002208919	0.035208825
ab1631	CEAM5,6,8	CEACAM5	-0.08	10.83	0.150327649	0.481387536
ab1086	TNF13	TNFSF13	0	10.82	0.976939704	0.997013353
ab1451	CD52	CD52	0.01	10.81	0.934552957	0.989880319
ab1562	CD33	CD33	-0.17	10.81	0.001311931	0.026541366
ab1734	IL18	IL18	0.02	10.81	0.670071389	0.929967152
ab1754	OX2G	CD200	0.13	10.81	0.346611019	0.73515079
ab1792	VCAM1	VCAM1	0.21	10.8	0.149659858	0.481387536

ab2146	SCRB2	SCARB2	-0.05	10.79	0.472218754	0.839145488
ab2412	CADH1	CDH1	0.02	10.79	0.636103746	0.916799244
ab2469	VEGF165, VEGF121	VEGFA	0.04	10.79	0.303679624	0.694873637
ab1534	ITB1	ITGB1	-0.01	10.78	0.929179156	0.989368899
ab1618	VGFR1	FLT1	0	10.77	0.962844073	0.995308645
ab1519	IFNA1	IFNA1; IFNA13	-0.04	10.76	0.70617887	0.939560929
ab1573	ITAE	ITGAE	-0.21	10.73	0.044173198	0.22779512
ab2172	IL3	IL3	-0.06	10.73	0.664759639	0.929956303
ab1498	CRLF2	CRLF2	-0.16	10.72	0.003315456	0.044716144
ab1661	TSLP	TSLP	0.09	10.71	0.445533439	0.816552575
ab1741	IL27A	IL27	0.05	10.71	0.429439252	0.808892945
ab1537	CD38	CD38	-0.13	10.7	0.291818363	0.690267287
ab1651	TNFA	TNF	-0.01	10.68	0.844387385	0.975520601
ab1502	BDNF	BDNF	-0.03	10.65	0.83010475	0.975520601
ab1823	PD1L1	CD274	-0.18	10.64	0.034116739	0.193519337
ab1503	CCL11	CCL11	-0.15	10.63	0.001691404	0.031188218
ab1836	IFNG	IFNG	0.11	10.63	0.132933466	0.460019756
ab1575	IL2RB	IL2RB	-0.12	10.6	0.035195945	0.194702025
ab1580	anti-FITC	NA	0.04	10.6	0.456774873	0.824579234
ab1484	EGLN	ENG	0.11	10.58	0.098181119	0.373496709
ab1576	SDC1	SDC1	-0.17	10.58	0.002509346	0.036994417
ab1606	K1C18	KRT18	-0.04	10.58	0.517637994	0.868287631
ab1622	VGFR3	FLT4	0.04	10.58	0.556706037	0.896316765
ab1888	IL1B	IL1B	0.55	10.58	2.18E-05	0.001177684
ab1518	KSYK	SYK	-0.03	10.56	0.603915051	0.916799244
ab1596	CCL13	CCL13	0.04	10.56	0.608257751	0.916799244
ab2794	LAG3	LAG3	0.06	10.55	0.453658953	0.82284348
ab1457	DAF	CD55	0.05	10.54	0.316573162	0.711613177
ab2073	TNF10	TNFSF10	-0.21	10.54	0.475193385	0.839428173
ab1892	CRTAM	CRTAM	-0.01	10.51	0.908125449	0.977109373
ab1389	ITAX	ITGAX	-0.05	10.48	0.611978539	0.916799244
ab1552	CD139	NA	0.01	10.47	0.887336993	0.977109373
ab1137	TNR4	TNFRSF4	0	10.46	0.954984895	0.995308645
ab2113	TNR18	TNFRSF18	-0.1	10.46	0.190561052	0.561299095
ab1509	IL10	IL10	0.14	10.45	0.256679531	0.652323236
ab1951	IL17B	IL17B	-0.05	10.45	0.403464082	0.797827471
ab1344	TGM2	TGM2	-0.1	10.44	0.127027786	0.4463802
ab1869	CCL1	CCL1	0.32	10.44	0.141758601	0.481064672
ab1568	B3GA1	B3GAT1	-0.21	10.43	1.48E-05	0.000971559
ab1827	X3CL1	CX3CL1	-0.02	10.43	0.835678847	0.975520601
ab2014	CSF3	CSF3	0.12	10.42	0.098699701	0.373496709
ab2124	IL31	IL31	-0.03	10.41	0.663210621	0.929956303
ab1504	anti Fol.Dendr.Cells	NA	0.21	10.4	0.016560602	0.116145022
ab2011	CO5	C5	0.06	10.4	0.775615445	0.973684305

ab1577	CEAM8	CEACAM8	-0.05	10.38	0.443050823	0.816552575
ab2125	TREM1	TREM1	0.11	10.38	0.19101243	0.561299095
ab2466	IL33	IL33	-0.02	10.38	0.826132955	0.975520601
ab1445	CD45RO	PTPRC	0.01	10.37	0.82950416	0.975520601
ab2154	CCL27	CCL27	0.05	10.37	0.844940582	0.975520601
ab1412	CD22	CD22	0.04	10.34	0.722254971	0.945040087
ab1863	TGFB3	TGFB3	0.07	10.34	0.322053794	0.716771269
ab2476	FLT3L	FLT3LG	0.12	10.33	0.110916157	0.408600792
ab2680	IFNL3	IFNL3	0.02	10.33	0.802858051	0.975520601
ab2108	IL7	IL7	-0.04	10.32	0.381479687	0.777745408
ab1477	CD86	CD86	0.03	10.29	0.842189101	0.975520601
ab1636	CD235a	GYPA	0.03	10.28	0.774778145	0.973684305
ab1789	CCL15	CCL15	-0.03	10.28	0.864249487	0.975520601
ab1516	NTF4	NTF4	-0.12	10.27	0.007847067	0.068792624
ab2078	GDF15	GDF15	0.03	10.27	0.744377327	0.96202082
ab1428	CD37	CD37	-0.01	10.26	0.847414736	0.975520601
ab2122	CD40L	CD40LG	0.02	10.26	0.706596461	0.939560929
ab2718	JAG1	JAG1	-0.01	10.26	0.865849089	0.975520601
ab1475	CD79A	CD79A	-0.14	10.25	0.003876077	0.049727231
ab2480	IL1R2	IL1R2	0.03	10.25	0.883466056	0.977109373
ab1394	CD15	NA	-0.1	10.23	0.540626081	0.883134529
ab1986	CCL14	CCL14	0.01	10.23	0.880248975	0.977109373
ab2742	ICOS	ICOS	0.11	10.23	0.467871427	0.834238545
ab1629	CEAM3,5	CEACAM3	0.04	10.19	0.417875747	0.805137886
ab1749	IL19	IL19	0.24	10.19	0.111083485	0.408600792
ab1110	5NTD	NT5E	-0.02	10.18	0.716313724	0.940025388
ab2202	TF	F3	0.03	10.18	0.705593429	0.939560929
ab2492	IL17F	IL17F	0.18	10.17	0.034150177	0.193519337
ab1955	IL37	IL37	-0.04	10.16	0.55891996	0.896316765
ab2005	SIGL9	SIGLEC9	0.07	10.16	0.383394854	0.77863202
ab2157	CD244	CD244	-0.03	10.16	0.804875641	0.975520601
ab2506	CSF3R	CSF3R	-0.06	10.16	0.498578299	0.862671662
ab2440	IL23A	IL23A	0.08	10.12	0.695951914	0.939560929
ab1739	CCL21	CCL21	-0.08	10.1	0.192555399	0.562689665
ab1460	CD57	NA	-0.14	10.09	0.442311877	0.816552575
ab2813	CDCP1	CDCP1	0.1	10.09	0.119438141	0.427377293
ab1084	TR13C	TNFRSF13C	-0.05	10.08	0.604891125	0.916799244
ab1489	CD177	CD177	-0.07	10.07	0.240533955	0.635783217
ab1589	IL25	IL25	0.17	10.07	0.059373887	0.278845219
ab1134	KI2L2	KIR2DL2	0.01	10.06	0.919820523	0.984318758
ab1171	TNFL8	TNFSF8	0	10.06	0.960990739	0.995308645
ab1476	CD80	CD80	-0.06	10.06	0.200901901	0.574242563
ab1920	NRG1	NRG1	-0.1	10.06	0.049893711	0.240771485
ab1882	TIE2	TEK	-0.06	10.04	0.500896645	0.863841428
ab1515	NTAL	LAT2	0.04	10.03	0.422141931	0.808892945
ab2058	CXCL9	CXCL9	-0.13	10.03	0.076135632	0.325588151

ab2300	CXL14	CXCL14	0.03	10.03	0.729758373	0.95013095
ab2812	LEPR	LEPR	-0.05	10.03	0.67487766	0.931720863
ab1793	BMP2	BMP2	0.04	10.02	0.351884299	0.740364564
ab1517	P53	TP53	0.03	10.01	0.624391441	0.916799244
ab1968	IFNL2	IFNL2	0.06	10.01	0.396701501	0.788940334
ab1520	PGH1	PTGS1	-0.01	10	0.831073171	0.975520601
ab2487	TNF18	TNFSF18	-0.03	10	0.833910322	0.975520601
ab2315	IL6RB	IL6ST	0.05	9.99	0.294971886	0.690267287
ab2734	PD1L2	PDCD1LG2	0.05	9.99	0.283262907	0.686296793
ab1595	TGFB1	TGFB1	0	9.98	0.996263738	0.997245684
ab1763	CCL16	CCL16	-0.11	9.98	0.309221972	0.704115831
ab1551	IL3RB	CSF2RB	0.21	9.93	0.001903624	0.031290813
ab1889	CNTF	CNTF	0.06	9.93	0.103907987	0.387628378
ab2175	CSF2	CSF2	-0.03	9.93	0.593336085	0.916799244
ab2335	IFNL1	IFNL1	0.14	9.92	0.147744604	0.481387536
ab2201	GDF2	GDF2	0.02	9.9	0.788418528	0.975520601
ab1223	TNF10_MOUSE	Tnfsf10	0.01	9.88	0.895138885	0.977109373
ab1449	CD48	CD48	-0.05	9.88	0.227051374	0.615613518
ab2265	HAVR1	HAVCR1	-0.01	9.87	0.90606143	0.977109373
ab1571	CD70	CD70	0.06	9.86	0.299203311	0.690267287
ab1591	IGF1	IGF1	-0.07	9.85	0.259834447	0.652323236
ab1926	CCL18	CCL18	0.02	9.85	0.608763557	0.916799244
ab2115	CXL11	CXCL11	0.07	9.8	0.112816846	0.41209487
ab1400	CD17	NA	-0.05	9.79	0.372398557	0.765162661
ab2687	I36RA	IL36RN	0.01	9.79	0.852169469	0.975520601
ab1496	pan HLA-class II	NA	-0.01	9.78	0.849433212	0.975520601
ab2041	IL3RA	IL3RA	0.03	9.78	0.63316278	0.916799244
ab1444	CD45RB	PTPRC	0.05	9.73	0.450662449	0.82284348
ab1803	FCG2B	FCGR2B	-0.03	9.73	0.816682185	0.975520601
ab2351	TGFB1,2,3	TGFB1	-0.02	9.71	0.640963762	0.921083315
ab1574	SEM7A	SEMA7A	-0.05	9.69	0.603742849	0.916799244
ab2100	IL1R1	IL1R1	-0.04	9.69	0.644408098	0.921083315
ab2508	CXCL6	CXCL6	0.01	9.64	0.938908321	0.991698347
ab2818	CADH5	CDH5	0.01	9.62	0.826452325	0.975520601
ab2276	CXL13	CXCL13	0.03	9.61	0.571441856	0.902637887
ab1036	LY75	LY75	-0.01	9.57	0.923919516	0.985764027
ab1936	ADAM8	ADAM8	0	9.57	0.906049229	0.977109373
ab1909	XCL1	XCL1	-0.02	9.54	0.704936337	0.939560929
ab1808	TNF12	TNFSF12	-0.06	9.48	0.177632429	0.543224755
ab1353	CD1A	CD1A	-0.04	9.45	0.631161045	0.916799244
ab2128	CXCL7	PPBP	-0.03	9.35	0.636181985	0.916799244
ab2252	IL9	IL9	0.02	9.25	0.760479345	0.968552386

Acknowledgments

First and foremost, I would like to sincerely thank Prof. Dr. Michael Hundemer, my dissertation supervisor. Michael Hundemer was the best example of a "*Doktorvater*". Your meticulous and dedicated support, your guidance throughout the project, immense scientific supervision and consistent encouragement shaped my way and will never be forgotten. I am very much grateful to you and I have learnt a lot from you, Thank you so much.

I would also like to thank Sergej Medenhoff, a colleague and a friend, who guided me from my first day, provided outmost support in the laboratory and in every aspect of life, without you, I would not have made it. I am very grateful to you!

I would like to thank our external collaborators who helped us throughout this project, Heiko Bruns, university hospital Erlangen, Hakim Echchannaoui, University of Johannes Gutenberg-Universität Mainz. Special thanks to the principal investigators, the study nurses, and study teams in the GMMG clinical study group. I am also heartfully grateful to the participating patients and their families for supporting this research project.

I humbly thank my colleagues and friends who helped me throughout this journey, Gigi Ton for always supporting me patiently and for her intellectual wealth which enriched my knowledge, Anna Schleich for her sincere laboratory work, interactive discussions, and helping me a lot, Mandy Medenhoff for her long contribution to the project from the beginning and organizing the patients` samples workflow. I appreciate your support so much.

My sincere gratitude also goes to Prof. Dr. Carsten Müller-Tidow and Prof. Dr. Hartmut Goldschmidt, for their tireless assistance, guidance, invaluable contributions, and encouragement throughout the project; to them I say Thank you so much.

My gratitude also goes to Prof. Dr. Markus Munder, for his critical comments, support, theoretical and practical contributions, and most importantly interactive revisions, I am indeed indebted to you.

To get through such a long way, I required more than academic support, so my beloved friends were always there to give me the essential emotional support. Shady Mahmoud: my childhood friend who was always on my side since I was 5 years old, thank you so much for always being there for me. Without a friend like you, providing me with a moral guidance, dedicated advice, and cheerful talks, I would have struggled searching my way, I owe you a lot. Peter Truckenmüller, being there helped me overcome many obstacles in

Germany and never to give up, thank you for making my world a better place. Shehab Elzoheiry, Julian Plaumann, Mostafa Youssef: your care, support, assistance, and the wonderful times I spent with you, were the incentive to keep going, I am very thankful to you. I am very grateful to my friends, family Mühl: Marianne, Sara & Moritz, Yasmin Demerdash, Iman Nafis, Fadwa El-Tahry, Nada Ragab, and Mohamed Belal.

Most importantly, I could have never achieved anything in my life without my beloved family. My parents, you made everything possible for me, thank for your daily support, calls, and messages. Your moral support was indispensable during my life. Your advice and guidance stood as a lighthouse to get safely from each storm I experienced. Few words and lines in the acknowledgment are never enough to described how am I indebted to you or to thank you. My siblings Linda, Laura, Liza, Sara, and Ahmed, you are my heroes, friends, and everything. Your unconditional love since I was a baby provided the intimacy needed to keep going. To my family: this work is nothing but a testament to your unconditional love and encouragement. I cannot love you more!

Eidesstattliche Versicherung

Bei der eingereichten Dissertation zu dem Thema

"The Effect of Elotuzumab on T cells in Patients with Multiple Myeloma"

handelt es sich um meine eigenständig erbrachte Leistung.

1. Ich habe nur die angegebenen Quellen und Hilfsmittel benutzt und mich keiner unzulässigen Hilfe Dritter bedient. Insbesondere habe ich wörtlich oder sinngemäß aus anderen Werken übernommene Inhalte als solche kenntlich gemacht.
2. Die Arbeit oder Teile davon habe ich bislang nicht an einer Hochschule des In- oder Auslands als Bestandteil einer Prüfungs- oder Qualifikationsleistung vorgelegt.
3. Die Richtigkeit der vorstehenden Erklärungen bestätige ich.

4. Die Bedeutung der eidesstattlichen Versicherung und die strafrechtlichen Folgen einer unrichtigen oder unvollständigen eidesstattlichen Versicherung sind mir bekannt. Ich versichere an Eides statt, dass ich nach bestem Wissen die reine Wahrheit erklärt und nichts verschwiegen habe.

Ort und Datum Unterschrift